Cyclodextrin-based Formulations for Pulmonary Delivery of Chemotherapeutic Molecules

Noratiqah Mohtar

Thesis submitted in accordance with the requirements of UCL for the degree of Doctor of Philosophy

August 2018

UCL School of Pharmacy
29-39 Brunswick Square
London WC1N 1AX
United Kingdom

Declaration

This work has been conducted in the School of Pharmacy, University College London between September 2014 and August 2018, under the supervision of Dr Satyanarayana Somavarapu, Professor Kevin M. G. Taylor and Dr Khalid Sheikh.

I, Noratiqah Mohtar, confirm that the research described in this thesis is original. I also certify that I have written all the text herein. Where information has been derived from other sources, I confirm that this has been indicated in this thesis.

Signature: _____   Date: _____

Acknowledgements

I would like to thank the staff of UCL School of Pharmacy, especially Ms Isabel Goncalves, Ms Catherine Baumber, Ms Kate Keen, Ms Allison Dolling, Ms Satinder Sembi, Ms Caitlin Broadbent, Mr David McCarthy, Mr Hardyal S. Gill, Mr Rob Wittwer, Dr Renu Datta, Mr Chris Cook, Mr Victor Diran and Dr Gabriella Caminotto, for their technical and administrative assistance.

Finally, I would like to express my utmost gratitude to my parents for their endless support. Their unconditional loves have given me the strength and confidence to pursue my dreams.

Thank you! May God bless all of you!

Abstract

This study investigated cyclodextrin-based formulations for the delivery of fisetin (a flavonoid) and erlotinib (a tyrosine kinase inhibitor) to the lung. In the first part of the study, complexation of fisetin with β-cyclodextrin (β-CD) and its derivatives, namely hydroxypropyl-β-cyclodextrin (HP-β-CD) and sulfobutylether-β-cyclodextrin (SBE-β-CD), was conducted. Complexation efficiency between fisetin and the cyclodextrins was in the order: SBE-β-CD > HP-β-CD > β-CD. Utilisation of 20% v/v ethanol during complexation with SBE-β-CD improved the solubilisation of fisetin 5.9-fold compared to using water alone. Spray-drying of the fisetin-SBE-β-CD complex from 20% v/v ethanol feed solution, produced a powder with a 2-fold increase in the fine particle fraction (FPF) compared to the spray-dried powder produced from a feed solution containing water alone, when characterised using the Next Generation Impactor (NGI). Addition of 20% w/w leucine into the powder produced from the ethanolic feed solution further improved the FPF by 2.3-fold compared to the powder without leucine. The preparation showed an unchanged cytotoxic activity of fisetin against the human lung adenocarcinoma (A549) cell line, when compared to fisetin solution. In the second part of the study, combinations of fisetin with three tyrosine kinase inhibitors (i.e. erlotinib, gefitinib, crizotinib) were evaluated for their cytotoxic activity against the A549 cell line. Combination of erlotinib and fisetin at 1: 2 molar ratio, showed the highest synergism in cell killing, when analysed using the median effect principle method. This combination was then used to form a complex with SBE-β-CD. Further improvement in the solubility of erlotinib and fisetin, was achieved with the addition of 50% v/v ethanol during complexation, compared to using water alone. The complex solution was lyophilised and reconstituted into a 3-times more concentrated preparation, prior to nebulisation into the NGI. The preparation showed a suitable aerosol size for inhalation of both drugs. In conclusion, cyclodextrin-based formulations in the form of a dry powder inhalation and nebuliser solution, showed promise for pulmonary delivery of fisetin and its combination with erlotinib, respectively, in the treatment of non-small cell lung cancer (NSCLC).

Research Impact Statement

Lung cancer caused 1.69 million deaths globally in 2015, with 85-90% of the cases caused by non-small cell lung cancer (NSCLC). More than 65% of patients diagnosed with NSCLC are presented with locally advanced or metastatic disease, which is treated with chemotherapy. The chemotherapeutic agents are often delivered via oral or intravenous routes, which can expose the patients to unwanted systemic side effects. Therefore, the aim of this study was to develop formulations containing chemotherapeutic molecules, which can be delivered via the pulmonary route for the treatment of NSCLC.

This study will help in our understanding of the potential of cyclodextrin-based formulations for pulmonary delivery of chemotherapeutic molecules, which maybenefit the NSCLC patients, improving their quality of life. Pulmonary delivery of the agents to the lung may reduce the systemic side effects compared to oral and intravenous routes, as well as increasing the drug concentration at the site of action with lower doses. Since chemotherapy is very costly, lower doses in localised therapy will reduce the cost of the drug, giving an economic benefit to the health sector.

In academia, this study can be a platform for application to other drugs for pulmonary delivery (e.g. anti-asthmatic drugs), in the treatment of other lung-associated diseases, although further studies need to be undertaken to improve the understanding of the work (e.g. safety of the formulation in pulmonary delivery). Good networks can also be generated between academia and industry, by exchanging the skills and knowledge, if the formulations in this study were to be further developed into marketed products.

Table of Contents

Chapter 4   Production of dry powder fisetin-SBE-β-CD complex for inhalation

List of Tables

15

List of Figures

19

List of Abbreviations

AKT	=	Serine/threonine kinase
ALK	=	Anaplastic lymphoma kinase
ANOVA	=	Analysis of variance
ATP	=	Adenosine triphosphate
BCR-ABL	=	Breakpoint cluster region-Abelson
BCS	=	Biopharmaceutics classification system
CD	=	Cyclodextrin
CE	=	Complexation efficiency
CFC	=	Chlorofluorocarbon
CI	=	Combination index
DMSO	=	Dimethylsulfoxide
DPI	=	Dry powder inhaler
DPPH	=	2,2-diphenyl-1-picrylhydrazyl
DRI	=	Drug reduction index
DS	=	Degree of substitution
EDTA	=	Ethylenediaminetetraacetic acid
EF	=	Emitted fraction
EGCG	=	(-)-epigallocatechin gallate
EGFR	=	Epidermal growth factor receptor
EML4-ALK	=	Echinoderm microtubule-associated protein-like 4-anaplastic lymphoma kinase
ERK	=	Extracellular signal-regulated kinase
FDA	=	US Food and Drug Administration
FPD	=	Fine particle dose
FPF	=	Fine particle fraction
FT-IR	=	Fourier transform infrared spectroscopy
GSD	=	Geometric standard deviation
HGFR	=	Hepatocyte growth factor receptor
HP-β-CD	=	2-hydroxypropyl-β-cyclodextrin
HPLC	=	High performance liquid chromatography

IC$_{50}$	=	Concentration that reduces 50% of the absorbance (in DPPH assay)
	=	Concentration that kills 50% of the cell population (in MTT assay)
ICH	=	International Council for Harmonisation
K$_s$	=	Stability constant
LA	=	Locally advanced
LOD	=	Limit of detection
LOQ	=	Limit of quantification
MAPK	=	Mitogen-activated protein kinase
MB	=	Mass balance
MMAD	=	Mass median aerodynamic diameter
MOC	=	Micro-orifice collector
mTOR	=	Mammalian target of rapamycin
MTT	=	3-(4,5-dimethylthiazol-2-yl)-2,5-diphenyltetrazolium bromide
NF-κB	=	Nuclear factor kappa-light-chain-enhancer of activated B cells
NGI	=	Next Generation Impactor
NSCLC	=	Non-small cell lung cancer
Pe	=	Peclet number
PI3K	=	Phosphatidylinositol 3-kinase
PLGA	=	Poly(D,L-lactic-co-glycolic acid)
pMDI	=	Pressurized metered-dose inhaler
RE	=	Relative error
RPMI	=	Roswell Park Memorial Institute
RSD	=	Relative standard deviation
SBE-β-CD	=	Sulfobutylether-β-cyclodextrin
SCLC	=	Small cell lung carcinoma
SEM	=	Scanning electron microscope
TFA	=	Trifluoroacetic acid
TGA	=	Thermogravimetric analysis
TKI	=	Tyrosine kinase inhibitor
UV	=	Ultraviolet

VEGF	=	Vascular endothelial growth factor
VMD	=	Volume median diameter
X_{10}	=	Particle size at the undersize value of 10%
X_{50}	=	Particle size at the undersize value of 50% or volume median diameter
X_{90}	=	Particle size at the undersize value of 90%
XRPD	=	X-ray powder diffraction
α-CD	=	α-cyclodextrin
β-CD	=	β-cyclodextrin
γ-CD	=	γ-cyclodextrin

Chapter 1

Introduction

1.1 Lung cancer

Cancer is a disease characterised by the abnormal growth of cells that can invade other parts of the body and/or spread to other organs. In 2015, cancer was reported to cause 8.8 million deaths, contributing to nearly 1 in 6 deaths globally (WHO, 2017). The most common cause of cancer death globally is lung cancer, contributing to 1.69 million deaths. Lung cancer is defined as tumours arising from respiratory epithelium and can be divided into two groups, according to its major pathological distinctions, namely small cell lung carcinoma (SCLC) and non-small cell lung carcinoma (NSCLC). NSCLC is responsible for 85-90% of lung cancers, while a reduced frequency of SCLC has been seen in many countries (Novello et al., 2016). NSCLC can be further divided into 3 major cell types; squamous cell carcinoma, large cell carcinoma and adenocarcinoma (Johnson et al., 2014). The latter is the most common subtype, accounting for more than 50% of lung cancer cases (Pao and Girard, 2011).

a) Squamous cell carcinoma

The morphologic features of squamous cell carcinoma include intercellular bridging, squamous pearl formation and individual cell keratinization. Squamous cell carcinoma often arises in segmental bronchi, extending to lobar and mainstem bronchus (Travis, 2011).

b) Large cell carcinoma

The tumours of large cell carcinoma usually consist of sheets and nests of large polygonal cells with vesicular nuclei and prominent nucleoli. These tumours are centrally located, but are often found in the lung periphery. They frequently appear as large necrotic tumours (Travis, 2011).

c) Adenocarcinoma

The morphologic features of adenocarcinoma include acinar and papillary tumours, lepidic adenocarcinoma and solid and micropapillary tumours (Travis et al., 2015). In advanced lung adenocarcinoma, molecular testing for epidermal growth factor receptor (EGFR) mutation and anaplastic lymphoma kinase (ALK) rearrangement, is

further conducted to determine the suitability for personalised medicine using specific tyrosine kinase inhibitors.

1.1.1 Treatment of non-small cell lung cancer (NSCLC)

Treatment of NSCLC depends on the cancer stages, which can be simplified as shown in Table 1.1. In stage I to III, surgery is often performed to remove the malignant tissues followed by cisplatin-based chemotherapy, to prevent systemic relapse which is responsible for >70% of all recurrences (Reck et al., 2013). In the advanced metastatic stage, systemic platinum-based chemotherapy or personalised medicine, which targets specific tyrosine kinase receptors, are being used. At this stage, determination of the histological subtypes is important to decide the suitability of tyrosine kinase inhibitors in the therapy (Novello et al., 2016).

Table 1.1 Treatment of NSCLC (according to NICE Guidance (2011) and European Society of Medical Oncology; adapted from Novello et al., 2016 and Postmus et al., 2017).

NSCLC stage	Treatment
Early stages (Stage I and II)	*Surgery and systemic therapy* Surgery followed by adjuvant chemotherapy (post-resection) containing cisplatin-based combinations with drugs including vinorelbine, docetaxel, gemcitabine and pemetrexed. *Primary radiotherapy* Alternative to surgery for medically unfit patients or patients refusing surgery.
Locally advanced (LA) stage (Stage III)	*Resectable LA NSCLC* Surgery followed by adjuvant chemotherapy as in the treatment of early stages NSCLC. *Non-resectable LA NSCLC* Concurrent chemotherapy and radiotherapy.
Metastatic stage (Stage IV)	*EGFR and ALK-negative disease* Chemotherapy with platinum-based regimens and third generation cytotoxics (cisplatin/paclitaxel, cisplatin/gemcitabine, cisplatin/docetaxel, carboplatin/paclitaxel). *EGFR-mutation positive NSCLC patients* Treatment with EGFR TKI (erlotinib, gefitinib, afatinib). *ALK-rearrangement positive NSCLC patients* Treatment with ALK TKI (crizotinib).

NICE: National Institute for Health and Care Excellence, LA: locally advanced, NSCLC: non-small cell lung cancer, EGFR: epidermal growth factor receptor, ALK: anaplastic lymphoma kinase, TKI: tyrosine kinase inhibitor.

1.1.2 The role of chemotherapeutic agents in lung cancer

Until the late 1990s, platinum-based combination therapy was used in the treatment of advanced lung cancer, regardless of the histological subtype. The later introduction of a new generation of cytotoxic drugs (e.g. gemcitabine, docetaxel and paclitaxel) improved overall survival, until a plateau of efficacy was achieved (Reck et al., 2013). At this point, the use of the conventional chemotherapeutic drugs was not able to improve overall survival, until newer drugs that target different histological subtypes and driver mutations were introduced.

In the concept of driver mutation, mutation in the gene that encodes signalling proteins involved in cellular proliferation and survival, may drive tumour formation and maintenance. For instance, overexpression of EGFR tyrosine kinase caused by the mutation is a critical factor in the development of NSCLC tumours. This mutation has been detected in 10-15% of NSCLC (National Institute for Health and Care Excellence, 2015). The single-mutant oncogenes can then be identified and utilised with specific targeted agents (Pao and Girard, 2011). The advancement in the lung cancer histology, as shown in Figure 1.1, has made a more specific and targeted treatment possible. These therapies target tyrosine kinase with genomic alterations including epidermal growth factor receptor (EGFR) mutations and echinoderm microtubule-associated protein-like 4-anaplastic lymphoma kinase (EML4-ALK) rearrangements. This has led to the recommendation in current guidelines to conduct EGFR and ALK testing in patients with adenocarcinoma or mixed tumours with adenocarcinoma components (Johnson et al., 2014).

Tyrosine kinases are the enzymes that play critical roles in normal cellular regulatory processes, by catalysing the transfer of γ phosphate groups from adenosine triphosphate (ATP) to target proteins (Arora and Scholar, 2005). Mutation of these enzymes can cause increases in tumour proliferation and growth, inhibition of apoptosis, and promotion of angiogenesis and metastasis. Small molecule inhibitors of tyrosine kinase will compete with the ATP binding site of the oncogenic enzymes, halting the signal transduction pathways. The small molecule inhibitors are aimed at various tyrosine kinases responsible for different cancers, including the breakpoint

28

cluster region-Abelson (BCR-ABL; e.g. imatinib mesylate), EGFR (e.g. erlotinib) and vascular endothelial growth factor (VEGF; e.g. semaxinib) tyrosine kinases (Arora and Scholar, 2005). As the best oncogenic targets for management of advanced NSCLC are the EGFR and ALK tyrosine kinases (Reck et al., 2013), the next section will further discuss erlotinib, an EGFR tyrosine kinase inhibitor used in the study.
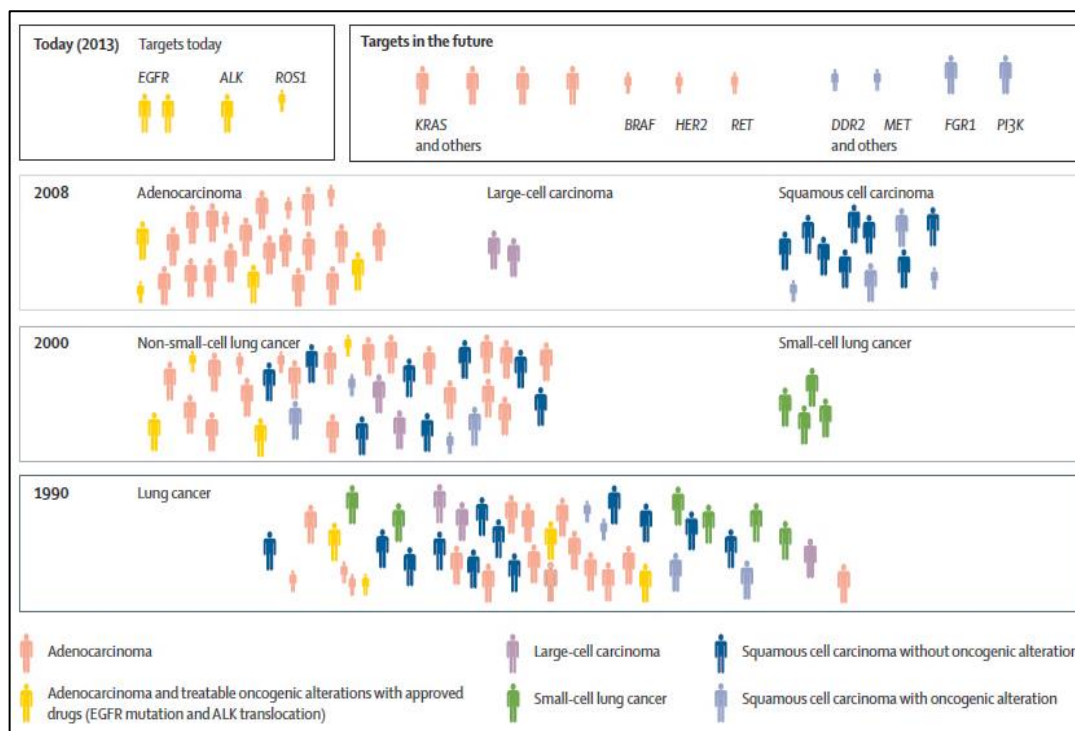
Figure 1.1 Development of lung cancer histology (Reck et al., 2013).

1.1.2.1 Erlotinib

Erlotinib or N-(3-ethynylphenyl)-6,7-bis(2-methoxyethoxy)-4-quinazolinamine is a reversible inhibitor of the EGFR tyrosine kinase, with a molecular weight of 393.44 g/mol (Figure 1.2). It is very poorly soluble in water, with reported aqueous solubility ~3-5 µg/mL (~7.6-12.7 µM) (Tóth et al., 2016; Truong et al., 2016). Erlotinib has a pH-dependent solubility; in its fully unionised form at pH 11, the log P octanol-water value is 2.75 and in its fully ionised form at pH 2, the log P value is 0.66 (Tóth et al., 2016).

Erlotinib has a low aqueous solubility and high permeability, such that the molecule is classified as Class II in the Biopharmaceutics Classification System

(BCS). Oral bioavailability of the drug is 59% and can be substantially improved, though highly variable, when administered with food (Frohna et al., 2006). As this could increase the risk of drug-related side effect (Iyer and Bhartuar, 2010), the drug is recommended to be taken on an empty stomach.
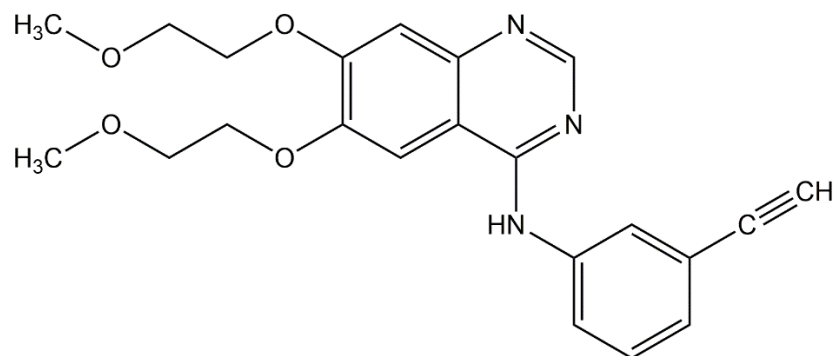
Figure 1.2 Chemical structure of erlotinib.

1.1.2.1.1 Formulation strategies for erlotinib

Erlotinib is currently available as a tablet (Tarceva®, Roche Products Ltd) in its hydrochloride form. In the UK, erlotinib is indicated for the treatment of locally advanced or metastatic NSCLC after failure of previous chemotherapy. It is also used as a monotherapy in the maintenance treatment of the disease, and in combination with gemcitabine in the treatment of metastatic pancreatic cancer (British National Formulary, 2017).

Erlotinib has been formulated into various pharmaceutical preparations to improve drug delivery, as shown in Table 1.2. The formulations include lipid-based nanoparticles, polymeric-based nanocarriers and water-soluble complexes, with most of them intended for cancer therapy.

Table 1.2 Formulation studies on erlotinib.

Formulation	Description	Intended treatment	Intended route of administration	Author
Lipid-based nanoparticles	Reverse micelle-loaded lipid nanocarrier	Pancreatic cancer	-	Vrignaud et al., 2012
	Co-encapsulation of erlotinib and doxorubicin in liposomes	Breast and lung cancer	Intravenous	Morton et al., 2014
	Co-encapsulation of erlotinib and doxorubicin in a pH-sensitive charge conversion nanocarrier, containing liposome-coated mesoporous silica nanoparticles	Non-small cell lung cancer	Intravenous	He et al., 2016
	Co-encapsulation of erlotinib and IL36α siRNA in amphiphilic lipid nanocarrier	Psoriasis	Topical	Boakye et al., 2017
	Anti-EGFR aptamer-conjugated chitosan-anchored liposomal complexes	Non-small cell lung cancer	-	Li et al., 2017b
	Co-encapsulation of oxygen and erlotinib by aptamer-modified liposomal complexes	Non-small cell lung cancer	Intravenous	Li et al., 2017a

Table 1.2 (cont.)

Formulation	Description	Intended treatment	Intended route of administration	Author
Lipid-based nanoparticles	Complexation of erlotinib with phospholipid	Pancreatic cancer	Oral	Dora et al., 2017
	PEGylated polypeptide lipid nanocapsules	Non-small cell lung cancer	Intravenous	Kim et al., 2017
	Liposomes modified with galactosylated lipid	Liver cancer	Intravenous	Xu et al., 2017
	Microparticles containing erlotinib-loaded solid lipid nanoparticles	Non-small cell lung cancer	Pulmonary	Bakhtiary et al., 2017
	Co-encapsulation of paclitaxel and erlotinib in solid lipid core nanocapsules with surface modification using PEG	Non-small cell lung cancer	-	Gupta et al., 2018
	Encapsulation of erlotinib in PEGylated liposomes	Non-small cell lung cancer	Intravenous	Zhou et al., 2018

Table 1.2 (cont.)

Formulation	Description	Intended treatment	Intended route of administration	Author
Polymeric-based nanocarriers	Poly(D,L-lactic-co-glycolic acid) (PLGA) nanoparticles	Non-small cell lung cancer	Oral	Marslin et al., 2009
	Embedding of erlotinib in a polymer matrix by using sub- or super-critical carbon dioxide	-	Oral	Jesson et al., 2014
	Lipid-polymer hybrid nanoparticles	Non-small cell lung cancer	Intravenous or pulmonary	Mandal et al., 2016
	Folate-conjugated thermosensitive O-maleoyl modified chitosan micellar nanoparticles	Ovarian cancer and non-small cell lung cancer	-	Fathi et al., 2017
	Embedding of erlotinib in a polyvinylpyrrolidone matrix using fat and supercritical fluid	Non-small cell lung cancer	Oral	Yang et al., 2017
	Co-encapsulation of erlotinib and doxorubicin in a poly(L-lactide)-b-polyethylene glycol (PLA-b-PEG) nanoparticles	Breast cancer	Intravenous	Zhou et al., 2017

Table 1.2 (cont.)

Formulation	Description	Intended treatment	Intended route of administration	Author
Water-soluble complexes	Complexation of erlotinib with HP-β-CD	Epidermoid carcinoma	Oral	Gontijo et al., 2015
	Complexation of erlotinib with SBE-β-CD	-	Oral	Devasari et al., 2015
	Cyclodextrin-based nanosponge complex	Pancreatic cancer	Oral	Dora et al., 2016
	Cyclodextrin complexes	-	-	Tóth et al., 2016
	Glutathione nanosponge	Non-small cell lung cancer	Intravenous	Momin et al., 2018
Others	Adsorption of erlotinib on gold nanoparticles	Non-small cell lung cancer	-	Lam et al., 2014
	Erlotinib-conjugated iron-oxide nanoparticles	Theranostic purpose in cancer treatment	Intravenous	Ali et al., 2016
	Solid self-emulsifying formulation	-	Oral	Truong et al., 2016
	Albumin nanoparticles	Pancreatic cancer	Intravenous	Noorani et al., 2017

Taking its hydrophobicity into consideration, a lipid-based system may be suitable as a carrier for erlotinib. Formulation of erlotinib in a reverse micelle-loaded lipid nanocarrier has been shown to maintain the cytotoxic activity of the drug against pancreatic human adenocarcinoma cell line (Vrignaud et al., 2012). Further, lipids such as cationic amphiphilic pyrrolidinium, has been used to enhance transdermal permeation of erlotinib. Nanocarriers made of the lipid, loaded with erlotinib and interleukin 36α siRNA, successfully delivered both drugs transdermally for the treatment of psoriasis in a mouse model (Boakye et al., 2017). Erlotinib has also been loaded into solid lipid nanoparticles which has shown to enhance its cytotoxicity against the human adenocarcinoma cell line (A549) compared to the free drug (Bakhtiary et al., 2017). The nanoparticles were further spray-dried in the presence of mannitol to produce microparticles with a reasonable fine particle fraction (FPF) of 30.98%. Complexation of erlotinib with phospholipid showed a higher cytotoxic and apoptotic activity against human pancreatic adenocarcinoma cell lines compared to free erlotinib (Dora et al., 2017). The complex showed a higher bioavailability in rats and less toxicity towards liver and renal in mice compared to the free drug.

Several lipid nanocarriers containing erlotinib were modified for targeting purposes. An anti-EGFR aptamer, a nucleic acid used to formulate targeted drug delivery system, was conjugated with chitosan prior to the anchoring with erlotinib-containing liposomes. The formulation enhanced erlotinib accumulation and induced more cycle arrest and apoptosis in a resistant lung cancer cells (H1975) (Li et al., 2017b). Co-delivery of erlotinib and oxygen in the carrier has also shown to overcome hypoxia-induced drug resistance in lung cancer cell lines with different EGFR gene status, i.e. A549, H1975 and PC-9 (Li et al., 2017a). Further, surface modification using β-D-galactose could mediate specific binding of liposomes with hepatocytes (Xu et al., 2017). The carrier has been shown to increase biodistribution of erlotinib in the liver which may help targeted delivery of the drug in the treatment of liver cancer.

Utilisation of polyethylene glycol (PEG) in surface modification of polypeptide lipid nanocapsule has been shown to effectively controlled the release of erlotinib from the nanocapsule core while showing a higher tumour regression in HCC-

827 xenograft tumour mice model (Kim et al., 2017). An increase in the cytotoxicity of erlotinib and paclitaxel combination in NCI-H23 cell line has also been shown in PEGylated solid lipid core nanocapsules (Gupta et al., 2018). PEG also has the ability to prolong circulation of liposomes which resulted in an increase in the erlotinib bioavailability in rats compared to the non-PEGylated liposomes (Zhou et al., 2018).

An amphiphilic lipid-based nanocarrier can also be utilised to co-encapsulate erlotinib and another hydrophilic drug. Incorporation of both drugs in different regions of the carrier, may enable a sequential release of each molecule. In one study, erlotinib was loaded into liposomes which were then used to coat amino-functionalised silica nanoparticles containing doxorubicin (He et al., 2016). The same drug combination was also loaded into the hydrophilic and hydrophobic regions of liposomes (Morton et al., 2014). In both studies, a staggered release of erlotinib followed by doxorubicin was achieved, potentially allowing a synergistic killing activity against different types of cancer cell lines, including lung and breast cancers.

Other than lipid nanocarriers, polymeric nanoparticles offer several advantages for the delivery of erlotinib. This type of carrier has been shown to improve the relative solubility of erlotinib (Jesson et al., 2014), and further improved bioavailability and reduced fed-fasted bioavailability variances of the drug (Yang et al., 2017). A lipid-polymeric hybrid nanoparticle can also provide mechanistic stability of the polymeric core and biomimetic properties of the lipid layer (Mandal et al., 2016). This formulation resulted in 25-fold decrease in the half maximal inhibitory concentration (IC_{50}) of erlotinib against the A549 cell line. Further, polymeric nanoparticles allowed slow release of erlotinib over time, which has been shown to reduce the sub-acute toxicity related to the drug (Marslin et al., 2009). The erlotinib-loaded PLGA nanoparticles produced no change in haematological, biochemical and histopathological profiles, after 4 weeks of oral treatment in rats.

The small size of the nanoparticles can be an advantage as they can extravasate the leaky vascular structure of newly blood vessels around the tumour and be trapped inside. Intravenous delivery of polymeric nanoparticles (~80 nm) containing erlotinib and doxorubicin had shown an increase in the retention time of the particles in breast

tumour in mice (Zhou et al., 2017). A targeted delivery of polymeric nanoparticles has also been studied in micelles made of folate-conjugated modified chitosan (Fathi et al., 2017). The preparation showed targeting of erlotinib in folate-positive cells (OVCAR-3), improving its cytotoxicity when compared to non-targeted micelles.

Complexation with water-soluble molecules (e.g. cyclodextrin) is another strategy to improve the solubility of erlotinib. β-cyclodextrin and its derivatives, including hydroxypropyl-β-cyclodextrin (HP-β-CD) and sulfobutylether-β-cyclodextrin (SBE-β-CD), were the most suitable hosts to enhance erlotinib's solubility (Tóth et al., 2016). As drug dissolution in the gastro-intestinal medium is the rate-limiting step for oral absorption, an improvement in the drug solubility will lead to an increase in the oral bioavailability. An improvement in bioavailability has been shown when erlotinib was complexed with SBE-β-CD (Devasari et al., 2015) and a cyclodextrin-based nanosponge (Dora et al., 2016). Inclusion of erlotinib into HP-β-CD had shown to maintain the anti-angiogenic activity of the drug against human epidermoid carcinoma cells (A431) compared to free erlotinib (Gontijo et al., 2015). Further, erlotinib activity could also be improved by using a glutathione cyclodextrin-based nanosponge. Targeting ability of glutathione linkage to lung tumour tissue in such formulation has been shown to increase erlotinib concentration in the tissue while minimising the distribution to other organs (Momin et al., 2018).

Erlotinib has also been incorporated into other carrier systems including a self-emulsifying formulation. This formulation was able to spontaneously form an oil-in-water emulsion upon aqueous dilution under gentle agitation in the gastrointestinal tract; thus, improving the oral bioavailability of erlotinib in rats (Truong et al., 2016). Further, gold nanoparticles (AuNPs) is another carrier which offers advantages such as low toxicity and biocompatibility. Erlotinib has been shown to efficiently adsorb onto the AuNPs and completely desorb from the nanoparticles inside NSCLC cell lines (Lam et al., 2014). Encapsulation of erlotinib in albumin nanoparticles (ANP) has been shown to facilitate pancreatic tumour targeting through albumin-receptor-mediated active transcytosis (Noorani et al., 2017). An improvement in erlotinib toxicity was seen in the ANP formulation compared to the free drug. In another study, erlotinib has been conjugated with iron oxide nanoparticles as a small molecule targeting agent (Ali

et al., 2016). The nanoparticles exhibited a theranostic (therapeutic and diagnostic) capabilities which can target cancer cells with overexpression of EGFR (i.e. CL1-5-F4) and could be monitored by magnetic resonance imaging (MRI) in xenograft-bearing mice. The above-mentioned formulation strategies highlight that extensive studies have been done to improve the delivery of erlotinib. In most cases, the formulation was intended for oral and intravenous administration, with the aim of improving the drug bioavailability or to reduce its systemic toxicity. In the case of NSCLC, pulmonary delivery of erlotinib may be an approach that can be explored to overcome bioavailability and systemic toxicity issues related to erlotinib, and directly target the cancer cells.

1.1.3 The role of phytochemicals in lung cancer

Apart from the standard pharmacological treatments, increasing attention is being given to the role of phytochemicals (e.g. flavonoids) in lung cancer therapy (Khan and Mukhtar, 2015). These compounds are commonly found in dietary plants, such as green tea (e.g. (-)-epigallocatechin gallate, EGCG), soybean (e.g. genistein), turmeric (e.g. curcumin), fruits and vegetables (e.g. fisetin). These compounds have shown cytotoxic activity against various lung cancer cell lines (Khan et al., 2012; Lev-Ari et al., 2014), and have also shown inhibition on lung metastases (Menon et al., 1998; Liu et al., 2012). The next section will discuss the physicochemical properties and formulation approaches for delivering fisetin, a flavonoid used in the study.

1.1.3.1 Fisetin

Fisetin or 3, 3', 4', 7-tetrahydroxyflavone (Figure 1.3) is a flavonoid that can be found in different fruits and vegetables including strawberry, apple, cucumber and onion (Khan et al., 2013). Fisetin is a hydrophobic molecule, with a molecular weight of 286.24 g/mol and log P octanol-water value ~3.2 (Mignet et al., 2012). It has a low solubility in water (< 1 mg/mL) and poor solubility in ethanol (< 14 mg/mL) (Ragelle et al., 2012).
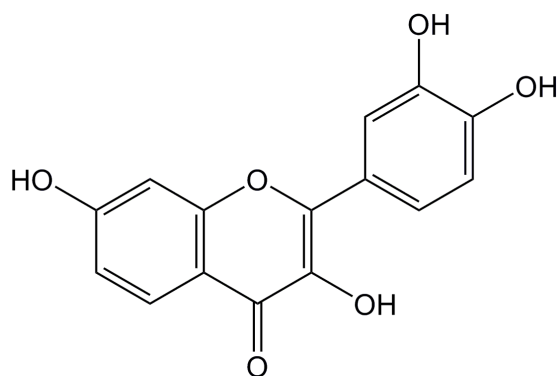
Figure 1.3 Chemical structure of fisetin.

1.1.3.1.1 Formulation strategies for fisetin

The low aqueous solubility of fisetin has been a hindrance to its formulation and delivery, thus leading to a number of formulation approaches aiming to improve its solubility and bioavailability (Table 1.3). The intraperitoneal bioavailability of fisetin has been shown to improve by 24- and 141-fold when administered in a nanoemulsion (Ragelle et al., 2012) and nanocochleate (Bothiraja et al., 2014) formulation, respectively. The nanocochleate structure, consisting of multi-layered solid-lipid bilayers in the form of a sheet rolled up in a spiral shape, also provides a sustained release of fisetin as the system slowly unwinds or dissociates.

Liposomes has been used as a carrier for fisetin, and following encapsulation in the carrier, fisetin has been shown to retain its biological activity against lung and colon carcinoma cell lines (Mignet et al., 2012). When administered intraperitoneally, the formulation showed an increase in relative bioavailability of fisetin by 47-fold and a slowing of the lung carcinoma growth in mice (Seguin et al., 2013).

Table 1.3 Formulation studies on fisetin.

Formulation	Intended treatment	Intended route of administration	Author
Nanoemulsion	Lung carcinoma	Intraperitoneal	Ragelle et al., 2012
Nanocochleate	Breast cancer	Intraperitoneal	Bothiraja et al., 2014
Liposome	Lung carcinoma and colon cancer	-	Mignet et al., 2012
Liposome	Lung carcinoma	Intraperitoneal	Seguin et al., 2013
α- and β-cyclodextrin complexes	-	-	Guzzo et al., 2006
γ-cyclodextrin complex	-	Parenteral	Pahari et al., 2013
β- and γ-cyclodextrin complexes	Cervical and breast cancer	-	Zhang et al., 2015
β-cyclodextrin and its derivatives complexes	Liver tumour	-	Sali et al., 2018
Cyclosophoroase dimer complex	Cervical adenocarcinoma	-	Jeong et al., 2013

Another strategy of improving the solubility of fisetin is by complexation with soluble organic compounds. Fisetin has been shown to form stable complexes with β-cyclodextrin (Guzzo et al., 2006) and γ-cyclodextrin (Pahari et al., 2013), which was confirmed by the molecular interactions of fisetin in the cavity of both cyclodextrins. Inclusion of fisetin into both cyclodextrins resulted in a better aqueous solubility and improved cytotoxic activity against human cervical and breast cancer cell lines (Zhang et al., 2015). As for β-cyclodextrin, a better aqueous solubility of fisetin was achieved when complexed with chemically-modified β-cyclodextrins, such as hydroxypropyl-β-cyclodextrin (HP-β-CD), compared to the native β-cyclodextrin (Sali et al., 2018).

The cytotoxic activity of fisetin against a liver tumour cell line was not affected for these complexes. Further, a novel cyclosophoroase dimer which was synthesized using cyclosophoroase, an epoxypolysaccharide produced by bacteria from the *Rhizobiaceae* family, was also used to form a complex with fisetin (Jeong et al., 2013). The complex showed a better solubility of fisetin when compared to β-cyclodextrin complex and a higher cytotoxic activity against a human cervical adenocarcinoma cell line.

Most of the formulations outlined above were intended for parenteral administration. None have yet explored the application of fisetin formulations for other routes such as by inhalation, which may be useful for a localised delivery of fisetin in the treatment of lung cancer.

1.1.4 Combination of chemotherapeutic agents and phytochemicals

In cancer therapy, combination of two or more agents is often employed to target different mechanisms or pathways to enhance efficacy. The same approach can also be used by combining chemotherapeutic agents and phytochemicals, resulting in an enhancement in the anti-proliferative and apoptotic effect of each molecule against cancer cells. The enhancement can be achieved by pre-treating the cells with the phytochemicals prior to the treatment with chemotherapeutic drug (Li et al., 2005c) or simultaneous treatment with both molecules (Gadgeel et al., 2009; Lev-Ari et al., 2014). Synergism in the killing activity may allow treatment using lower doses of both molecules, resolving the problem of dose-dependent side effects.

Further, multiple site targeting can also be used in the treatment of drug-resistant cell lines. Phytochemicals have been shown to cause re-sensitisation of resistant cells towards treatment with drugs such as cisplatin (Lev-Ari et al., 2014; Zhuo et al., 2015) and erlotinib (Milligan et al., 2009; Zhang et al., 2016). As erlotinib and fisetin were used in the study, the combination of both drugs with other agents will be discussed in the next section.

1.1.4.1 Combination of erlotinib and phytochemicals

Combination of erlotinib and flavonoids has attracted attention for providing synergistic activity in cancer treatment. Combination of erlotinib and a soy isoflavone (genistein) has been tested against various cell lines, including pancreatic cancer (El-Rayes et al., 2006) and NSCLC with EGFR mutation (Gadgeel et al., 2009). Potentiation and synergy of the cytotoxic activity were associated with down-regulation of EGFR by erlotinib and inhibition in the nuclear factor kappa-light-chain-enhancer of activated B cells (NF-κB) activity by genistein, which transcribes genes for cancer cell survival, invasion and metastasis.

Flavonoids have also been shown to reverse acquired erlotinib-resistance in NSCLC cell lines. Fisetin has been shown to cause reversal of erlotinib-resistance through inactivation of mitogen-activated protein kinase (MAPK) and protein kinase B (also known as Akt) pathway, and suppression of survivin (an anti-apoptotic signalling protein) expression (Zhang et al., 2016). A synergistic killing activity against erlotinib-resistant cell lines was also shown in a combination treatment of erlotinib and ampelopsin (a dietary flavonoid from *Ampelopsis grossedentata*). The cell death was induced by a signaling pathway related to reactive oxygen species (Hong et al., 2017).

1.1.4.2 Combination of fisetin and chemotherapeutic agents

In recent years, fisetin has attracted interest as many studies have shown its anti-carcinogenic effect on different cancer cell lines including lung, colon and prostate cancers. It has specifically shown anti-proliferative, apoptotic and anti-oxidant activities, as well as anti-inflammatory and neuroprotective activities (Khan et al., 2013).

Fisetin has shown benefit in combination therapy with other anti-cancer agents. It works synergistically by increasing the cytotoxicity of chemotherapeutic agents, such as cisplatin (Tripathi et al., 2011) and cyclophosphamide (Touil et al., 2011), at low doses. Enhancements in the anti-angiogenic and anti-tumour activities of the drugs were shown in embryonal and lung carcinoma xenograft models.

Fisetin can also work as an adjunct in cancer therapy to alleviate specific side effects related to a cytotoxic agent or other therapy. Fisetin has shown protection against ovariectomy-induced bone loss in mice via its anti-inflammatory activity, which caused repression of osteoclast differentiation process (Léotoing et al., 2013). Pre-treatment with fisetin has also shown a renoprotective effect in cisplatin-induced nephrotoxicity in rats, without altering cisplatin uptake in kidney tissue (Sahu et al., 2014). The renoprotection was associated with its free radical scavenging and strong anti-oxidant properties.

1.1.4.3 Proposed mechanism of action of erlotinib and fisetin combination in lung cancer

Erlotinib and the TKIs specifically target the mutated tyrosine kinases, including mutation in the EGFR (target for erlotinib and gefitinib) and rearrangement of the EML4-ALK (target for crizotinib). Inhibition of the enzyme will supress the downstream signalling pathway which will halt the progression of the cancer (Figure 1.4). The pathway can be divided into two parts; the pro-survival arm involving the PI3K-Akt, and the proliferative arm comprising the Ras-Raf-ERK pathway (Sharma et al., 2007).

A rational approach to enhance the cytotoxic activity of erlotinib is to combine the drug with an agent that inhibits activation of other sites in the signalling pathway. Fisetin has been shown to act at various sites of the pathway, including inhibition in the phosphorylation of Akt and mTOR (Khan et al., 2012). Inhibition of the mTOR alone can activate a negative feedback loop, by activating the Akt through the upregulation of the receptor tyrosine kinase. However, dual inhibition of fisetin on PI3K-Akt and mTOR signals in the A549 cell line helps to keep the feedback loop in check (Khan et al., 2012). Further, suppression on activation of the ERK-1 and ERK-2 signals in the A549 cell line has been shown to contribute to fisetin's ability to inhibit cell invasion and migration in metastatic process (Liao et al., 2009).

```
                          Tyrosine kinase

         PI3K                                    RAS

                                                  |

                                                 RAF

         AKT ———————— mTOR ———— MAPK/ERK

          ↓              ↓              ↓

     Cell survival   Protein synthesis   Cell growth
```
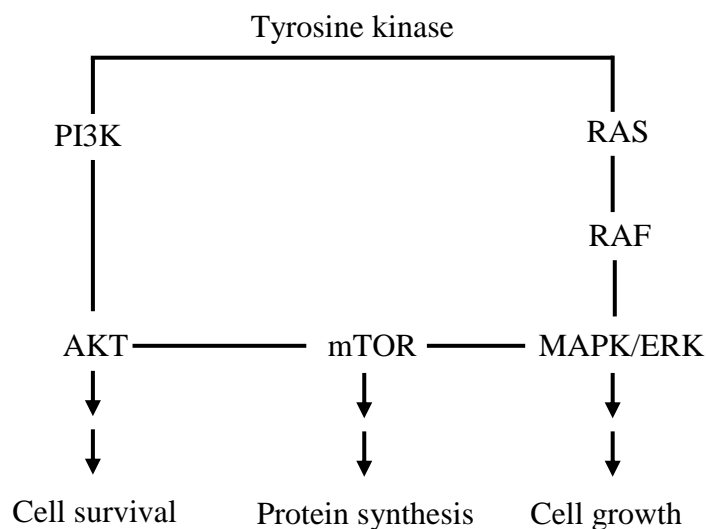
Figure 1.4 Cell survival pathways downstream of activated receptor tyrosine kinase (adapted from Sharma et al., 2007; Landi and Cappuzzo, 2014). PI3K, phosphatidylinositol 3-kinase; AKT, serine/threonine kinase; mTOR, mammalian target of rapamycin; MAPK, mitogen-activated protein kinase; ERK, extracellular signal-regulated kinase.

Other than the mentioned mechanisms, fisetin inhibits cell proliferation and tumour development in *in vivo* lung cancer models, through its anti-oxidative mechanism (Ravichandran et al., 2011). The effect was more pronounced when fisetin was used as a chemopreventive, rather than a chemotherapeutic agent. Therefore, targeting of erlotinib and fisetin to multiple sites in the cancer cell signalling pathway, may provide a synergistic activity against the lung cancer cells and may also cause re-sensitisation of erlotinib-resistant lung cancer cell lines.

1.2   Delivery of hydrophobic drugs

According to the Biopharmaceutics Classification System (BCS), drug substances can be classified based on their aqueous solubility and intestinal permeability (Amidon et al., 1995). Drugs in Class II and IV have poor aqueous solubility, which may hinder their oral absorption and leads to poor oral bioavailability. Approximately 75% of new chemical entities have low aqueous solubility and are classified as BCS Class II and IV molecules (Di et al., 2012). In local treatment, such as via inhalation, absorption

may not be the main concern if the drug is not intended for systemic delivery. Although hydrophobicity is beneficial for tissue uptake of the drug, solubilisation and stabilisation of the agent can be a problem at the formulation stage.

The solubility and dissolution rate of a drug can be improved via physical and chemical modifications, such as micronisation, salt formation (Li et al., 2005b) and co-crystallisation (Basavoju et al., 2008). Another strategy is to incorporate the drug into a range of nanocarriers (e.g. liposome, cyclodextrin complex and nanoemulsion), which can improve the drug delivery and may offer other advantages. Coating of the liposomes with folate and polyethylene glycol has been shown to help tumour targeting while prolonging the circulation of erlotinib (Morton et al. 2014). Further, an improvement in the oral bioavailability of drugs has been reported with a cyclodextrin complex (Ren et al., 2014) and a nanoemulsion preparation (Shen et al., 2011).

The next section will focus on inclusion complexation with cyclodextrins, which was used to improve the solubility of erlotinib and fisetin in the study.

1.2.1   Inclusion complexation with cyclodextrins

Cyclodextrins are cyclic oligosaccharides produced by the activity of a bacterial enzyme (*cyclomaltodextrin glucanotransferase*) on starch. The most common marketed cyclodextrins contain six (α-cyclodextrin), seven (β-cyclodextrin), and eight (γ-cyclodextrin) (α-1,4)-linked α-D-glucopyranose units (Table 1.4). β-cyclodextrin is the most commonly used cyclodextrin as it has a good 'fit' with many compounds used in various applications, including pharmaceutical and cell culture (Caligur, 2008). This is mainly because the small cavity of α-cyclodextrin limits the size of the guest molecule and the larger cavity of γ-cyclodextrin prevents an effective interaction between the cavity and the guest molecule to facilitate the complexation. However, β-cyclodextrin has the poorest aqueous solubility compared to the other two cyclodextrins and causes adverse effects including nephrotoxicity, if given parenterally. Substitution of multiple hydroxyl groups on the β-cyclodextrin with hydroxypropyl and sulfobutylether groups (Table 1.4), improves the aqueous solubility and toxicological profile of the parent cyclodextrin molecule (Kurkov and Loftsson, 2013).

45

Table 1.4 Structural and physicochemical properties of selected cyclodextrins (adapted from Brewster and Loftsson, 2007).
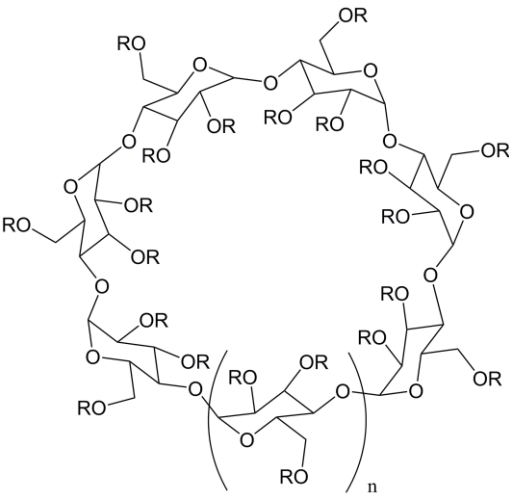
Cyclodextrin	n	R	MW[a] (Da)	Solubility in water[b] (mg/mL)
α-cyclodextrin (α-CD)	0	–H	972	145
β-cyclodextrin (β-CD)	1	–H	1135	18.5
2-hydroxypropyl-β-cyclodextrin (HP-β-CD)	1	$-CH_2CHOHCH_3$	1400	>600
Sulfobutylether-β-cyclodextrin sodium salt (SBE-β-CD)	1	$-(CH_2)_4SO_3^-\,Na^+$	2163	>500
γ-cyclodextrin (γ-CD)	2	–H	1297	232

[a] MW: molecular weight
[b] Solubility in pure water at approximately 25°C

The cyclodextrin molecule has a truncated cone structure, due to the chair conformation of the glucopyranose unit (Figure 1.5). Orientation of the hydroxyl groups on the cone exterior and positioning of the skeletal carbons and the oxygens in the central cavity, produces a molecule with a hydrophilic exterior and a hydrophobic cavity (Brewster and Loftsson, 2007). Complexation of a cyclodextrin and a drug molecule occurs in the form of an inclusion complex or host-guest complex (Figure 1.5). The hydrophobic molecule, with an appropriate size, will act as a guest and enter the lipophilic cavity of cyclodextrin, which act as a host to form a non-permanent inclusion complex. The complex depends on the dimensional fit between the host and

the guest without formation or breakage of covalent bonds (Del Valle, 2004). Further, the complex formation involves physical interactions including van der Waals', electrostatic, hydrophobic and charge-transfer interactions (Loftsson et al., 2005b). The ability to form soluble complexes makes cyclodextrin a useful complexing agent for lipophilic drugs, as it can improve the stability and bioavailability of the drug (Brewster and Loftsson, 2007). The next section will discuss the SBE-β-CD, a cyclodextrin used in the study.
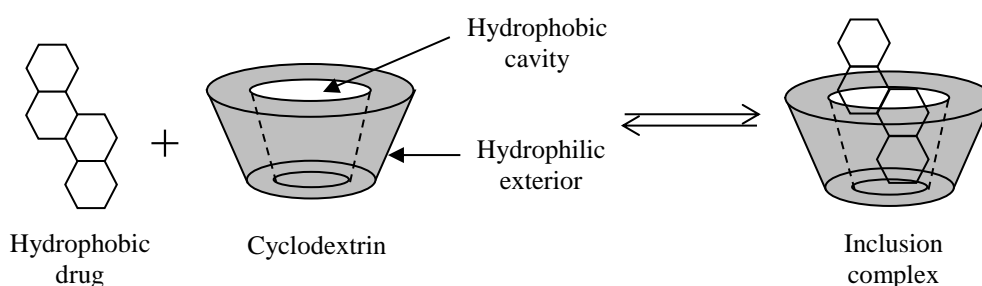
Figure 1.5 Schematic drawing of drug-cyclodextrin complex formation (adapted from Loftsson and Brestwer, 2012).

1.2.1.1 Sulfobutylether-β-cyclodextrin (SBE-β-CD)

SBE-β-CD is a modified β-CD which has been approved by the US Food and Drug Administration (FDA) as a pharmaceutical excipient. It has been used as a solubilizing or complexing agent in formulations for several routes of administration including parenteral, oral and pulmonary.

A number of studies have highlighted the benefit of using SBE-β-CD as a solubilising agent, to eliminate the side effects related to some parenteral formulations. In one study, SBE-β-CD was used as a solubilising agent for an etomidate preparation (McIntosh et al., 2004). The IV administration of the formulation was compared with Amidate® (a commercial etomidate product with propylene glycol as a co-solvent) in beagle dogs. The SBE-β-CD formulation showed similar pharmacokinetic and pharmacodynamic behaviour, but with a 10-fold reduction in *in vivo* haemolysis compared to Amidate®. This study suggested the SBE-β-CD formulation of etomidate can be used as an alternative to diminish the propylene glycol-related side effects of

Amidate®. In another study, a preparation containing propofol in SBE-β-CD was compared with the marketed propofol lipid emulsion (Diprivan®) in a porcine model (Egan et al., 2003). IV infusion of the SBE-β-CD formulation exhibited similar pharmacokinetic and pharmacodynamic behaviour as Diprivan®. Therefore, the authors suggested that the SBE-β-CD formulation may be a suitable alternative to Diprivan® to reduce the lipid emulsion-related side effects (e.g. pain on injection and allergic reaction). However, the following investigation on healthy human volunteers showed that the preparation failed to reduce the pain on injection related to propofol (Wallentine et al., 2011).

Different formulations of drug-SBE-β-CD complexes have also been studied and compared with oral marketed products. An oral preparation of aprepitant-SBE-β-CD complex was reported to enhance the solubility of the drug (Ren et al., 2014). The SBE-β-CD-containing formulation showed a better solubility and dissolution rate, with a comparable bioavailability to Emend® (a marketed aprepitant capsule). In another study, complexation of amiodarone hydrochloride with SBE-β-CD enhanced the solubility and dissolution of the drug (Wang et al., 2017). Oral administration of the complex was shown to diminish the food-effect, leading to an unaltered pharmacokinetic profile in a fasted state, when compared to the commercial amiodarone tablet (Cordarone®).

Pulmonary delivery of SBE-β-CD formulations has been investigated for the treatment of lung infections. Nebulisation of a marketed intravenous formulation of voriconazole-SBE-β-CD (Vfend®) was studied for prevention of invasive pulmonary aspergillosis (Tolman et al., 2009). The aerosolised formulation showed an improved survival, fewer signs of invasive disease and better histological findings in a murine model, compared to the intraperitoneal administration of amphotericin B. In one study, a dry powder inhalation of rifampicin-loaded phospholipid lipospheres containing SBE-β-CD and vitamin C, was produced (Singh et al., 2015). The preparation showed a better aerosolisation performance and *in vitro* anti-tuberculotic activity, compared to the formulation without SBE-β-CD. The improvement in the anti-tuberculotic activity was associated with the removal of cholesterol from the cell membrane by the SBE-β-CD, reducing available nutrients for the cells, thus causing cell death.

1.2.1.2 Cyclodextrin formulations and safety in pulmonary delivery

Studies on complexation of drugs with different types of cyclodextrins have been conducted with several formulations reaching the pharmaceutical market. These complexes are available for many routes of administration including oral (e.g. Sporanox®, Nimedex®), intravenous (e.g. Vfend®, Mitozytrex®), intramuscular (e.g. Abilify®, Geodon®), sublingual (e.g. Nicorette®, Nitropen®) and intranasal (e.g. Aerodiol®) (Kurkov and Loftsson, 2013), though none has yet been marketed for inhalation (EMA, 2017). Pulmonary drug delivery can be a practical route for local treatment of lung-related diseases (e.g. asthma, chronic obstructive pulmonary disease, lung cancer), although it can also be employed for systemic delivery, due to the large absorptive surface area, high blood flow, low enzymatic activity and avoidance of first-pass metabolism (Ibrahim et al., 2015).

Utilisation of cyclodextrin to increase the solubility of an insoluble drug can give advantages of increased drug absorption, faster onset of action and decreased clearance. Cyclodextrins are readily absorbed from the lung; the rate of absorption varies between different cyclodextrins with one study reporting HP-β-CD as the best candidate as a drug carrier for sustained pulmonary delivery (Cabral Marques et al., 1991). In general, cyclodextrins that are considered to be the safest for parenteral formulations (i.e. γ-CD, HP-β-CD and SBE-β-CD) are also considered safe for pulmonary application (Loftsson et al., 2005b). γ-CD has been shown to be the safest among the natural cyclodextrins (α- and β-CD) in a study using human bronchial adenocarcinoma-derived Calu-3 cells (Matilainen et al., 2008). Further, hydroxyalkylation of the hydroxyl group on α- and β-CD, has been shown to make the molecules safer than the parent cyclodextrins.

1.3 Pulmonary drug delivery

The lungs are the primary organs of the respiratory system in humans, which are responsible for the gas exchange in the body. The lungs can be divided into two main parts (Figure 1.6); the conducting airways (consist of trachea, bronchi and bronchioles) and the sac-like alveoli (Patton and Byron, 2007). The alveoli, where the gas exchange takes place, have a large surface area of more than $100m^2$.
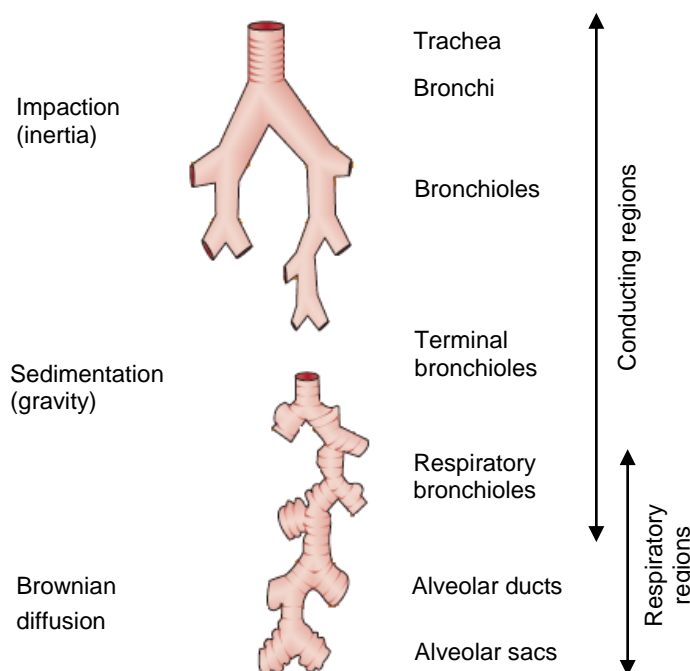
Figure 1.6 Predominant mechanisms of particle deposition in the human airways (adapted from Patton and Byron, 2007).

The pulmonary route has been used to deliver drugs for effective local therapy (e.g. asthma, chronic obstruction pulmonary disorder) and systemic delivery (e.g. proteins, peptides). The drug formulation is delivered in the form of solid or liquid aerosols, with a high surface area to volume ratio. However, the efficacy of therapeutic aerosols depends on the ability for droplets or particles to be deposited in the peripheral airways. The main mechanisms involved in the deposition of inhaled particles in lungs are impaction, sedimentation and diffusion (Lippman et al., 1980; Patton and Byron, 2007). In the upper airways, the change in the direction of the airstream causes impaction of larger particles (> 5 µm) on the airways' wall. Impaction is driven by the inertial force, causing particles to break free from the airstream. The smaller particles (1-5 µm), which escape impaction, are then removed from the airstream by gravitational sedimentation. This mechanism is important in small airways with low air velocity, including the bronchioles and alveolar spaces. Particles of < 0.5 µm will undergo Brownian diffusion, which is a random motion caused by impaction of

submicron particles with gas molecules in the respiratory tract. The collision will cause the particles to move out from the airstream and deposit on the wall of small airways and alveoli.

1.3.1 Aerodynamic diameter in pulmonary drug delivery

In the development of inhalation products, certain parameters are critical to ensure optimal delivery of the drug to the deep lung region. The most important parameter is the particle's aerodynamic diameter which is defined as the diameter of an equivalent unit density sphere with the same terminal settling velocity as the investigated particle (Telko and Hickey, 2005). An optimum aerodynamic diameter to reach the lower respiratory tract is between 0.5 and 5 µm as particles larger than 5 µm will tend to deposit in the oropharynx and upper airways. On the other hand, particles smaller than 0.5 µm will be influenced by Brownian motion causing a very slow deposition of the particles or they may not deposit at all (Pilcer and Amighi, 2010).

The aerodynamic diameter (d_a) of particles is influenced by the density and shape of the particles as shown in the following equation;

$$d_a = d_{geo}\sqrt{\frac{\rho_p}{\rho_0\chi}} \qquad\qquad \text{Eq 1.1}$$

where d_{geo} is the physical diameter of the particle, ρ_p is the particle density, ρ_0 is the unit density, and χ is the dynamic shape factor. The dynamic shape factor is the ratio of the actual resistance force of a non-spherical falling particle to the resistance force of a sphere with the same volume (Pilcer and Amighi, 2010). Based on the equation, a smaller aerodynamic diameter can be achieved by decreasing the particle size, decreasing the particle density and/or increasing the dynamic shape factor.

One strategy in designing aerosol particles is to create low density particles with relatively large geometric sizes. In one study, smaller non-porous particles were compared to larger porous particles, having a nearly identical aerodynamic diameter (Edwards et al., 1997). The latter showed a higher respirable fraction, possibly attributed to their smaller surface-to-volume ratio, leading to less aggregation during the aerosolisation. This led to a better systemic absorption of insulin and testosterone

in rats. Further, the shape of the particles also has a strong effect on particle behaviour. Pollen-shaped particles have shown better flowability, aerosolisation and deposition properties compared to other shapes including sphere, needle, cube and plate (Hassan and Lau, 2009). Although particles of all shapes had a higher dynamic shape factor compared to the spherical particles, the surface feature of the pollen-shaped particles increased the distance between two interacting particles, reducing the contact surface. The low inter-particulate force led to less particle aggregation, resulting in improved emitted dose and fine particle fraction.

1.3.2 Delivery devices

Devices used in the pulmonary delivery can be divided into three broad types; the nebulisers, dry powder inhalers (DPIs) and pressurised metered-dose inhalers (pMDIs). This section will be focusing on the nebulisers and DPIs, as they were the devices used in the study.

1.3.2.1 Nebulisers

Nebulisers are devices that convert a solution or suspension into small droplets or aerosols, to be inhaled into the lung. Although most of the nebulisers are not portable, they offer the advantage of delivering a larger volume of drug solution over an extended period, which is favourable in the delivery of drugs with a large therapeutic dose, such as antibiotics (Traini and Young, 2009). Further, no special inhalation technique is needed during the administration, as the drug is inhaled during normal tidal breathing through a mouthpiece or facemask. Therefore, nebulisation may be convenient in paediatric patients, the elderly, acutely dyspnoeic or uncooperative patients.

The nebulisers that are available in the market are the pneumatic/jet, ultrasonic and mesh nebulisers (Table 1.5). The jet nebuliser uses compressed air, which is passed through a small aperture to create an area of negative pressure, causing the liquid to be drawn up a feed tube from the reservoir (Vecellio, 2006). The drawn liquid is broken down into droplets, with the small droplets leaving the nebuliser to be inhaled by the patient, and the large droplets impacted by the baffle to be recycled in the liquid

reservoir. The problem with the conventional nebuliser is some of the drug may be lost to the environment during exhalation. Therefore, inhalation and exhalation valves have been introduced (e.g. Pari LC$^©$ nebuliser), to help generate more aerosols using a negative pressure created during the inspiration and minimising the drug wastage during exhalation phase (Ari, 2014).

Ultrasonic nebulisers use the high-frequency vibration (> 1 MHz) of a piezoelectric crystal to generate standing waves of the drug solution (Dolovich and Dhand, 2011). The waves are then broken up, creating large and small droplets. The small droplets are available to be inhaled by the patient, while the large droplets are thrown onto the nebuliser's wall to be recycled by the nebuliser (Vecellio, 2006). The mesh nebuliser also uses energy from a vibrating piezoelectric crystal which is attached to the horn transducer, producing vibrations around the mesh with multiple apertures. The vibrating mesh pumps and loads the holes with liquids, creating respirable aerosols (Vecellio, 2006).

Based on the mode of operation, the high shearing forces in the jet nebuliser may be disruptive to formulations such as liposomes (Elhissi et al., 2007). However, addition of materials such as cholesterol in liposomes (Bridges and Taylor, 1998) and polycationic peptide in a lipid DNA complex (Birchall et al., 2000), has been shown to protect the formulations against the shearing force of the device to some extent, maintaining their integrity. Vibrating mesh nebulisers are the latest generation of nebuliser with improved features compared to conventional jet nebulisers, including better output rate and lower residual volume. Although, ultrasonic nebulisers have been shown to be suitable to deliver formulations, such as liposomes (Kleeman et al., 2007), denaturation of liposomes caused by the elevated temperature has also been reported (Bridges and Taylor, 1998). On the other hand, mesh nebulisers are less disruptive to formulation with sensitive structures, such as liposomes (Elhissi et al., 2007; Kleeman et al., 2007) and peptides (Manunta et al., 2011). Despite the advantages of the other nebulisers, the jet nebuliser is still widely used in clinical practice due to the ease of use and its low-cost.

Table 1.5 Comparison of different nebulisers (adapted from Dolovich and Dhand, 2011; Taylor, 2018).

Features	Jet	Ultrasonic	Vibrating mesh
Mechanism			
Power source	Compressed gas or electrical mains	Electrical mains	Batteries or electrical mains
Portability	Restricted	Restricted	Portable
Output rate	Low	High	High
Residual volume	0.8-2.0 mL	Variable but low	≤ 0.2 mL
Cost	Low	High	High
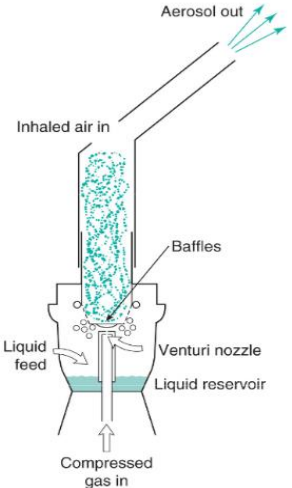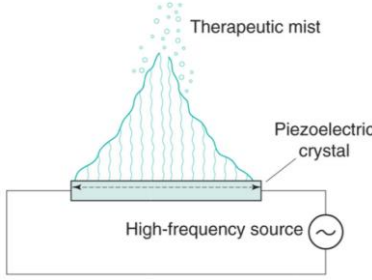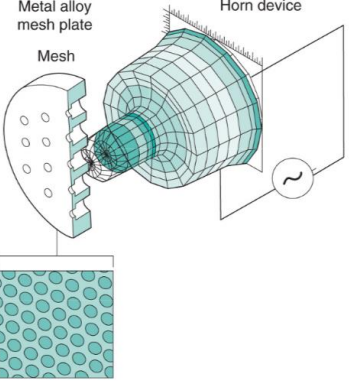
1.3.2.2 Pressurised metered-dose inhalers (pMDIs)

pMDIs are multi-dose devices that include a pressurised canister containing dissolved or suspended drug in a liquid propellant or a mixture of liquid propellants, together with other excipients (Figure 1.7). The canister is fitted with a metering valve, which upon actuation releases a predetermined dose in a spray form. The pMDIs are the most widely used inhalation devices for the treatment of asthma and chronic obstructive pulmonary disease (Dolovich and Dhand, 2011), offering benefits of portability and shorter time of administration compared to nebulisers. The original pMDIs were not environmental friendly as they employed chlorofluorocarbon (CFC) as a propellant, which can damage the stratospheric ozone. However, alternative propellants, namely hydrofluoroalkanes are now used (Boulet et al., 1999).
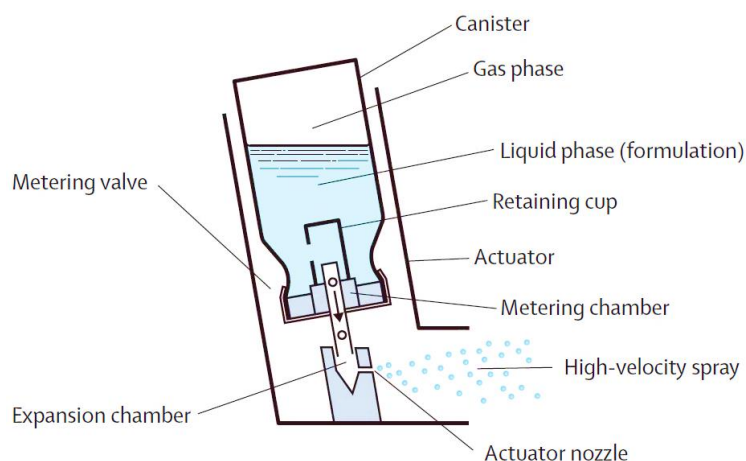
Figure 1.7 The components of a pMDI (Dolovich and Dhand, 2011).

A disadvantage of pMDIs is the need for actuation and inhalation coordination by patients, which can cause variation in the fraction of drug reaching the lung (Pilcer and Amighi, 2010). The problem has been overcome by the introduction of breath-actuated pMDI devices (e.g. Autohaler®, Easi-breathe®), which diminish the need for coordination as the device can sense the inhalation through the actuator and fire the dose in synchrony. Alternatively, spacer devices or valved holding chambers may be used to minimise the need for coordination, especially in young children.

1.3.2.3 Dry powder inhalers (DPIs)

Dry powder inhalers (DPIs) combine device design and powder technology to deliver dry particles as aerosols to the lung. The DPI removes the propellant and the breath-actuation coordination issues of the pMDIs, with better stability compared to liquid formulations (Pilcer and Amighi, 2010). There are two types of DPIs, namely the single-dose and multi-dose devices (Figure 1.8). Examples of the single-dose device are the Aerolizer®/Cyclohaler® and Handihaler®. In the example of Aerolizer®, a pre-packaged drug is delivered in a hard gelatin capsule. The capsule is placed into the device and pierced by metal needles on both sides of the capsules. An inhaled airflow through the device causes the powder to disperse to the capsule walls and out through the holes into the inspired air (Schering Corporation, 2010).

Multi-unit or multi-dose DPIs contain either multiple doses in foil blisters (e.g. Ellipta® and Diskus®/Accuhaler®) or a reservoir of drug from which the metered-dose will be delivered for each inhalation (e.g. Easyhaler® and Turbohaler®). In the example of the Ellipta® inhaler, the foil-covered blister pockets preloaded with individual doses are peeled off as each dose is advanced (GlaxoSmithKline, 2017). Separate pre-metering and packaging of each dose minimizes the exposure of the content to ambient condition, protecting the formulation from humidity. In the example of the Easyhaler® (reservoir-based device), a dose is accurately measured and delivered from a formulation reservoir, preloaded with 200 doses of inhaled medication (Juntunen-Backman et al., 2002). A metered-dose is loaded to the dosing chamber by pressing the overcap of the device. In both examples, the devices are equipped with a dose counter which can be used to track the number of actuations used from the inhaler.
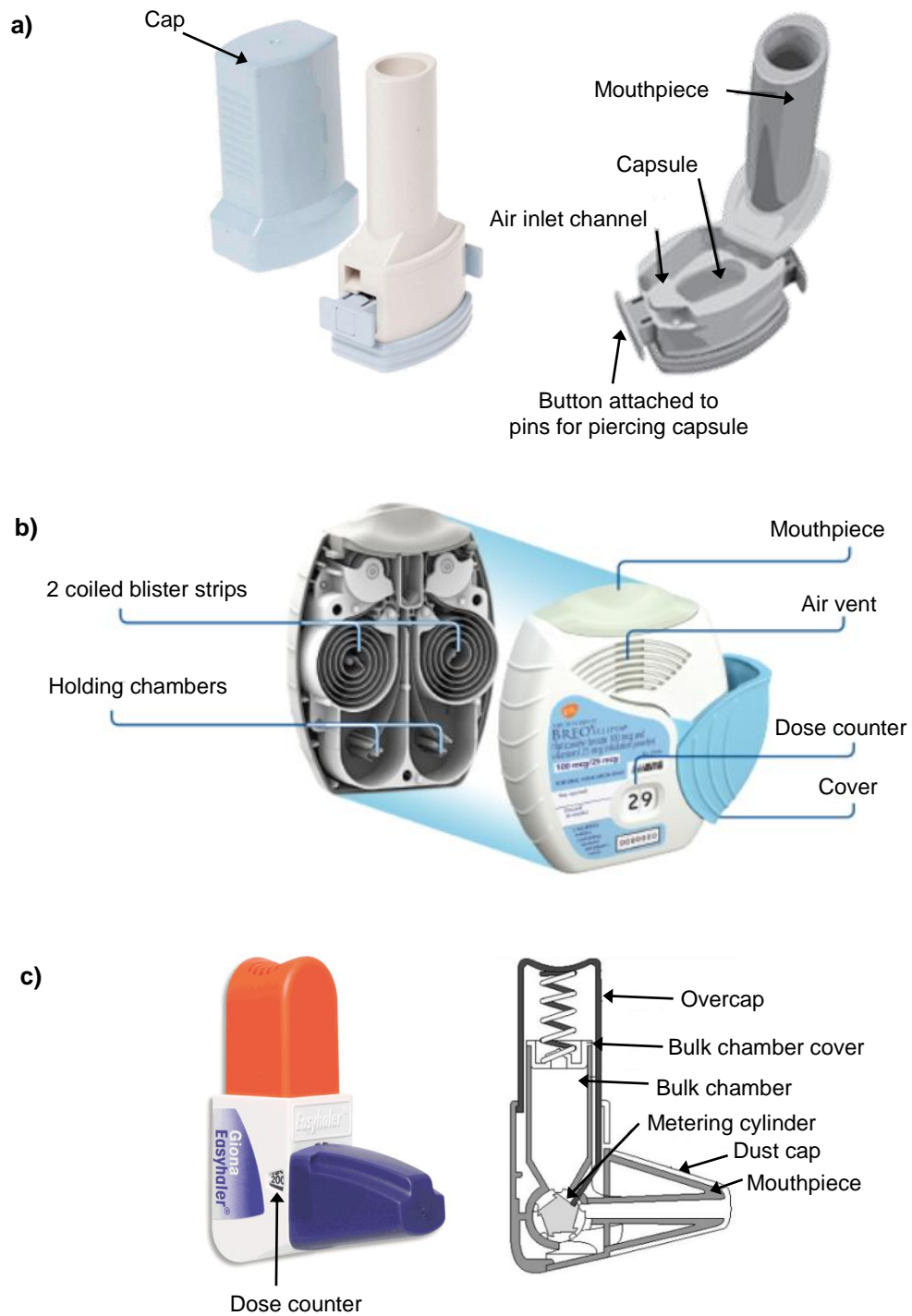
Figure 1.8 Selected dry powder inhaler devices; a) Aerolizer®, b) Ellipta® and c) Easyhaler® (adapted from Juntunen-Backman et al., 2002; Schering Corporation, 2010; GlaxoSmithKline, 2017).

1.3.2.3.1   Excipients used in DPIs

The DPI formulation often consists of a micronised drug with poor flow properties, caused by its static, cohesive and adhesive nature. Addition of excipients helps to improve the flowability as well as providing bulk to aid handling and dosing of the drug. The drug particles are mixed with larger carrier particles, such as lactose, to produce a mix in which the small drug particles attach to the surface of a larger carrier particle (Figure 1.9). The drug particles are then separated from the carrier during inhalation to be carried deep into the lung, whereas the larger particles impact in the oropharynx (Telko and Hickey, 2005).
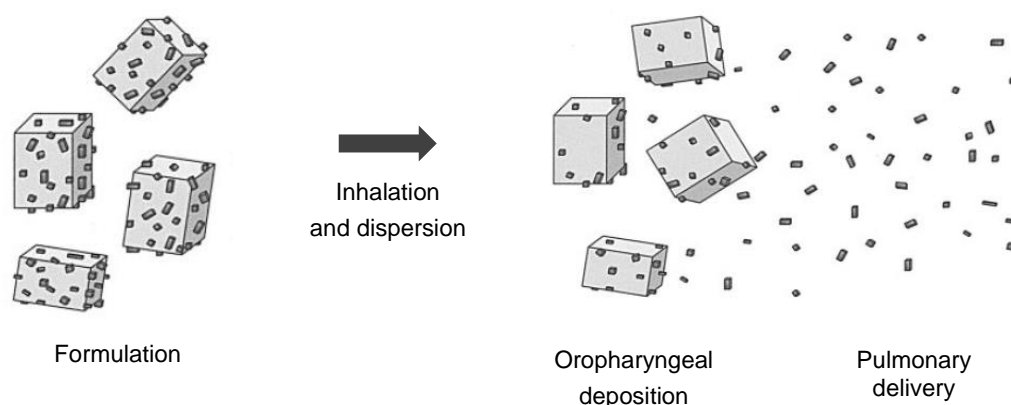
Figure 1.9 Principle of dry powder inhaler design (adapted from Telko and Hickey, 2005).

Inadequate drug-carrier separation can occur when the drug particles bind to the high-energy sites of the carrier particles, producing a strong interaction and reducing the drug deposition efficiency (Pilcer and Amighi, 2010). This problem can be overcome by producing a ternary mixture containing coarse and fine carrier particles. In one study, micronised lactose was added to coarse lactose particles to fill in the high-energy sites on the larger particles, leaving only low-energy sites for the binding of salbutamol sulphate (Zeng et al., 1999). The ternary mixture enhanced detachment of the drug particles during inhalation, showed by a higher deposition

efficiency, compared to the binary mixture containing coarse lactose and salbutamol sulphate only.

Additionally, different materials can be used to modify adhesion properties of drug and carrier particles. Magnesium stearate has been used to reduce the electrostatic repulsion between lactose particles, leading to improved interaction between the fine and coarse lactose (Guchardi et al., 2008). This resulted in a smaller interaction between the carrier and formoterol fumarate, improving the aerodynamic performance. Amino acids such as leucine have also been used as a dispersibility enhancer in a spray-dried powder for inhalation (Seville et al., 2007). Addition of leucine resulted in formation of a wrinkled surface, reducing the interaction between particles. The surface modification led to enhanced dispersibility and deposition efficiency of salbutamol sulphate.

1.3.3 Particle engineering in pulmonary delivery

In addition to the device design and patient's inhalation technique, powder formulation is an important consideration for DPIs. The drug powder needs to be in the respirable range (preferably < 5 µm) to be able to reach the peripheral airways. One of the techniques to reduce particle size is micronisation, including vibration milling, ball milling and jet milling. In the milling process, the starting material undergoes many impact and/or attrition events to achieve the required particle size distribution. This process can induce electrostatic charges, which often leads to a powder with poor flow properties. In one study, flowability of micronised decapeptide cetrorelix was improved by preparing an adhesive mixture, consisting of the micronised drug attached to the surface of coarse lactose as a carrier (Irngartinger et al, 2004). The adhesive mixture produced using pearl-milled decapeptide cetrorelix showed a better inhalation performance compared to the adhesive mixture produced using spray-dried decapeptide cetrorelix.

However, the milling technique is limited to reducing the particle size using mechanical stress, which can not be used to engineer complex structures such as porous/hollow, surface-modified, coated or encapsulated particles (Chen et al., 2016). Alternative techniques include spray drying (Tajber et al., 2009; Meenach et al., 2013),

spray-freeze drying (Saluja et al., 2010) and supercritical antisolvent precipitation (Ober et al., 2013). From the mentioned techniques, spray drying will be discussed in the next section as it was used in the preparation of dry powders in the study.

1.3.3.1 Spray drying

Spray drying is a technique to produce micron-sized particles, during which a drug-containing liquid feed in the form of a solution, emulsion or suspension, is converted into dry particles. Spray drying involves three main steps (Figure 1.10); i) atomisation of the feed solution from a nozzle, ii) drying of the droplets in a drying chamber, and iii) separation of the dry powder in a cyclone (Peltonen et al., 2010).
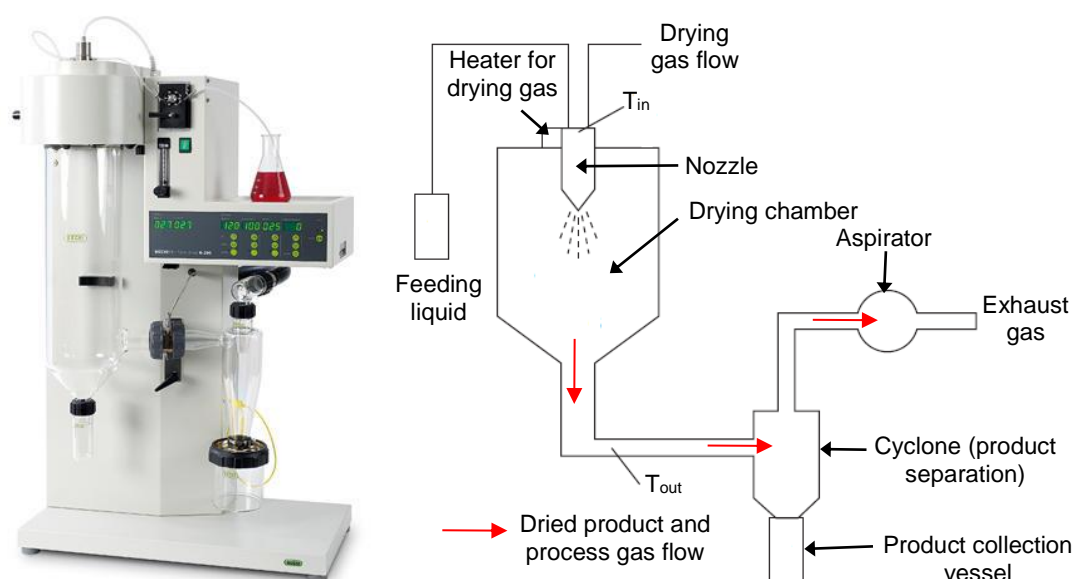
Figure 1.10 Büchi mini spray dryer B-290 used in the study and a schematic diagram of a spray dryer (adapted from Peltonen et al., 2010).

Spray drying allows building up of the particle to be in the desired size distribution, density, particle shape and morphology (Hoppentocht et al., 2014). This can be done by controlling formulation parameters such as composition and nature of the ingredients, viscosity, solid content and solvent type, as well as process parameters such as the inlet air temperature, feed rate and droplet size (Chen et al., 2016). The Peclet number (Pe) can be used to explain the particle formation process by spray

drying (Vehring, 2008). The Peclet number describes the ratio of diffusion coefficient of the solute (D_i) and the evaporation rate (κ), as in the following equation;

$$Pe = \frac{\kappa}{8D_i}$$

Eq 1.2

A small Peclet number indicates slower evaporation of the solvent which gives time for the solute to distribute homogeneously in the droplets, giving solid structure of the particles (Figure 1.11). In contrast, a high Peclet number signifies rapid evaporation of the solvent and/or slow diffusion of the solute from the surface, leading to shell formation. Different morphologies can be produced depending on the size and properties of the shell; solid hollow spheres, dimpled or wrinkled particles (Vehring, 2008).
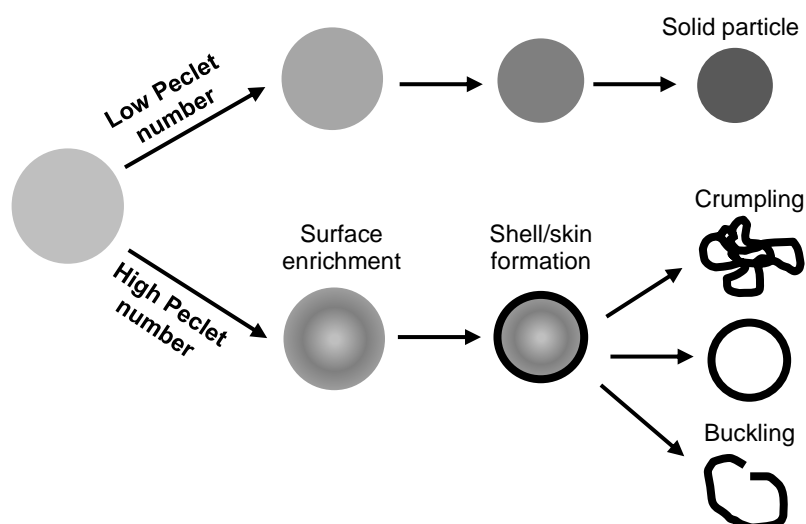
Figure 1.11 Proposed particle formation process according to Peclet number (adapted from Vehring, 2008).

Porous or hollow particles can be advantageous for aerosol drug delivery because of their low density, contributing to a lower aerodynamic diameter (Eq 1.1). Spray drying of an ethanolic feed solution has been shown to produce large porous particles with a mass median aerodynamic diameter (MMAD) of $< 5\ \mu m$ (Vanbever et al., 1999). A sufficient fine particle fraction was achieved, resulting in a sustained insulin plasma level in rats, similar to a subcutaneous injection. An excipient-free nanoporous microparticles of budesonide was also produced by spray-drying ethanolic

solution of the drug (Nolan et al., 2009). The low-density particles showed an improvement in the fine particle fraction compared to the micronised and non-porous spray-dried particles, comparable to the marketed budesonide preparation (Cyclocaps®).

Alternatively, volatile excipients or pore forming agents can be used to produce the porous structure. In the marketed tobramycin inhalation powder (PulmoSphere™, Tobi® Podhaler®), a volatile oil (i.e. perfluorooctyl bromide) was used to produce an oil-in-water emulsion of tobramycin, together with other excipients (e.g. distearoylphosphatidylcholine) (Geller et al., 2011). Spray drying of the emulsion caused formation of droplets with a shell made up of the slow-diffusing excipients and a core containing readily-diffused tobramycin. Further drying of the droplets caused evaporation of perfluorooctyl bromide, forming the pores.

1.3.3.2 Spray drying of inhalable nanocarriers

Suspensions containing nanocarriers (e.g. nanoliposomes, polymeric nanoparticles) can be spray dried to form inhalable nanostructured microparticles for the treatment of lung-related or systemic diseases. The nanocarriers are often dried in the presence of bulking materials (e.g. lactose, trehalose) to form a continuous matrix in which the nanoparticles are dispersed homogenously (Peltonen et al., 2010). In one study, dapsone-loaded nanoliposomes were spray dried in the presence of various bulking materials (i.e. sucrose, lactose, hydrolysed gelatin) and a dispersibility enhancer (i.e. leucine) for the treatment of cystic fibrosis (Chougule et al., 2008). The hydrolysed gelatin-based preparation showed a high fine particle fraction and a prolonged *in vitro* release of dapsone, up to 16 h.

Inhalable nanocomposite particles were also prepared by spray drying a solution containing PLGA nanoparticles loaded with TAS-103 (a novel topoisomerase inhibitor) and trehalose dihydrate (Tomoda et al., 2009). Delivery of the preparation by inhalation resulted in a higher drug concentration in the lung compared to the intravenous administration of the free drug in rats, offering targeted drug delivery in the treatment of lung cancer. Further, inhalable powders containing isoniazid-loaded chitosan nanoparticles were spray dried in the presence of different excipients (i.e.

lactose, mannitol, maltodextrin) and leucine (Pourshahab et al., 2011). The lactose-based preparation showed a capability of delivering higher fine particle fractions compared to other preparations, while providing a sustained release of isoniazid and better killing against a mycobacterium strain.

The above-mentioned studies produced spray-dried inhalable powders from feed liquids containing the drug-loaded nanocarriers and excipients. Alternatively, spray drying can be used to prepared micron-sized powders of the formulation, prior to the mixing with larger-particle carriers. In one study, spray drying of an inclusion complex of beclometasone dipropionate with γ-cyclodextrin was performed and the powders were mixed with different larger-particle carriers (i.e. lactose, trehalose) (Cabral-Marques and Almeida, 2009). The preparations showed better deposition profiles compared to a commercial beclometasone inhalation product (Beclotaine Rotacaps), with less deposition in the upper compartment of a two stage glass impinger. This indicated likely low deposition in the oropharynx, possibly reducing the chances of oral candidiasis related to beclometasone treatment in patients.

These studies showed the application of spray drying in the production of inhalable dry powder inhalation for the treatment of various diseases. Local delivery by inhalation and sustained release of the drug from the nanocarriers, will offer possibilities of less frequency of administration and a reduction in systemic toxicities related to the drug.

1.4 Problem statement

Fisetin is a dietary flavonoid that has shown anti-oxidant and anti-cancer activities against various types of cancer, including lung cancer. However, its low solubility in water is a challenge to the delivery of the molecule. One way of increasing its solubility is to form an inclusion complex of fisetin with cyclodextrins, which has been studied before; no study has yet explored the formulation of fisetin for pulmonary delivery. Inhalation of the complexes in the form of a dry powder may give an opportunity of local treatment in lung-associated diseases (e.g. lung injury and NSCLC).

Additionally, combination of fisetin and TKIs should be explored to address the dose-related toxicity and drug-resistance problems of the TKIs. To date, only an oral dosage form is approved for the delivery of the TKIs, with bioavailability ~40-60%. Therefore, the synergistic combination and its local delivery to the lung may offer opportunities for dose reduction, as well as increasing the bioavailability to the target site, which may be cost-effective and able to reduce the systemic side effects related to the drug. Moreover, targeting of fisetin and the TKI at different sites of the signalling pathway, may prevent occurrence of drug-resistance or re-sensitize resistant lung cancer cells towards TKI therapy. The low solubility of both fisetin and the TKI may be resolved by forming co-complexes with cyclodextrins to improve solubility while minimising the use of excipients. Ultimately, localised delivery of fisetin and its combination with the TKI will hopefully contribute to a better outcome when treating of NSCLC.

1.5 Aim and objectives of the study

This study aims to improve the solubility of fisetin and a tyrosine kinase inhibitor, and subsequently to develop inhalable formulations suitable for pulmonary delivery of both molecules. The study was conducted with the following objectives:

1) To screen the most suitable β-cyclodextrin to form an inclusion complex with fisetin in order to provide optimal solubility and complexation efficiency.

2) To develop and optimise a dry powder formulation of fisetin and the most suitable β-CD complex for pulmonary delivery.

3) To analyse the combinations of fisetin and different tyrosine kinase inhibitors, to find the most synergistic combination against the NSCLC cell line. The selected combination will be used to form inclusion complexes with cyclodextrins.

4) To optimise the cyclodextrin complex containing fisetin and the tyrosine kinase inhibitor, to be suitable for nebulisation.

The flow of the project outlined in this thesis is shown in Figure 1.12. The project began with a study of the complexation of fisetin with cyclodextrins (***Chapter 3***), followed by the spray drying of a fisetin-SBE-β-CD complex to produce a dry powder suitable for inhalation (***Chapter 4***). Subsequently, the cytotoxic activity of fisetin and its combination with tyrosine kinase inhibitors, against the human lung adenocarcinoma (A549) cell line was analysed in ***Chapter 5***, and the combination with the most synergistic killing activity (i.e. erlotinib and fisetin) was used to form complexes with cyclodextrins. The erlotinib-fisetin-SBE-β-CD complex was then optimised to be suitable for nebulisation (***Chapter 6***).

Production of cyclodextrin-based formulations for pulmonary delivery of chemotherapeutic molecules

Complexation of fisetin with cyclodextrins
A study on solubilisation of fisetin in different cyclodextrins and investigation of ethanol addition on the formation of the complex
(*Chapter 3*)

Production of a dry powder fisetin-SBE-β-CD complex for inhalation
Preparation of the dried complex using spray drying. An investigation of different feed solution compositions and incorporation of leucine on the physicochemical and aerodynamic properties of the powder
(*Chapter 4*)

Combination of fisetin and tyrosine kinase inhibitors (TKIs)
Analysis of fisetin and its combinations with the TKIs against the human lung adenocarcinoma (A549) cell line using median effect principle method
(*Chapter 5*)

Co-complexation of erlotinib and fisetin with cyclodextrins
A study on solubilisation of both drugs in different cyclodextrins and investigation of ethanol addition on the formation of the complex
(*Chapter 5*)

Production of an erlotinib-fisetin-SBE-β-CD complex for nebulisation
Optimisation of the formulation compositions and lyophilisation of the complex for nebulisation
(*Chapter 6*)

Figure 1.12 Schematic of the thesis describing production of cyclodextrin-based formulations of fisetin and its combination with TKIs for pulmonary delivery.

Chapter 2

General materials and methods

2.1 Materials

Materials used in the study were as follows;

2.1.1 Active pharmaceutical ingredients

Fisetin (3,3',4',7-tetrahydroxyflavone, >98%) was purchased from Carbosynth (Berkshire, UK). Erlotinib (free base, >99%) and gefitinib (free base, >99%) were procured from LC Laboratories (Woburn, USA) and crizotinib (>98%) was purchased from Insight Biotechnology (Middlesex, UK).

2.1.2 Excipients

Sulfobutylether-β-cyclodextrin (SBE-β-CD, Captisol®, MW: 2163, DS: 7) was a gift from Cydex Pharmaceuticals (La Jolla, USA). β-cyclodextrin (β-CD, Kleptose® DC, MW: 1135) and hydroxypropyl-β-cyclodextrin (HP-β-CD, Kleptose® HP, MW: 1480, DS: 5.6) was a kind gift from Roquette Pharma (Northamptonshire, UK). L-leucine was purchased from EMD Chemicals Inc. (San Diego, USA).

2.1.3 Reagents and solvents

Absolute ethanol (99.9%) was procured from Fisher Scientific (Loughborough, UK). Acetonitrile, water, dimethyl sulfoxide (DMSO) and trifluoroacetic acid (TFA) of HPLC grades and DPPH˙ (2,2-diphenyl-1-picrylhydrazyl) free radical, L-ascorbic acid and methanol of analytical grades were obtained from Sigma-Aldrich (Dorset, UK).

The Roswell Park Memorial Institute (RPMI 1640) medium, phosphate buffered saline (pH7.4), foetal bovine serum (FBS), 0.05% trypsin-EDTA solution and penicillin-streptomycin solution were purchased from Gibco (USA). The 3-(4,5-dimethylthiazol-2-yl)-2,5-diphenyltetrazolium bromide (MTT) was obtained from Sigma (USA).

2.2   Phase solubility study

A phase solubility study was conducted according to the method of Higuchi and Connors (1965) to investigate the influence of cyclodextrins on the solubilisation of the drug. An excess amount of drug was added into 5 mL deionized water containing different concentrations of β-CD, HP-β-CD and SBE-β-CD. The mixture was mixed in a bath sonicator (Clifton, UK) for 15 min and left for further mixing at 100 rpm and 37°C for 24 h in an orbital incubator shaker (Sanyo Gallenkamp, Leicester, UK). The uncomplexed drug was filtered from the solution using a 0.45-μm syringe filter (Merck Millipore Ltd., Ireland). The filtrate was diluted accordingly with DMSO and measured using validated HPLC methods (see Section 2.6).

The concentration of solubilised drug (mM) was plotted against different concentrations of cyclodextrin (mM). The slope and y-intercept (S_0) of the straight lines were used to calculate the complexation parameters as follows;

$$\text{Stability constant, } K_s = \frac{\text{slope}}{S_0 \, (1\text{-slope})} \qquad \text{Eq 2.1}$$

$$\text{Complexation efficiency, } CE = \frac{\text{slope}}{1\text{-slope}} \qquad \text{Eq 2.2}$$

$$\text{Molar ratio of drug: } CD = 1: \frac{(CE + 1)}{CE} \qquad \text{Eq 2.3}$$

2.3   Freeze drying

Freeze drying was used to remove water from the drug-cyclodextrin complex solution. In the method, 5 mL of sample solution was transferred into a 14 mL glass vial and frozen at -20°C for 24 h. The frozen solution was placed into the freeze-drying system (Savant MicroModulyo, Thermo Electron, USA) equipped with a condenser operating at -50°C. The drying process was carried out under vacuum for 48 h.

2.4   Spray drying

Spray drying was utilised to prepare an inhalable dry powder from a drug-cyclodextrin complex solution. The complex solutions were spray dried using a mini laboratory spray dryer, model B-290 (Büchi Labortechnik, Switzerland), in an open loop mode configuration using compressed air as the drying gas. The process was done under the following conditions; inlet temperature (T_{in}): 120°C, corresponding to an outlet temperature $T_{(out)}$: 66°C, spray gas flow: 536 L/h, pump: 20% (4.83 mL/min), aspirator: 100% (35 m^3/h).

2.5   Determination of yield and the amount of solubilised drug

The yield of the spray-dried powder was calculated using the following equation;

$$\text{Yield (\%)} = \frac{\text{Weight of the spray-dried powder (mg)}}{\text{Initial weight of drug and excipients (mg)}} \times 100 \qquad \text{Eq 2.4}$$

In the complex solution, the free drugs were removed by filtering the solution using a 0.45-µm syringe filter. In the dried-powder preparations, a known amount of the powder was redispersed in a known amount of deionized water and vortexed for 5 s. The uncomplexed drugs were removed using a 0.45-µm syringe filter. In both cases, an aliquot of sample before filtration and in the filtrate was diluted with DMSO, and was injected into the HPLC (Section 2.6) to determine the amount of drug. The amount of solubilised drug was calculated according to the following equation;

$$\text{Solubilised drug (\%)} = \frac{\text{Amount of drug in the filtrate (mg)}}{\text{Amount of drug in the unfiltered solution (mg)}} \times 100 \qquad \text{Eq 2.5}$$

2.6   Quantification of drugs using high performance liquid chromatography (HPLC)

All drugs used in the experiments were quantified using a HPLC-UV method. Analysis was performed using an Agilent 1260 series HPLC system (Agilent Technologies, USA) equipped with quaternary pump VL, standard autosampler, thermostatted column compartment and variable wavelength detector VL. The data were acquired and analysed using OpenLab CDS ChemStation Edition (B.04.03) software. The

chromatographic separation was performed using an ether-linked phenyl column with polar endcapping (Synergi^{TM} 4 µm Polar-RP 80°A, 250 x 4.6 mm i.d, 4 µm particle size).

2.7 Determination of particle size distribution by laser diffraction analysis

The particle size distribution of the dried powder was determined using a Sympatec HELOS BF laser diffraction analyzer (Sympatec GmbH, Clausthal-Zellerfeld, Germany) with RODOS/M dry powder disperser. The sample was loaded into a sealed sample tube and the tube was inserted into the micro-dosing device (ASPIROS). Sufficient sample was loaded to obtain an obscuration of >1 and each sample was measured in triplicate at an air pressure of 4 bar. Results were analysed using Windox 5 (version 5.7.0.0) software.

Results were analysed based on the Mie Evaluation Extended (MIEE) algorithm for spherical, isotropic and homogeneous particles, which converted the scattered light data into particle size information. The complex refractive index value used in the analysis was 1.550, with air as the continuous phase.

Results were expressed as the volume mean particle size and percentage undersize at 10% (X_{10}), 50% (X_{50}) and 90% (X_{90}). The X_{50} is also known as the volume median diameter (VMD) of the particles. The width of the size distribution was expressed as the Span according to following equation;

$$\text{Span} = \frac{X_{90} - X_{10}}{X_{50}} \qquad \text{Eq 2.6}$$

2.8 X-ray powder diffraction (XRPD) analysis

The raw materials, physical mixtures and selected formulations, in powder form, were analyzed for their crystallinity and physical interaction using XRPD analysis. The powder was placed on the circular sample holder and was evenly spread using a glass slide. The excess powder was removed and the sample holder was placed in the Rigaku

MiniFlex 600 X-ray diffractometer (Rigaku, Japan). The analysis was conducted at room temperature. The Cu anode X-ray tube was operated at a generator voltage of 40 kV and a current of 15 mA. Diffraction patterns were recorded over the diffraction angle (2θ) of 5-37°, a scanning rate of 5°(2θ)/min and a scan step of 0.05° (2θ).

2.9 Fourier transform infrared (FT-IR) spectroscopy

FT-IR analysis was done to evaluate the chemical interaction of all materials in the mixtures or drug-cyclodextrin complexes. FT-IR analysis of raw materials, physical mixtures and selected formulations was undertaken using a Spectrum 100 FT-IR spectrometer (Perkin Elmer, Massachusetts, USA). The sample powder was placed on the sample slot and the compression probe was lowered onto the sample by turning the knob clockwise. The knob was adjusted to give a pressure value of around 130. Spectra were recorded over the range 4000-650 cm^{-1} with a resolution of 4 cm^{-1} and scanning speed of 0.2 cm/s.

2.10 Thermogravimetric analysis (TGA)

The residual solvent content of the spray-dried powders was determined using a thermogravimetric analyser (Discovery TGA, TA instrument, USA). Samples were loaded onto aluminium pans and placed in sample holders. The analysis was carried out under a nitrogen purge of 20 mL/min. A heating rate of 10°C/min over a range of room temperature to 400°C was applied to each sample and each measurement was performed in triplicate.

2.11 Scanning electron microscopy (SEM)

A scanning electron microscope (SEM) was used to examine the surface morphology of produced powders. In the analysis, the sample was placed on the surface of a double-sided adhesive black carbon tab which was attached to a 12.5 mm aluminium stub. The sample was sputter-coated with gold (Quorum Q150R; Quorum Technologies, Sussex, UK) prior to observation under SEM (FEI Quanta200F SEM; FEI, Eindhoven, Netherlands) at an acceleration voltage of 5 kV.

2.12 Aerosol deposition study using the Next Generation Impactor (NGI)

The aerosol properties of an inhalation preparation can be characterised using inertial techniques, as described in the European Pharmacopoeia (2016). These techniques use the principle of inertial impaction to distribute the aerosols throughout the stages. The collection surface where the particles impact can be a dry impaction plate or cup (in the Andersen Cascade Impactor and Next Generation Impactor) or liquid (in the Glass Impinger and Multistage Liquid Impinger).

Cascade impactors allow fractionation of aerosols according to the particle's inertia without the need to know the particle density or shape (Figure 2.1). In the analysis, sample-loaded air is drawn into the impactor, flowing through a series of stages each made up of a plate with a specific nozzle arrangement. As the particle inertia depends on the velocity and aerodynamic particle size, particles of large aerodynamic diameter will impact on a certain stage while smaller particles will remain in the air stream to be passed to the next stage. A smaller air jet increases the air velocity, collecting finer particles. Any remaining particles are collected by the micro-orifice collector (MOC) (Shekunov et al., 2007; Copley Scientific, 2015).
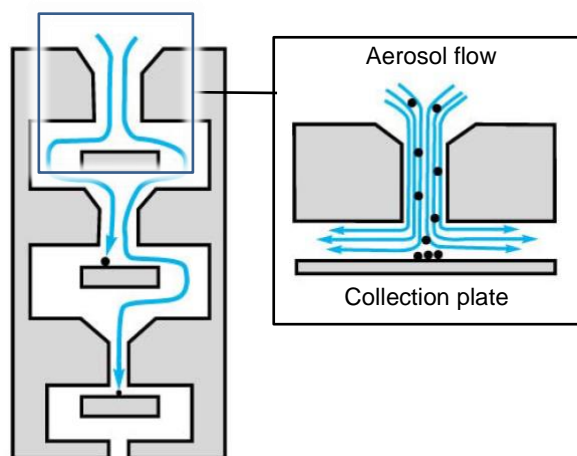
Figure 2.1 Principle of operation of a cascade impactor (Copley, 2007).

The Next Generation Impactor (NGI; Apparatus E, Chapter 2.9.18, European Pharmacopoiea) was used in this study. The NGI (Figure 2.2) was fitted with a 90° bend 'induction port' to mimic the human throat and comprises 7 impaction stages and

the MOC. The NGI can be used with air flow rates between 15 and 100 L/min, characterising particles between 0.5 and 5 µm with five stages, with cut-off diameters in the appropriate range, over most operating conditions (Copley, 2007). As characterisation of dry powder and nebulised aerosols involve different compendial procedures, the methods will be explained in detail in the relevant chapters.
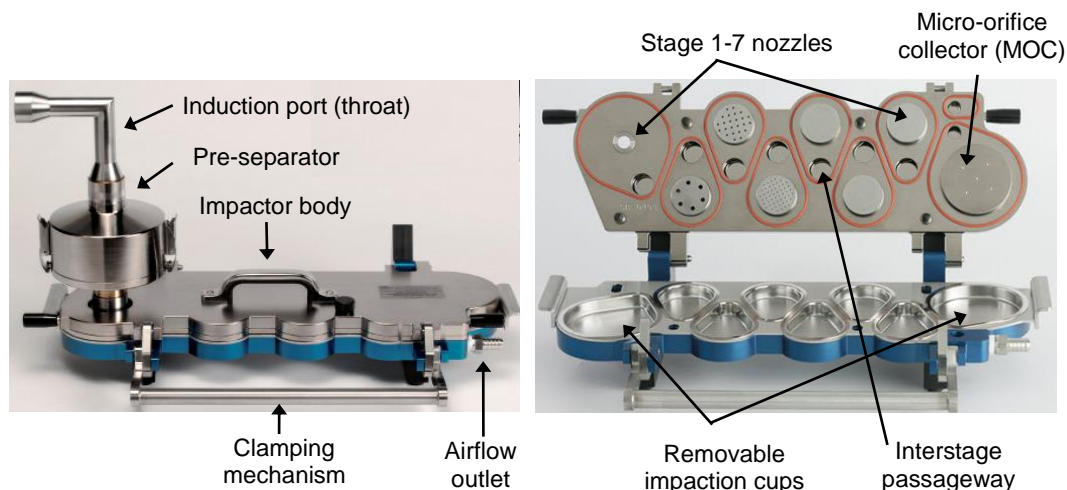
Figure 2.2 The Next Generation Impactor (a) showing the induction port and pre-separator in place (b) showing the component parts (adapted from Copley Scientific, 2015).

2.13 *In vitro* cell toxicity study (MTT assay)

2.13.1 Cell culture

The human lung adenocarcinoma cell line, A549 (purchased from American Type Culture Collection; ATCC), was used in the study. A549 cells are alveolar basal epithelial cells, which are responsible for the diffusion of substances (e.g. water and electrolytes) across the alveoli in a normal lung. The A549 (passage number: 29 to 31) was chosen in this study as it has been used to study the effect of chemotherapeutic molecules and their formulations (Zhou et al., 2013; Mandal et al., 2016), and to study the mechanism of actions (Liao et al., 2009; Zhang et al., 2014) involved in the treatment of NSCLC.

The cells were cultured in a complete media, which consisted of RPMI 1640 with L-glutamine supplemented with 10%v/v foetal bovine serum, 100 µg/mL streptomycin and 100 U/mL penicillin. The cell cultures were maintained in an incubator at 37°C with a humidified environment of 5% CO_2 and 95% air. The cells were harvested with 1.5 mL trypsin-EDTA solution when reaching 70-80% confluence during the exponential growth phase and sub-cultured into 96-well plates for further assay.

2.13.2 Analysis of cell viability

Cell viability was evaluated using the MTT assay, which is one of the cell-based assays used to screen the direct cytotoxic effect or the effect of the test preparations on cell proliferation. In this assay, the yellow-coloured tetrazolium reagent (MTT) is reduced by the active metabolism of viable cells into purple-coloured formazan as shown in Figure 2.3 (Riss et al., 2016). As the dead cells lose the ability to convert the MTT into formazan, the change in the colour can be used as a marker to estimate the number of the viable cells.
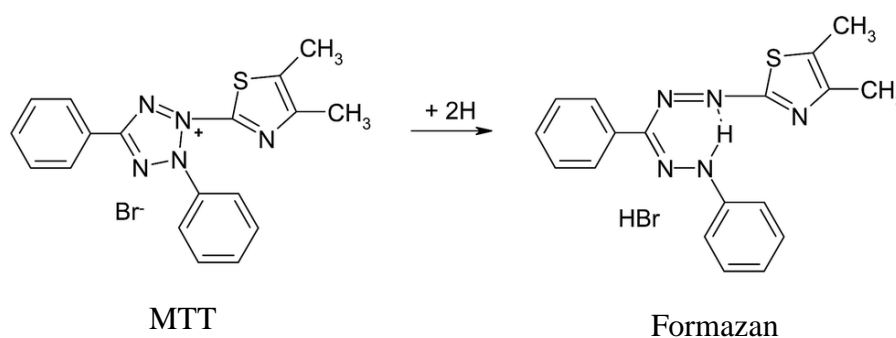
MTT   Formazan

Figure 2.3 Structures of MTT and formazan product.

In brief, the cells were seeded at a density of 2 x 10^4 cells per well in a 96-well plate and incubated for 24 h at 37°C (5% CO_2/95% air). Then, 200 µL of treatment solutions were added at different concentrations in the treated wells and 200 µL complete media solution was used in the untreated wells. For all treatments, stock solution of the free drugs was prepared in DMSO and diluted using complete media, with DMSO concentration of not more than 0.1%v/v. Therefore, the cells were also

treated with 0.1% v/v DMSO in the media to evaluate DMSO-derived toxicity. In this assay, treatment with complete media was used as a negative control and experiments were done in triplicate on three different days.

After a defined incubation time (48 or 72 h), the medium was replaced with 110 µL MTT solution and further incubated for 2 h. The MTT solution was prepared by dissolving 5 mg MTT in 1 mL saline phosphate buffer solution and 10 mL complete media solution (0.45 mg/mL). Then, the MTT solution was removed and the generated formazan was solubilised in 150 µL DMSO. The plate was shaken for 10 min prior to optical density (OD) measurement using a multi-mode microplate reader (SpectraMax® M2^e, Molecular Devices, USA) at 570 nm. The percentage of cell viability was calculated as follows;

$$\text{Cell viability (\%)} = \frac{\text{OD of treated cells}}{\text{OD of untreated cells}} \times 100 \qquad \text{Eq 2.7}$$

The cell viability curve was plotted and the effective concentration to kill 50% of the cells (EC_{50}) was analysed using OriginPro® 2016 software (OriginLab Corporation, USA).

2.14 Statistical analysis

All parameters were statistically analysed using a t-test for independent groups or one-way analysis of variance (ANOVA) with a post-hoc Tukey HSD test. For all analyses, differences were considered statistically significant when $p < 0.05$.

Chapter 3

Complexation of fisetin with β-cyclodextrins

3.1 Introduction

Fisetin is a natural flavonoid with promising pharmacological activities for treatment or prevention of various diseases. However, its poor water solubility has been a hindrance in the delivery and absorption of the molecule. Several studies have been undertaken to improve the solubility and hence the bioavailability of fisetin by incorporating the compound into nanocochleates (Bothiraja et al., 2014), nanoemulsions (Ragelle et al., 2012), liposomes (Mignet et al., 2012; Seguin et al., 2013) and cyclosophoroase dimer complex (Jeong et al., 2013).

Few studies have investigated complexation of fisetin with different types of cyclodextrins (i.e. α-, β- and γ-cyclodextrin) (Guzzo et al., 2006; Pahari et al., 2013). These studies involving cyclodextrins were limited to investigating the suitability of cyclodextrins to form complexes with fisetin at the molecular interaction level. From these studies, only β- and γ-cyclodextrins were proven to form stable complexes with fisetin. Inclusion of fisetin into β- and γ-cyclodextrins also resulted in a higher cytotoxic activity of fisetin against human cervical and breast cancer cell lines (Zhang et al., 2015). Another study reported a better complexation of fisetin with chemically modified β-cyclodextrins, while maintaining the cytotoxic activity against a liver tumour cell line (Sali et al., 2018). Although plenty of studies has been done on the complexation of fisetin with cyclodextrins, none has yet explored the pulmonary delivery of the complexes, which can give an advantage of localised delivery in the treatment of lung-associated diseases such as lung injury or lung cancer.

Development and production of a fisetin-cyclodextrin complex, suitable for inhalation, will be covered in 2 chapters. In this chapter, complexation of fisetin with different types of β-cyclodextrins (i.e. β-CD, HP-β-CD and SBE-β-CD) was investigated and the anti-oxidant activity of fisetin in the complexes was evaluated. A complex with the highest complexation efficiency was chosen for further investigation using different drying processes and a co-solvent approach to increase the complexation efficiency. This chapter will also describe the development and validation of a simple and specific HPLC-UV method for the quantification of fisetin

according to the International Conference of Harmonisation (ICH) guideline (ICH, 1994). The HPLC-UV method will be used throughout the whole study.

3.2   Methods

3.2.1   Development and validation of an HPLC-UV method for quantification of fisetin

3.2.1.1   Instrumentation

Analysis was performed using the HPLC-UV system as described in Section 2.6. The HPLC conditions are as follows;

Table 3.1 HPLC conditions for quantification of fisetin.

Settings	Conditions
Column	Synergi™ 4 µm Polar-RP 80°A
	(250 x 4.6 mm i.d., 4 µm particle size)
Mobile phase	Acetonitrile: 0.1%v/v TFA in water (30:70; v/v; pH 2)
Column temperature	40°C
Flow rate	1 mL/min
Injection volume	30 µL
Detection wavelength	362 nm
Run time	12 min

0.1%TFA in water was prepared by mixing 1 mL TFA in 1000 mL HPLC water. The solution was mixed with acetonitrile using the quartenary pump system in the HPLC, to produce the mobile phase.

3.2.1.2   Specificity

Specificity of the method was assessed to ensure the absence of interference from other excipients at the retention time of the analyte (ICH, 1994). The evaluation was

conducted by comparing the chromatographs of fisetin, β-CD, HP-β-CD, SBE-β-CD and fisetin-SBE-β-CD complex solution.

3.2.1.3 Preparation of calibration standards and quality control samples

A primary stock solution of fisetin (200 µg/mL) was prepared by dissolving 5 mg fisetin in 25 mL DMSO. Calibration standards were prepared by appropriate dilution of the stock solution with DMSO to give a set of concentrations in the range 2 to 60 µg/mL. Quality control samples were prepared at low, medium and high concentrations of 15, 35 and 55 µg/mL, respectively.

3.2.1.4 Validation of the method

a) Limit of detection and limit of quantitation

Determination of both limits was carried out by injecting low concentrations of fisetin solution. The limit was determined at a signal to noise ratio of 3: 1 and 10: 1 for the limit of detection (LOD) and limit of quantitation (LOQ), respectively (ICH, 1994). The LOQ is also defined as the lowest quantifiable amount with a precision (%RSD) and accuracy (%RE) within ± 10% (Sistla et al., 2005).

b) Linearity

The linearity of the method was evaluated by constructing five calibration curves on five consecutive days using a concentration range of 2 to 60 µg/mL. Results were plotted as peak area of fisetin against corresponding concentrations using linear regression analysis.

c) Precision and accuracy

Precision is described as the percentage of relative standard deviation (%RSD) while accuracy is defined as percentage of relative error (%RE) as shown in following equations;

$$\text{Precision (\%RSD)} = \frac{\text{Standard deviation}}{\text{Mean value}} \times 100\%$$

Eq 3.1

$$\text{Accuracy (\%RE)} = \frac{\text{(Calculated concentration} - C_{std})}{C_{std}} \times 100\%$$

Eq 3.2

where C_{std} is nominal concentration of the standard solution.

Evaluation of intra- and inter-day variations was conducted in triplicate for each quality control sample within the same day and within 3 days, respectively.

3.2.2 Phase solubility study

An excess amount of fisetin (5 mg) was added into 5 mL deionized water containing different concentrations of β-CD, HP-β-CD and SBE-β-CD (0.156-10 mM). Then, the phase solubility study was conducted as described in Section 2.2.

3.2.3 Investigation of spray and freeze drying of fisetin-SBE-β-CD complex

The complex was prepared at 1: 1 molar ratio as 1 molecule of cyclodextrin was found to form a complex with one molecule of fisetin, from the phase solubility study. This was done by adding 66.4 mg fisetin into 10 mL deionized water containing 500 mg SBE-β-CD. The mixture was then introduced to bath sonication (Clifton, UK) for 15 min, prior to mixing in an orbital incubator shaker (Sanyo Gallenkamp, Leicester, UK) at 100 rpm and 37°C for 24 h. The solution was then filtered using 0.45-µm syringe filter and subjected to different drying processes, namely freeze drying and spray drying (Section 2.3 and 2.4). The powder produced by both methods was immediately transferred to a desiccator at room temperature until further characterisation for particle size distribution.

3.2.4 Investigation of different complexation methods of fisetin-SBE-β-CD complex

Complexation of fisetin with SBE-β-CD was carried out at a 1: 1 molar ratio (5 mg fisetin and 37.65 mg SBE-β-CD) using two different methods of complexation, namely the aqueous method and the co-solvent method.

In the aqueous method, fisetin and SBE-β-CD were dissolved in 10 mL deionized water and mixed in a bath sonicator for 15 min. The mixture was further mixed for 24 h in a shaking incubator at 100 rpm and 37°C.

The co-solvent method involved solubilisation of fisetin in 2 mL absolute ethanol and SBE-β-CD in 8 mL deionized water. The solutions were mixed and sonicated in a bath sonicator for 15 min prior to solvent evaporation under vacuum at 80°C, using a rotary evaporator (RC900, KNF Neuberger, UK). The dried complex was rehydrated with rotation at 80°C using 10 mL deionized water and left to cool to room temperature. In both methods, final solutions were filtered using 0.45-µm syringe filter to separate the uncomplexed fisetin, and the filtrates were used for further studies.

3.2.5 Determination of *in vitro* anti-oxidant activity

The anti-oxidant activity of free fisetin and the complex solutions was determined using the DPPH assay described previously (Shang et al., 2010; Prabhu et al., 2011). The activity was determined by measuring scavenging of stable free-radical DPPH$^{\bullet}$ using a UV spectrophotometer at 517 nm. In this assay, addition of anti-oxidant into the DPPH$^{\bullet}$ solution will cause bleaching of the deep purple colour proportional to the concentration and anti-oxidant activity of the sample (Figure 3.1).

Control   Increasing concentration of fisetin solution
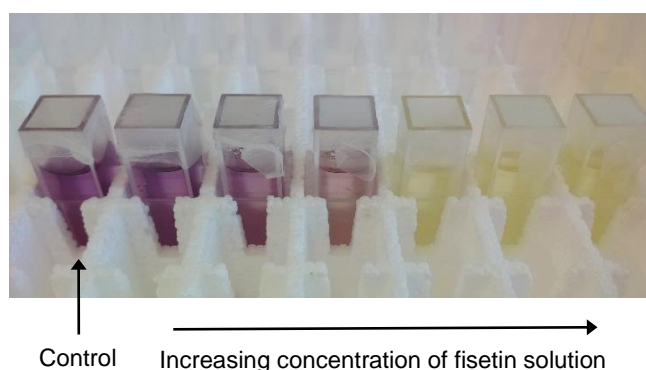
Figure 3.1 Mixture of DPPH solution and sample after 40 min incubation in the dark.

A 100 µM methanolic solution of DPPH$^{\bullet}$ was prepared by dissolving 7.88 mg DPPH in 200 mL methanol. The solution was protected from light and kept at -15°C until further use. Each test sample was prepared at 5 or 6 different concentrations prior

to the assay. Then, 1 mL of each concentration was added into 1 mL methanolic solution of DPPH$^{\bullet}$ and the solutions were mixed by aspiration, in a disposable cuvette. An equal amount of deionized water was added into 1 mL of DPPH$^{\bullet}$ solution to serve as a control. The cuvette was covered with a parafilm and the mixture was kept in the dark at ambient temperature for 40 min, prior to measurement in the UV spectrophotometer (Cary 100 UV-Vis, Agilent Technologies, USA) at 517 nm. The percentage of inhibition was calculated as follows;

$$\text{Inhibition (\%)} = \frac{\text{Abs Control} - \text{Abs Test}}{\text{Abs Control}} \times 100 \qquad \text{Eq 3.3}$$

The concentration at which the absorbance decreased by 50% (IC_{50}) was determined from a linear correlation between concentration of fisetin (mM) against the inhibition (%) for all tested samples. The anti-oxidant assay for each sample was done in triplicate and the IC_{50} was compared to ascorbic acid as a standard.

3.3 Results and discussion

3.3.1 Development and validation of HPLC-UV method for quantification of fisetin

Reported methods for determination of fisetin by HPLC used a combination of solvent (acetonitrile or methanol) and acidified water (2% v/v glacial acetic acid) as a mobile phase for separation on a C18 column (Mignet et al., 2012; Ragelle et al., 2012; Seguin et al., 2013). In this study, separation of fisetin on a C18 column was initially undertaken using acetonitrile and 0.1% v/v TFA in water as the mobile phase. However, the method produced a broad and non-symmetric peak of fisetin, which may be caused by the poor separation of the re-used column. Therefore, separation of fisetin using the same mobile phase was conducted on a Polar-RP column, an ether-linked phenyl column with polar endcapping, which was already available in the lab. The column is specific for maximizing the retention and selectivity of polar and aromatic analytes (Phenomenex, 2015) such as fisetin, thus producing a good-shaped and symmetric peak indicating a good separation.

Different compositions for the mobile phase were investigated to optimise retention time and the shape of the peak. A composition of 30: 70 (acetonitrile: 0.1%v/v TFA) was chosen as it gave a retention time ~8 min and a peak with a good symmetry. In this method, an analysis temperature of 25°C was not possible as the high aqueous composition caused a very high pressure in the column. Therefore, the separation was conducted at a column temperature of 40°C to reduce the viscosity of the mobile phase. This setting gave a column pressure of around 100 bar and produced a stable baseline within a short period of time.

Fisetin was dissolved in different solvent systems and stability of the solutions were evaluated visually. Fisetin was found to be stable in DMSO for more than 3 days while precipitation of fisetin in methanol was observed after 1 day. Thus, DMSO was used to prepare the stock solution, calibration and quality control samples. Literatures reported analysis of fisetin at a UV wavelength 360 nm (Mignet et la., 2012; Ragelle et al., 2012; Seguin et al., 2013; Bothiraja et al., 2014). In this study, the λ max of fisetin in DMSO was found to be at 362 nm (Figure 3.2), thus this wavelength was used in the study.
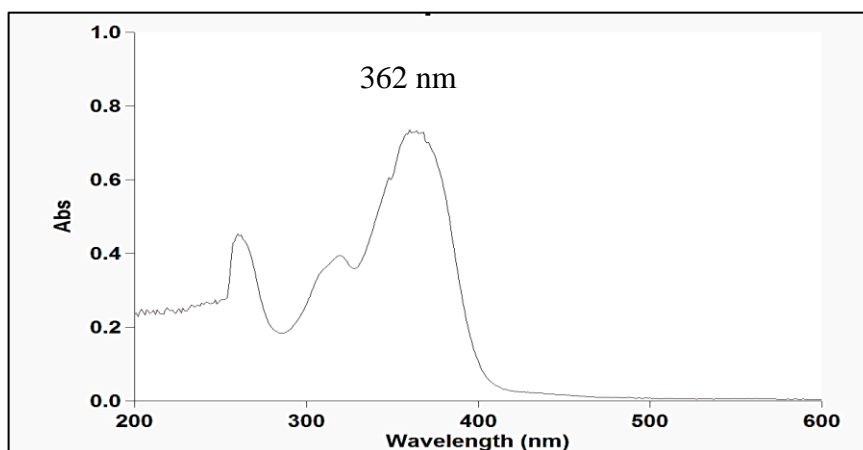
Figure 3.2 UV absorbance spectrum of fisetin in DMSO.

3.3.1.1 Specificity

Figure 3.3A shows a chromatogram of fisetin with a retention time of 8.4 min. Chromatograms of β-CD (Figure 3.3B), HP-β-CD (Figure 3.3C), SBE-β-CD (Figure 3.3D) and fisetin-SBE-β-CD complex (Figure 3.3E) show no interference from the excipients at the retention time of fisetin. Thus, the method was found to be specific and suitable for quantification of fisetin in all β-CD complexes.
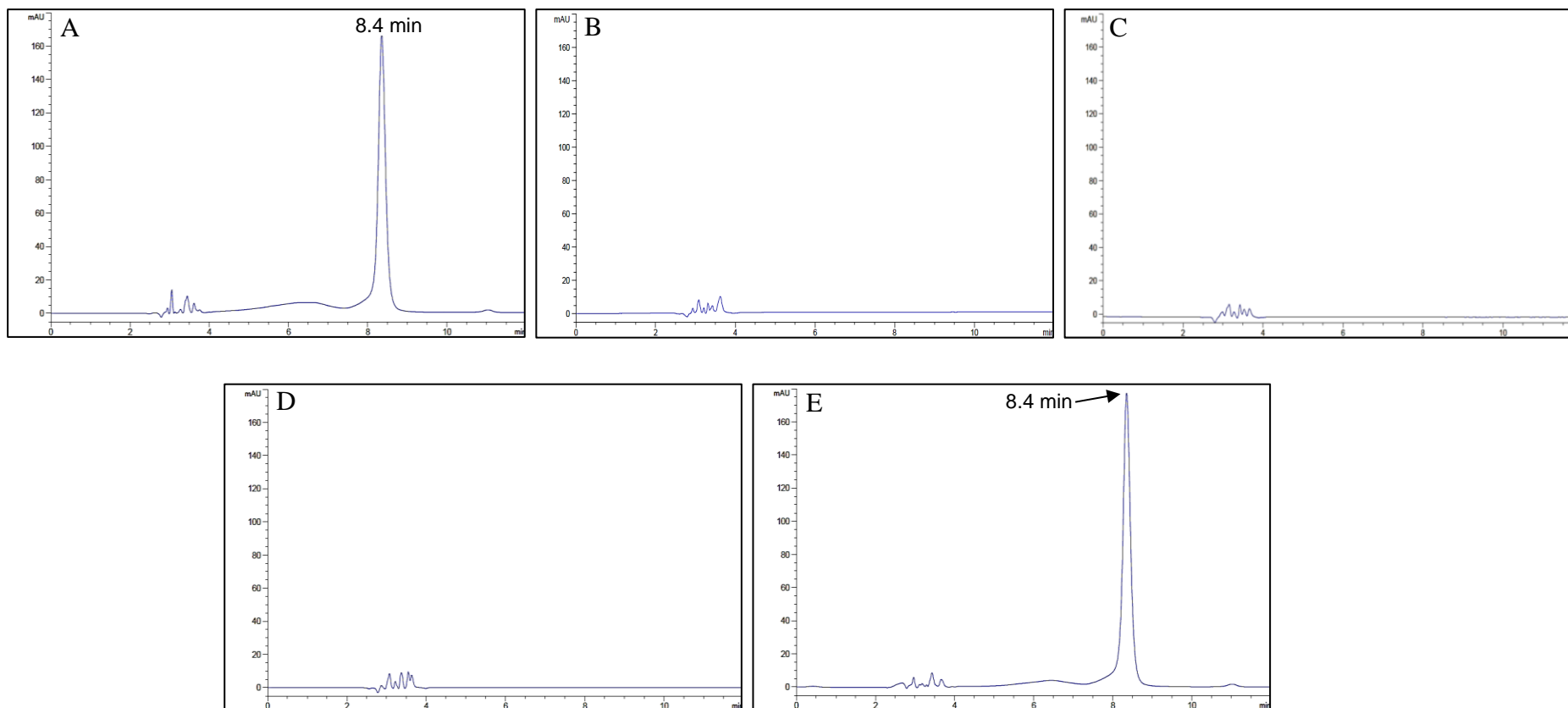
Figure 3.3 HPLC chromatograms of (A) fisetin solution, (B) β-CD solution, (C) HP-β-CD solution, (D) SBE-β-CD solution, and (E) fisetin-SBE-β-CD complex solution.

3.3.1.2 Validation of the analytical method

a) Limit of detection and limit of quantitation

The LOD and LOQ of the method were 0.4 µg/mL and 2 µg/mL, respectively. The LOQ showed a precision of 6.34% and accuracy of 7.50% which was within the limit of ±10% (Sistla et al., 2005).

b) Linearity

The precision and accuracy of all calibration points are presented in Table 3.2. The precision ranged from 2.92 to 6.34% and the accuracy ranged from -1.04 to 7.50%. The calibration points were found to be linear from 2 to 60 µg/mL (Figure 3.4). The mean linear regression equation from five calibration curves was y = 79.4022 (±2.5280)x − 22.9295 (±15.4958) with a coefficient of determination of 0.9998 (±0.0002).

Table 3.2 Calibration standards for fisetin. Mean ± s.d., $n = 5$.

Nominal concentration (µg/mL)	Calculated concentration (µg/mL)	Precision (%RSD)	Accuracy (%RE)
2	2.15 ± 0.14	6.34	7.50
10	9.95 ± 0.48	4.86	-0.53
20	19.79 ± 0.95	4.78	-1.04
30	29.95 ± 1.12	3.73	-0.15
40	40.14 ± 1.53	3.82	0.35
50	50.08 ± 1.46	2.92	0.16
60	59.93 ± 2.18	3.63	-0.11
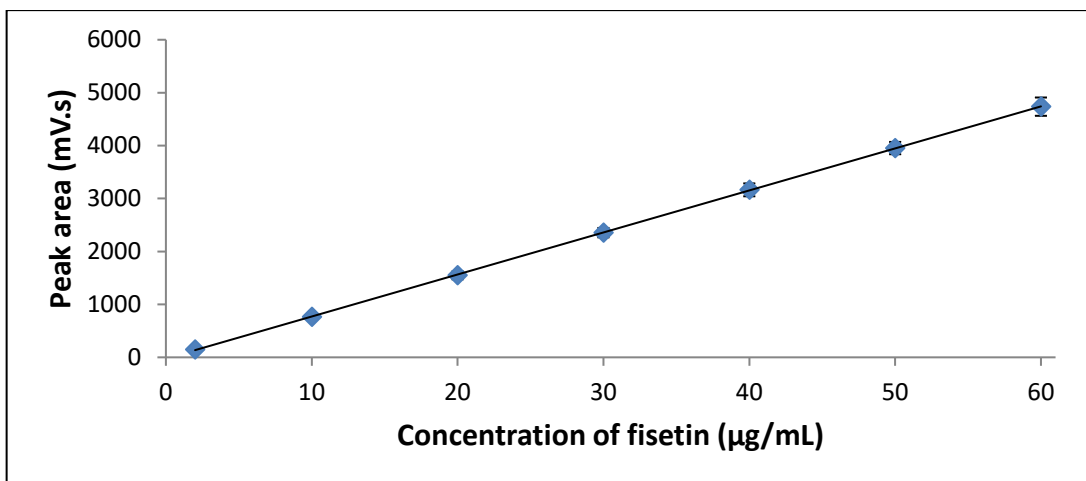
Figure 3.4 Calibration curves of fisetin. Mean ± s.d., $n = 5$.

c) Intra-day and inter-day validation

The intra-day precision ranged from 0.34 to 1.26% while the accuracy ranged from -1.62 to -2.52% (Table 3.3). The inter-day precision and accuracy was in the range of 2.94 to 3.20% and 1.20 to 2.21%, respectively. The intra- and inter-day validation of the method shows that all results were within the limit of ±5% (Sistla et al., 2005).

Table 3.3 Inter-day and intra-day validation of the method for fisetin. Mean ± s.d.

Nominal concentration (µg/mL)	Intra-day[a]			Inter-day[b]		
	Measured concentration (µg/mL)	%RSD	%RE	Measured concentration (µg/mL)	%RSD	%RE
15	14.67 ± 0.18	1.26	-2.18	15.21 ± 0.49	3.20	1.40
35	34.43 ± 0.18	0.34	-1.62	35.78 ± 1.05	2.94	2.21
55	53.61 ± 0.23	0.42	-2.52	55.66 ± 1.76	3.17	1.20

[a] three replicates for each concentration on the same day
[b] nine replicates for each concentration (day 1, $n = 3$; day 2, $n = 3$; day 3, $n = 3$)

3.3.2 Phase solubility study

A phase solubility plot of fisetin in three different cyclodextrins is shown in Figure 3.5. The plot depicts a Higuchi A_L type of phase solubility behaviour for all complexes;

a linear increase in solubility of fisetin with increasing concentration of cyclodextrins. The linearity can be confirmed as all systems show R^2 values greater than 0.99 (Table 3.4). The stability constant (K_s) is used to determine the solubilising efficiency of cyclodextrins for a drug (Pralhad and Rajendrakumar, 2004; Borghetti et al., 2009). The solubilising efficiency of fisetin in different cyclodextrins was in following order; SBE-β-CD > HP-β-CD > β-CD (Table 3.4). The K_s value of fisetin in the β-CD system was in agreement with a previous study of the complex in a neutral solution at 35°C, which was reported as 510 ± 30 M^{-1} (Guzzo et al., 2006). The K_s values corresponded to a greater solubilisation of fisetin at 10 mM SBE-β-CD (4.474 ± 0.239 mM) compared to the systems containing HP-β-CD and β-CD with values of 2.291 ± 0.046 and 0.628 ± 0.099 mM, respectively. All three complexes showed an increase in fisetin solubility in the aqueous solution compared to the free drug alone (0.110 ± 0.004 mM).
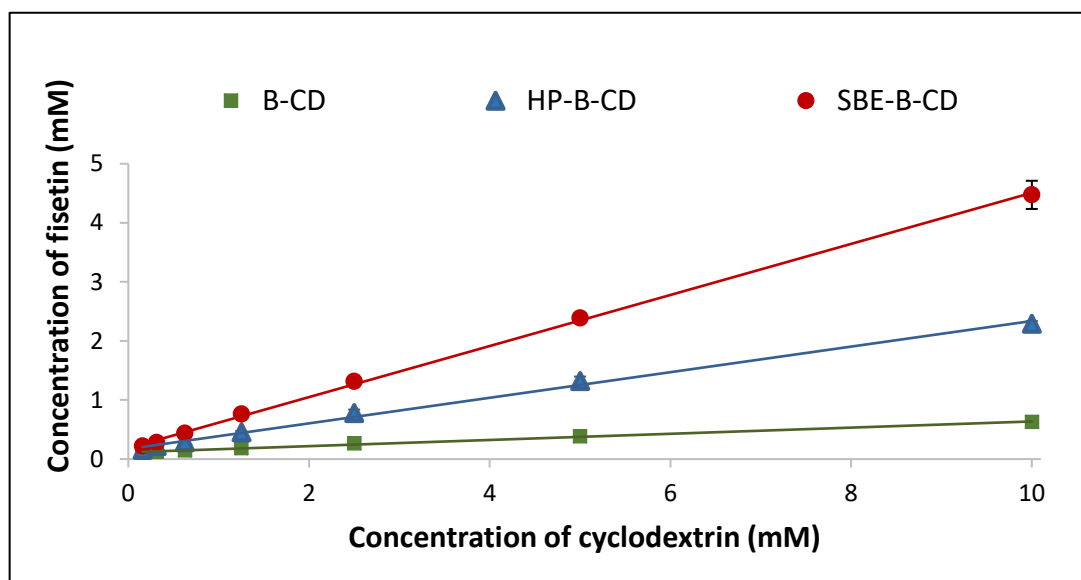
Figure 3.5 Phase solubility plots of fisetin in solutions of different cyclodextrins. Mean $\pm$ s.d., $n = 3$.

Table 3.4 shows complexation parameters for all fisetin-cyclodextrin complexes; 1: 1 stoichiometry (i.e. one molecule of cyclodextrin will form a complex with one molecule of fisetin) can be assumed as all slopes have values below 1 (Brewster and Loftsson, 2007). Complexation efficiency (CE) describes the ratio between cyclodextrin complex and free cyclodextrins. This parameter is more reliable than the K_s value, as it is independent of both the intrinsic solubility and the y-intercept,

as shown in Eq 2.1 and Eq 2.2 (Loftsson and Brewster, 2012). The CE values showed comparable results to that of the K_s values. The molar ratio calculated using Eq 2.3 shows that the best corresponding molar ratio of fisetin to respective cyclodextrins was in SBE-β-CD system (Table 3.4; i.e. 1 out of every 2 SBE-β-CD molecules forms a complex with fisetin). Lower molar ratio of drug to cyclodextrin is favoured as less cyclodextrin will be needed to form a soluble complex, thus reducing the bulkiness of the formulation. Thus, SBE-β-CD was chosen for further optimisation with fisetin.

Table 3.4 Complexation parameters of fisetin in different types of cyclodextrin. Mean $\pm$ s.d., $n = 3$.

Cyclodextrin	Slope	y-intercept, S_0 (mM)	Stability constant, K_s (M^{-1})	R^2	Complexation efficiency, CE	Molar ratio (Fisetin: CD)
β-CD	0.052 ± 0.009	0.114 ± 0.009	481.66 ± 67.38	0.9939 ± 0.0026	0.055 ± 0.010	1: 19
HP- β-CD	0.217 ± 0.001	0.171 ± 0.029	1647.25 ± 264.88	0.9942 ± 0.0045	0.277 ± 0.002	1: 5
SBE- β-CD	0.432 ± 0.019	0.184 ± 0.009	4138.84 ± 199.27	0.9985 ± 0.0007	0.763 ± 0.058	1: 2

3.3.3 Determination of anti-oxidant activity

The anti-oxidant activities of fisetin in the complexes formed by all three cyclodextrins were compared to that of the fisetin solution (Figure 3.6). The IC_{50} values of all samples were determined from interpolation of the graph concentration of fisetin against the percentage of inhibition (see example in Appendix A). There was no significant difference in the IC_{50} values ($p > 0.05$) suggesting that complexation with all cyclodextrins maintained the anti-oxidant activity of fisetin. An unchanged anti-oxidant activity has also been reported when resveratrol (a dietary polyphenol) was complexed with β-CD and HP-β-CD (Lu et al., 2009). Further, the solutions of free fisetin and fisetin-cyclodextrin complexes showed significantly lower IC_{50} values ($p < 0.05$) compared to ascorbic acid, suggesting better anti-oxidant activity in all fisetin-containing solutions. The DPPH assay was also conducted on blank cyclodextrins solution. The cyclodextrins did not show any inhibition in the DPPH activity up to 50 mM concentration, confirming that the anti-oxidant activity of all formulations was solely a function of fisetin.
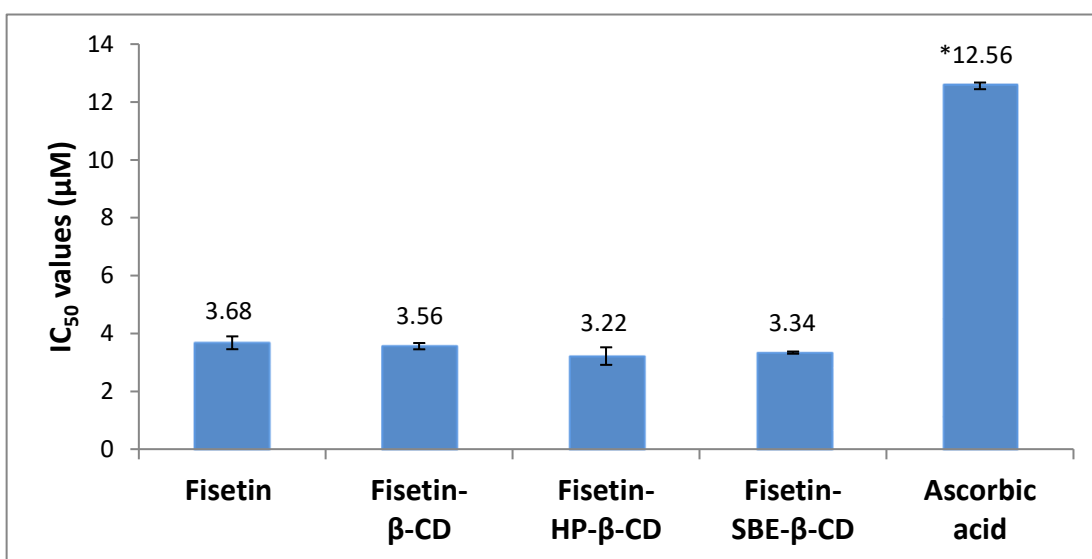
Figure 3.6 IC_{50} values of fisetin, fisetin-cyclodextrin complexes and ascorbic acid. Mean ± s.d., $n = 3$, *significant difference compared to fisetin solution, $p < 0.05$. Concentration of fisetin has been normalised in all samples.

3.3.4 Investigation of spray and freeze drying of fisetin-SBE-β-CD complex

3.3.4.1 Particle size distribution

The effect of two different drying methods on powder characteristics and anti-oxidant activities of the dried complexes was investigated. Table 3.5 shows that the spray-dried complex had a smaller particle size (X_{50}: 1.74 µm) compared to the freeze-dried complex (X_{50}: 24.93 µm). The former powder also showed a narrower particle size distribution compared to the latter as indicated by the Span values of 1.66 and 2.65, respectively. In terms of particle size and distribution, the spray-dried powder is more suitable for inhalation purpose as 50% of the particles were below 5µm (EMA, 2006).

Table 3.5 Physical properties of the dried fisetin-SBE-β-CD complex from different drying methods. Mean ± s.d., $n = 3$, *p < 0.05.

Sample	X_{50} (µm)	Span
Spray-dried complex	*1.74 ± 0.09	*1.66 ± 0.01
Freeze-dried complex	24.93 ± 1.06	2.65 ± 0.14

3.3.4.2 Anti-oxidant activity

In the DPPH assay, no significant change (p > 0.05) was observed in the IC_{50} values of the dried complexes compared to fisetin solution and fisetin-SBE-β-CD complex solution (Figure 3.7). The results indicate that both drying methods did not affect the *in vitro* anti-oxidant property of fisetin within the complex.
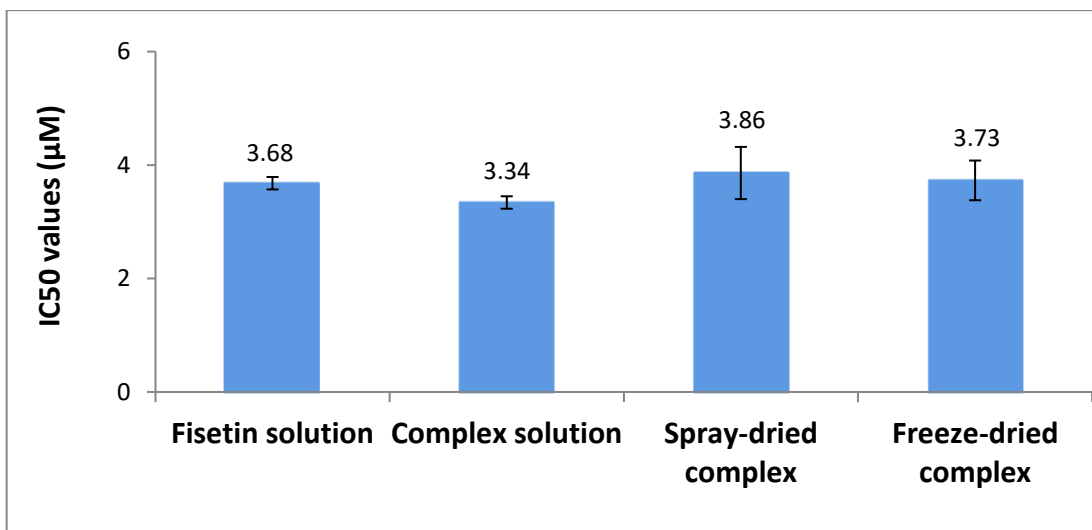
Figure 3.7 IC$_{50}$ values of fisetin in the dried SBE-β-CD complexes in comparison to the solutions. Mean ± s.d., $n = 3$.

3.3.5 Investigation of different complexation methods of fisetin-SBE-β-CD complex

In the preparation of drug-cyclodextrin complexes, ethanol has previously been used as a solvent (Cabral-Marques and Almeida, 2009; Zheng and Chow, 2009; Bhise, 2011). In this study, ethanol alone could not be used as the solvent system, as SBE-β-CD is not soluble in ethanol. Co-solvency (i.e. addition of solvent into aqueous solution) can be used to enhance the complexation process as the solvent can help to increase the solubility of a hydrophobic drug (Loftsson and Brewster, 2012). In a preliminary study, different ratios of ethanol and water were studied to find an optimal composition that would facilitate and enhance the complexation process. The ethanol content affected the stability of the formed complexes, with sub-optimal compositions resulting in precipitation of fisetin within 3 h of preparation. It has been reported that ethanol content should be optimised, as too high solvent content reduces the inclusion of drug, as solvent will competitively bind to the cyclodextrin molecules (Li et al., 2009). In this study, this may cause the expulsion of fisetin from the cavity of the cyclodextrin, causing precipitation. Thus, 20%v/v of ethanol in water was selected for the co-solvent method, based on optimal drug inclusion and minimal precipitation.

The percentage of solubilised fisetin in complexes prepared using the aqueous and co-solvent methods was 15.2 ± 1.1 and $90.2 \pm 3.9\%$, respectively, indicating that complexes produced by the co-solvent method had a 5.9-fold higher ($p < 0.05$) content of solubilised fisetin (Figure 3.8).

A higher molar ratio of fisetin to SBE-β-CD was tested in the co-solvent method. However, a higher ratio was unable to increase the amount of fisetin forming complexes with SBE-β-CD. Therefore, a molar ratio of 1: 1 was maintained for further studies.
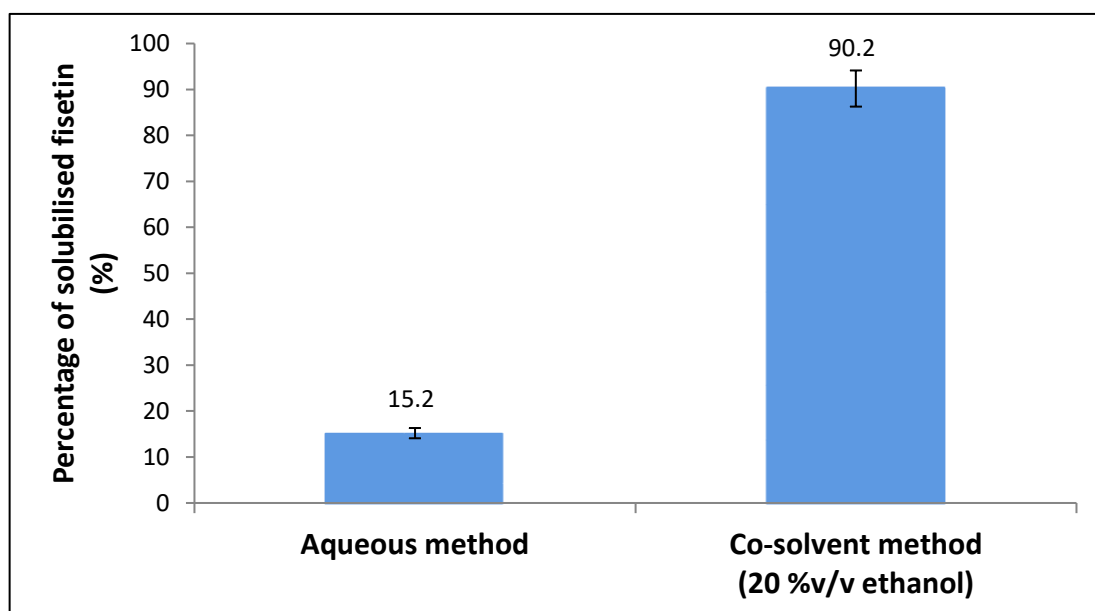
Figure 3.8 Percentage of solubilised fisetin in complexes produced by two methods. Mean $\pm$ s.d., $n = 3$.

3.4 Conclusion

In this chapter, a new reliable HPLC method was developed for determination of fisetin using UV detection. The method used a simple mobile phase composition, comprising acetonitrile: 0.1%v/v TFA in water (30: 70) which was easy to prepare, and the method was validated according to the relevant ICH guideline. The method was shown to be simple, specific, precise and accurate for quantification of fisetin in the study.

Complexation of fisetin with three different cyclodextrins (i.e. β-CD, HP-β-CD and SBE-β-CD) was successfully undertaken and the best complexation efficiency was shown with fisetin-SBE-β-CD complex. Complexation with all three cyclodextrins was able to enhance the solubility of fisetin without altering its *in vitro* anti-oxidant activity. Drying of fisetin-SBE-β-CD complex solution using freeze-drying and spray-drying methods did not affect the anti-oxidant activity of fisetin, while spray drying was found to be suitable to produce a dry powder with appropriate size properties for inclusion in inhalable formulations. Two methods were compared for the complexation of fisetin with SBE-β-CD, namely aqueous and co-solvent method. The co-solvent method, using a mixture of water and ethanol (20%v/v), resulted in an improvement in the percentage of solubilised fisetin by 5.9-fold compared to the aqueous method. Thus, the co-solvent method is used in the next chapter for further optimisation.

Chapter 4

Production of a dry powder fisetin-SBE-β-CD complex for inhalation

4.1 Introduction

In Chapter 3, spray drying was found to be capable of producing a dry powder of fisetin-SBE-β-CD complex with physical size suitable for inhalation purposes. In this chapter, fisetin-SBE-β-CD complex prepared using the co-solvent method was chosen for further investigation. The co-solvent method was found to increase the amount of solubilised fisetin in the preparation. As the preparation was in solution, it was imperative to remove the organic solvent (i.e. ethanol) by rotary evaporation, and the complex was then rehydrated with water. As spray drying was introduced at a later stage to produce an inhalable powder, the ethanol could also be removed by that process. An omission of evaporation and rehydration steps was considered an interesting approach, worth of investigation, to simplify the preparation steps. Therefore, the physical characteristics and *in vitro* aerosol deposition profile of the dry powders produced from two types of feed solutions (i.e. feed solution containing water and feed solution containing 20%v/v ethanol in water) were investigated.

Addition of dispersibility enhancers such as leucine into formulations prior to spray drying, has been shown to yield powders with improved aerosolisation properties (Li et al., 2003; Rabbani and Seville, 2005; Seville et al., 2007). Thus, this chapter will also present and discuss the use of leucine in some formulations as a means of improving the physical and aerosolisation properties of the spray-dried powders.

4.2 Methods

4.2.1 Investigation of different feed solution compositions for spray drying

Fisetin-SBE-β-CD complex was prepared using the co-solvent method containing 20%v/v ethanol in water and a 1: 1 molar ratio of fisetin to SBE-β-CD. In brief, 66.4 mg fisetin and 500 mg SBE-β-CD were dissolved in 27 mL ethanol and 106 mL deionized water, respectively, prior to mixing in a bath sonicator for 15 min. This preparation produced a 1.74 mM concentration of both the drug and excipient. The

mixture was then treated differently to produce two feed solutions for spray drying (Figure 4.1).
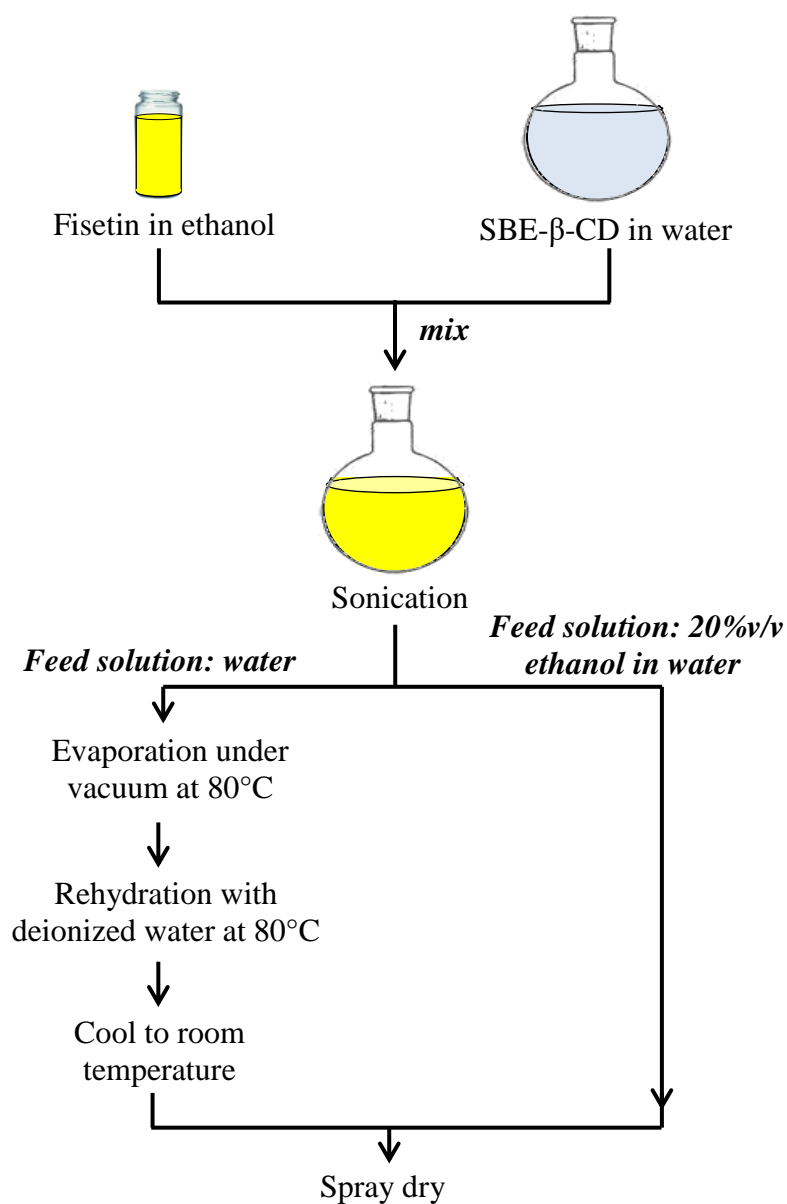
Figure 4.1 Schematic diagram of spray drying steps from different feed solutions.

For the feed solution containing 20% v/v ethanol in water, the mixture was directly subjected to spray drying. This preparation was coded as SD_20% Eth. For the feed solution containing water alone, the mixture containing 20% v/v ethanol in water was subjected to solvent evaporation under vacuum at 80°C using a rotary evaporator, to remove the ethanol. Then, the dried complex was rehydrated with 133 mL deionized

water for 10 min at 80°C and left to cool to room temperature. This preparation was coded as SD_ H_2O.

Both solutions in a final total powder mass of 0.4%w/v were spray dried and the dried powder produced by both methods was immediately transferred to a desiccator at room temperature until further analysis.

4.2.2   Incorporation of leucine as a dispersibility enhancer

It was found in the study that spray drying from the feed solution containing 20%v/v ethanol produced a powder with better aerosolisation properties compared to the feed solution containing water alone. Therefore, incorporation of leucine into the former feed solution was done to further improved aerosolisation properties of the preparation. Fisetin-SBE-β-CD complex solution containing 20%v/v ethanol in water was prepared as in Section 4.2.1 and leucine was added at a concentration of 0, 5, 10 and 20%w/w prior to spray dying (Table 4.1). The solution was stirred with magnetic stirring for 10 min, producing a final total powder mass of 0.4%w/v in every formulation. The formulations were spray dried and stored in a desiccator at room temperature.

Table 4.1 Composition of fisetin-SBE-β-CD complex preparations containing leucine.

Formulation Code	Leucine (%w/w)	Fisetin (mg)	SBE-β-CD (mg)	Leucine (mg)	Total weight (mg)
SD_20%Eth	0	66.4	500.0	-	566.4
SD_20%Eth5%Leu	5	63.1	475.0	28.3	566.4
SD_20%Eth10%Leu	10	59.8	450.0	56.6	566.4
SD_20%Eth20%Leu	20	53.1	400.0	113.3	566.4

4.2.3 Characterisation of the preparations

Preparations were characterised for yield and amount of solubilised drug as described in Section 2.5. They were also characterised for particle size distribution, XRPD, FT-IR, TGA and SEM, as described in Section 2.7, 2.8, 2.9, 2.10, and 2.11, respectively .

4.2.4 Assessment of aerosol properties using the Next Generation Impactor (NGI)

The aerosol properties of the dry powders were evaluated using the NGI (Copley Scientific Limited, Nottingham, UK) conducted under pharmacopoeial conditions (Apparatus E, European Pharmacopoeia, Chapter 2.9.18). Air flow through the apparatus was adjusted to 60 ± 3 L/min using the vacuum pump and two-way solenoid valve timer. The air flow rate was tested using a flow meter (DFM2000, Copley Scientific Limited, Nottingham, UK) prior to testing.

In the setting of powder inhalation, a pre-separator is placed above Stage 1 to collect large masses of non-respirable particles (Figure 2.2). The central cup of the pre-separator insert was filled with 15 mL deionized water and the micro-orifice collector (MOC) stage was fitted with a $1.6\,\mu$m glass microfiber filter (Whatman, UK). The impaction cups were coated with 1%v/v silicone oil in hexane prior to analysis, and left to dry for 1 h. The coating was done to minimise particle bounce that may cause re-entrainment of the particles into the air stream, causing them to be carried to a lower stage (Copley Scientific, 2015). Powder samples (30 ± 1 mg) were accurately weighed and filled into no. 3 hard gelatine capsules (Alchemists Apothecary, Derbyshire, UK) and were individually loaded into the dosage chamber of an Aerolizer® device (Novartis, Surrey, UK; Figure 1.8a). The capsule was pierced and the Aerolizer® mouth-piece was inserted into a mouth-piece adaptor. The powder was drawn via an induction port into the NGI and tested for 4 s at 60 L/min, using 3 capsules for each sample. After all three actuations, powders in capsules, device, mouthpiece, induction port, pre-separator and stage 1-8 of the NGI were collected with thorough rinsing using deionized water into separate volumetric flasks. The solutions were mixed in a bath sonicator for 15 min and appropriately diluted prior to fisetin

determination using HPLC (Section 3.2.1). Under these conditions, the cut-off diameter for each NGI stage are as in Table 4.2.

Table 4.2 Cut-off diameter of each NGI stage at 60 L/min (Apparatus E, European Pharmacopoeia, Chapter 2.9.18).

Stage	Cut-off diameter (µm)
1	8.06
2	4.46
3	2.82
4	1.66
5	0.94
6	0.55
7	0.34
8	Micro-Orifice Collector (MOC)

The amount of fisetin on each stage was quantified and the aerosolisation parameters were calculated. Mass balance (MB) is expressed as percentage of total weight of fisetin recovered from all parts of the NGI in comparison to the initial total amount of loaded fisetin;

$$MB = \frac{\text{Mass of fisetin from capsule to Stage 8}}{\text{Initial mass of fisetin loaded into the capsule}} \times 100 \qquad \text{Eq 4.1}$$

Emitted fraction (EF) is the percentage of total mass of fisetin coming out from the capsules after each impactor run;

$$EF = \frac{\text{Mass of fisetin from device to Stage 8}}{\text{Mass of fisetin from capsule to Stage 8}} \times 100 \qquad \text{Eq 4.2}$$

The fine particle dose (FPD) was determined by plotting the cumulative mass of fisetin versus cut-off diameter of the corresponding stage (see example in Appendix B). The FPD was calculated by interpolation of the mass of fisetin less than 5 µm. Fine particle fraction (FPF) is defined as percentage of the FPD in comparison to the total recovered dose;

$$FPF = \frac{Fine\ particle\ dose}{Total\ recovered\ mass\ of\ fisetin\ in\ all\ stages} \times 100 \qquad Eq\ 4.3$$

Mass median aerodynamic diameter (MMAD) is determined as the particle size at the 50% of cumulative fraction by mass for the aerosolised powders. It is calculated from the graph of cumulative fraction against effective cut-off diameter on log probability axes (see example in Appendix C). Geometric standard deviation (GSD) is a measure of the width of an aerodynamic particle size distribution. It is calculated using the same plot as for calculation of MMAD using the following formula;

$$GSD = (d_{84}/d_{16})^{1/2} \qquad Eq\ 4.4$$

where d_{84} and d_{16} describe the diameters of which 84% and 16% of the aerosol mass is included, respectively.

4.2.5 *In vitro* cell toxicity of fisetin and the spray-dried formulation (MTT assay)

The cell culture and MTT assay were conducted as described in Section 2.13, to compare the toxicity of fisetin in the solution and in the optimised formulation (SD_20%Eth20%Leu). The treatment solutions included fisetin, spray-dried powder containing 20%w/w leucine and the blank formulation (containing SBE-β-CD and leucine), at concentrations of fisetin ranging from 4.69 to 600 µM.

In the preparation of treatment solutions, a stock solution of fisetin (350 mM) was prepared by dissolving 5 mg fisetin in 50 µL DMSO. The solution was then diluted with complete media to produce 4.69-600 µM fisetin solution. 10 mg of the spray-

dried complex (SD_20%Eth20%Leu) was dissolved in 1 mL complete media and diluted into solutions containing 4.69-600 µM fisetin. The blank formulation was dissolved separately in 1 mL complete media and diluted according to the dilution of the formulation.

The A549 cells were seeded at a density of 2 x 10^4 cells per well, in a 96-well plate. The cells were incubated for 24 h at 37°C (5% CO_2/95% air), prior to removal of the media. The cells were then treated with 200 µL treatment solutions. As the highest concentration of fisetin samples contained the highest concentration of DMSO (0.1% v/v), the cells were also treated with 0.1% v/v DMSO in the media to evaluate the DMSO-derived cytotoxicity. Treatment with complete media was used as a negative control and experiments were done in triplicate on three different days. The cells were incubated with the treatments for 48 h prior to the MTT assay, as described in Section 2.13.2. The cell viability was calculated according to Eq 2.7.

4.3 Results and discussion

4.3.1 Investigation of different feed solution compositions for spray drying

4.3.1.1 Particle size distribution, yield and residual solvent content

Particle size analysis of the powders by laser diffraction was conducted using air dispersion at 4 bar as a lower pressure was not sufficient to adequately disperse the particles. The spray-dried powder produced from the feed solution containing water alone (SD_H$_2$O) showed a unimodal particle size distribution (Figure 4.2) with all particles less than 5 µm. The particles showed a narrow size distribution with an X_{50} value of 1.50 ± 0.18 µm and Span value of 1.55 ± 0.25 (Table 4.3). The spray-dried product was in the form of a fine powder which may contribute to its ability to disperse easily (Figure 4.3A).

The spray-dried powder produced from a feed solution containing 20% v/v ethanol (SD_20%Eth) displayed a bimodal size distribution with a group of particles having a mode less than 3 µm, and another population of particles in the size range: approximately 3-20 µm probably indicating agglomeration of smaller particles. The

wider particle size distribution resulted in a Span value of 3.14 ± 0.51, though the X_{50} value was 1.48 ± 0.08 µm (Table 4.3). The powder appeared to be sticky and was in the form of large clumps, which were easy to break up (Figure 4.3B). This may explain the product's tendency to agglomerate into bigger particles.
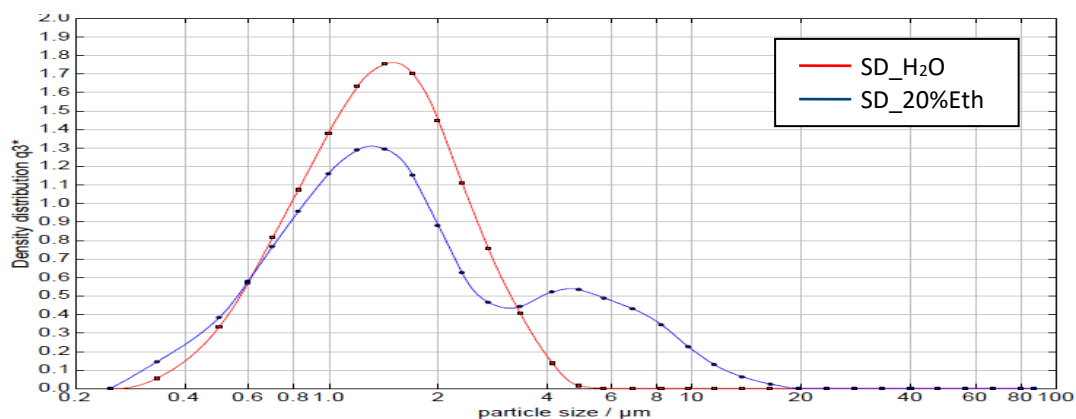
Figure 4.2 Particle size distribution of the spray-dried powders from different feed solutions.
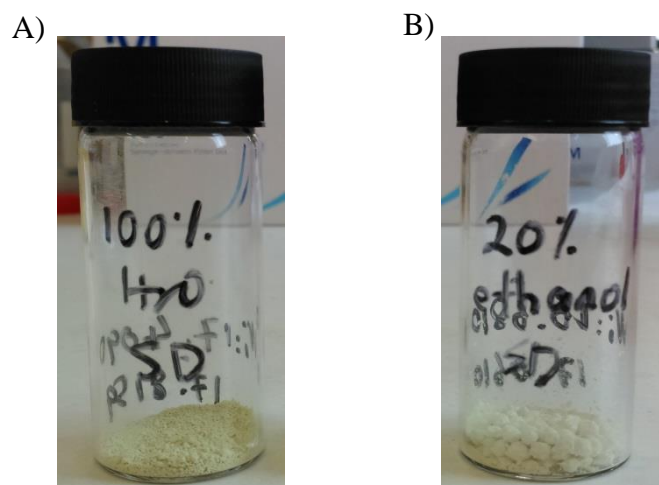
Figure 4.3 Spray-dried powder of fisetin-SBE-β-CD complexes, A) SD_H$_2$O and B) SD_20%Eth.

Table 4.3 shows that 90% of particles (X_{90}) produced from a feed solution containing water alone were significantly smaller ($p < 0.05$) compared to particles produced from a feed solution containing 20% v/v ethanol, with the size of 3.05 and 5.31 µm, respectively. Nevertheless, both powders were suitable for inhalation as majority of the particles were below 5 µm. The powder produced from the feed

solution containing 20 %v/v ethanol, gave a yield of 63.9 ± 2.7% which was lower than the powder produced from feed solution containing water alone (74.4 ± 0.9%). This may be caused by the cohesive properties of the former powder, which can be seen from the large clumps (Figure 4.3B). Cohesive powder has been shown to result in low spray drying yield (Li et al., 2005a) and the lower yield may also indicate adhesive particles with a greater tendency to adhere to the wall of the spray dryer (Seville et al., 2007).

The formulations showed no difference ($p > 0.05$) in the residual solvent contents, with values of 7.75% for the powder produced from feed solution containing water and 8.31% for the powder produced from feed solution containing 20%v/v ethanol (Table 4.3). The residual solvent content of spray-dried powders varies between formulations, with some reports of ~3% (Chang et al., 2014) and others between 6 and 11% (Maa et al., 1998; Gilani et al., 2005), and depends on the hygroscopicity of the material. Evaporation of the solvent molecules in the drying chamber of the spray dryer will cause an increase in the vapour concentration within the instrument. A hygroscopic material will tend to take up more water during the spray-drying process, causing a higher residual solvent content in the final formulation (Gilani et al., 2005). SBE-β-CD 7 used in this study has been shown to be hygroscopic and absorb more moisture compared to other substituted SBE-β-CD (i.e. SBE-β-CD 4 and 5; the number indicates the average number of substituted sulfobutylether groups per CD) (Jain and Adeyeye, 2001). Thus, giving a high residual solvent content.

Despite the residual solvent, the powders were able to be adequately dispersed during measurement in laser diffraction analyser and NGI, giving acceptable particle size distribution and FPF.

Table 4.3 Physical properties of spray-dried complexes produced from different feed solution compositions. Mean $\pm$ s.d., $n = 3$.

Preparation	Particle size (μm)[a]				Yield (%)	Solubilised fisetin (%)	Residual solvent (%)
	X_{10}	X_{50}	X_{90}	Span			
SD_H$_2$O	*0.70 $\pm$ 0.03	1.50 $\pm$ 0.18	*3.05 $\pm$ 0.71	*1.55 $\pm$ 0.25	*74.4 $\pm$ 0.9	96.15 $\pm$ 3.58	7.75 $\pm$ 0.37
SD_20%Eth	0.63 $\pm$ 0.02	1.48 $\pm$ 0.08	5.31 $\pm$ 1.03	3.14 $\pm$ 0.51	63.9 $\pm$ 2.7	96.75 $\pm$ 5.02	8.31 $\pm$ 0.53

[a] analyzed by a laser diffraction analyzer at a dispersion pressure of 4 bar.
* $p < 0.05$

4.3.1.2 FT-IR analysis of the spray-dried complexes produced from different feed solution compositions

The infrared spectra of all samples are presented in Figure 4.4. The fisetin crystal showed a characteristic O-H stretch at 3344.18 and 1205.94 cm^{-1}. These peaks are still evident in the spectrum of a physical mixture of fisetin and SBE-β-CD, suggesting that fisetin remained in its crystalline state without any interaction in the mixture. However, the peaks are absent on the spectra of spray-dried formulations (Figure 4.4d and e) indicating restriction of vibration and bending of fisetin molecules in the host cavity of the inclusion complex. Further, SBE-β-CD had a broad peak at 3382.94 cm^{-1}, which indicates O-H stretch of the alcoholic group in the molecule (Figure 4.4b). It also has a C-H stretch of the alkane group at 2928.98 cm^{-1}. These peaks are less obvious on the spectrum of the physical mixture, but can be clearly seen in the spectra of spray-dried formulations. No new peaks were seen in the spectra of the complex, indicating no chemical interaction between fisetin and SBE-β-CD molecules. This was expected as the host-guest complex is reported to depend on hydrophobic interaction between the lipophilic cavity of the cyclodextrin and the drug, without formation or breakage of covalent bonds (Del Valle, 2004).
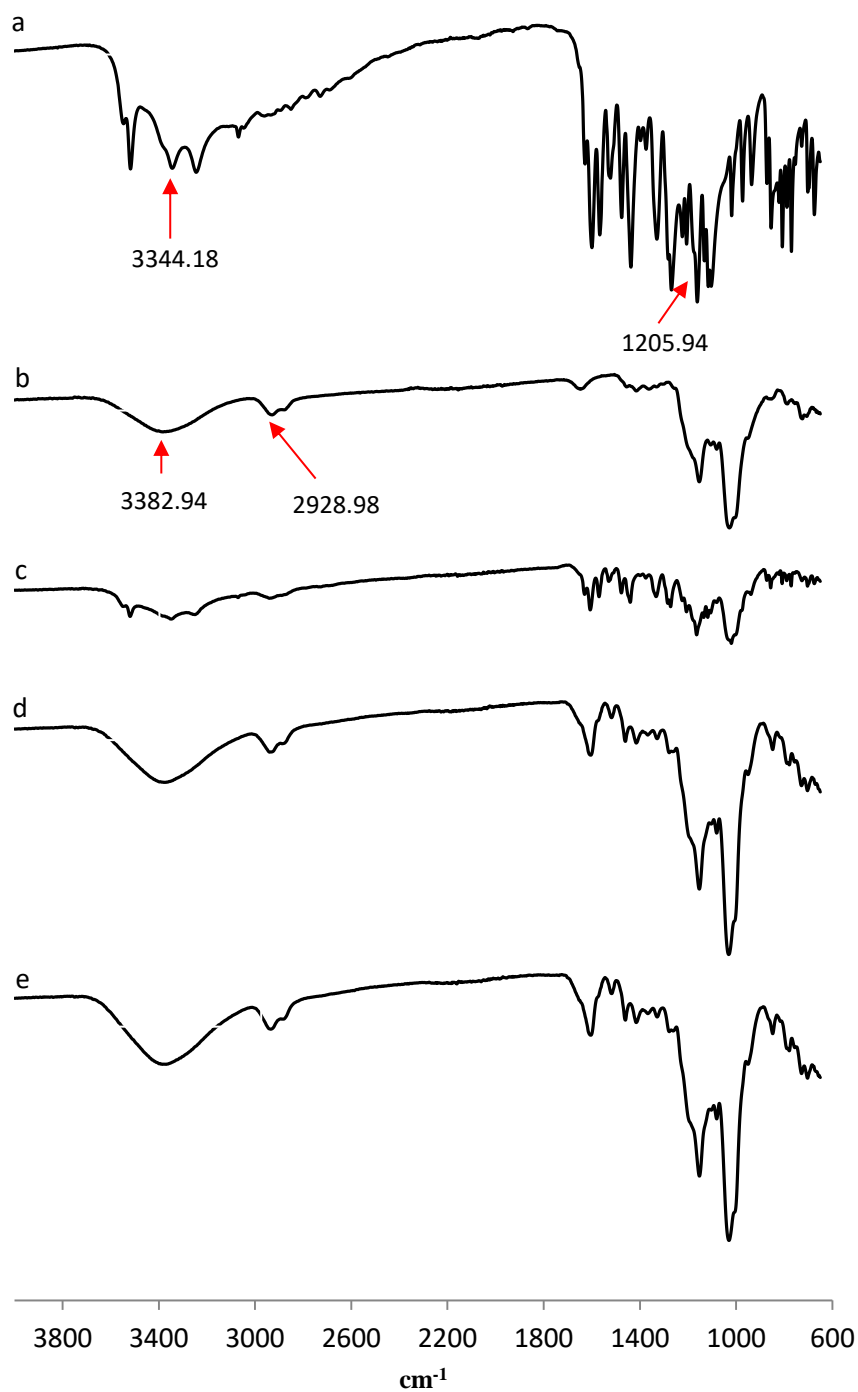
Figure 4.4 FT-IR spectra of a) fisetin, b) SBE-β-CD, c) physical mixture, d) SD_H$_2$O and e) SD_20%Eth.

4.3.1.3 XRPD analysis of the spray-dried complexes produced from different feed solution compositions

The diffractogram of pure fisetin (Figure 4.5a) indicated a typical crystalline nature with a large number of sharp diffraction peaks, especially at 12.35, 15.50, 24.05, 26.25 and 28.25° (2θ). In contrast, broad and diffused peaks with low intensities were recorded for pure SBE-β-CD, indicating its amorphous state (Figure 4.5c). Some diffraction peaks from the crystalline fisetin are visible on the diffractogram of the physical mixture (labelled with arrows, Figure 4.5d), but with lower intensities as fisetin was diluted with SBE-β-CD. Spray drying of fisetin from 20%v/v ethanol solution was also done (Figure 4.5b), to determine if the drying process has any impact on the crystallinity of the drug. The spray-dried fisetin showed low intensities and less diffraction peaks (labelled with arrows) compared to the pure fisetin, indicating the presence of a mixture of amorphous and crystalline state in the preparation. A mixture of both states was caused by the difference in the solubility of the drug in different solvents. A low solubility of fisetin in water led to a formation of crystalline powder, while an increased solubility of fisetin in ethanol led to a formation of amorphous powder. However, complexation of fisetin with SBE-β-CD improved the solubility of the drug in both aqueous and ethanolic feed solutions, producing amorphous powder as shown by the broad and diffused peaks and the disappearance of sharp peaks (Figure 4.5e and f).
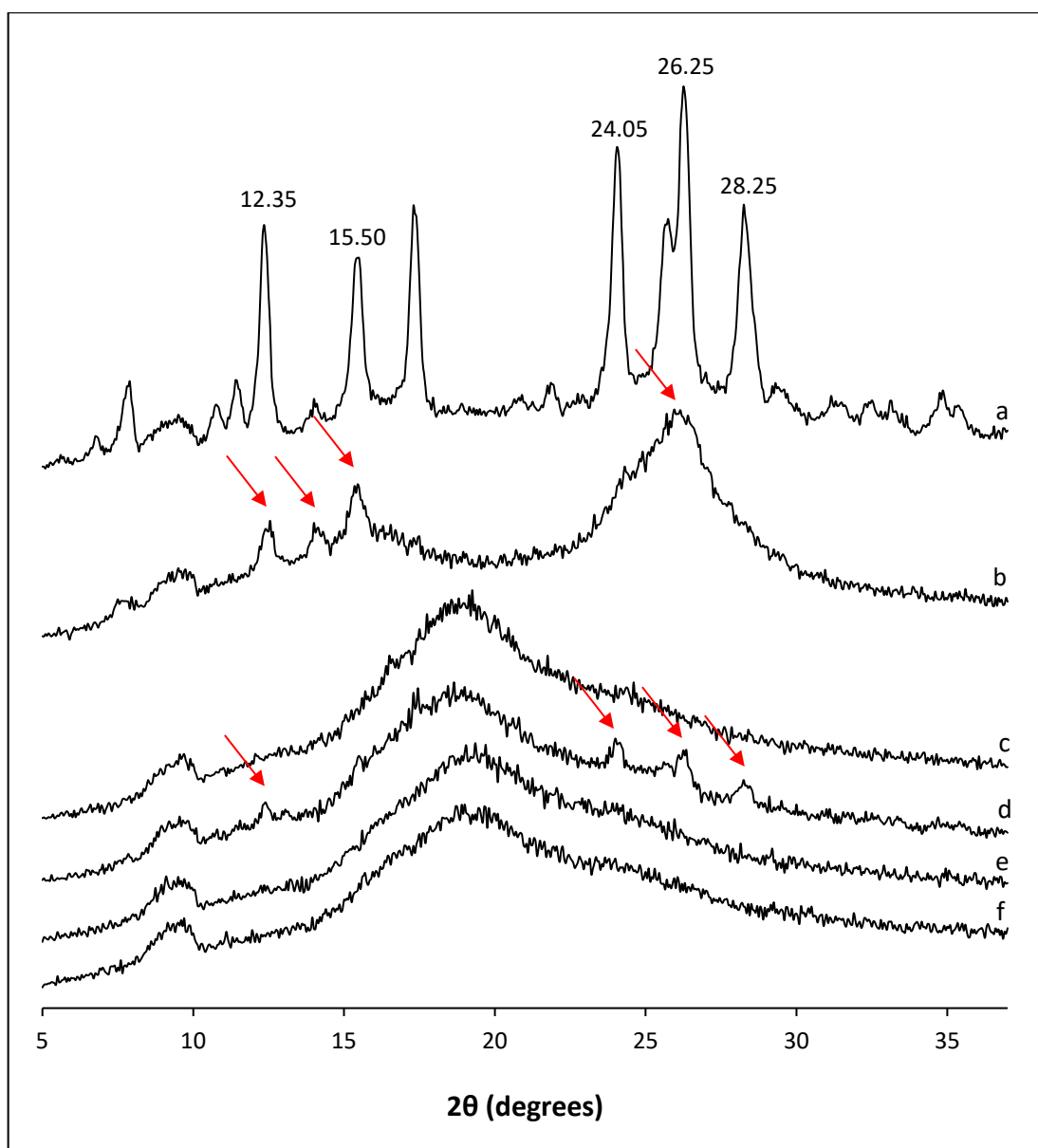
Figure 4.5 XRPD diffractograms of a) fisetin, b) spray-dried fisetin in 20%v/v ethanol in water, c) SBE-β-CD, d) physical mixture, e) SD_H$_2$O and f) SD_20%Eth. The red arrows showing fisetin's peaks.

4.3.1.4 *In vitro* **aerosol deposition study of the spray-dried complexes produced from different feed solution compositions**

In the NGI, an air flow of 60 L/min was used, as for previous impactor studies using the Aerolizer® (Son and McConville, 2012; Scalia et al., 2013). Figure 4.6 shows the distribution of fisetin in the NGI. The spray-dried powder produced from a feed solution containing 20%v/v ethanol showed improved aerosolisation, based on lower deposition in the capsules to pre-separator stage but higher deposition in Stage 2 onwards compared to powder produced from a feed solution in water.

Table 4.4 shows the aerosol properties for both formulations calculated from the NGI deposition results. The powder which was produced from a feed solution containing 20%v/v ethanol had a higher fine particle fraction (FPF) compared to spray-dried powder produced from a feed solution containing water alone. The powder produced from 20%v/v ethanol also showed a 2-fold increase ($p < 0.05$) in the fine particle dose (FPD). The difference in the FPF and FPD between both powders may be explained by the possible difference in the particle formation process from each feed solution, which can be explained using the Peclet number (P*e*).

Droplets produced from the feed solution containing water alone will have a lower evaporation rate compared to the ethanolic feed solution, as the boiling point of water (100ºC) is higher than ethanol (78.4ºC). From the equation (Eq 1.2), lower evaporation rate and/or high diffusion coefficient will result in a lower P*e* (i.e. ≤ 1). In this condition, the slow evaporation rate of solvent from the droplet gives the solutes adequate time to redistribute within the drying droplets, leading to dense solid particles.

Meanwhile, a higher evaporation rate of solvent from the droplets produced from an ethanolic feed solution, will lead to formation of a shell as the solutes do not have sufficient time to diffuse from the surface. Rapid solidification of the shell will form hollow or more porous particles, with lower density (Rizi et al., 2010). In this study, the powder produced from the ethanolic feed solution was fluffier and lighter compared to the powder produced from the feed solution containing water only. Even though the powder had a higher X_{90} value (Table 4.3) compared to the powder

produced from the feed solution containing water alone, lower density will cause a reduction in the aerodynamic diameter (Eq 1.1), making the powder move more readily to the lower stages of the NGI. An improvement in the FPF and FPD has also been shown when a powder was spray-dried from an aqueous feed solution containing a solvent (i.e. isopropyl alcohol), which has a lower boiling point than water (Stigliani et al., 2013).
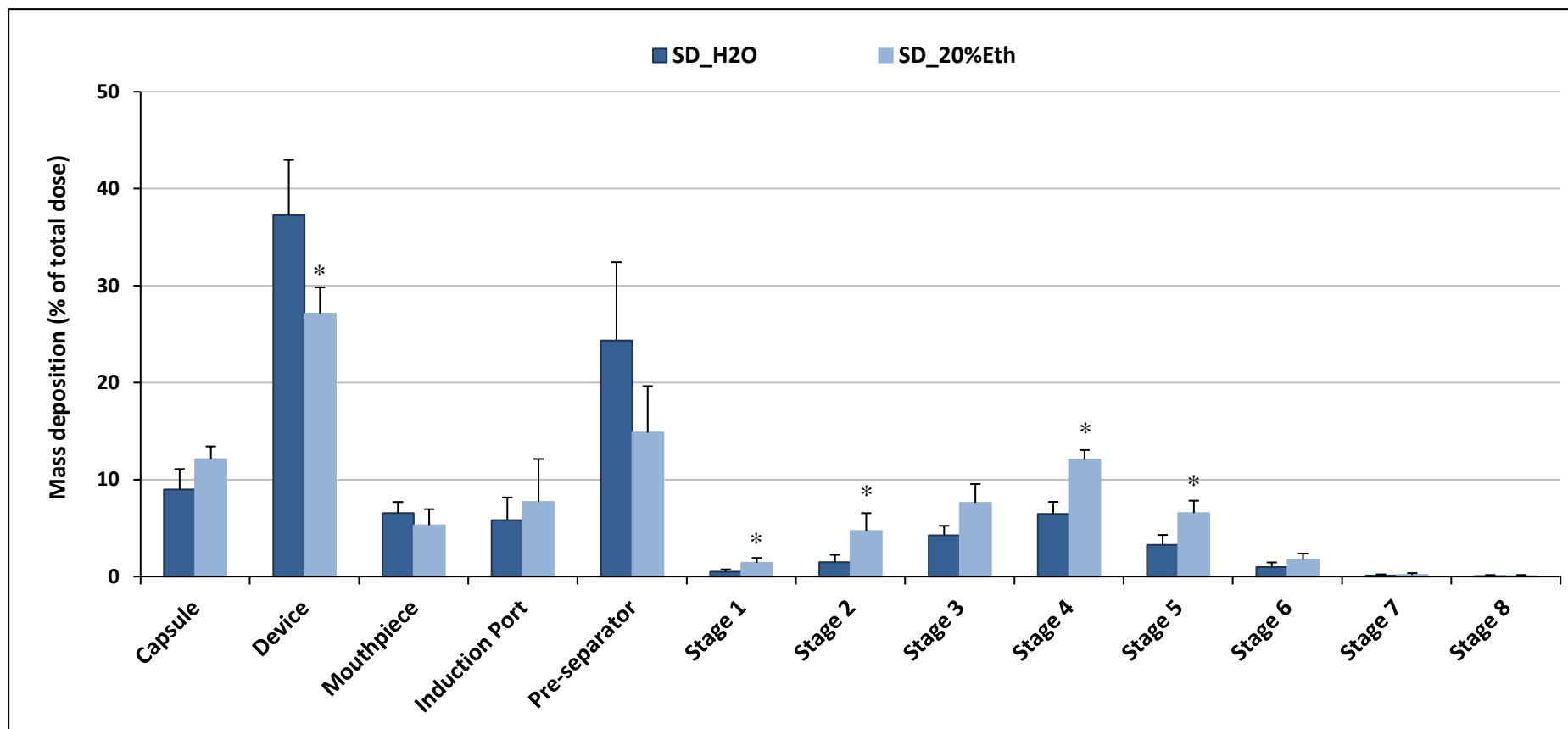
Figure 4.6 Distribution of spray-dried powder preparations of fisetin in the NGI. Mean ± s.d., $n = 3$, * p < 0.05.

Table 4.4 Aerosolisation properties of the spray-dried complexes from different feed solutions. Mean ± s.d., $n = 3$.

Preparation	MB (%)	EF (%)	FPF[a] (%)	FPD (mg)	MMAD (μm)	GSD
SD_H$_2$O	96.49 ± 1.07	91.01 ± 2.12	*16.78 ± 2.65	*1.92 ± 0.33	2.35 ± 0.37	1.68 ± 0.03
SD_20%Eth	98.89 ± 5.43	88.08 ± 1.29	32.87 ± 2.43	3.80 ± 0.26	2.45 ± 0.32	1.75 ± 0.07

MB: Mass balance, EF: Emitted fraction, FPF: Fine particle fraction, FPD: Fine particle dose, MMAD: Mass median aerodynamic diameter, GSD: Geometric standard deviation.

[a] Fraction of particles < 5 μm

* $p < 0.05$

In this study, almost 100% of fisetin loaded into the capsules was recovered which meets the requirement by the European Pharmacopoeia (75 to 125%). Approximately 90% of fisetin was successfully emitted from the capsules for both formulations. The MMAD and GSD for both formulations were similar ($p > 0.05$). However, the MMADs for both formulations were significantly higher ($p < 0.05$) than the values of volume median diameter (X_{50}), suggesting that the particles may not be optimally dispersed during aerosolisation.

4.3.1.5 SEM analysis of the spray-dried complexes produced from different feed solution compositions

Figure 4.7 shows scanning electron micrographs of the spray-dried powders. The spray-dried fisetin powder from 20% v/v ethanol solution (Figure 4.7A) had spherical particles with the appearance of fisetin crystals on the surface. This corresponds with the XRPD results showing a mixture of both amorphous and crystalline states in the preparation. Particles of the spray-dried SBE-β-CD powder from the same solvent composition were spherical in form (Figure 4.7B).

The spray-dried powders from the feed solution containing water alone, comprised of pitted spherical particles (Figure 4.7C). The majority of the particles were approximately 2 µm in diameter. The spray-dried powders from the feed solution containing 20% v/v ethanol also showed pitted spherical morphology, but with greater variation in size (Figure 4.7D). The individual size of the particles of the latter powders (Figure 4.7D) were mostly smaller than the MMAD value from the NGI (2.45 µm), suggesting that the particles moved in aggregate form during dispersion as an aerosol. This may be caused by the tendency of the product to agglomerate due to its stickiness, as discussed in Section 4.3.1.1. In both powders, fisetin crystals were not apparent, confirming the amorphosity of the preparations.
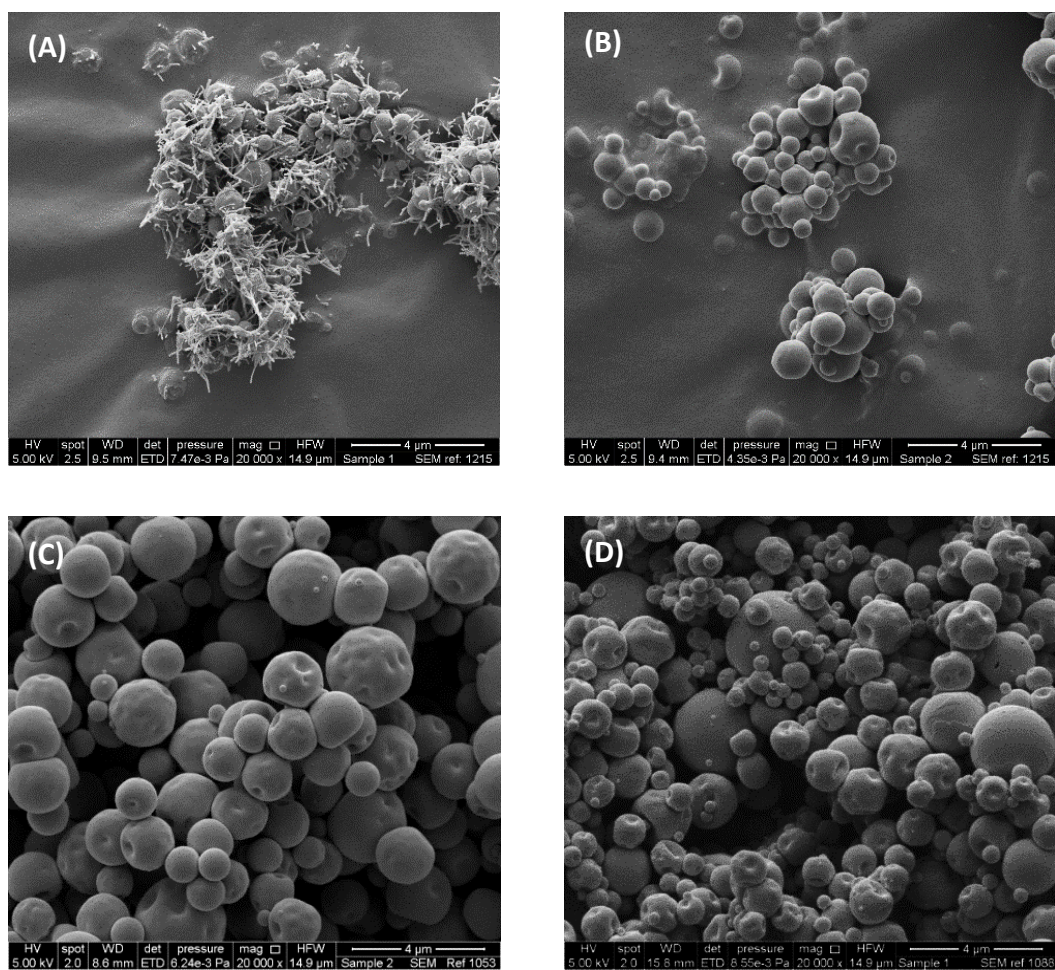
Figure 4.7 Scanning electron micrographs of spray-dried (A) fisetin, (B) SBE-β-CD, and spray-dried fisetin-SBE-β-CD complex from feed solution containing (C) water and (D) 20%v/v ethanol.

4.3.2 Incorporation of leucine as a dispersibility enhancer

4.3.2.1 Particle size distribution, yield and residual solvent content

The spray dried formulation from the feed solution containing 20%v/v ethanol (SD_20%Eth) was chosen for further investigation by adding leucine as a dispersibility enhancer. This formulation was chosen as it gave better aerosolisation properties compared to the spray-dried formulation from the feed solution containing water alone (SD_H$_2$O).

Addition of leucine into the spray-dried formulation changed the particle size distribution of the powder from bimodal to unimodal distribution, regardless of the amount of leucine added (Figure 4.8). This can be attributed to the improvement in the powder flowability. In one study, incorporation of leucine at levels as low as 5%w/w was shown to reduce the cohesiveness and improve the flowability of a spray-dried herbal extract powder (Chang et al., 2014). The change in the flowability can be explained by the irregular or wrinkled surfaces formed by the coating of the particles with leucine. Uneven surface lead to reduced inter-particulate contact points compared to the smooth surfaces, reducing the adhesiveness and cohesiveness of the particles (Chew and Chan, 2001). The improvement in the particle size distribution is also shown by the Span values presented in Table 4.5. Addition of leucine caused a reduction in Span value ($p < 0.05$) from 3.14 in the formulation without leucine, to the lowest value of 1.22 in the formulation with 20%w/w leucine.

Table 4.5 shows that incorporation of leucine as low as 5%w/w reduced the volume median diameter (X_{50}) from 1.48 ± 0.08 to 1.25 ± 0.01 µm ($p < 0.05$). Incorporation of leucine into the preparation caused a small reduction ($p < 0.05$) in the yields, regardless of the concentration. This result was not expected as previous studies have shown that leucine has the ability to modify the physicochemical properties of spray dried powder, making it less cohesive and less adhere to the wall, leading to higher yields during the spray drying process (Seville et al., 2007; Chang et al., 2014). The reduction in the yield may be related to the smaller size of the powder particles containing leucine, which made them likely to be pulled from the cyclone together with the air into the exhaust, giving slightly lower yield compared to the preparation

without leucine. Further, addition of leucine into the formulation did not affect formation of the fisetin-SBE-β-CD complex as shown by the same percentage of solubilised fisetin.
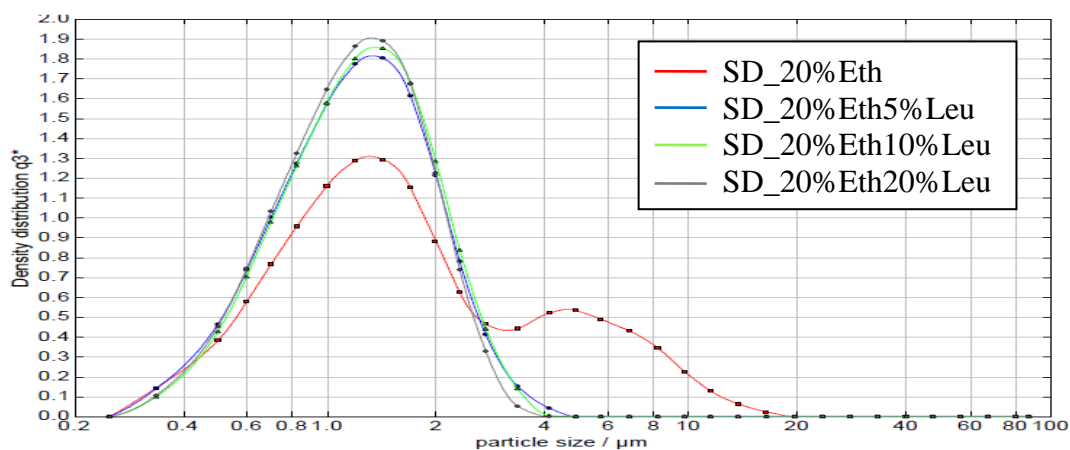
Figure 4.8 Particle size distributions of spray-dried powders, in the presence of different contents of leucine.

The leucine coating has been shown to provide a hydrophobic layer, protecting the particles against moisture and temperatures, allowing preservation of the structural integrity (Raula et al., 2008). The protection against the moisture can be seen from the results where a significant reduction ($p < 0.05$) in the residual solvent content was seen in the formulation containing 10% w/w leucine from 8.31 to 6.64% (Table 4.5), and further increase in the amount of leucine to 20% w/w did not affect the residual solvent content ($p > 0.05$).

The spray-dried formulation containing 20% w/w leucine, showed an increase in the aqueous solubility of fisetin from 31.51 ± 1.16 µg/mL to 1006.19 ± 37.08 µg/mL.

Table 4.5 Physical properties of spray-dried complexes in the presence of leucine. Mean ± s.d., $n = 3$.

Preparation	Particle size (µm)[a]				Yield (%)	Solubilised fisetin (%)	Residual solvent (%)
	X_{10}	X_{50}	X_{90}	Span			
SD_20%Eth	0.63 ± 0.02	1.48 ± 0.08	5.31 ± 1.03	3.14 ± 0.51	63.9 ± 2.7	96.8 ± 5.0	8.31 ± 0.53
SD_20%Eth5%Leu	0.62 ± 0.01	*1.25 ± 0.01	*2.29 ± 0.07	*1.33 ± 0.05	*56.4 ± 2.5	96.3 ± 0.9	7.27 ± 0.49
SD_20%Eth10%Leu	0.63 ± 0.03	*1.24 ± 0.05	*2.21 ± 0.11	*1.27 ± 0.02	*56.4 ± 1.1	97.6 ± 0.4	*6.64 ± 0.56
SD_20%Eth20%Leu	0.63 ± 0.02	*1.23 ± 0.04	*2.14 ± 0.09	*1.22 ± 0.02	*52.3 ± 0.8	98.8 ± 0.8	*6.05 ± 0.66

[a] analysed by laser diffraction at a dispersion pressure of 4 bar
* significant difference compared to formulation without leucine, $p < 0.05$

4.3.2.2 XRPD analysis of the spray-dried complexes containing leucine

Figure 4.9 shows diffractograms of raw materials and spray-dried powders containing leucine. Diffractogram of the physical mixture (containing fisetin, SBE-β-CD and leucine) showed crystalline peaks of fisetin (labelled with arrows, Figure 4.9c) and leucine, with lower intensities due to the dilution with SBE-β-CD, confirming that no physical interaction occurred between the materials. On the other hand, the diffractograms of spray-dried complexes containing leucine (Figure 4.9d, e and f) showed the disappearance of the crystalline peaks of fisetin and leucine, confirming that all formulations were in the amorphous form, similar to the SD_20%Eth formulation (Figure 4.5f).
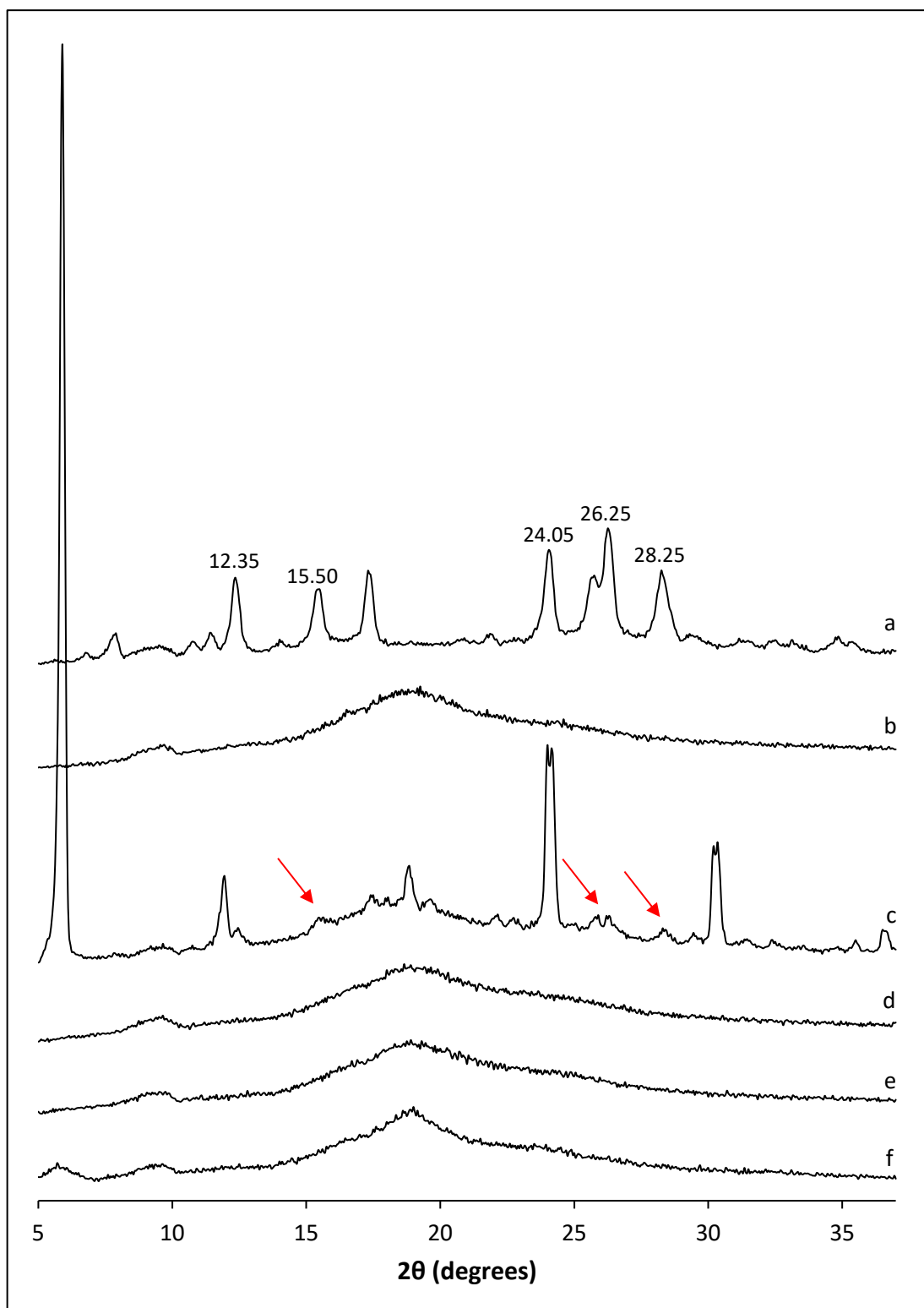
Figure 4.9 XRPD diffractograms of a) fisetin, b) SBE-β-CD, c) physical mixture, d) SD_20%Eth5%Leu, e) SD_20%Eth10%Leu and f) SD_20%Eth20%Leu. The red arrows showing fisetin's peaks.

4.3.2.3 *In vitro* aerosol deposition study of the spray-dried complexes containing leucine

Figure 4.10 shows the distribution of aerosolised fisetin in the NGI, in the presence leucine. An increase in the amount of leucine resulted in a significant reduction ($p < 0.05$) in the deposition of fisetin in capsules, device and mouthpiece stages. An increase in the deposition of fisetin in Stage 2 to Stage 8 was also seen, though most of the increases for individual stages were not significant ($p > 0.05$), with the highest NGI deposition seen in formulation containing 20%w/w leucine.

Table 4.6 shows aerosolisation properties of the investigated formulations. The mass balance and MMAD were not influenced by the presence of leucine. However, the MMAD values of all preparations were significantly higher ($p < 0.05$) than their respective volume median diameters (X_{50}). This suggests that the particles performed as aggregates during aerosolisation, and were not completely dispersed.

The emitted fraction from the capsules was improved in formulations containing 10 and 20%w/w leucine. The value increased ($p < 0.05$) from 88.08% without the presence of leucine to 97.31% in the formulation containing 20%w/w leucine. This may be caused by the low residual solvent content in both formulations compared to the formulation without leucine (Table 4.5). Low residual solvent content may reduce the adhesive interaction between capsule wall and particles, thus increasing the number of particles emitted into the NGI. This may also explain the reduction in the amount of fisetin in capsules during the deposition study in NGI (Figure 4.10).
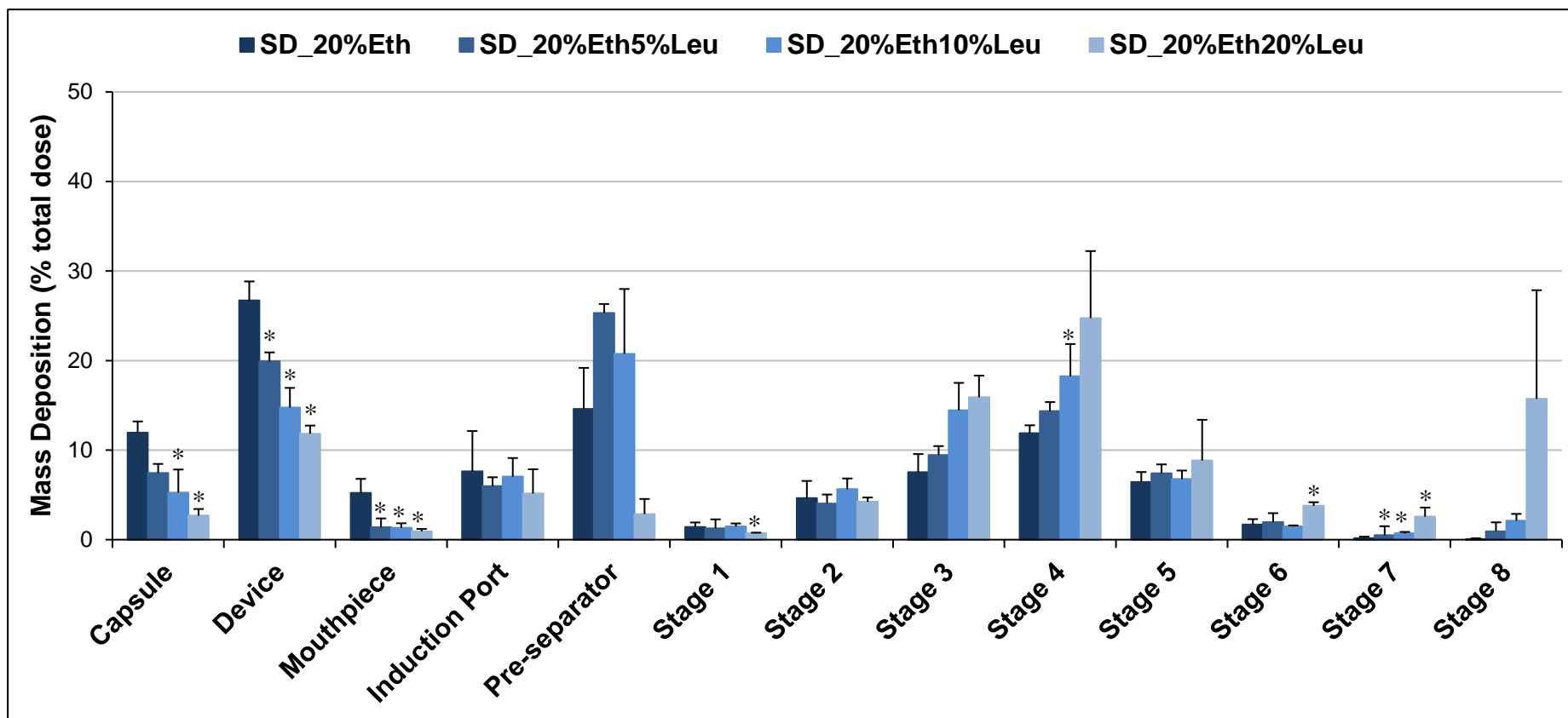
Figure 4.10 Distribution of spray-dried powder preparations containing leucine in the NGI. Mean ± s.d., $n = 3$, *significant difference compared to SD_20%Eth, $p < 0.05$.

Table 4.6 Aerosolisation properties of the spray-dried complexes in the presence of leucine. Mean ± s.d., $n = 3$.

Preparation	MB (%)	EF (%)	FPF (%)[a]	FPD (mg)	MMAD (µm)	GSD
SD_20%Eth	98.89 ± 5.43	88.08 ± 1.29	32.87 ± 2.43	3.80 ± 0.26	2.45 ± 0.32	1.75 ± 0.07
SD_20%Eth5%Leu	105.64 ± 4.81	92.54 ± 1.80	39.18 ± 2.22	4.67 ± 0.12	2.34 ± 0.16	1.75 ± 0.02
SD_20%Eth10%Leu	108.02 ± 2.95	*94.73 ± 2.56	*50.32 ± 9.18	*5.77 ± 0.93	2.54 ± 0.08	1.72 ± 0.02
SD_20%Eth20%Leu	98.80 ± 0.93	*97.31 ± 0.74	*76.31 ± 3.29	*7.10 ± 0.30	2.11 ± 0.01	1.73 ± 0.12

MB: Mass balance, EF: Emitted fraction, FPF: Fine particle fraction, FPD: Fine particle dose, MMAD: Mass median aerodynamic diameter, GSD: Geometric standard deviation.

[a] Fraction of particles < 5 µm

* significant difference compared to SD_20%Eth, $p < 0.05$

An increase in FPF was found for formulations containing 10 and 20%w/w leucine. The value increased from $32.87 \pm 2.43\%$ in formulation without leucine to $50.32 \pm 9.18\%$ in formulation with 10%w/w leucine (p < 0.05). An increase in the amount of leucine to 20%w/w caused further improvement in the FPF to $76.31 \pm 3.29\%$ (p < 0.05). Addition of 20%w/w leucine increased the FPD from 3.80 mg in the formulation without leucine, to 7.10 mg (p < 0.05).

The results show that the aerosolisation properties of the powder were improved in the presence of leucine. Although all powders were prone to form aggregates, as shown from the higher MMAD values compared to the X_{50} values, addition of leucine improved the fraction of fisetin that was < 5 µm. As previously explained, the irregular and wrinkled surface caused by the deposition of leucine on the surface of the particle, reduces the sites for interparticulate cohesion and may facilitate de-aggregation of the particles. This results in an improvement in the FPD and FPF by inclusion of leucine, as has also been shown in the spray-dried powders containing salbutamol sulphate (Seville et al., 2007) and ketoprofen lysinate (Stigliani et al., 2013).

4.3.2.4 SEM analysis of the spray-dried complexes containing leucine

The SEM images showed that incorporation of leucine into the formulation, at a concentration of as low as 5%w/w caused an alteration in the surface morphology, giving a wrinkled spherical shape particle. The wrinkled and rough surface becomes more pronounced with increased leucine content (Figure 4.11B-D). The change in morphology can be explained by the enrichment of leucine on the surface of the particles. Leucine has a hydrophobic nature and has a tendency to act as a weak surfactant (Gliński et al., 2000), which causes an accumulation of leucine at air-solution interfaces, leading to enrichment of the amino acid on particle surfaces during spray-drying (Chang et al., 2014). This forms a leucine film that collapses when solvent is removed by evaporation, thus forming the observed surface.
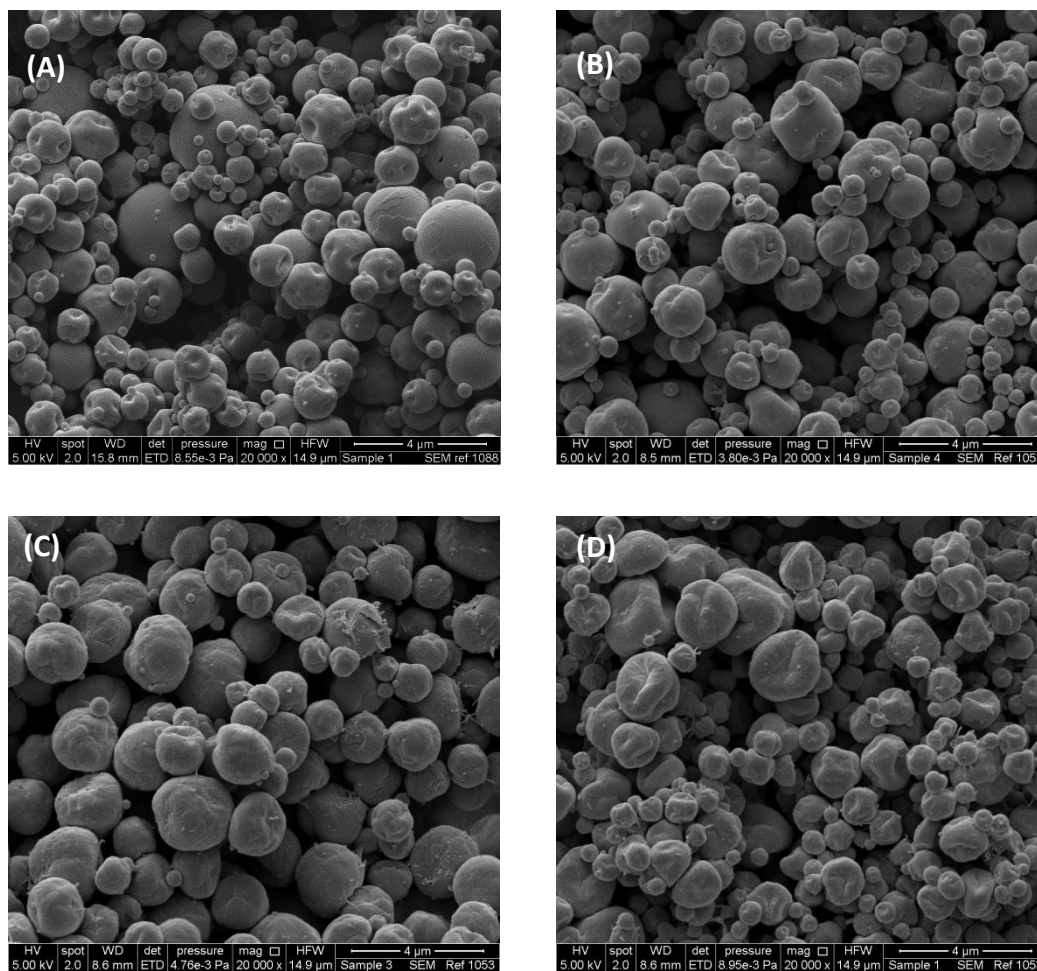
Figure 4.11 Scanning electron micrographs of spray-dried powder (A) without leucine; and in the presence of (B) 5%w/w, (C) 10%w/w and (D) 20%w/w leucine.

4.3.2.5 *In vitro* cell cytotoxicity of fisetin and the spray-dried complex containing leucine (SD_20%Eth20%Leu)

In a preliminary study, 2×10^4 cells was found to be the optimum number of cells to be seeded into each well as this was sufficient to reach ~70% confluency after 24 h incubation (see Appendix D). Studies have reported different treatment incubation time of the cells, ranging from 24 to 96 h (Liao et al., 2009; Zhuo et al., 2015). In this study, 48 h treatment incubation time was chosen as there was no difference in the cell viability curve between 48 and 72 h. Further, the cells were incubated with MTT for 2 h as there was no difference in the UV absorbance between 2 and 4 h.

The A549 cell viability curve is shown in Figure 4.12. The blank formulation, containing SBE-β-CD and leucine, showed no cytotoxic activity at all investigated concentrations (up to 495 µM for SBE-β-CD and 2313 µM for leucine). The cells also showed no DMSO-derived cytotoxicity at a concentration of 0.1%v/v DMSO in the media. Fisetin and the formulation containing 20%w/w leucine (SD_20%Eth20%Leu) showed a similar growth inhibition curve with no significant difference ($p > 0.05$) in the cytotoxic activities (Figure 4.12). The EC_{50} values of fisetin and fisetin in SD_20%Eth20%Leu preparation were 67.97 ± 14.48 and 75.86 ± 18.11 µM, respectively. The result shows that complexation with SBE-β-CD and the spray-drying process did not alter the cytotoxicity of fisetin in the A549 cell line.
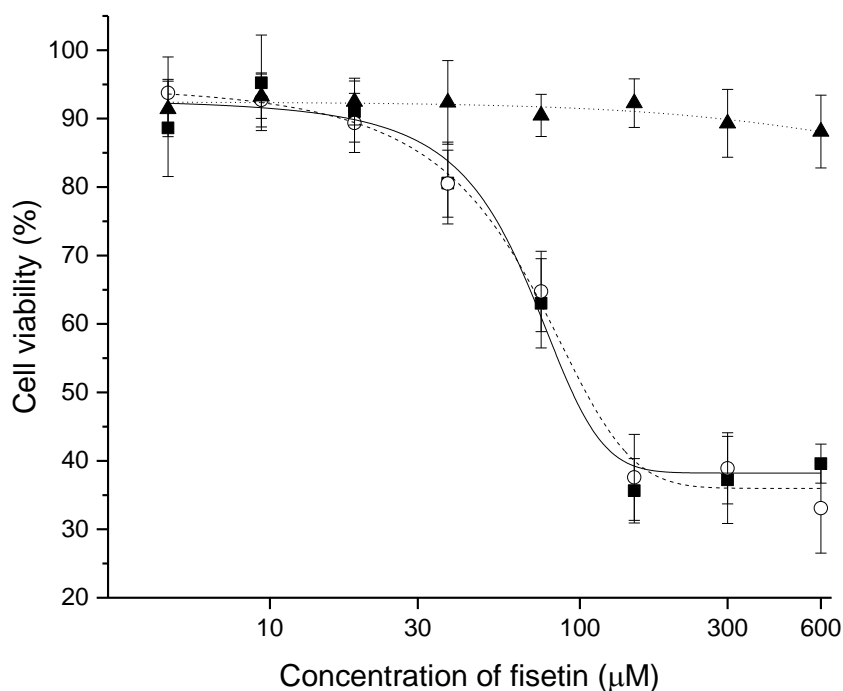
Figure 4.12 Cell viability (%) of A549 cells after treatment with fisetin (■), SD_20%Eth20%Leu preparation (○) and blank formulation (▲) after 48 h. Mean ± s.d., $n = 3$.

4.4   Conclusion

In this chapter, spray drying of fisetin-SBE-β-CD complex in an aqueous solution containing 20%v/v ethanol produced a powder with a bimodal size distribution compared to spray drying of the complex in aqueous solution, which produced a powder with a unimodal distribution. Despite that, both powders were of an appropriate size for inhalation; with ~90% of the powder < 5 µm. Formation of an inclusion complex between fisetin and SBE-β-CD was confirmed from the FT-IR analysis and both spray-dried powders were in the amorphous form. Both powders showed the same values in the emitted fraction, MMAD and GSD. However, the spray-dried powder produced from the co-solvent system showed an approximate 2-fold increase in the fine particle fraction compared to the other preparation. This may be attributed by the low density of the particles.

The spray-dried complex in the co-solvent system was further optimised using leucine as a dispersibility enhancer. Addition of leucine into the preparation generated

a powder with improved particle size distribution showed by the change in the distribution from bimodal to unimodal. Incorporation of 10 and 20%w/w leucine showed a reduction in the residual solvent content and the powders were in the amorphous form. The preparation with 20%w/w leucine showed an improvement in the emitted fraction by 1.1-fold and an increase in the deposition of fisetin to the lower regions of the NGI by 2.3-fold, compared to the preparation without leucine. The preparation also showed an unchanged cytotoxic activity of fisetin against the A549 cell line.

These results suggest the dry powder inhalation formulation of fisetin-SBE-β-CD complex may provide an improvement in the solubility of fisetin and be capable of delivering high amounts of fisetin to the deep lung region for therapeutic applications. Although fisetin may not be an ideal candidate for pulmonary delivery because of the relatively high dose needed, this study demonstrates how its formulation and delivery can be optimised and provides data that can be applied to other anti-cancer agents. Additionally, synergistic combination of fisetin with other anti-cancer agents will be explored in the next chapter, for pulmonary delivery using a SBE-β-CD complex.

Chapter 5

Analysis of drug combinations and co-complexation of fisetin and erlotinib with cyclodextrins

5.1 Introduction

Combination of anti-cancer agents with flavonoids has attracted attention for providing synergistic activity and to reverse acquired drug resistance in cancer treatment. Fisetin has shown a synergistic and beneficial combination with other anti-cancer agents, including cisplatin (Tripathi et al., 2011) and cyclophosphamide (Touil et al., 2011), allowing dose reduction of those agents. It has also been shown to reverse acquired resistance in different lung cancer cell lines, making the cells more sensitive towards cisplatin (Zhuo et al., 2015) and erlotinib (Zhang et al., 2016). Thus, combination of this flavonoid as an adjuvant with other anti-cancer agents used in the treatment of NSCLC (e.g. tyrosine kinase inhibitors) is an interesting approach, especially in lung cancer therapy.

Interaction between two or more agents can be studied using standard cytotoxicity assays (e.g. MTT and sulphorhodamine B assays), in which different concentrations of the single agents and their combinations are tested against the cell line to generate a growth inhibition curve (Bijnsdorp et al., 2011). A combination can be defined as synergistic, additive or antagonistic depending on the activity of the drug in combination compared to its individual activity. However, the evaluation is not straightforward due to the complexity of biological system. Thus, various mathematical methods and programs was developed to calculate the activity, including isobologram, fractional effect analysis and median-drug effect analysis (Bijnsdorp et al., 2011).

The isobologram and fractional effect analysis have limited applicability in this type of study, as the former method does not give an information of the extent of interaction and the latter assumes a linear concentration-effect relationship of the agents. On the other hand, the median-drug effect analysis allows calculation of the extent of the interaction and it assumes a sigmoidal concentration-effect curves of the agents and their combinations (Chou and Talalay, 1984), using a software programme CompuSyn. The median-drug effect analysis has been widely used to analyse anti-cancer agent combinations against different cancer cell lines, including the NSCLC

(Edelman et al., 2001), human ovarian adenocarcinoma (Ganta and Amiji, 2009) and renal carcinoma cell line (Hongrapipat et al., 2008).

This chapter aims to evaluate the combination of fisetin with three tyrosine kinase inhibitors (TKIs; erlotinib, gefitinib and crizotinib; Table 5.1) against the A549 cell line. Interaction between the drugs was analysed using the median-effect principle to find the most synergistic combination. The combination of fisetin and a TKI was then used to be formulated with cyclodextrins, to co-deliver both drugs locally for the treatment of NSCLC. The first approach was to optimise a cyclodextrin complex containing the TKI alone. This complex, in a dried powder form, can then be combined with the spray-dried fisetin-SBE-β-CD complex prepared in Chapter 4. The second approach was to co-complex both fisetin and the TKI in a cyclodextrin system, to deliver both drugs through nebulisation. Multiple complexation of molecules in cyclodextrins has been done previously (Loftsson et al., 2002; Yatsu et al., 2013), and this approach may be useful to optimise the use of excipients and reduce the bulkiness of the formulation.

Table 5.1 Summary of the properties of TKIs used in the study.

Drug	Molecular structure	Physicochemical properties	Indication	Drug target
Erlotinib		*Molecular weight* 393.44 g/mol *Solubility* Water: very poorly soluble DMSO: 100 mg/mL *Log P* 2.75	i) Metastatic pancreatic cancer. ii) Locally advanced or metastatic NSCLC.	Reversible inhibitor of EGFR tyrosine kinase domain.
Gefitinib		*Molecular weight* 446.90 g/mol *Solubility* Water: very poorly soluble DMSO: 100 mg/mL *Log P* 3.2	Locally advanced or metastatic NSCLC.	Reversible inhibitor of EGFR tyrosine kinase domain.
Crizotinib		*Molecular weight* 450.34 g/mol *Solubility* Water: very poorly soluble DMSO: 25 mg/mL *Log P* 1.83	Treatment of previously treated ALK-positive advanced NSCLC.	Inhibitor of ALK and c-Met/ hepatocyte growth factor receptor (HGFR).
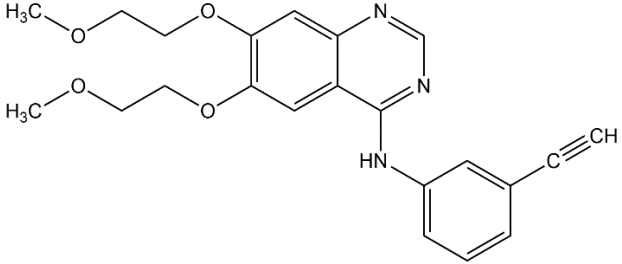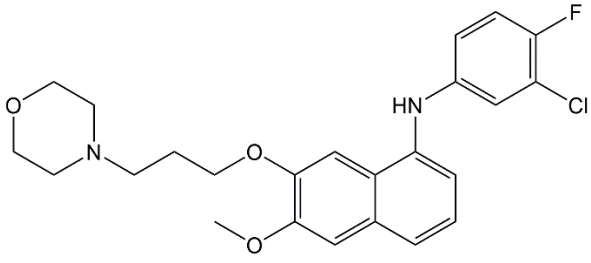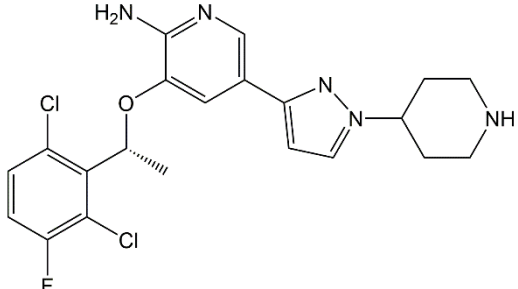
5.2 Methods

5.2.1 Analysis of drug combinations

5.2.1.1 *In vitro* cytotoxicity of individual drugs and combinations (MTT assay)

The *in vitro* cytotoxicity of individual drugs and their combinations was determined using the MTT assay, as described in Section 2.13.2. Stock solutions were prepared by dissolving an accurate amount of the drug in DMSO, as shown in Table 5.2. The stock solutions were further diluted with complete media to prepare the individual and combination treatment solutions as in Table 5.3.

Table 5.2 Concentration of the stock solution for each drug.

Drug	Amount of drug (mg)	Volume of DMSO (µL)	Concentration of stock solution (mM)
Fisetin	5	50	349
Erlotinib	5	50	254
Gefitinib	5	100	112
Crizotinib	5	100	111

Table 5.3 Concentration of individual and combination treatments in each well.

Treatment (Molar ratio)	Concentration of treatment solution in each well (µM)					
	1st	2nd	3rd	4th	5th	6th
Fisetin	150.0	75.0	37.5	18.8	9.4	4.7
Erlotinib	200.0	100.0	50.0	25.0	12.5	6.3
Fisetin: Erlotinib (1: 1)	100.0: 100.0	50.0: 50.0	25.0: 25.0	12.5: 12.5	6.3: 6.3	3.1: 3.1
Fisetin: Erlotinib (2: 1)	200.0: 100.0	100.0: 50.0	50.0: 25.0	25.0: 12.5	12.5: 6.3	6.3: 3.1
Fisetin: Erlotinib (4: 1)	100.0: 25.0	50.0: 12.5	25: 6.3	12.5: 3.1	6.3: 1.6	3.1: 0.8
Gefitinib	60.0	50.0	40.0	30.0	20.0	10.0
Fisetin: Gefitinib (2: 1)	100.0: 50.0	50.0: 25.0	25.0: 12.5	12.5: 6.3	6.3: 3.1	3.1: 1.6
Fisetin: Gefitinib (3: 1)	75.0: 25.0	37.5: 12.5	18.8: 6.3	9.4: 3.1	4.7: 1.6	2.3: 0.8
Crizotinib	25.0	12.5	6.3	3.1	1.6	0.8
Fisetin: Crizotinib (10: 1)	150.0: 15	75.0: 7.5	37.5: 3.8	18.8: 1.9	9.4: 0.9	4.7: 0.5
Fisetin: Crizotinib (15: 1)	150.0: 10.0	75.0: 5.0	37.5: 2.5	18.8: 1.3	9.4: 0.6	4.7: 0.3

The A549 cells were seeded in a 96-well plate, at a density of 2×10^4 cells per well. After 24 h incubation at 37°C (5% CO_2/95% air), the media was removed and the cells were treated with 200 µL treatment solutions. Treatment with complete media was used as a negative control and treatment with 10% v/v DMSO was used as a positive control. The cells were also treated with 0.1% v/v DMSO in the media to assess the DMSO-derived cytotoxicity, as all samples contained DMSO up to 0.1% v/v. Six replicates were made for each test condition and the 96-well plates were incubated for 72 h prior to the MTT assay, described in Section 2.13.2. The percentage of cell viability was calculated according to Eq 2.7.

5.2.1.2 Dose-effect analysis and determination of combination index (CI)

Results from the MTT assay were analysed using the median effect analysis to determine the interaction in binary combination treatment. The analysis assumes that the agents alone and the combinations will result in sigmoid (not linear) concentration-effect curves (Bijnsdorp et al., 2011). Analysis was undertaken using CompuSyn Ver. 1.0 (ComboSyn, Inc., NJ, USA) software. The fraction affected (FA) was calculated from the percentage of cell viability as follows;

$$FA = 1 - \left(\frac{\% \text{ Cell viability}}{100} \right) \qquad \text{Eq 5.1}$$

The FA values were entered into the software for each tested concentration of the single and combination drug treatments. The software analysed the combined effect of the drugs using the median effect principle of the mass action law (Chou and Talalay, 1984). The median effect equation is described as

$$f_a/f_u = (D/D_m)^m \qquad \text{Eq 5.2}$$

where f_a and f_u are the fraction affected and fraction unaffected, respectively, D is the dose required to produce f_a, D_m is the dose required to produce the median effect (e.g. IC_{50}) and m is the coefficient representing the shape of the dose-effect curve.

Linearisation of the equation was achieved by making a logarithmic conversion of Eq 5.2 as follows;

$$\log (f_a/f_u) = m \log (D) - m \log (D_m) \qquad \text{Eq 5.3}$$

and the median effect plot was constructed using $y = \log (f_a/f_u)$ versus $x = \log (D)$, where m is the slope and D_m is the antilog of the x-intercept.

Combination index (CI) is a quantitative measure of the degree of drug interaction which indicates synergism, additive or antagonism effect. In this study, each drug used in the combinations has a different mechanism of action. Thus, the mutually non-exclusive CI was calculated using the following equation (Chou and Talalay, 1984; Bijnsdorp et al., 2011);

$$CI = [(D)_1/(D_x)_1] + [(D)_2/(D_x)_2] + [(D)_1(D)_2/(D_x)_1(D_x)_2] \qquad \text{Eq 5.4}$$

where $(D)_1$ and $(D)_2$ are the doses of the drug in a fixed-ratio combination that inhibit x% cell growth, while $(D_x)_1$ and $(D_x)_2$ represent the doses of the drug in the individual treatment that also inhibit x% cell growth.

The dose-reduction index (DRI) measures the dose reduction of each drug in a synergistic combination, when compared to the dose of each drug alone (Chou and Martin, 2005). Based on Eq 5.4, the DRI value was calculated using the following equation;

$$(DRI)_n = (D_x)_n/(D)_n \qquad \text{Eq 5.5}$$

5.2.2 HPLC-UV method for quantification of erlotinib

This section will discuss quantification of erlotinib as it was the TKI chosen to be used in combination with fisetin to develop the cyclodextrin formulation. Quantification of erlotinib was achieved using a HPLC-UV method, previously developed in the laboratory. As the method was already validated according to the ICH guidelines (ICH, 1994), this chapter will only discuss the specificity of the method and preparation of the calibration curves to be used in the study. Analysis was performed using the HPLC-UV system described in Section 2.6 and the conditions are described in Table 5.4.

Table 5.4 HPLC conditions for the quantification of erlotinib.

Settings	Conditions
Column	Synergi^{TM} 4 µm Polar-RP 80°A (250 x 4.6 mm i.d., 4 µm particle size)
Mobile phase	Acetonitrile: 0.1%v/v TFA in water (50: 50; v/v)
Column temperature	25°C
Flow rate	1 mL/min
Injection volume	10 µL
Detection wavelength	246 nm

5.2.2.1 Specificity

Specificity of the method was assessed to ensure the absence of interference from the excipients in the formulation, by comparing the chromatographs of erlotinib, β-CD, HP-β-CD, SBE-β-CD and erlotinib-SBE-β-CD complex solution.

5.2.2.2 Preparation of calibration curve

A primary stock solution of erlotinib was prepared by dissolving 5 mg erlotinib in 25 mL DMSO (200 µg/mL). The stock solution was used to prepare calibration standards by making appropriate dilutions using DMSO, to obtain concentrations in the range 3-70 µg/mL. The linearity of the method was evaluated by constructing five calibration curves on five consecutive days and the results were plotted as peak area of erlotinib against corresponding concentrations using linear regression analysis.

5.2.3 Complexation of erlotinib with cyclodextrins

5.2.3.1 Phase solubility study

Phase solubility studies were conducted by adding an excess amount of erlotinib (5 mg) into 5 mL HPLC water, containing 5-35 mM β-CD, HP-β-CD or SBE-β-CD. Samples were then handled as described in Section 2.2.

5.2.3.2 Investigation of co-solvency and pH adjustment on erlotinib-HP-β-CD complex

Data from the phase solubility study showed that erlotinib has the highest complexation efficiency in HP-β-CD. Therefore, further improvement in the complexation of erlotinib with HP-β-CD was done by using co-solvency method and pH adjustment of the solution. Complexation of erlotinib with HP-β-CD was carried out at a 1: 1 molar ratio (5 mg erlotinib and 18.8 mg HP-β-CD) in 10 mL HPLC water. In the investigation of the co-solvency effect, erlotinib and HP-β-CD were dissolved in different volumes of ethanol and HPLC water, respectively (Table 5.5). Both solutions were mixed using bath sonication for 15 min. The mixture was then evaporated under vacuum at 80°C using a rotary evaporator, to remove the solvents. The dried film was rehydrated with 10 mL HPLC water at 80°C and left to cool to room temperature. The solution was then filtered using 0.45-µm syringe filter and appropriately diluted with DMSO. An aliquot of 10 µL was injected into the HPLC (Section 5.2.2) for quantification of erlotinib.

Table 5.5 Solvent composition in the preparation of erlotinib-HP-β-CD complex.

Ethanol composition (%v/v)	Erlotinib (mg)	HP-β-CD (mg)	Volume (mL)	
			Ethanol	HPLC water
0	5.0	18.8	0	10
30	5.0	18.8	3	7
50	5.0	18.8	5	5
70	5.0	18.8	7	3
90	5.0	18.8	9	1

In the investigation of the pH effect, 18.8 mg HP-β-CD was dissolved in 10 mL HPLC water. The cyclodextrin solution was found to be at pH 7.7, and the solution was adjusted to pH 4.0, 3.0 and 2.0 ($\pm$ 0.2) using 0.1N hydrochloric acid (HCl). Then, 5 mg erlotinib was added into the solution and mixed with bath sonication for 15 min. The solution was left for further mixing at 100 rpm and 37°C for 24 h, prior to filtration with 0.45-µm syringe filter. Then, 10 µL aliquot of the appropriately diluted filtrate was injected onto the HPLC.

5.2.4 Co-complexation of erlotinib and fisetin with cyclodextrins

5.2.4.1 Phase solubility study

In this study, HP-β-CD and SBE-β-CD were used to complex both drugs, as they gave the highest complexation efficiency for erlotinib and fisetin, respectively. An excess amount of erlotinib and fisetin (5 mg each) was added into 5 mL HPLC water containing different concentrations of HP-β-CD and SBE-β-CD (1-10 mM). Then, the samples were handled as described in Section 2.2.

5.2.4.2 Investigation of the effect of co-solvency on the erlotinib-fisetin-SBE-β-CD complex

Co-complexation of erlotinib and fisetin with SBE-β-CD, in the presence of ethanol, was carried out at different solvent compositions (Table 5.6). SBE-β-CD was used in this experiment as it gave the highest complexation efficiency for both drugs in the co-complex solution, from the phase solubility study. Both drugs were dissolved in ethanol, and SBE-β-CD was dissolved in HPLC water. Complexes were prepared as described in Section 5.2.3.2. Then aliquots of 10 and 30 µL of appropriately diluted samples, were injected into the HPLC for quantification of erlotinib (Section 5.2.2) and fisetin (Section 3.2.1), respectively.

Table 5.6 Solvent compositions in the preparation of erlotinib-fisetin-SBE-β-CD complex.

Ethanol composition (%v/v)	Erlotinib (mg)	Fisetin (mg)	SBE-β-CD (mg)	Volume (mL)	
				Ethanol	HPLC water
0	5	5	27.47	0	10
30	5	5	27.47	3	7
50	5	5	27.47	5	5
70	5	5	27.47	7	3
90	5	5	27.47	9	1

5.3   Results and discussion

5.3.1   Analysis of drug combinations

Interactions between fisetin and three TKIs (erlotinib, gefitinib and crizotinib) were analysed using the median effect principle of the mass action law (Chou and Talalay, 1984). Results from the MTT assay were entered into the CompuSyn software to generate the fraction affected plot (see Figure 5.1 and Appendix E-I) and median effect

plot (see examples in Appendix J and K) for all tested samples. Combination ratios were decided based on the IC_{50} value of each drug (Table 5.7). For example, the IC_{50} of fisetin and erlotinib was 77.43 and 91.72 µM, respectively. Thus, the possible combination ratio was 1: 1. A few ratios for each combination were tested against the A549 cell line in a preliminary study. From the study, ratios with the low combination index (CI) were chosen to be repeated, as shown in Table 5.7. The results show that all combinations required less median dose (D) of both fisetin and TKIs to inhibit the cell growth, compared to the individual drug treatment. Reduction in the dose can be caused by additive or synergistic activities between the drugs, which can be determined from the CI values. Interaction between the drugs was analysed using the CompuSyn software; CI values of <1, =1 and >1 indicate synergism, additive and antagonism effect, respectively. Determination of CI confirmed that all combinations had a synergistic effect, showed by the value of less than 1. Combination of fisetin: erlotinib (2: 1 molar ratio), showed the lowest CI, signifying the strongest synergistic activity as it was closer to 0 (Bijnsdorp et al., 2011).

The synergistic activity of fisetin with all TKIs may be caused by targeting of both drugs at different sites of the signalling pathway (Figure 1.4). The TKIs act on the mutated tyrosine kinase; having EGFR mutation (a target for erlotinib and gefitinib) and EML4-ALK rearrangement (a target for crizotinib). On the other hand, fisetin acts on multiple sites of the downstream signalling pathway of tyrosine kinase, including PI3K-Akt, mTOR (Khan et al., 2012) and ERK (Liao et al., 2009). Inhibition of mTOR alone will lead to activation of the Akt through upregulation of tyrosine kinases. However, this negative feedback loop can be prevented by dual inhibition of fisetin on PI3K-Akt and mTOR signalling (Khan et al., 2012).

Synergism between two drugs which act on different targeting sites was reported in a previous study by Rao et al. (2005). In the study, combination of an EGFR inhibitor (EKI-785) with an mTOR inhibitor (rapamycin) was shown to give a synergistic anti-proliferative and proapoptotic effects on glioblastoma multiforme (GBM) cells. The study suggested that a simultaneous inhibition of multiple enzyme activities can overcome the compensatory signalling mechanism, which limits the efficacy of single-agent therapies.

Table 5.7 Parameters of the dose-effect curves and combination index of the treatments in A549 cell lines. Mean ± s.d., $n = 6$.

Drug combination		Molar ratio	D_m (µM)[a]	D/IC$_{50}$ (µM)[b]		Combination index (CI)[c]	m[d]	r[e]
Drug A	Drug B			Drug A	Drug B			
Fisetin	-	-	77.43 ± 7.61	77.43 ± 7.61	-	-	1.83 ± 0.23	0.98 ± 0.02
-	Erlotinib	-	91.72 ± 35.83	-	91.72 ± 35.83	-	0.55 ± 0.14	0.98 ± 0.01
Fisetin	Erlotinib	1: 1	70.32 ± 14.17	35.16 ± 7.09	35.16 ± 7.09	0.90 ± 0.18	1.26 ± 0.27	0.96 ± 0.03
Fisetin	Erlotinib	2: 1	33.24 ± 11.79	22.16 ± 7.86	11.08 ± 3.93	0.42 ± 0.10*	2.01 ± 0.37	0.97 ± 0.02
Fisetin	Erlotinib	4: 1	56.29 ± 11.96	45.03 ± 9.57	11.26 ± 2.39	0.74 ± 0.15	1.43 ± 0.26	0.98 ± 0.01
-	Gefitinib	-	54.70 ± 13.68	-	54.70 ± 13.68	-	2.76 ± 1.96	0.96 ± 0.05
Fisetin	Gefitinib	2: 1	52.97 ± 7.82	35.31 ± 5.21	17.66 ± 2.61	0.79 ± 0.15	3.34 ± 1.52	0.95 ± 0.03
Fisetin	Gefitinib	3: 1	44.85 ± 7.56	33.64 ± 5.67	11.21 ± 1.89	0.64 ± 0.07*	1.60 ± 0.18	0.91 ± 0.04

Table 5.7 (cont.)

Drug combination		Molar ratio	D_m (µM)[a]	D/IC$_{50}$ (µM)[b]		Combination index (CI)[c]	m[d]	r[e]
Drug A	Drug B			Drug A	Drug B			
-	Crizotinib	-	5.54 ± 1.69	-	5.54 ± 1.69	-	1.54 ± 0.75	0.97 ± 0.02
Fisetin	Crizotinib	10: 1	28.78 ± 4.76	26.17 ± 4.32	2.62 ± 0.43	0.84 ± 0.17	2.31 ± 0.17	0.96 ± 0.01
Fisetin	Crizotinib	15: 1	35.82 ± 6.51	33.58 ± 6.11	2.24 ± 0.41	0.85 ± 0.13	2.02 ± 0.36	0.97 ± 0.02

[a] D_m represents the total median dose, at 50% inhibition of the cell growth.
[b] D is the median dose of each drug, at 50% inhibition of the cell growth.
[c] Combination index values at the median dose.
[d] Coefficient of the dose-effect curve.
[e] Correlation coefficient of the linear curve.
* significant difference compared to other ratios of the same drugs combination, $p < 0.05$.

Multiple site targeting can also overcome resistance towards a single-agent treatment as shown in a study by Ihle et al. (2005). Combination of an EGFR inhibitor (gefitinib) and a PI3K inhibitor (PX-866) was able to overcome resistance towards gefitinib in an A549 xenograft. Sensitivity of the cell line towards gefitinib was partly associated with inhibition of PI3K/Akt signalling, which is critical for cancer survival. In another study, combination of an EGFR inhibitor (erlotinib) and fisetin has been shown to overcome resistance towards erlotinib in an erlotinib-resistant human EGFR mutant NSCLC cell line (HCC827) (Zhang et al., 2016). Fisetin was shown to cause reversal of resistance through inactivation of MAPK and the Akt pathway and suppression of survivin (an anti-apoptotic signalling protein) expression.

Table 5.7 also showed the coefficient describing the shape of the dose-effect curve (m) of every individual and combination treatment. All treatments showed m values >1, indicating a sigmoidal dose-effect curve, except for erlotinib treatment which showed a value of <1, indicating a flat sigmoidal curve (Chou and Talalay, 1984). The difference in these two curves is shown in Figure 5.1; showing a more plateau killing activity of erlotinib at higher concentrations, compared to fisetin. These two types of dose-effect curves are common in cellular and animal systems (Chou, 2010). The linear correlation coefficient (r) for every individual and combination treatment curves was > 0.9, showing that the data were applicable to this analysis method (Chou and Talalay, 1984).
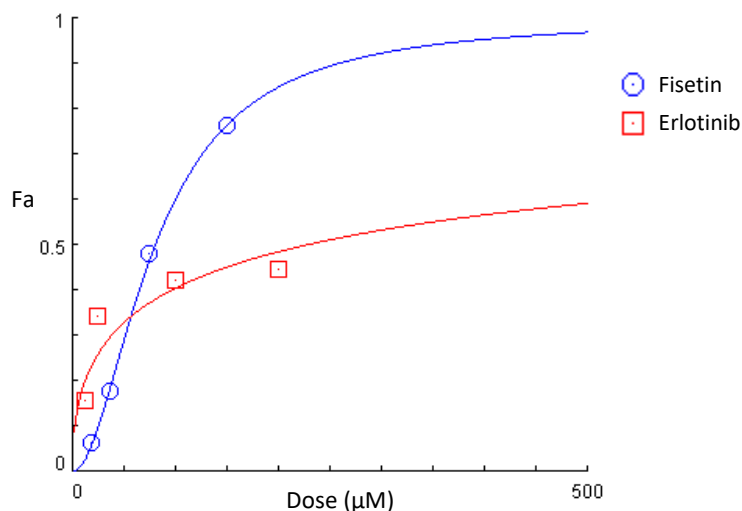
Figure 5.1 Fraction affected (FA) plot, showing a sigmoidal dose-effect curve for fisetin and a flat sigmoidal curve for erlotinib.

The drug reduction index (DRI) in Table 5.8, signifies the fraction of the drug concentration that can be reduced to achieve 50% inhibition of the cell growth. For instance, the IC_{50} values were 77.43 and 91.72 µM for fisetin and erlotinib, respectively, in single agent treatments (Table 5.7). However, combination of fisetin: erlotinib (2: 1 molar) could inhibit 50% of cell growth using only 22.16 µM fisetin and 11.08 µM erlotinib. This represents 3.63- and 8.98-fold decreases in fisetin and erlotinib concentrations, respectively. Based on the results, lower doses of fisetin and the TKIs can be used if the drugs are given together. The highest reduction in the doses of both drugs was seen in a combination of fisetin and erlotinib (2: 1 molar ratio).

Erlotinib treatment has been associated with dose-related side effects, including dermatologic reaction (e.g. rash and acneiform eruptions), stomatitis and diarrhoea (Shepherd et al., 2005; Bovenschen and Alkemade, 2009). Thus, the dose reduction of erlotinib may be useful clinically, to improve the patient's adherence and quality of life.

147

Table 5.8 Dose reduction index (DRI) of combined treatments in A549 cell lines. Mean ± s.d., $n = 6$.

Drug combination		Molar ratio	Drug reduction index (DRI)[a]	
Drug A	Drug B		Drug A	Drug B
Fisetin	Erlotinib	1: 1	2.17 ± 0.29	2.66 ± 1.07
Fisetin	Erlotinib	2: 1	3.63 ± 0.83	8.98 ± 4.60
Fisetin	Erlotinib	4: 1	1.71 ± 0.27	8.62 ± 4.14
Fisetin	Gefitinib	2: 1	2.32 ± 0.54	3.18 ± 0.98
Fisetin	Gefitinib	3: 1	2.42 ± 0.44	4.93 ± 1.21
Fisetin	Crizotinib	10: 1	3.03 ± 0.13	2.17 ± 0.73
Fisetin	Crizotinib	15: 1	2.37 ± 0.17	2.52 ± 0.73

[a] Drug reduction index values at D_m or IC_{50}.

5.3.2 HPLC-UV method for quantification of erlotinib

5.3.2.1 Specificity

Figure 5.2A shows the chromatogram for erlotinib with a retention time of 4.7 min. Figure 5.2B-E show no interference from all excipients (β-CD, HP-β-CD and SBE-β-CD) at the retention time of erlotinib, indicating specificity of the method for quantification of erlotinib in the β-CD complexes.
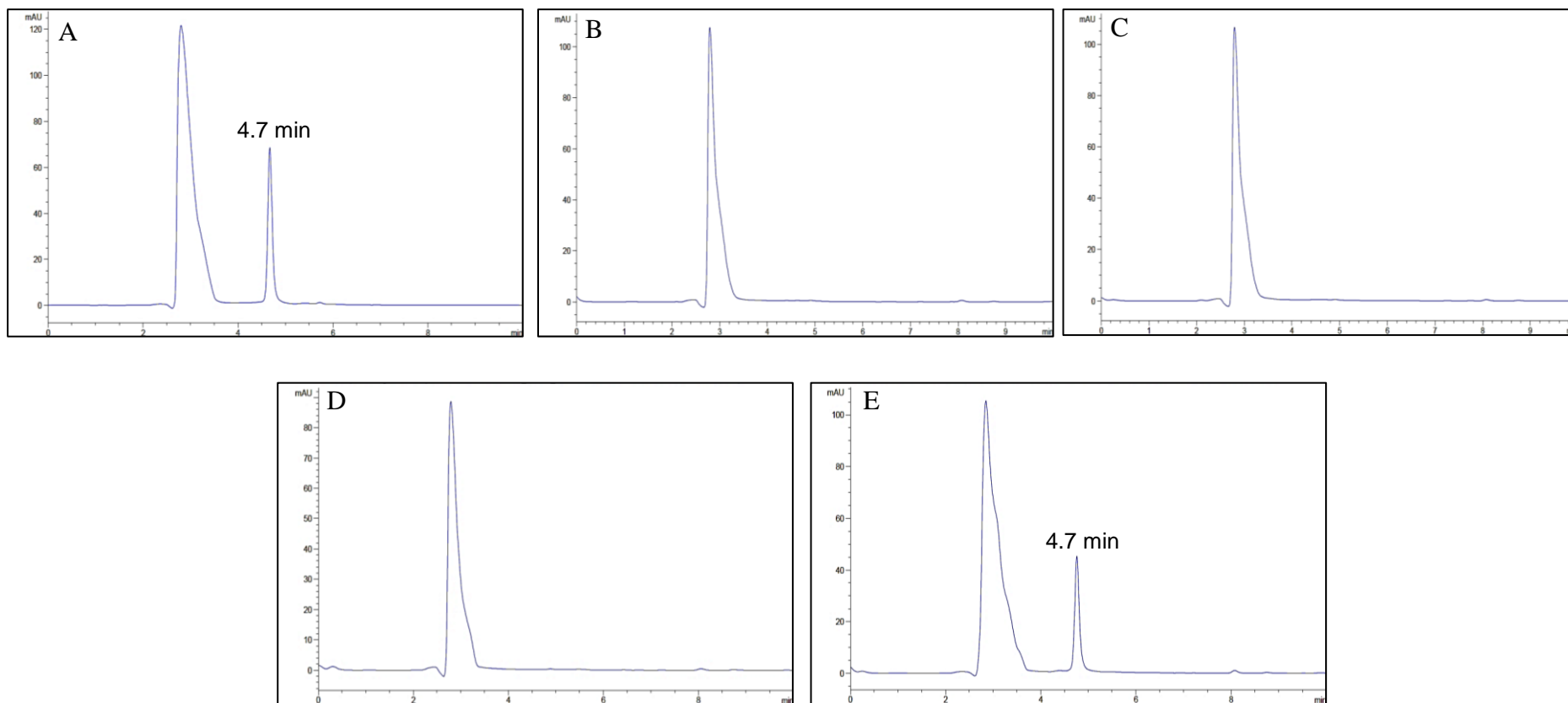
Figure 5.2 HPLC chromatograms of (A) erlotinib solution, (B) β-CD solution, (C) HP-β-CD solution, (D) SBE-β-CD solution and (E) erlotinib-SBE-β-CD complex solution.

5.3.2.2 Calibration curves

A calibration curve of erlotinib in DMSO was prepared for the use in this study (Figure 5.3). The curve was linear in the range 3-70 µg/mL with a mean linear regression equation of $y = 44.00 \ (\pm 1.22)x - 9.93 \ (\pm 7.81)$ from five calibration curves. The R^2 value 0.9998 ($\pm$0.0002) showed that the calibration curve was linear and suitable for quantification of erlotinib, as stated in the guideline (ICH, 1994).
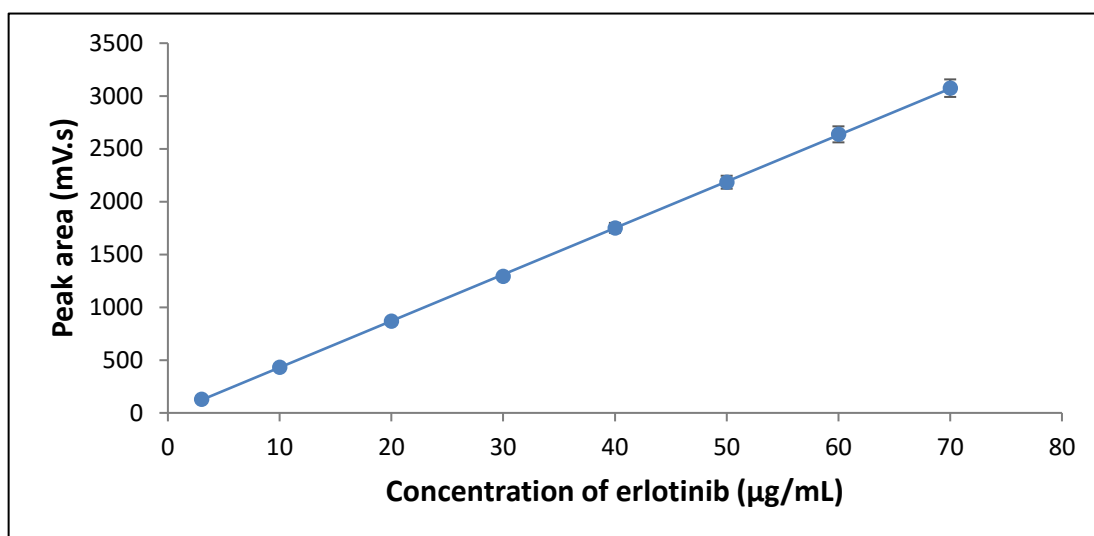
Figure 5.3 Calibration curves of erlotinib. Mean $\pm$ s.d., $n = 5$.

5.3.3 Complexation of erlotinib with cyclodextrins

5.3.3.1 Phase solubility study

Figure 5.4 shows phase solubility plots of erlotinib in the β-CD, HP-β-CD and SBE-β-CD, displaying a Higuchi A_L type of phase solubility behaviour for all complexes. All plots showed a linear increase in the solubility of erlotinib with increasing concentration of cyclodextrins, as confirmed by the R^2 values greater than 0.99 in all systems (Table 5.9).
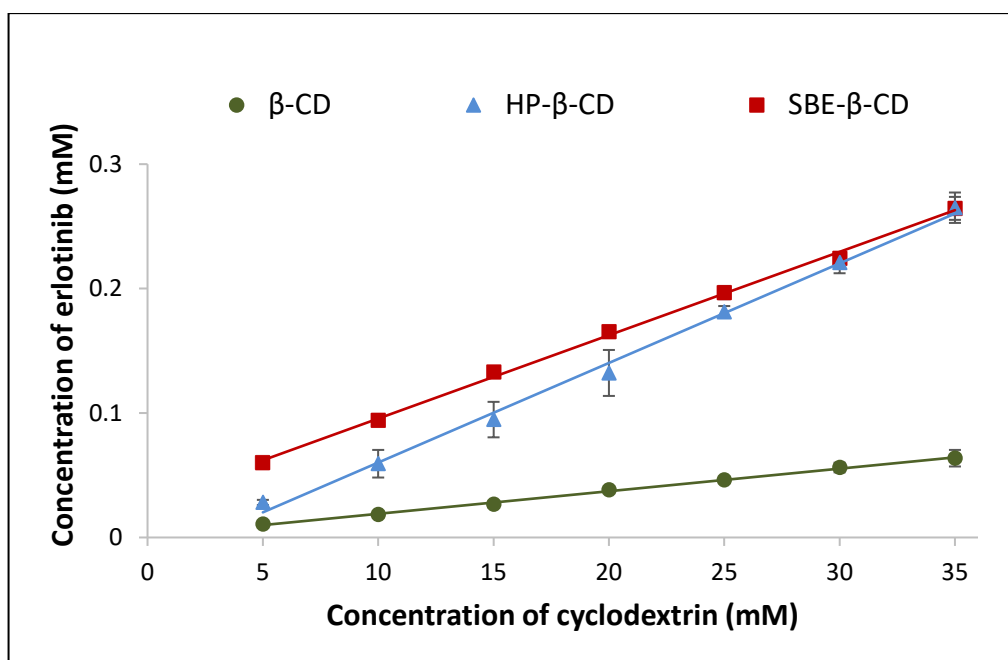
Figure 5.4 Phase solubility plots of erlotinib in solutions of different cyclodextrins. Mean ± s.d., $n = 3$.

Table 5.9 shows complexation parameters of erlotinib in the three cyclodextrins; slope values < 1 showed that all complexes were in 1: 1 stoichiometry. The solubilising efficiency of erlotinib in each cyclodextrin, determined by the K_s values, was in the following order β-CD > HP-β-CD > SBE-β-CD. The values did not correspond to the phase solubility plot that showed a better solubilising profile in HP-β-CD and SBE-β-CD (Figure 5.4). This finding can occur in the case of poorly soluble drug (aqueous solubility < 0.1 mM), where the difference between intrinsic solubility and y-intercept of the phase solubility diagram will cause erroneous K_s value (Loftsson et al., 2005a). The erroneous K_s values of erlotinib may be caused by the low solubilising efficiency of the drug in the cyclodextrins, giving a very low and inaccurate y-intercept values, affecting the calculation of the K_s values. This was different in fisetin's case, as the y-intercept values was ~10-times higher than erlotinib.

Generally, K_s is used to determine the solubilising efficiency of cyclodextrins for a drug, as in the case of fisetin (Section 3.3.2). However, in this case, complexation efficiency (CE) may be more suitable to be used as it is independent of both intrinsic solubility and the y-intercept (Loftsson and Brewster, 2012). The CE values (Table

5.9) show an increment of solubility in the following order HP-β-CD > SBE-β-CD > β-CD, comparable to the results of the phase solubility diagram. The best molar ratio was in HP-β-CD system; 1 out of every 124 HP-β-CD molecules forms a complex with erlotinib.

Previous studies reported better solubilising efficiency of erlotinib in SBE-β-CD compared to β-CD and HP-β-CD (Devasari et al., 2015; Tóth et al., 2016). The difference in the results may be caused by the difference in the condition of experiments, including the range of cyclodextrin concentrations and method of complex preparation.

Table 5.9 Complexation parameters of erlotinib in different cyclodextrins. Mean $\pm$ s.d., n = 3.

Cyclodextrin	Slope	y-intercept, S_0 (mM)	Stability constant, K_s (M^{-1})	R^2	Complexation efficiency, CE	Molar ratio (Erlotinib: CD)
β-CD	0.002 ± 0.000	0.002 ± 0.001	1919.06 ± 1706.86	0.9906 ± 0.0030	0.002 ± 0.000	1: 556
HP-β-CD	0.008 ± 0.000	0.020 ± 0.007	444.57 ± 160.40	0.9909 ± 0.0073	0.008 ± 0.000	1: 124
SBE-β-CD	0.007 ± 0.000	0.029 ± 0.004	240.89 ± 45.72	0.9956 ± 0.0014	0.007 ± 0.000	1: 150

5.3.3.2 Investigation of co-solvency and pH adjustment on erlotinib-HP-β-CD complex formation

HP-β-CD was used to form a complex with erlotinib, as it showed the highest CE in the phase solubility study (Table 5.9). A co-solvency method was used to further improve the complex formation, using different compositions of ethanol (0-90% v/v). Table 5.10 shows that 90% v/v ethanol was needed to significantly improve the amount of solubilised erlotinib from $0.74 \pm 0.05\%$ to $1.92 \pm 0.32\%$ ($p < 0.05$). Nonetheless, the relative amount of solubilised erlotinib to HP-β-CD, as shown by the mass ratio 1: 188 in the formulation, was too small to be carried forward in the study.

Table 5.10 Effect of different ethanol compositions on the complexation of erlotinib with HP-β-CD. Mean $\pm$ s.d., $n = 3$.

Ethanol compositions (% v/v)	Amount of HP-β-CD (mg)	Amount of solubilised erlotinib		Mass ratio of solubilised erlotinib to HP-β-CD
		mg	%	
0	18.8	0.04 ± 0.00	0.74 ± 0.05	1: 470
30	18.8	0.04 ± 0.00	0.76 ± 0.09	1: 470
50	18.8	0.05 ± 0.02	1.10 ± 0.33	1: 376
70	18.8	0.06 ± 0.01	1.24 ± 0.19	1: 313
90	18.8	0.10 ± 0.02	$1.92 \pm 0.32*$	1: 188

*significant difference compared to formulation without ethanol, $p < 0.05$.

Another way of enhancing the CE is by drug ionisation. Normally, a more lipophilic unionised form of a drug shows greater affinity towards the hydrophobic cyclodextrin cavity. However, ionisation of a poorly water-soluble drug can also increase the CE by increasing the intrinsic solubility (Loftsson and Brewster, 2012). Erlotinib has a pH-dependent solubility in water, with log P 2.75 at pH 11 and log P 0.66 at pH 2 (Tóth et al., 2016). Therefore, complexation of erlotinib with HP-β-CD at a lower pH can increase ionisation of the drug, thus increasing the solubility (Table 5.11). At lower pH, an increase in the intrinsic solubility of erlotinib can be seen where

a higher amount of the drug was solubilised without HP-β-CD, showing that solubility was less affected by the presence of cyclodextrin. Only 13.79% of the solubility was significantly contributed by complexation with HP-β-CD ($p < 0.05$) at pH 3, while HP-β-CD did not contribute at all to the solubility of erlotinib at pH 2 ($p > 0.05$).

Table 5.11 Effect of pH on the solubilisation of erlotinib without and in the presence of HP-β-CD. Mean ± s.d., n = 3.

pH	Amount of solubilised erlotinib			
	Without HP-β-CD		With HP-β-CD	
	mg	%	mg	%
7.7	0.01 ± 0.00	0.14 ± 0.02	0.02 ± 0.00*	0.32 ± 0.02*
4.0	0.19 ± 0.04	3.74 ± 0.77	0.21 ± 0.08	4.22 ± 1.69
3.0	2.61 ± 0.12	52.19 ± 2.33	3.30 ± 0.25*	65.98 ± 5.02*
2.0	5.00 ± 0.09	100.01 ±1.81	5.45 ± 0.45	109.04 ± 8.95

*significant difference compared to preparations without HP-β-CD, $p < 0.05$.

Preparation in pH 2, without HP-β-CD, showed the highest solubility of erlotinib (100%). Ideally, pH of liquid preparations for nebulisation should be between 3 and 10 (British Pharmacopoeia, 2017). Lower pH and hyper- or hypo-osmolar solutions may result in bronchoconstriction, coughing and irritation of the lung mucosa (Labiris and Dolovich, 2003). As a safer option with reasonable improvement in the solubility of erlotinib, erlotinib solution or erlotinib-HP-β-CD complex at pH 3 may be suitable to be carried forward for further study. Spray drying of the solution into a dry powder, suitable for inhalation, also merits investigation. The dried preparation can then be combined with the spray-dried fisetin-SBE-β-CD complex (as prepared in Chapter 4), to be delivered to the lung. However, spray drying of this cytotoxic drug needs a safe and appropriate setting, with protection of the environment and co-workers, which was not available in our laboratory. Another feasible option is to prepare a nebulisation solution containing cyclodextrin complexes of both erlotinib and fisetin, which can minimise the risk of exposure. This will be discussed in the following sections.

5.3.4 Co-complexation of erlotinib and fisetin with cyclodextrins

5.3.4.1 Phase solubility study

Figure 5.5 shows the phase solubility plot of erlotinib and fisetin in two cyclodextrin systems, when both drugs were present in the cyclodextrin solutions. The cyclodextrins used in this study were the two cyclodextrins that showed the best solubilising profile for fisetin (i.e. SBE-β-CD) and erlotinib (i.e. HP-β-CD). Both drugs showed a Higuchi A_L type behaviour in both cyclodextrin complexes, with greater solubilisation in SBE-β-CD. Both drugs show a linear increase in their solubility with increasing concentrations of cyclodextrins, confirmed by the R^2 values > 0.99 (Table 5.12). At 10 mM SBE-β-CD, fisetin shows 15-fold higher solubility (2.70 ± 0.12 mM) compared to erlotinib (0.18 ± 0.01 mM).

Table 5.12 shows that all complexes were in 1: 1 stoichiometry, as the slope values are all below 1. The solubilising efficiency (K_s value) of fisetin was higher in the SBE-β-CD system, corresponding to the phase solubility plot. However, the K_s value of erlotinib was higher in HP-β-CD which does not correspond to the phase solubility plot. This may be caused by the difference between intrinsic solubility and y-intercept, as previously discussed in Section 5.3.3.1. Thus, CE values are more reliable to show a greater solubilisation of both drugs in SBE-β-CD.
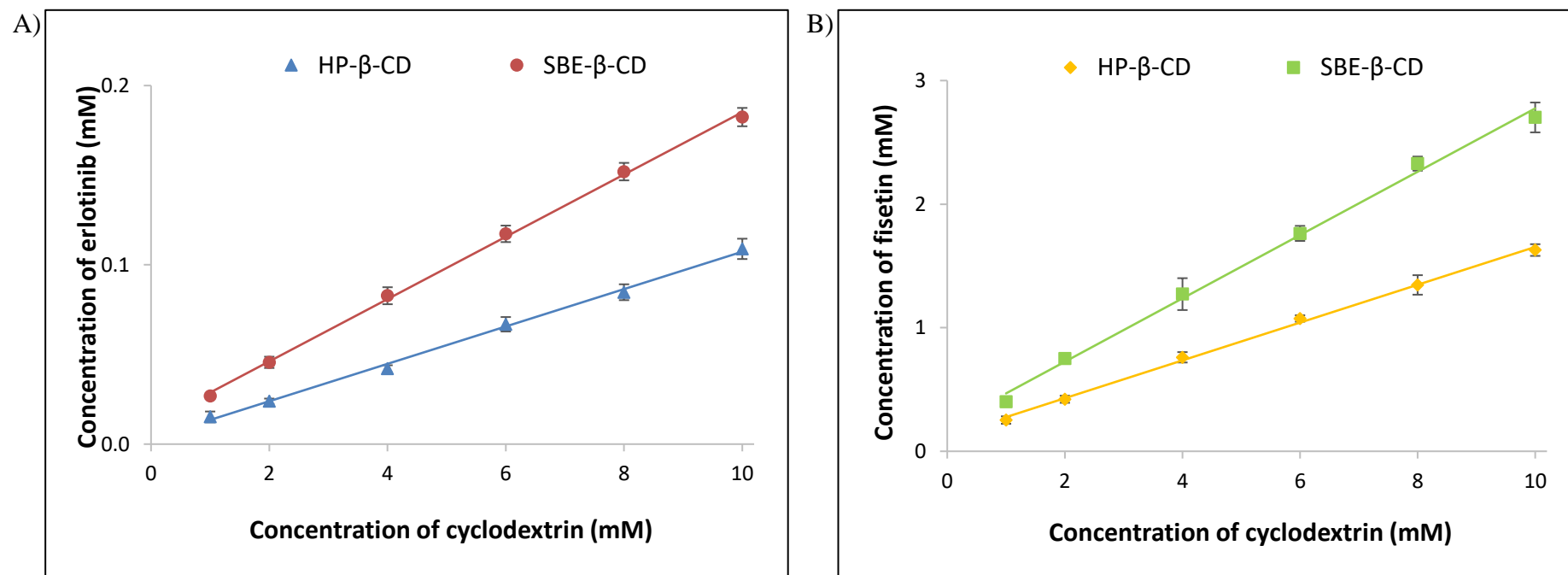
Figure 5.5 Phase solubility plot of A) erlotinib and B) fisetin in different cyclodextrins; with both drugs present in the complex solutions. Mean ± s.d., $n = 3$.

Table 5.12 Co-complexation parameters of fisetin and erlotinib in different cyclodextrins. Mean $\pm$ s.d., n = 3.

Cyclodextrin	Slope	y-intercept, S_0 (mM)	Stability constant, K_s (M^{-1})	R^2	Complexation efficiency, CE	Molar ratio (Drug: CD)
Fisetin						
HP-β-CD	0.153 ± 0.003	0.124 ± 0.026	1507.00 ± 321.31	0.9963 ± 0.0025	0.181 ± 0.004	1: 6
SBE-β-CD	0.256 ± 0.011	0.212 ± 0.025	1642.70 ± 246.06	0.9935 ± 0.0047	0.345 ± 0.020	1: 4
Erlotinib						
HP-β-CD	0.010 ± 0.001	0.003 ± 0.002	5935.05 ± 5720.37	0.9963 ± 0.0022	0.011 ± 0.001	1: 97
SBE-β-CD	0.017 ± 0.001	0.011 ± 0.001	1553.26 ± 64.19	0.9982 ± 0.0013	0.018 ± 0.001	1: 58

Although both drugs showed better solubilising profiles in SBE-β-CD, the molar ratio of erlotinib to the cyclodextrin (i.e. 1 out of every 58 SBE-β-CD molecules forms a complex with erlotinib) was lower compared to the ratio for fisetin (i.e. 1 out of every 4 molecules of SBE-β-CD forms a complex with fisetin). As formation of the inclusion complex depends on dimensional fit, the difference in the size and molecular structure between erlotinib and fisetin may cause the variation in the CE. Erlotinib has a higher molecular weight (393.44 g/mol, Figure 1.2) and a bulkier molecular structure, having two methoxyethoxy functional groups, compared to fisetin (286.24 g/mol, Figure 1.3). This may cause a hindrance during the inclusion of the drug into cyclodextrin's cavity, resulting in a lower CE. Moreover, fisetin has a higher log P value (i.e. 3.2) compared to erlotinib (i.e. 2.75 at its fully unionised form). Thus, a more lipophilic molecule such as fisetin will have a greater affinity to the hydrophobic cavity of the cyclodextrin.

Table 5.13 shows complexation parameters of both drugs in single and binary drug-CD complexes. Co-complexation improved the CE of erlotinib by 1.3- and 2.6-fold in HP-β-CD and SBE-β-CD, respectively, compared to the single complexes (Table 5.13). Contrarily, CE of fisetin was decreased by 1.5- and 2.2-fold in HP-β-CD and SBE-β-CD, respectively, in the presence of erlotinib. The change in the CE may be explained by the interaction between both drugs, affecting their intrinsic solubility. Based on Eq 5.6, which is derived from Eq 2.1 and 2.2, alteration of the intrinsic solubility will affect the CE of the drug.

$$\text{Complexation efficiency, } CE = S_0 \text{ x } K_s \qquad\qquad \text{Eq 5.6}$$

In this case, fisetin may increase the intrinsic solubility of erlotinib and erlotinib may reduce the intrinsic solubility of fisetin, causing such CE values.

Table 5.13 Complexation parameters of erlotinib and fisetin in single and binary drug-cyclodextrin complexes. Mean ± s.d., n = 3.

Cyclodextrin	Erlotinib				Fisetin			
	Complexation efficiency, CE		Molar ratio (Drug: CD)		Complexation efficiency, CE		Molar ratio (Drug: CD)	
	Individual	Binary	Individual	Binary	Individual	Binary	Individual	Binary
HP-β-CD	0.0081 ± 0.0002	0.0104 ± 0.0008	1: 124	1: 97	0.2766 ± 0.0015	0.1806 ± 0.0036	1: 5	1: 6
SBE-β-CD	0.0067 ± 0.0002	0.0174 ± 0.0005	1: 150	1: 58	0.7630 ± 0.0582	0.3448 ± 0.0198	1: 2	1: 4

Solubilisation of erlotinib through a non-inclusion complex may also explain the increase in the CE value of the drug, in the presence of fisetin. Fisetin-cyclodextrin complexes may self-associate to form water-soluble aggregates of several complexes. The aggregates can further solubilise erlotinib through non-inclusion complexation, in a similar manner to drug solubilisation by micelles. The ability of drug-cyclodextrin complexes to form a non-inclusion complex with another drug has been reported previously (Loftsson et al., 2002). An increase in the solubilisation of 17β-estradiol and diethylstilbestrol, when complexed with HP-β-CD, was seen in the presence of other drugs. The improvement in the solubilisation was associated with the formation of non-inclusion complexes of both drugs by ibuprofen- or diflunisal-HP-β-CD complexes.

These results suggest that co-complexation of erlotinib and fisetin with SBE-β-CD, allows optimisation of the use of excipients in the preparation, as well as improving the solubility of erlotinib.

5.3.4.2 Investigation of the effect of co-solvency on the erlotinib-fisetin-SBE-β-CD complex

Preparation of the complex in the mixture of ethanol and water improved the amount of erlotinib and fisetin solubilised (Table 5.14). In this study, 50%v/v ethanol was found to significantly improve the solubilisation of both drugs ($p < 0.05$) when compared to the formulation without ethanol, from 2.83 to 11.93% for erlotinib and from 29.61 to 56.34% for fisetin. Further increases in ethanol content did not improve the solubilisation ($p > 0.05$). At 50%v/v ethanol, the mass ratio of erlotinib to SBE-β-CD was improved by 4.3-fold, and the mass ratio of fisetin to SBE-β-CD was improved by 1.8-fold, compared to the formulation without ethanol; suggesting a preparation with lower amount of excipients was achievable with a higher drug loading.

Table 5.14 Complexation of erlotinib and fisetin with SBE-β-CD, in different ethanol compositions. Mean ± s.d. $n = 3$.

Ethanol composition (%v/v)	Amount of SBE-β-CD (mg)	Amount of solubilised erlotinib		Mass ratio of solubilised erlotinib to CD	Amount of solubilised fisetin		Mass ratio of solubilised fisetin to CD
		mg	%		mg	%	
0	27.47	0.14 ± 0.03	2.83 ± 0.50	1: 196	1.48 ± 0.12	29.61 ± 2.47	1: 18
30	27.47	0.18 ± 0.03	3.56 ± 0.66	1: 152	2.21 ± 0.29	44.13 ± 5.78	1: 12
50	27.47	0.60 ± 0.15	11.93 ± 2.93*	1: 45	2.82 ± 0.07	56.34 ± 1.39*	1: 10
70	27.47	0.71 ± 0.14	14.17 ± 2.90*	1: 38	2.47 ± 0.36	49.36 ± 7.27*	1: 11
90	27.47	0.87 ± 0.08	17.32 ± 1.65*	1: 31	2.75 ± 0.58	55.01 ± 11.50*	1: 10

*significant difference compared to formulation without ethanol, $p < 0.05$.

5.4 Conclusions

In the analysis, all fisetin-TKI combinations showed synergistic killing activity against the A549 cell line, with the most synergistic combination of erlotinib and fisetin being a 1: 2 molar ratio. The observed synergism may be caused by both drug molecules targeting multiple sites in the tyrosine kinase signalling pathway. This combination may also give a clinical benefit, as it allows reduction in the dose needed to reach IC_{50} by 8.98- and 3.63-fold for erlotinib and fisetin, respectively. Thus, a cyclodextrin-based formulation containing both drugs was prepared for further investigation in the study.

The first approach investigated a single drug complex of erlotinib with different cyclodextrins. Erlotinib showed the highest complexation efficiency with HP-β-CD, when compared to β-CD and SBE-β-CD. Addition of ethanol in the complexation process improved the amount of solubilised erlotinib, but the high excipient content in the preparation meant this was not viable to be carried forward in the study. pH reduction increased the aqueous solubility of erlotinib, up to a point that addition of cyclodextrin did not contribute to the drug solubility at all. Erlotinib solution or erlotinib-HP-β-CD complex solution at pH 3 showed a reasonable improvement in the solubility of erlotinib. However, spray-drying of the the solutions, to be combined with the previously prepared spray-dried fisetin-SBE-β-CD complex, was not possible due to unavailability of a suitable instrument which could protect the environment and operator.

The second approach was to prepare a binary drug-CD complex of erlotinib and fisetin with different cyclodextrins. The highest CE for both drugs, when co-complexed, was found in the SBE-β-CD system. The CE of erlotinib and fisetin was increased by 2.6-fold and decreased by 2.2-fold, respectively, when compared to the single drug-cyclodextrin complexes. The improvement in erlotinib solubility may results from the formation of non-inclusion complexes of the drug with fisetin-CD complex aggregates. Addition of 50%v/v ethanol during the complex preparation, improved complexation by 4.3- and 1.8-fold for erlotinib and fisetin, respectively, making the preparation less bulky with a higher drug loading.

This optimal preparation was further optimised in the next chapter to make it suitable for inhalation purposes.

Chapter 6

Optimisation of an erlotinib-fisetin-SBE-β-CD complex for nebulisation

6.1 Introduction

Several formulation approaches have been reported for both erlotinib and fisetin, and these approaches have been discussed for fisetin in Chapter 3. Erlotinib has been formulated into lipid-based nanoparticulate systems (Vrignaud et al., 2012; Morton et al., 2014; He et al., 2016; Boakye et al., 2017; Li et al., 2017a; Li et al., 2017b; Dora et al., 2017; Kim et al., 2017; Xu et al., 2017; Bakhtiary et al., 2017; Gupta et al., 2018; Zhou et al., 2018), polymeric-based nanocarriers (Marslin et al., 2009; Jesson et al., 2014; Mandal et al., 2016; Fathi et al., 2017; Yang et al., 2017; Zhou et al., 2017), nanosponge complexes (Dora et al., 2016; Momin et al., 2018), gold nanoparticles (Lam et al., 2014), iron-oxide nanoparticles (Ali et al., 2016), albumin nanoparticles (Noorani et al., 2017) and a solid self-emulsifying formulation (Truong et al., 2016).

Although the combination of erlotinib and fisetin in erlotinib-resistant human EGFR mutant NSCLC cell line (HCC827) has been reported (Zhang et al., 2016), no further study on formulation of the combination has been conducted. Complexation of the single drug with cyclodextrins have been reported for erlotinib (Devasari et al., 2015; Gontijo et al., 2015; Tóth et al., 2016) and fisetin (Guzzo et al., 2006; Pahari et al., 2013; Zhang et al., 2015). However, there are no reports of co-complexation of both drugs in cyclodextrins, specifically in SBE-β-CD.

This chapter will discuss further optimisation of erlotinib-fisetin-SBE-β-CD complex, to make it suitable for nebulisation. Nebulisation of the preparation over an extended period may be able to deliver a larger volume of the solution, thus allowing delivery of a higher dose of the drug.

6.2 Methods

6.2.1 Investigation of different formulation compositions

Different compositions of erlotinib-fisetin-SBE-β-CD complex were investigated to find out the optimal preparation. The experiment was carried out by varying the amount of one ingredient while maintaining the amount of other ingredients at a time. Therefore, the experiment was conducted into two parts (Table 6.1).

Table 6.1 Different compositions of erlotinib-fisetin-SBE-β-CD complex.

	Erlotinib (mg)	Fisetin (mg)	SBE-β-CD (mg)	Mass ratio
Part 1	5	5	27.47	1: 1: 5
	5	5	54.94	1: 1: 11
	5	5	109.88	1: 1: 22
Part 2	5	1.2	109.88	4: 1: 92
	2.5	1.2	109.88	2: 1: 92
	1.25	1.2	109.88	1: 1: 92
	0.625	1.2	109.88	1: 2: 92

The first part was carried out using different amounts of SBE-β-CD and a fixed amount of erlotinib (5 mg) and fisetin (5 mg). The second part was undertaken using a different amount of erlotinib and fixed amount of fisetin (1.2 mg) and SBE-β-CD (109.88 mg). In both parts, erlotinib and fisetin were dissolved in 5 mL absolute ethanol, and SBE-β-CD was dissolved in 5 mL HPLC water, making the total volume of 10 mL. Complexation of both drugs with SBE-β-CD was carried out in 50%v/v ethanol, as described in Section 5.2.3.2. The final solution was filtered using a 0.45-µm syringe filter and the appropriately diluted filtrates were injected into the HPLC for quantification of erlotinib and fisetin, as described in Section 5.2.2 and Section 3.2.1, respectively. The amount of solubilised drugs was quantified immediately after preparation (Day 0), and after 1 (Day 1) and 2 (Day 2) days of preparation.

6.2.2 Lyophilisation and investigation of different redispersion concentrations of the complex

In order to prepare a more concentrated complex solution, the preparation was freeze-dried and reconstituted to different concentrations using HPLC water. In this experiment, the optimal preparation chosen from Section 6.2.1 was used. The complex was prepared in 50%v/v ethanol using 0.625 mg erlotinib, 1.2 mg fisetin and 109.88

mg SBE-β-CD, as described in Section 5.2.3.2. After rehydration with HPLC water, the complex was left to cool to room temperature prior to freeze drying, as described in Section 2.3. The lyophilised samples were kept in a desiccator at room temperature, until reconstitution.

Different amounts of the lyophilised complex were reconstituted with 5 mL HPLC water to produce 1-, 2-, 3- and 4-times more concentrated complex solutions. The reconstituted solutions were filtered using a 0.45-µm syringe filter, and the amount of solubilised drugs in each solution was quantified using HPLC. The quantification was made immediately after reconstitution (0 hour), and 1 h after reconstitution (1 hour).

The lyophilised sample, physical mixture and raw materials were also characterised using XRPD and FT-IR, as described in Section 2.8 and 2.9, respectively.

6.2.3 Assessment of aerosol properties of the complex solution using the Next Generation Impactor (NGI)

Assessment of the nebulised aerosol was done according to European Pharmacopoeia (Apparatus E, Chapter 2.9.44) using the NGI. The micro-orifice collector (MOC) stage was fitted with a 1.6 µm glass microfiber filter (Whatman, UK). The induction port and the assembled impactor body were pre-cooled in a refrigerator at 5°C for at least 90 min. Meanwhile, 4 mL of the complex solution was placed into a Pari LC$^©$ Sprint jet nebuliser (Figure 6.1) attached to a Pari Boy compressor (PARI Medical Ltd., Surrey, UK).
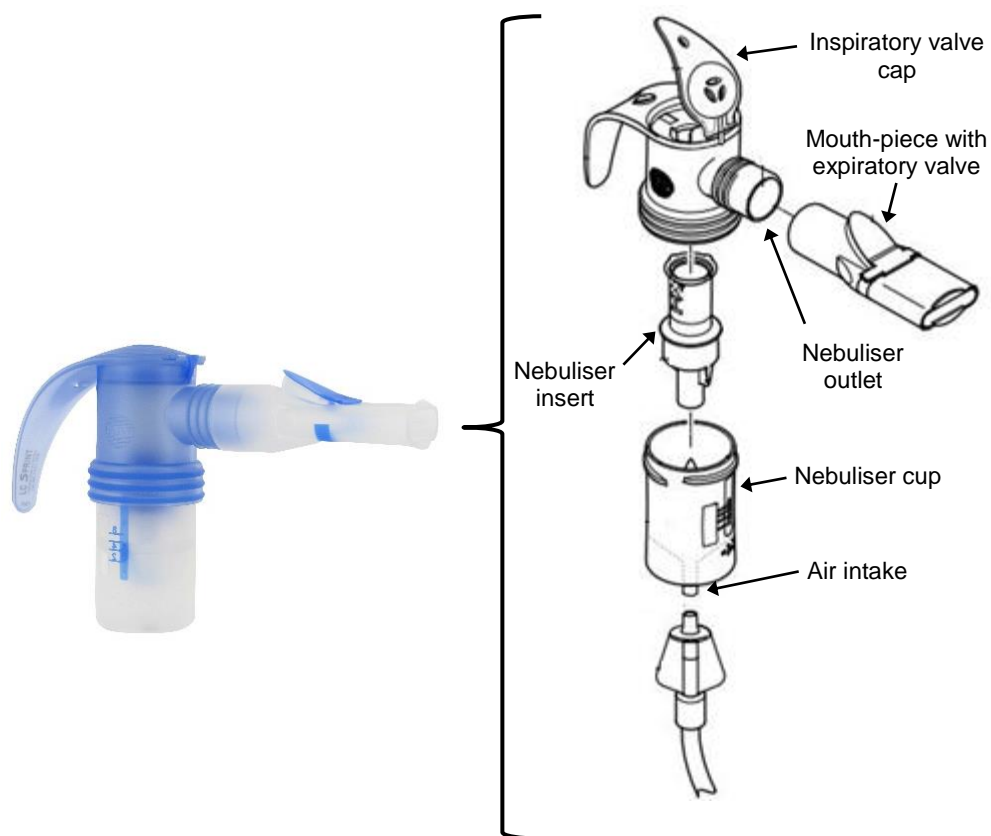
Figure 6.1 Pari LC$^©$ Sprint jet nebuliser and its component parts (adapted from Pari, 2018).

Air flow through the pre-cooled equipment was adjusted to 15 ± 0.75 L/min using a vacuum pump and tested using the flow meter. The flow meter was removed and the nebuliser mouth-piece was inserted into a mouth-piece adaptor, attached to the induction port. The compressor for the nebuliser was then switched on and nebulisation was carried out for 10 min. After the nebulisation process, the solution in nebuliser, induction port and stage 1-8 of the NGI were rinsed thoroughly using ethanol into separate volumetric flasks. The solutions were mixed in a bath sonicator for 15 min and filtered using 0.45-µm syringe filter to remove undissolved SBE-β-CD. The filtrate was then injected into the HPLC for quantification of erlotinib and fisetin.

Under these conditions, the cut-off diameter for each NGI stage are as shown in Table 6.2 (Apparatus E, Chapter 2.9.44, European Pharmacopoeia);

Table 6.2 Cut-off sizes for the NGI at 15 L/min.

Stage	Cut-off diameter (μm)
1	14.1
2	8.61
3	5.39
4	3.30
5	2.08
6	1.36
7	0.98

The aerosolisation parameters were calculated as follows;

$$\text{Mass balance (MB)} = \frac{\text{Mass of drug from nebuliser to Stage 8}}{\text{Initial mass of drug in the nebuliser solution}} \times 100 \qquad \text{Eq 6.1}$$

$$\text{Emitted fraction (EF)} = \frac{\text{Mass of drug from induction port to Stage 8}}{\text{Mass of drug from nebuliser to Stage 8}} \times 100 \qquad \text{Eq 6.2}$$

The fine particle dose (FPD), fine particle fraction (FPF), mass median aerodynamic diameter (MMAD) and geometric standard deviation (GSD) were calculated as described in Chapter 4.2.4.

6.2.4 *In vitro* cell toxicity of erlotinib and fisetin in the nebulisation solution

The cytotoxic activity of the drugs in the complex was compared to that of the free drugs using the MTT assay. The molar ratio of erlotinib to fisetin in the formulation was slightly different, compared to the optimal ratio determined in Section 5.3.1. Therefore, the cytotoxic activity of the combination used in the formulation (erlotinib:

fisetin; 1: 2.6 molar ratio) was compared to the optimal combination (erlotinib: fisetin; 1: 2 molar ratio), together with the freeze-dried erlotinib-fisetin-SBE-β-CD complex and blank SBE-β-CD-complex.

The drug combinations were prepared, as described in Section 5.2.1.1, at erlotinib concentrations 0.20-100 µM. 55 mg of the lyophilised erlotinib-fisetin-SBE-β-CD complex was dissolved in 1.67 mL sterile HPLC water, and diluted into solutions containing 0.39-200 µM erlotinib using complete media. The same amount of blank SBE-β-CD complex was dissolved separately using the same volume of sterile HPLC water, and diluted according to the dilution of the formulation.

The A549 cells were seeded in a 96-well plate, at a density of 2×10^4 cells per well. After 24 h incubation at 37°C (5% CO_2/95% air), the media was removed and the cells were treated with 200 µL treatment solutions. Treatment with complete media was used as a negative control and treatment with 10%v/v DMSO was used as a positive control. As the samples of drug combinations contained DMSO, the cells were treated with 0.1%v/v DMSO in the media, to evaluate the DMSO-derived cytotoxicity. Three replicates were made for each test condition on different days, and the cells were incubated with the treatment for 72 h prior to the MTT assay, as described in Section 2.13.2.

6.3 Results and discussion

6.3.1 Investigation of different concentrations of SBE-β-CD

In this study, the amount of SBE-β-CD was increased to obtain a higher concentration of the complex in the solution. An increase in the drug solubilisation would be expected as more cyclodextrin was available to form complexes with the drug molecules. This trend can be seen for fisetin; an increase in solubilisation from 43.8 to 105.8%, when SBE-β-CD was increased from 27.47 to 109.88 mg (Table 6.3). However, the amount of solubilised erlotinib remained at ~15-20%, despite the increasing amount of SBE-β-CD (Table 6.3). This may be caused by the easiness of fisetin's molecule to go inside the hydrophobic cavity of SBE-β-CD, due to its less bulky molecular structure (Figure 1.3) and higher log P value (3.2) compared to

erlotinib (Figure 1.2, log P 2.75). Therefore, more fisetin will form complexes with SBE-β-CD molecules, leaving less or no available space for erlotinib.

Table 6.3 Solubilisation of erlotinib and fisetin in preparations containing different amount of SBE-β-CD. Mean ± s.d., $n = 3$.

Composition of preparation (mg)				Solubilisation of erlotinib		Solubilisation of fisetin	
Erlotinib	Fisetin	SBE-β-CD	Mass ratio	Amount (mg)	Percentage (%)	Amount (mg)	Percentage (%)
5	5	27.47	1: 1: 5	0.77 ± 0.11	15.4 ± 2.2	2.19 ± 0.23	43.8 ± 4.7
5	5	54.94	1: 1: 11	1.04 ± 0.12*	20.7 ± 2.5*	4.53 ± 0.09*	90.6 ± 1.9*
5	5	109.88	1: 1: 22	0.75 ± 0.07	15.0 ± 1.4	5.29 ± 0.31*	105.8 ± 6.2*

*significant difference compared to formulation containing 27.47 mg SBE-β-CD, $p < 0.05$.

Figure 6.2 shows stability of the complexes at room temperature over 2 days. The highest amount of SBE-β-CD (109.88 mg) provided better stability for retention of both drugs in the complex. Preparation of the complex with less than 109.88 mg SBE-β-CD caused significant reduction ($p < 0.05$) in the amount of solubilised drug remaining, as early as 1 day after preparation, suggesting instability of the complex. However, the complex was stable within 2 days after preparation, when prepared with 109.88 mg SBE-β-CD.

The results show that 109.88 mg SBE-β-CD in 10 mL preparation, was able to provide higher solubilisation and better stability for fisetin, but could only provide the latter for erlotinib in the complex. This may be explained by the limited ability of water-soluble fisetin-SBE-β-CD complex aggregates (as discussed in Section 5.3.4.1) to form non-inclusion complexes with erlotinib molecules. Thus, further increase in the concentration of fisetin-SBE-β-CD could only improve stability of the formed inclusion complexes.
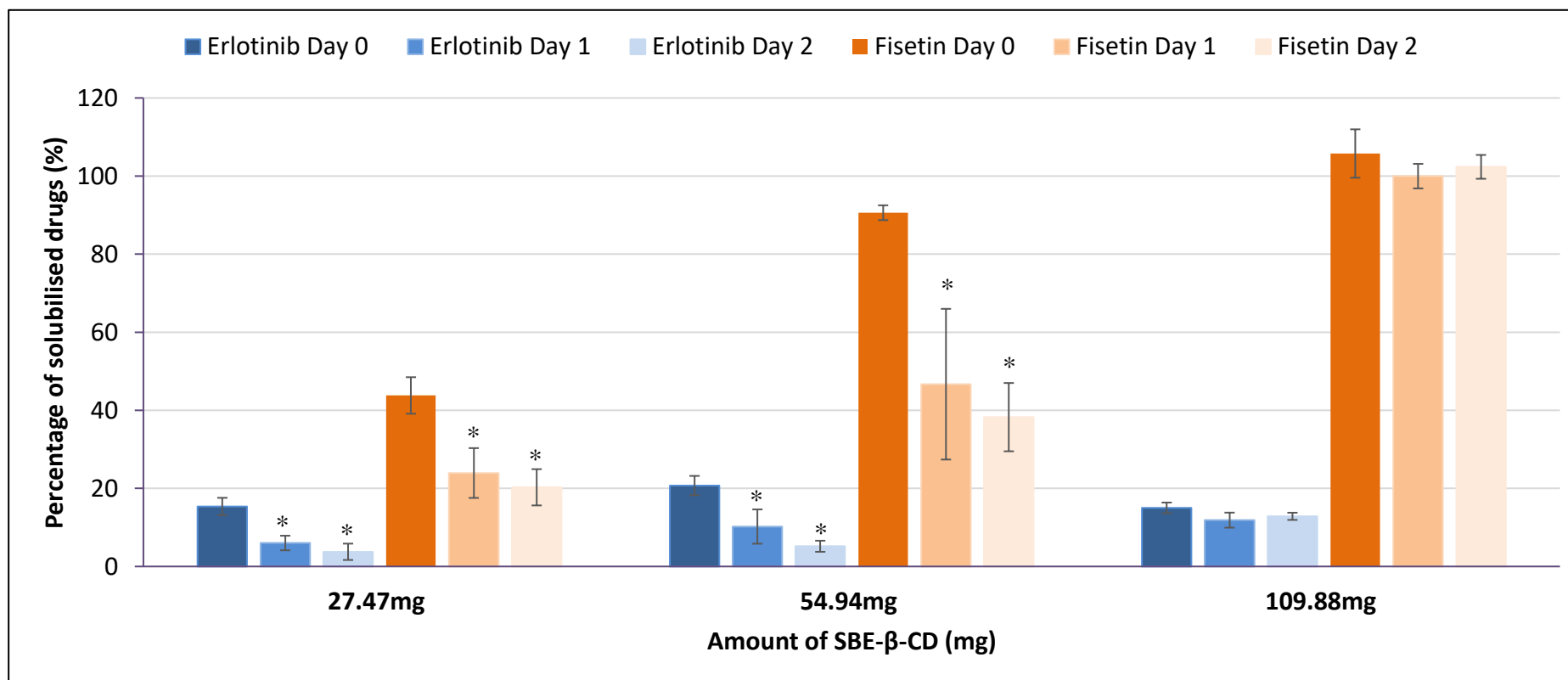
Figure 6.2 Stability of erlotinib-fisetin-SBE-β-CD complex containing different amounts of SBE-β-CD in 10 mL, at room temperature. Mean ± s.d., $n = 3$, *significant difference compared to the same formulation on Day 0, $p < 0.05$.

6.3.2 Investigation of different amounts of erlotinib in complexes

Section 5.3.1 showed that the most synergistic combination of erlotinib and fisetin occurred with a molar ratio of 1: 2 (mass ratio 1: 1.46). Table 6.3 shows that the erlotinib amount that could form stable complexes with SBE-β-CD was ~0.8 mg. Therefore, the amount of fisetin was fixed at 1.2 mg (~1.46-times higher than 0.8 mg), and the amount of erlotinib was varied from 5 to 0.625 mg.

Table 6.4 shows that all fisetin's molecules formed complexes with SBE-β-CD, with ~90-100% of the drug being solubilised in all preparations. In the case of erlotinib, reducing the drug amount from 5 to 0.625 mg, improved the percentage of solubilised erlotinib from 8.1 to 95% ($p < 0.05$). The increase in the percentage of solubilised erlotinib was expected as the value was calculated in relative to the amount of erlotinib used in the formulation. The smaller the amount of erlotinib used, the higher the calculated percentage. The preparation containing 1.25 mg erlotinib showed a great improvement in the amount of solubilised erlotinib (0.96 mg), compared to other preparations. However, the formed complexes were not stable as the amount of solubilised erlotinib was significantly reduced from 0.96 ± 0.00 to 0.49 ± 0.03 mg ($p < 0.05$, Figure 6.3), 1 day after of preparation. Meanwhile, other preparations demonstrated better stability of the complexes over 2 days after preparation. The preparation containing 0.625 mg erlotinib was chosen to be nebulised, as it showed the least amount of excess drugs, with $95.0 \pm 3.5\%$ erlotinib and $90.3 \pm 8.2\%$ fisetin being solubilised, and sufficient stability of the complexes in the solution.

176

Table 6.4 Solubilisation of erlotinib and fisetin in preparations containing different amounts of erlotinib. Mean $\pm$ s.d., $n = 3$.

Composition of preparation (mg)				Solubilisation of erlotinib		Solubilisation of fisetin	
Erlotinib	Fisetin	SBE-β-CD	Mass ratio	Amount (mg)	Percentage (%)	Amount (mg)	Percentage (%)
5	1.2	109.88	4: 1: 92	0.41 ± 0.01	8.1 ± 0.3	1.23 ± 0.11	102.1 ± 8.8
2.5	1.2	109.88	2: 1: 92	0.49 ± 0.02*	19.5 ± 0.9*	1.20 ± 0.15	99.9 ± 12.9
1.25	1.2	109.88	1: 1: 92	0.96 ± 0.00*	76.6 ± 0.2*	1.15 ± 0.10	95.5 ± 8.2
0.625	1.2	109.88	0.5: 1: 92	0.59 ± 0.02*	95.0 ± 3.5*	1.08 ± 0.10	90.3 ± 8.2

*significant difference compared to formulation containing 5 mg erlotinib, $p < 0.05$.
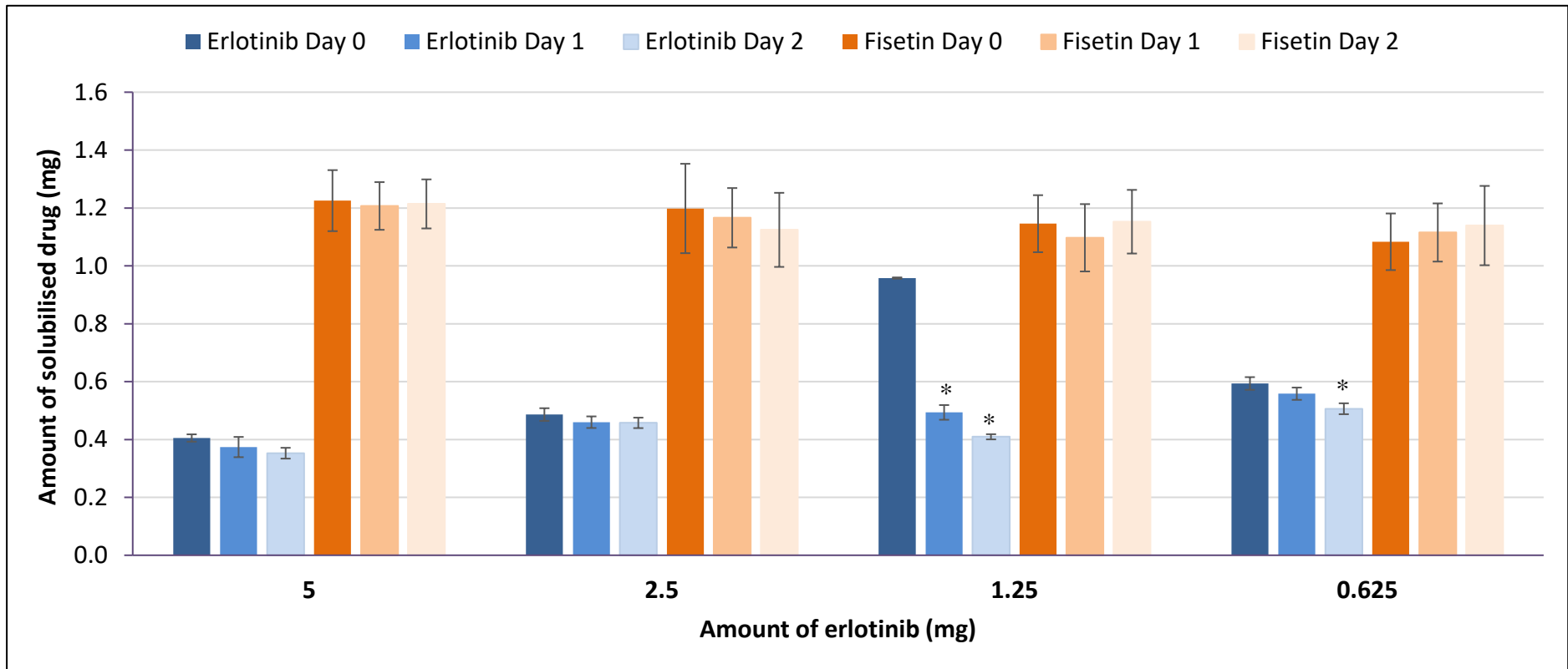
Figure 6.3 Stability of fisetin-erlotinib-SBE-β-CD complex containing different amounts of erlotinib, at room temperature. Mean ± s.d., $n = 3$, *significant difference compared to the same formulation on Day 0, $p < 0.05$.

6.3.3 Lyophilisation and investigation of different redispersion concentrations of the complexes

The optimised complex preparation contained 0.625 mg erlotinib, 1.2 mg fisetin and 109.88 mg SBE-β-CD in 10 mL solution. Thus, the concentration of both drugs in the preparation was 62.5 µg/mL and 120 µg/mL of erlotinib and fisetin, respectively. Characterisation of this solution nebulised into the NGI was not possible, as the amount of erlotinib collected at all NGI stages was below the limit of quantitation of the HPLC method. One way to address this problem is by increasing the concentration of the complex in the solution. Solidification of the complex by freeze drying and reconstitution of the dried complex with smaller volume of water, may help to produce a more concentrated preparation, with the need for stability in a shorter time.

Table 6.5 shows that reconstitution of the dried-complex to 4-times more concentrated solution significantly reduced the amount of solubilised erlotinib from 96.5 to 90.1% ($p < 0.05$). However, reconstitution of the dried-complex did not change solubilisation of fisetin ($p > 0.05$). The results show that lyophilisation and reconstitution of the preparation slightly affected stability of erlotinib-SBE-β-CD complex, but not fisetin-SBE-β-CD complex.

Table 6.5 Solubilisation of erlotinib and fisetin in different reconstitution concentrations. Mean $\pm$ s.d., $n = 3$.

Preparation	Sample's weight (mg)	Reconstitution volume (mL)	Solubilisation of erlotinib		Solubilisation of fisetin	
			Amount (mg)	Percentage (%)	Amount (mg)	Percentage (%)
Before lyophilisation	-	-	0.32 ± 0.01	96.5 ± 0.5	1.18 ± 0.05	91.7 ± 4.7
1x-concentrated	52.93 ± 0.71	5	0.26 ± 0.01	77.3 ± 3.5*	0.58 ± 0.02	96.3 ± 0.6
2x-concentrated	105.33 ± 1.02	5	0.59 ± 0.01	90.7 ± 0.2*	1.18 ± 0.04	96.5 ± 0.5
3x-concentrated	159.83 ± 1.29	5	0.90 ± 0.02	92.5 ± 0.2	1.80 ± 0.08	99.1 ± 1.6*
4x-concentrated	209.17 ± 13.83	5	1.15 ± 0.03	90.1 ± 2.1*	2.43 ± 0.09	97.2 ± 2.6

*significant difference compared to the preparation before lyophilisation, $p < 0.05$.

Figure 6.4 shows the stability of the reconstituted complex 1 h after reconstitution, as ~30min to 1 h was needed for nebulisation and aerosol characterisation of the preparation. Fisetin was shown to be stable in the complex 1 h after reconstitution at all concentrations. However, the amount of solubilised erlotinib was significantly reduced ($p < 0.05$) to 83.0 ± 2.4 and $85.3 \pm 2.3\%$ in 2- and 3-times more concentrated solutions, respectively, 1 h after reconstitution. Although 4-times more concentrated solution showed insignificant reduction in the amount of solubilised erlotinib ($p > 0.05$), high variation of the values may signify instability of the complex. Therefore, the 3-times more concentrated solution was chosen as the final preparation to be nebulised and characterised using the NGI, based on sufficient drug solubility and stability of the complex.
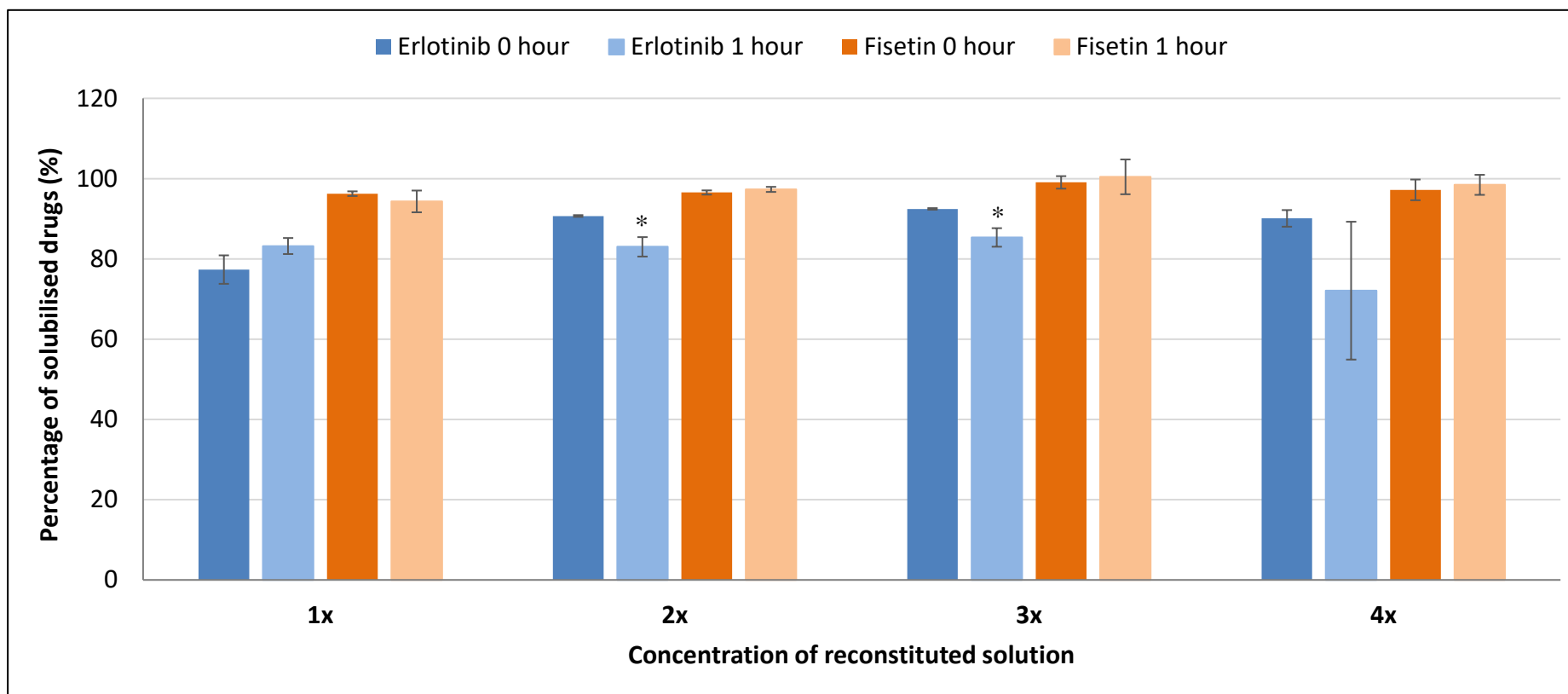
Figure 6.4 Stability of the complex in different reconstitution concentrations at room temperature. Mean ± s.d., $n = 3$, *significant difference compared to the formulation at 0 hour, $p < 0.05$.

6.3.4 Assessment of aerosol properties of nebulised complex solutions using the NGI

In this study, a flow rate of 15 L/min was used, as it represents a good estimation to the mid-inhalation flow rate by a tidally breathing healthy adult (500 mL tidal volume) (European Pharmacopoeia, Chapter 2.9.44). The NGI was calibrated at this flow rate as outlined in the European Pharmacopoeia standard.

Figure 6.5 shows the distribution of the deposited nebulised drugs in the NGI, with the majority of drugs deposited on Stage 3 and 4. Although both drugs show a normal distribution, the mass ratio of erlotinib to fisetin differed in the nebuliser and in all stages of the NGI. Higher mass ratio of fisetin in Stage 1 to 6, compared to the ratio in nebuliser, shows that less erlotinib was being emitted into the NGI and was left in the nebuliser. This is confirmed with a lower emitted fraction of erlotinib (52.56%) when compared to fisetin (67.41%) in Table 6.6 ($p < 0.05$). This led to a fine particle dose (FPD) ratio of 1: 3.1 (erlotinib: fisetin), dissimilar to the ratio in the initial reconstituted solution (1: 1.9).

The non-uniform ratio of drugs may be caused by the presence of insoluble drugs. One hour after reconstitution, the preparation had a higher amount of insoluble erlotinib compared to insoluble fisetin, indicated by the percentage of solubilisation 85.3 ± 2.3 and $100.4 \pm 4.3\%$, respectively. Further, the intense shear of liquid in the jet nebuliser may cause disruption of the inclusion and non-inclusion complexes, as previously reported in other formulations including liposomes (Elhissi et al., 2007; Kleeman et al., 2007) and lipid-peptide-DNA complexes (Birchall et al., 2000). Evaporation of the solvent during jet nebulisation will cause a decrease in the solution's concentration and temperature, affecting viscosity of the preparation (Steckel and Eskandar, 2003). These changes could also cause recrystallisation of a drug from solution which was nebulised at the limit of the drug solubility, or recrystallisation of a drug with a temperature-dependent solubility in the nebuliser solution (Taylor et al., 1992). These factors can cause release/precipitation of the complexed drugs into the solution in medication reservoir, leading to a non-uniform emission of the insoluble drug into the NGI.
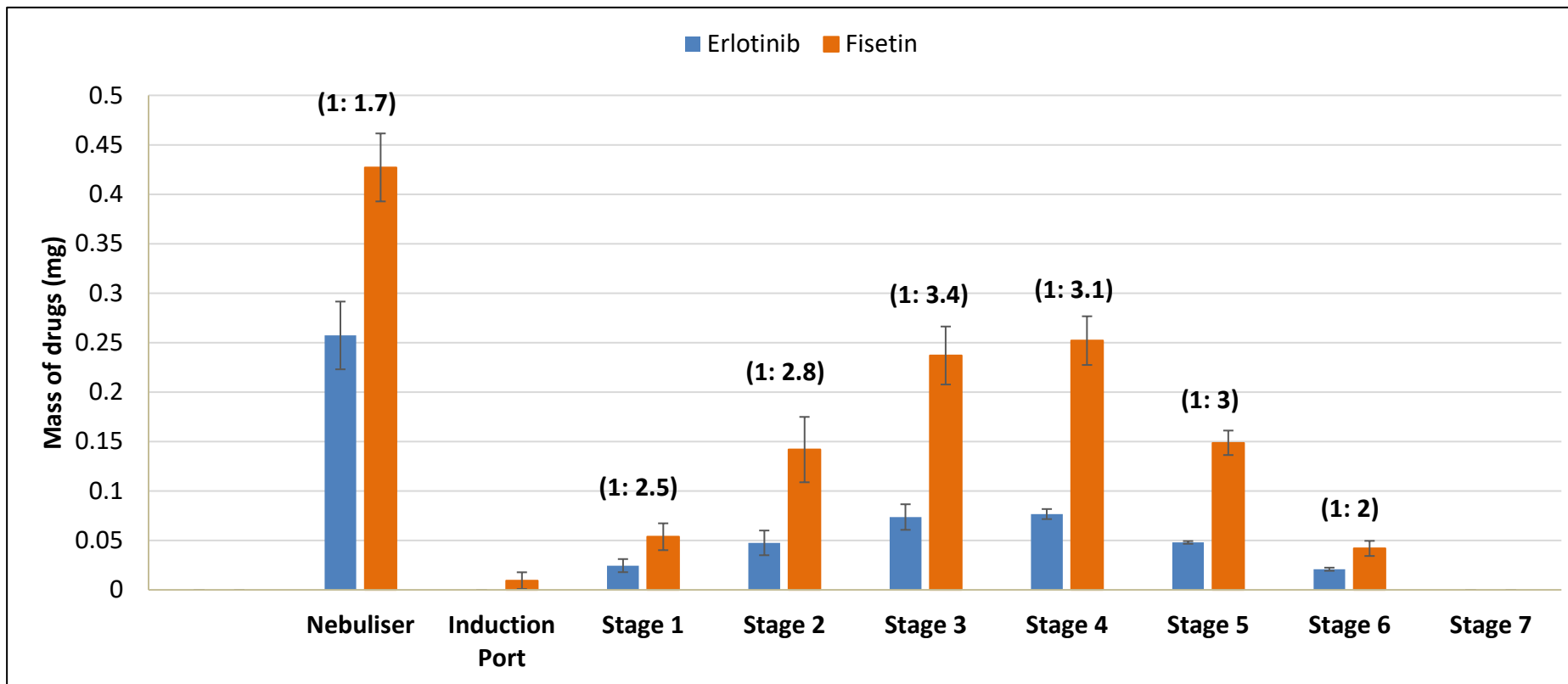
Figure 6.5 Distribution of erlotinib and fisetin in the NGI following nebulisation of erlotinib-fisetin-SBE-β-CD complex. Mean ± s.d., $n = 3$. In bracket: mass ratio of erlotinib to fisetin.

Table 6.6 Aerosolisation properties of the nebulised complex in the NGI. Mean ± s.d., $n = 3$.

Parameters	Values	
	Erlotinib	Fisetin
Mass balance (%)	82.98 ± 3.87	84.67 ± 3.19
Emitted fraction (%)	52.56 ± 4.78	67.41 ± 2.86
Fine particle dose (mg)	0.20 ± 0.01	0.62 ± 0.03
Fine particle fraction (%)[a]	70.10 ± 6.19	71.61 ± 6.64
Mass median aerodynamic diameter (µm)	5.39 ± 0.51	5.36 ± 0.51
Geometric standard deviation	1.94 ± 0.07	1.83 ± 0.05

[a] Fraction of particles < 5 µm

The mass balance quantified the percentage of total mass of drug recovered during the assessment, which was ~80% for both drugs. The loss may be explained by some solution left on the interstage passageways of the NGI, which was not collected. Nonetheless, the values met the requirement by European Pharmacopoeia (75 to 125%). The mass median aerodynamic diameter (MMAD) was ~5.4 µm for both drugs, signifying that almost 50% of the drugs were in the droplet size of ≤ 5 µm, which was suitable for inhalation (EMA, 2006).

The fraction of emitted solution from the jet nebuliser was < 70% for both drugs. This is common in the jet nebuliser system, as the residual volume can vary between 0.8 to 2 mL depending on the preparation (Dolovich and Dhand, 2011), representing 20-50% of the 4 mL complex solution. Further, the fine particle dose showed that 0.20 and 0.62 mg of erlotinib and fisetin, respectively, were in the aerosol size < 5 µm. This represents the amount of drugs that could reach the deep lung region during the 10 min nebulisation. Although the oral dose of erlotinib (150 mg; British National Formulary, 2017) and fisetin (25 mg/kg in mice; Ravichandran et al., 2011) are high, synergistic combination and localised delivery (i.e. nebulisation) of both

drugs may further reduce the doses. A reduced in the dose needed has been shown when a drug (e.g. salbutamol) is inhaled rather than taken orally. However, a longer duration of nebulisation may be needed to deliver the therapeutic doses of both drugs to the lung.

6.3.5 XRPD analysis of the lyophilised erlotinib-fisetin-SBE-β-CD complex

Figure 6.6 shows diffractograms of erlotinib and fisetin with plenty of sharp diffraction peaks, signifying the crystalline nature of the compounds. On the other hand, the diffractogram of SBE-β-CD and the lyophilised complex showed broad and diffused peaks with low intensities, indicating their amorphous nature. Although the lyophilised complex was in the amorphous form, formation of erlotinib-fisetin-SBE-β-CD inclusion complex could not be confirmed from the result, as the amount of both drugs were too diluted (mass ratio drug: SBE-β-CD; 1: >90). This can be seen from the diffractogram of the physical mixture, showing only amorphous form of the SBE-β-CD without any crystalline peaks of the drugs.
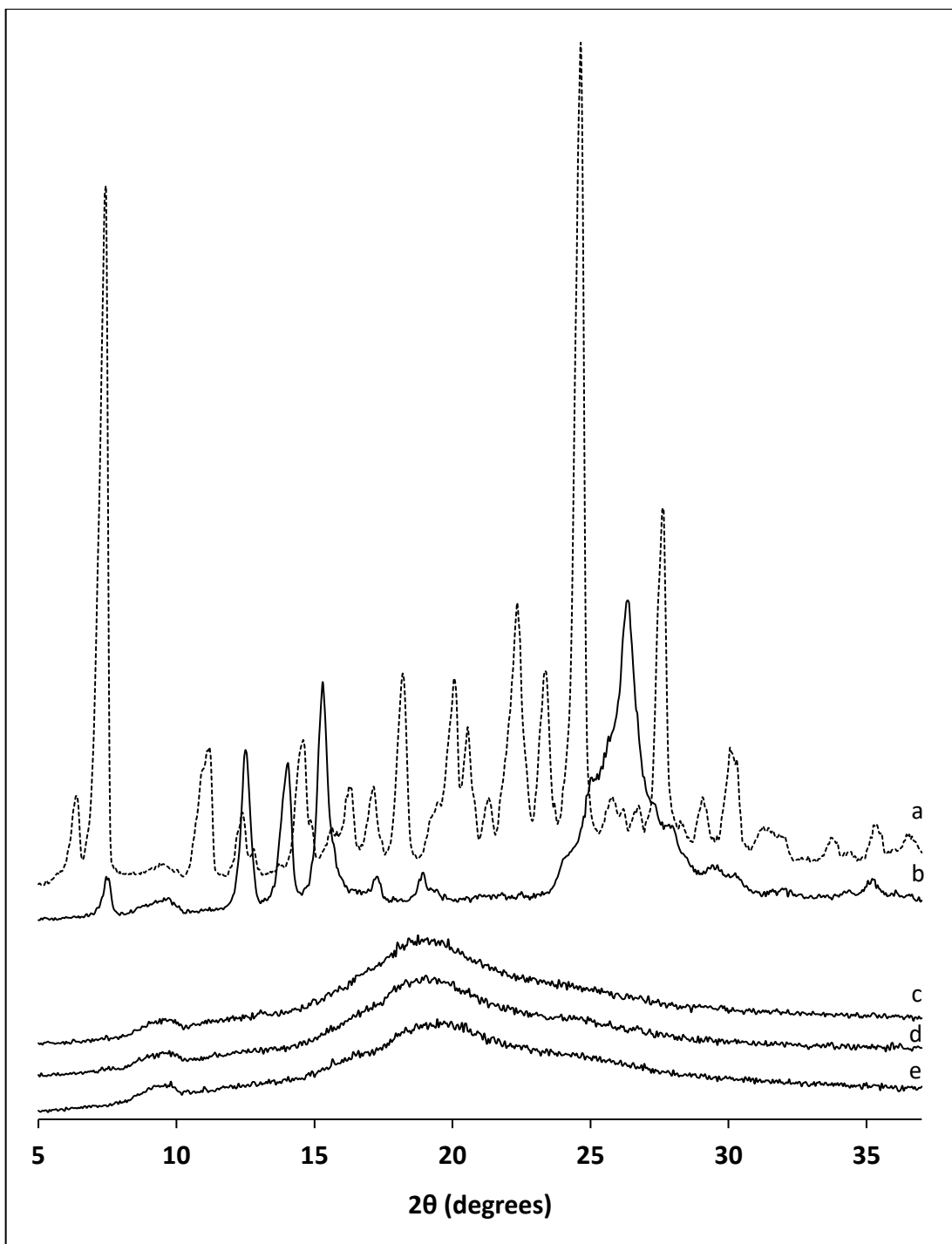
Figure 6.6 XRPD diffractograms of a) erlotinib, b) fisetin, c) SBE-β-CD, d) physical mixture and e) lyophilised erlotinib-fisetin-SBE-β-CD complex.

6.3.6   FT-IR analysis of the lyophilised erlotinib-fisetin-SBE-β-CD complex

Figure 6.7 shows the FT-IR spectra of the raw materials, a physical mixture and the complex. The erlotinib spectrum showed characteristic bands at 3250, 1511 and 1029 cm^{-1}, corresponding to the N-H stretching of the secondary amine, C-C stretching of aromatic groups and C-O stretching of ether, respectively. The fisetin spectrum showed characteristic O-H stretches at 3222 and 1205 cm^{-1}, and aromatic C-C stretch at 1594 cm^{-1}. Both the physical mixture and the lyophilised complex showed the same spectra as SBE-β-CD, illustrated by alcoholic O-H and C-O stretch at 3375 and 1153 cm^{-1}, respectively. SBE-β-CD also showed an alkane C-H stretch at 2929 cm^{-1}.

Interaction between the drugs and SBE-β-CD could not be concluded from the FT-IR results, as the amount of drugs in the preparation was too small compared to SBE-β-CD (mass ratio drug: SBE-β-CD; 1: >90). This is shown by the non-visibility of the drug peaks in the spectrum of the physical mixture.
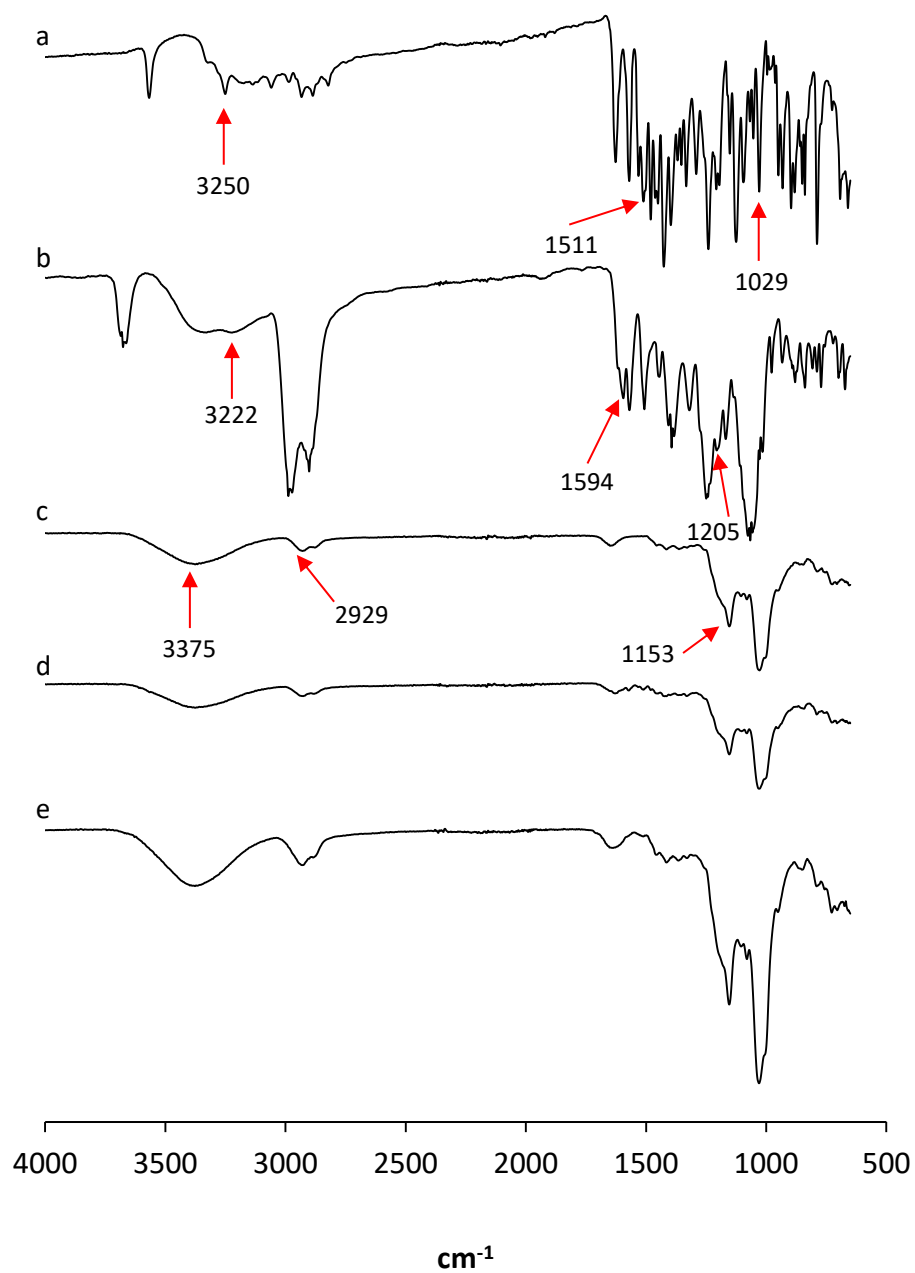
Figure 6.7 FT-IR spectra of a) erlotinib, b) fisetin, c) SBE-β-CD, d) physical mixture and e) lyophilised erlotinib-fisetin-SBE-β-CD complex.

6.3.7 *In vitro* cell toxicity of erlotinib and fisetin in the nebulisation solution

Table 6.7 shows the cytotoxic activity in the A549 cells after being treated with the samples for 72 h. The molar ratio of erlotinib to fisetin (1: 2.6) used in the formulation, showed no significant difference in toxicity ($p > 0.05$) compared to the optimal ratio (1: 2) found in Section 5.3.1. The IC_{50} of the drug combination in the formulation, were higher than the drug combination in solution ($p > 0.05$). The difference may be caused by the insoluble fraction of the drug (especially erlotinib) in the reconstituted preparation. As discussed in Section 6.3.3, the amount of solubilised erlotinib was significantly reduced from 92.5 ± 0.2 to $85.3 \pm 2.3\%$ ($p < 0.05$), 1 h after reconstitution. Since the cells were incubated with the treatment for 72 hr, the instability of erlotinib-SBE-β-CD complex will change the ratio of solubilised erlotinib: fisetin, thus affecting the cytotoxic activity.

Table 6.7 Cytotoxic activities of erlotinib and fisetin in the drug combinations, in solution and in the complex, Mean $\pm$ s.d., $n = 3$.

Samples (molar ratio)	IC_{50} (µM)	
	Erlotinib	**Fisetin**
Erlotinib: Fisetin (1: 2)	15.11 ± 3.64	30.22 ± 7.28
Erlotinib: Fisetin (1: 2.6)	13.79 ± 3.25	35.84 ± 8.45
Lyophilised erlotinib-fisetin-SBE-β-CD (1: 2.6)	$23.91 \pm 2.90*$	$62.16 \pm 7.53*$

*significant difference compared to Erlotinib: Fisetin (1: 2.6)

The A549 cell viability plots (Figure 6.8) show sigmoidal inhibition curves for the drug combinations in solution and in the complex. The blank SBE-β-CD complex showed a killing activity at the highest concentration, which may be caused by the osmotic effect of the preparation. In the assay, the highest concentration of the complex solution contained 42%v/v water in the media, which could create a hypotonic environment in the treatment well. This will cause the movement of water molecule from the diluted treatment solution into the cells. The uptake of the excess

water may produce sufficient pressure to induce lysis or rupturing of the cell wall, causing cell death.When the same concentration of lyophilised blank SBE-β-CD complex was dissolved in the media, no killing activity against the A549 cell line was seen (cell viability: 87.48 ± 3.85%, $n = 3$). This result show that SBE-β-CD did not show cytotoxic activity at all investigated concentrations (up to 14 mM).
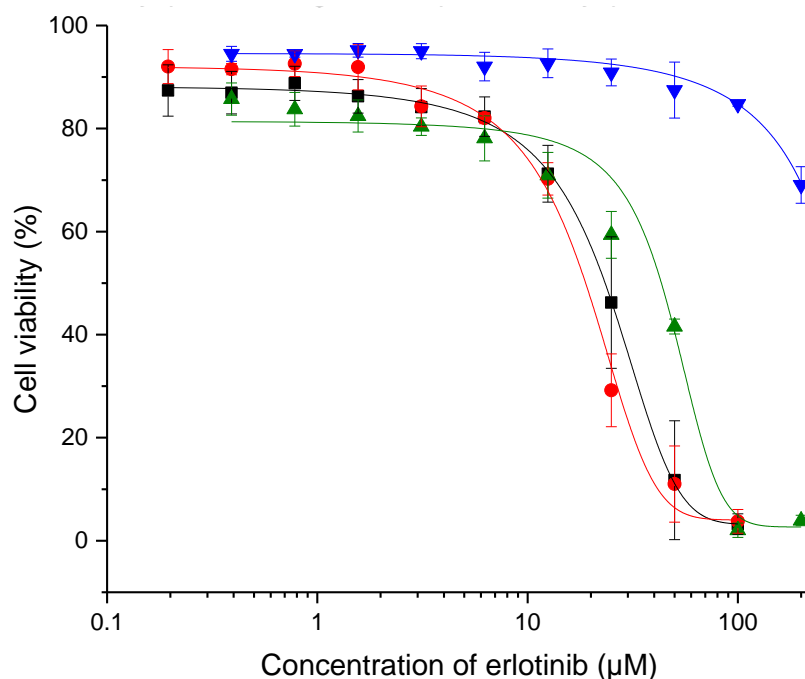
Figure 6.8 Cell viability (%) of A549 cells after treatment with erlotinib: fisetin (1: 2 molar) (■), erlotinib: fisetin (1: 2.6 molar) (●), lyophilised erlotinib-fisetin-SBE-β-CD complex (▲), lyophilised blank SBE-β-CD complex after 72 h (▼). Mean ± s.d., $n = 3$.

6.4 Conclusions

This chapter has focused on the optimisation of erlotinib-fisetin-SBE-β-CD complex, to be suitable for nebulisation. Increasing the amount of SBE-β-CD in the preparation, resulted in an increase in the amount of solubilised fisetin but did not affect solubilisation of erlotinib. However, the preparation with 109.88 mg SBE-β-CD in 10 mL showed a better stability for the complexes over 2 days after preparation.

Reducing the amount of erlotinib in the preparation did not affect the solubilisation of fisetin (90-100% solubilisation). However, the preparation containing 0.625 mg erlotinib, showed a significant increase in the amount of solubilised erlotinib compared to the preparation containing 5 mg erlotinib, with the least amount of excess drug. The preparation also showed sufficient stability for the complex over 2 days after preparation.

Reconstitution of the lyophilised complex into 3-times more concentrated preparation, was able to provide sufficient concentration of both drugs to be quantified following nebuliser delivery into the NGI. The nebulisation preparation showed sufficient stability 1 h after reconstitution. However, nebulisation of the preparation showed a non-uniform ratio distribution of both drugs in the NGI, which was likely to be caused by instability of the complexes in the jet nebuliser. Despite that, the nebulised erlotinib-fisetin-SBE-β-CD complex was shown to have a suitable aerosol size for inhalation.

The optimised nebulisation preparation showed a lower killing activity against the A549 cells compared to the drug solution. The difference may be caused by the instability of the complex during the incubation period of the treatment, which could cause change in the ratio of solubilised drugs.

Chapter 7

General discussion and future work

7.1   General discussion and conclusion

Pulmonary delivery has long been used to deliver drugs for effective local therapy of lung-associated diseases, such as asthma and chronic obstructive pulmonary disorder. Direct delivery of a drug to the site of action allows the use of a lower dose compared to the oral or intravenous routes, reducing systemic absorption and thus reducing systemic side effects (Traini and Young, 2009). One of the diseases that might also benefit from this delivery route is non-small cell lung cancer (NSCLC).

One treatment approach in NSCLC is personalised therapy, including EGFR (e.g. erlotinib and gefitinib) and ALK (e.g. crizotinib) tyrosine kinase inhibitors. These molecules inhibit the tyrosine kinase enzyme with genomic alterations, which causes the cancer. Apart from standard therapy, attention has also been given to the role of phytochemicals (e.g. fisetin), in lung cancer therapy (Khan and Mukhtar, 2015). Fisetin is a flavonoid that has shown anti-carcinogenic effects on different cancer cell lines including lung, colon and prostate cancers (Khan et al., 2013). It has also shown synergistic cytotoxic activity with other chemotherapeutic agents such as cisplatin (Tripathi et al., 2011) and cyclophosphamide (Touil et al., 2011) against different types of cancer. Therefore, utilisation of fisetin, individually or in combination with the tyrosine kinase inhibitors, should be considered as an alternative treatment for NSCLC.

A challenge to the delivery of these molecules is their low solubility in water, which can cause non-uniformity of the dose and instability of the preparation. Aqueous solubility can be improved by forming an inclusion complex of the molecule with cyclodextrins. The drug-cyclodextrin complexes can then be delivered to the lung via dry powder inhalation or nebulisation, giving an opportunity of local treatment in NSCLC. The work in this thesis commenced with the aim to improve the solubility of fisetin and erlotinib, by preparing cyclodextrin complexes containing both molecules, and subsequently to develop suitable formulations for pulmonary delivery of the drugs. The work was divided into two parts; i) the production of a dry powder fisetin-SBE-β-CD complex for inhalation and ii) the production of an erlotinib-fisetin-SBE-β-CD complex for nebulisation.

The first part of the work described in this thesis focused on the development of fisetin-cyclodextrin complexes, suitable for pulmonary delivery. Several studies have investigated incorporation of fisetin into different nanocarriers for the treatment of lung carcinoma (Mignet et al., 2012; Ragelle et al., 2012; Seguin et al., 2013), but were limited to the delivery of the nanocarriers via the intraperitoneal route. Therefore, pulmonary delivery of fisetin-cyclodextrin complexes can give an advantage of localised delivery in the treatment of lung cancer. Complexation of fisetin with β-cyclodextrins was undertaken in **Chapter 3** to improve its aqueous solubility. SBE-β-CD was found to be the best cyclodextrin to solubilise fisetin, demonstrated by the highest complexation efficiency, compared to β-CD and HP-β-CD. The anti-oxidant activity of fisetin was not affected when it was complexed with the cyclodextrins, and the activity was maintained after drying of the complex using freeze- and spray-drying methods. The spray-drying method produced a dry powder with a particle size suitable for inhalation. Addition of ethanol improved the complexation of fisetin with SBE-β-CD, with 20%v/v ethanol in water improving the solubility of fisetin 5.9-fold compared to using water alone.

Initially, the fisetin-SBE-β-CD complex produced by the co-solvency method was subjected to rotary evaporation to remove the ethanol. The dried film of the complex was then rehydrated with warm water and characterised. Subsequently, in **Chapter 4**, spray drying was utilised to produce an inhalable powder, which could also remove the ethanol and omit the evaporation and rehydration steps. The dry powder produced using these two feed solutions (i.e. feed solution containing water and feed solution containing 20%v/v ethanol) were compared. The powder produced from both feed solutions showed sizes appropriate for inhalation, with most of the powder < 5 µm. Even though the powder produced from the 20%v/v ethanolic feed solution showed a bimodal size distribution, a ~2-fold increase in the fine particle fraction was achieved when the powder was delivered from an Aerolizer® DPI device, compared to the other preparation. The improvement in the fine particle fraction can be attributed to the less dense particles, produced from ethanolic feed solution during spray drying process. The lower density will cause reduction in the aerodynamic diameter, allowing the particles to move more readily to the lower stages of NGI,

resulting in an increase in the fine particle fraction (Stigliani et al., 2013). Therefore, the spray-dried powder produced from the ethanolic feed solution was selected and its aerosol performance was further optimised using the dispersibility enhancer, leucine.

Addition of leucine to the powder formulation improved its dispersibility, shown by the change in particle size distribution from bimodal to unimodal. An enhancement in the dispersibility of the powders was also shown by a 2.3-fold increase in the fine particle fraction, when 20%w/w leucine was incorporated into the preparation. The improvement in the flowability and dispersibility can be explained by the presence of leucine at the particle surface, forming an irregular or wrinkled surface. Such surfaces will cause a reduction in the inter-particulate contact points, reducing the adhesiveness and cohesiveness of the particles (Chew and Chan, 2001). A reduction in adhesive and cohesive forces between particle may improve flowability of the powder and facilitate de-aggregation of the particles, causing an increase in the fine particle fraction (Seville et al., 2007; Stigliani et al., 2013). Further, the preparation showed an unchanged cytotoxic activity of fisetin against the A549 cell line, when compared to fisetin solution.

To conclude the first part of the work, the spray-dried fisetin-SBE-β-CD complex containing leucine showed an improvement in the solubility of fisetin and may be capable of delivering high amounts of fisetin to the deep lung (fine particle dose: 7.1 mg). From the literature, 21 mg/kg of fisetin in different nanocarriers was delivered to the rats via intraperitoneal injection (Seguin et al., 2013; Bothiraja et al., 2014) and 25 mg/kg of fisetin was delivered via the oral route (Ravichandran et al., 2011), for the treatment of lung carcinoma. In this case, ~1500-1700 mg total of fisetin may be needed for both delivery routes in humans. As the intraperitoneal and oral route involve systemic circulation of fisetin prior to reaching the lung, a lower dose may be needed if fisetin is delivered locally to the lung. However, 7.1 mg may not be sufficient for fisetin to exert its anti-cancer activity, considering > 200-fold reduction of the dose. This can be resolved by giving multiple inhalations in one dose and/or increasing the dosing frequency to achieve sufficient concentration of fisetin in the lung.

Fisetin alone may not be as potent as other anti-cancer drugs, shown by the high dose needed for its cytotoxic activity. However, its combination with other anti-cancer drugs, including cisplatin (Tripathi et al., 2011) and cyclophosphamide (Touil et al., 2011), has shown synergism in the cytotoxic effect, allowing dose reduction of those agents. Therefore, the second part of the work explored the combination of fisetin with tyrosine kinase inhibitors to find combinations with synergistic killing activity against the A549 cells. In **Chapter 5**, the cytotoxic activity of combinations of fisetin with three tyrosine kinase inhibitors (i.e. erlotinib, gefitinib and crizotinib) against the A549 cells was evaluated using the median effect principle method (Chou and Talalay, 1984). The results showed a synergistic killing activity in all combinations of fisetin and tyrosine kinase inhibitors, which was likely caused by targeting of both molecules in combinations at different sites of the cancer signalling pathways (Rao et al., 2005). The greatest synergism was found with a combination of erlotinib and fisetin, at 1: 2 molar ratio. The synergism resulted in a dose reduction to achieve IC_{50} of 8.98- and 3.63-fold for erlotinib and fisetin, respectively, which may offer a clinical benefit due to reduced side effects related to erlotinib. The combination was further formulated using cyclodextrins, to improve the solubility of both drugs.

In considering pulmonary delivery of the complexes, the first approach was to prepare a spray-dried erlotinib-cyclodextrin complex, to be combined with the inhalable dry powder fisetin-SBE-β-CD complex that was prepared in **Chapter 4**. HP-β-CD showed the best solubilising efficiency for erlotinib, followed by SBE-β-CD and β-CD. Complexation of erlotinib and HP-β-CD was further optimised using a co-solvent (i.e. ethanol). Although an improvement in the solubilisation of erlotinib was seen with the addition of 90%v/v ethanol, the relative amount of solubilised erlotinib to HP-β-CD (mass ratio 1: 188) was too small to be carried forward in the study. Further, adjustment of the solution to acidic pH, increased the aqueous solubility of erlotinib, up to a point that addition of HP-β-CD did not contribute to the solubilisation at all. In this case, erlotinib-HP-β-CD complex in pH 2 and 3 showed sufficient solubilisation of erlotinib, and may be suitable to be spray-dried. However, the pH was at the lower limit of the pH range suitable for inhalation (pH 3-10; British Pharmacopoeia, 2018), which may result in bronchoconstriction, coughing and

irritation of the lung mucosa (Labiris and Dolovich, 2003). Moreover, a suitable instrument to spray dry the solution containing erlotinib was not available, that could protect the environment and operator. Therefore, spray drying of erlotinib-HP-β-CD was not carried out in the study.

The second approach was to prepare a nebuliser solution containing a co-complex of both drugs with a cyclodextrin, which can minimise the use of excipients in the formulation. In this study, HP-β-CD and SBE-β-CD were used to form the co-complex, as they were the cyclodextrins that showed the best solubilising profile for erlotinib and fisetin, respectively. A higher solubilising efficiency of erlotinib was found in the co-complexation with fisetin using SBE-β-CD, which was better than the single erlotinib-SBE-β-CD complex. This may be attributed to the formation of fisetin-SBE-β-CD complex aggregates, which can further solubilise erlotinib through non-inclusion complexes. Further improvement in the drug solubility was achieved with addition of 50%v/v ethanol during complexation (i.e. 4.3- and 1.8-fold increase in solubility for erlotinib and fisetin, respectively).

The erlotinib-fisetin-SBE-β-CD complex was further optimised in **Chapter 6**, to prepare a solution suitable for nebulisation. A preparation composed of 109.88 mg SBE-β-CD, 0.625 mg erlotinib and 1.2 mg fisetin gave sufficient solubility and stability of the preparation. However, this preparation was too diluted to be quantified by the HPLC following nebuliser delivery into the NGI. Thus, lyophilisation of the erlotinib-fisetin-SBE-β-CD complex was undertaken and reconstitution of the powder into a 3-times more concentrated preparation was sufficient to allow accurate quantification of both drugs by HPLC. Nebulisation of the preparation from a Pari LC$^©$ Sprint jet nebuliser, showed a non-uniform ratio of the two drugs in different stages of the NGI. Such distribution may be caused by instability of the erlotinib-fisetin-SBE-β-CD complex during intense shear of the jet nebuliser (Elhissi et al., 2007; Kleeman et al., 2007) and recrystallisation of the drugs in the solution (Taylor et al., 1992), resulting in a non-uniform ratio of the insoluble drugs delivered into the NGI. This caused a change in the ratio of erlotinib: fisetin in the fine particle dose (1: 3.1) compared to the solution before nebulisation (1: 1.9). Despite the instability, the

preparation showed a suitable aerosol size for inhalation of both drugs (MMAD ~5 μm).

To conclude the second part of the work, an erlotinib-fisetin-SBE-β-CD complex with sufficient solubility and stability of both drugs was successfully prepared. The fine particle dose after nebulisation of the preparation, showed that 0.20 mg erlotinib and 0.62 mg fisetin may be delivered to the deep lung. The doses needed in the oral treatment of erlotinib and fisetin are 150 and ~1500 mg, respectively. As the oral route involves systemic distribution of the drug prior to reaching the lung, a lower dose of both drugs may be needed if delivered via nebulisation to the lung. The synergistic combination of erlotinib and fisetin will further allow dose reduction of both drugs. This may represent a positive advance in the treatment of erlotinib, which is currently available only via the oral route. Erlotinib undergoes extensive first-pass metabolism following oral administration (Smith et al., 2008), leading to an oral bioavailability of ~59% (Frohna et al., 2006). Delivery of the drug via inhalation can ensure a high concentration at the target site without the need for high doses. Localised delivery of erlotinib may also help to reduce/diminish the systemic side effects (e.g. dermatologic reaction, stomatitis and diarrhoea), improving patient's adherence and quality of life.

The fine particle dose achieved in this study, may or may not be enough for the treatment of NSCLC. However, the dosing can be adjusted by shortening or prolonging the nebulisation time to get the desired dose. Jet nebulisation may not be the best choice to deliver the erlotinib-fisetin-SBE-β-CD complex, as it affected stability of the preparation. In this case, another nebulisation device (e.g. mesh nebuliser), which is less disruptive towards the formulation, may be used. The devices will be further discussed in the future work.

In conclusion, the aim of the thesis was achieved as cyclodextrin-based formulations, with improved aqueous solubility of fisetin and erlotinib, were developed and optimised to be suitable for pulmonary delivery. Local delivery of fisetin, individually and in combination with erlotinib, to the lung showed some

promising results, which may contribute to a better outcome in the treatment of NSCLC.

7.2 Future work

The present study has investigated the suitability of fisetin and its combination with erlotinib to be complexed using SBE-β-CD. The complexes have been formulated and optimised such that they are suitable for pulmonary delivery, via dry powder inhalation and/or nebulisation. However, further studies should be considered to improve the understanding of the formulations prepared in this work.

a) Stability studies of the dried complexes

In the study, fisetin-SBE-β-CD and erlotinib-fisetin-SBE-β-CD complexes were spray- and freeze-dried, respectively. After drying, both preparations were kept in a desiccator prior to the analysis.

In the real-world situation, the dried powder may be stored at different temperatures and humidity. SBE-β-CD is a hygroscopic material (Jain and Adeyeye, 2001), which will tend to take up moisture, causing recrystallisation of the powder thus affecting stability of the inclusion complexes. In the case of the spray-dried fisetin-SBE-β-CD complex, the moisture will also cause recrystallisation and agglomeration of the particles, which could affect dispersibility during inhalation. Even though leucine has been shown to protect the integrity of spray-dried particles against moisture as high as 65%RH within 7 days (Raula et al., 2008), a longer storage stability at certain conditions (e.g. 25 ± 2ºC/ 60 ± 5%RH) should be studied to determine the best storage condition for the preparations, according to the relevant international guidelines (ICH, 2003).

b) Utilisation of other devices for the nebulisation of the erlotinib-fisetin-SBE-β-CD complex

Nebulisation of the erlotinib-fisetin-SBE-β-CD complex prepared in this study, was performed using a jet nebuliser. The non-uniform distribution of the two drugs in the aerosolised product in the NGI, might suggest instability of the complex caused by the

intense shear of the nebuliser or temperature effects. In contrast to jet nebulisers, mesh nebulisers have been shown to be less disruptive towards formulations (Elhissi et al., 2007; Kleeman et al., 2007) with little or no temperature effects and may improve the emitted fraction of drugs into the NGI, as they have a small residual volume. Therefore, nebulisation of the complex using a mesh nebuliser should be studied to find a suitable device to deliver the preparation optimally to the lung.

c) In vivo animal study of the SBE-β-CD-based preparations

The work in this thesis describes formulation development of inhalable SBE-β-CD-based formulations, and characterisation of the aerosol performance *in vitro* using the NGI. An in vivo animal study should be performed to evaluate the inhalation performance and efficacy of the preparation. Different methods of delivering the preparation to the animal lung may be applied according to the formulations;

i) The dry powder fisetin-SBE-β-CD complex can be delivered by insufflation of the powder to the lungs, using an insufflator device (Kim et al., 2012). Another method is to deliver the powder through forced ventilation, using a ventilator which is connected to an endotracheal tube (Vanbever et al., 1999).

ii) The erlotinib-fisetin-SBE-β-CD complex solution can be delivered via intratracheal instillation of the solution to the mouse lung or whole-body nebulisation (Rudolph et al., 2004). In the whole-body nebulisation, the preparation is nebulised into an acrylic glass box containing the mice.

d) Formulation development of other potential combinations

In the study, combinations of fisetin and all three tyrosine kinase inhibitors (i.e. erlotinib, gefitinib, crizotinib) showed synergistic killing activity against the A549 cells. However, only the combination of erlotinib and fisetin (1: 2 molar ratio) was chosen to be developed into an inhalable preparation, as it showed the highest synergism. Based on the results, combination of fisetin and gefitinib/crizotinib should also be developed into inhalable formulations. Although the drug reduction index (DRI) of gefitinib and crizotinib was not as high as erlotinib (Table 5.8), a 2- to 5-fold reduction of the dose may significantly reduce the treatment cost, especially for an

expensive drug like crizotinib (Table 7.1). However, a cost benefit analysis has to be done as pulmonary delivery of a drug will also add to the treatment cost (e.g. inhaler device).

Table 7.1 Estimated price for the treatment using tyrosine kinase inhibitors, calculated according to British National Formulary (2017).

Drugs	Estimated price	Treatment dose	Estimated price for daily treatment
Erlotinib	£54.38/ 150 mg tablet	150 mg OD	£54.38
Gefitinib	£72.26/ 250 mg tablet	250 mg OD	£72.26
Crizotinib	£78.15/ 250 mg capsule	250 mg BD	£156.30

References

ALI, A. A. A., HSU, F. T., HSIEH, C. L., SHIAU, C. Y., CHIANG, C. H., WEI, Z. H., CHEN, C. Y. & HUANG, H. S. (2016) Erlotinib-conjugated iron oxide nanoparticles as a smart cancer-targeted theranostic probe for MRI. *Scientific Reports*, 6, 36650.

AMIDON, G. L., LENNERNÄS, H., SHAH, V. P. & CRISON, J. R. (1995) A theoretical basis for a biopharmaceutics drug classification: The correlation of in vitro drug product dissolution and in vivo bioavailability. *Pharmaceutical Research*, 12, 413-420.

ARI, A. (2014) Jet, ultrasonic, and mesh nebulizers: An evaluation of nebulizers for better clinical outcomes. *Eurasian Journal of Pulmonology*, 16, 1-7.

ARORA, A. & SCHOLAR, E. M. (2005) Role of tyrosine kinase inhibitors in cancer therapy. *Journal of Pharmacology and Experimental Therapeutics*, 315, 971-979.

BAKHTIARY, Z., BARAR, J., AGHANEJAD, A., SAEI, A. A., NEMATI, E., EZZATI NAZHAD DOLATABADI, J. & OMIDI, Y. (2017) Microparticles containing erlotinib-loaded solid lipid nanoparticles for treatment of non-small cell lung cancer. *Drug Development and Industrial Pharmacy*, 43, 1244-1253.

BASAVOJU, S., BOSTRÖM, D. & VELAGA, S. P. (2008) Indomethacin-saccharin cocrystal: Design, synthesis and preliminary pharmaceutical characterization. *Pharmaceutical Research*, 25, 530-541.

BHISE, S. D. (2011) Effect of hydroxyropyl β-cyclodextrin inclusion complexation on solubility of fenofibrate. *International Journal of Research in Pharmaceutical and Biomedical Sciences,* 2, 596-604.

BIJNSDORP, I. V., GIOVANNETTI, E. & PETERS, G. J. (2011) Analysis of Drug Interactions. IN: CREE, A. I. (Ed.) *Cancer Cell Culture: Methods and Protocols*. Totowa, NJ, Humana Press, pp. 421-434.

BIRCHALL, J. C., KELLAWAY, I. W. & GUMBLETON, M. (2000) Physical stability and in-vitro gene expression efficiency of nebulised lipid-peptide-DNA complexes. *International Journal of Pharmaceutics*, 197, 221-231.

BOAKYE, C. H. A., PATEL, K., DODDAPANENI, R., BAGDE, A., MAREPALLY, S. & SINGH, M. (2017) Novel amphiphilic lipid augments the co-delivery of erlotinib and IL36 siRNA into the skin for psoriasis treatment. *Journal of Controlled Release*, 246, 120-132.

BORGHETTI, G. S., LULA, I. S., SINISTERRA, R. D. & BASSANI, V. L. (2009) Quercetin/β-cyclodextrin solid complexes prepared in aqueous solution followed by spray-drying or by physical mixture *AAPS PharmSciTech,* 10, 235-242.

BOTHIRAJA, C., YOJANA, B. D., PAWAR, A. P., SHAIKH, K. S. & THORAT, U. H. (2014) Fisetin-loaded nanocochleates: formulation, characterisation, in vitro anticancer testing, bioavailability and biodistribution study. *Expert Opinion on Drug Delivery*, 11, 17-29.

BOULET, L. P., BECKER, A., BÉRUBÉ, D., BEVERIDGE, R. & ERNST, P. (1999) Canadian asthma consensus report. *Canadian Medical Association Journal*, 161, S1-S62.

BOVENSCHEN, H. J. & ALKEMADE, J. A. (2009) Erlotinib-induced dermatologic side-effect. *International Journal of Dermatology*, 48, 326-328.

BREWSTER, M. E. & LOFTSSON, T. (2007) Cyclodextrins as pharmaceutical solubilizers. *Advanced Drug Delivery Reviews*, 59, 645-666.

BRIDGES, P. A. & TAYLOR, K. M. G. (1998) Nebulisers for the generation of liposomal aerosols. *International Journal of Pharmaceutics*, 173, 117-125.

BRITISH NATIONAL FORMULARY (2017). 74th ed. London: BMJ Group and Pharmaceutical Press.

BRITISH PHARMACOPOEIA (2018). London: TSO.

CABRAL-MARQUES, H. & ALMEIDA, R. (2009) Optimisation of spray-drying process variables for dry powder inhalation (DPI) formulations of corticosteroid/cyclodextrin inclusion complexes. *European Journal of Pharmaceutics and Biopharmaceutics,* 73, 121-129.

CABRAL MARQUES, H. M., HADGRAFT, J., KELLAWAY, I. W. & TAYLOR, G. (1991) Studies of cyclodextrin inclusion complexes. III. The pulmonary absorption of β-, DM-β- and HP-β-cyclodextrins in rabbits. *International Journal of Pharmaceutics*, 77, 297-302.

CALIGUR, V. (2008) Cyclodextrins. *BioFiles.*[Online]. [Accessed 11th October 2015]. Available at http://www.sigmaaldrich.com.

CHANG, Y. X., YANG, J. J., PAN, R. L., CHANG, Q. & LIAO, Y. H. (2014) Anti-hygroscopic effect of leucine on spray-dried herbal extract powders. *Powder Technology,* 266, 388-395.

CHEN, L., OKUDA, T., LU, X. Y. & CHAN, H. K. (2016) Amorphous powders for inhalation drug delivery. *Advanced Drug Delivery Reviews*, 100, 102-115.

CHEW, N. Y. K. & CHAN, H. K. (2001) Use of solid corrugated particles to enhance powder aerosol performance. *Pharmaceutical Research*, 18, 1570-1577.

CHOU, T. C. (2010) Drug combination studies and their synergy quantification using the Chou-Talalay method. *Cancer Research*, 70, 440-446.

CHOU, T. C. & MARTIN, N. (2005) CompuSyn for drug combination and for general dose-effect analysis: User's guide. *ComboSyn, Inc*. [Online]. [Acessed 30th August 2017]. Available at www.combosyn.com.

CHOU, T. C. & TALALAY, P. (1984) Quantitative analysis of dose-effect relationships: the combined effects of multiple drugs or enzyme inhibitors. *Advances in Enzyme Regulation*, 22, 27-55.

CHOUGULE, M., PADHI, B. & MISRA, A. (2008) Development of spray dried liposomal dry powder inhaler of Dapsone. *AAPS PharmSciTech*, 9, 47-53.

COPLEY, M. (2007) Understanding cascade impaction and its importance for inhaler testing. [Online]. [Accessed 12th February 2018]. Available at http://www.copleyscientific.com/files/ww/articles/Understanding%20Cascade%20Impaction%20White%20Paper.pdf.

COPLEY SCIENTIFIC (2015) Quality solutions for inhaler testing. [Online]. [Accessed 25th November 2017]. Available at http://www.copleyscientific.com/files/ww/brochures/Inhaler%20Testing%20Brochure%202015_Rev4_Low%20Res.pdf.

COUNCIL OF EUROPE (2016) *European Pharmacopoeia.* Strasbourg: Council of Europe.

DEL VALLE, E. M. M. (2004) Cyclodextrins and their uses: a review. *Process Biochemistry*, 39, 1033-1046.

DEVASARI, N., DORA, C. P., SINGH, C., PAIDI, S. R., KUMAR, V., SOBHIA, M. E. & SURESH, S. (2015) Inclusion complex of erlotinib with sulfobutyl ether-β-cyclodextrin: Preparation, characterization, in silico, in vitro and in vivo evaluation. *Carbohydrate Polymers*, 134, 547-556.

DI, L., FISH, P. V. & MANO, T. (2012) Bridging solubility between drug discovery and development. *Drug Discovery Today*, 17, 486-495.

DOLOVICH, M. B. & DHAND, R. (2011) Aerosol drug delivery: developments in device design and clinical use. *The Lancet*, 377, 1032-1045.

DORA, C. P., KUSHWAH, V., KATIYAR, S. S., KUMAR, P., PILLAY, V., SURESH, S. & JAIN, S. (2017) Improved oral bioavailability and therapeutic efficacy of erlotinib through molecular complexation with phospholipid. *International Journal of Pharmaceutics*, 534, 1-13.

DORA, C. P., TROTTA, F., KUSHWAH, V., DEVASARI, N., SINGH, C., SURESH, S. & JAIN, S. (2016) Potential of erlotinib cyclodextrin nanosponge complex to enhance solubility, dissolution rate, in vitro cytotoxicity and oral bioavailability. *Carbohydrate Polymers*, 137, 339-349.

EDELMAN, M. J., QUAM, H. & MULLINS, B. (2001) Interactions of gemcitabine, carboplatin and paclitaxel in molecularly defined non-small-cell lung cancer cell lines. *Cancer Chemotherapy and Pharmacology*, 48, 141-144.

EDWARDS, D. A., HANES, J., CAPONETTI, G., HRKACH, J., BEN-JEBRIA, A., ESKEW, M. L., MINTZES, J., DEAVER, D., LOTAN, N. & LANGER, R. (1997) Large porous particles for pulmonary drug delivery. *Science*, 276, 1868-1872.

EGAN, T. D., KERN, S. E., JOHNSON, K. B. & PACE, N. L. (2003) The pharmacokinetics and pharmacodynamics of propofol in a modified cyclodextrin formulation (Captisol®) versus propofol in a lipid formulation (Diprivan®): An electroencephalographic and hemodynamic study in a porcine model. *Anesthesia & Analgesia*, 97, 72-79.

EL-RAYES, B. F., ALI, S., ALI, I. F., PHILIP, P. A., ABBRUZZESE, J. & SARKAR, F. H. (2006) Potentiation of the effect of erlotinib by genistein in pancreatic cancer: The role of Akt and nuclear factor-ΚB. *Cancer Research*, 66, 10553-10559.

ELHISSI, A. M. A., FAIZI, M., NAJI, W. F., GILL, H. S. & TAYLOR, K. M. G. (2007) Physical stability and aerosol properties of liposomes delivered using an air-jet nebulizer and a novel micropump device with large mesh apertures. *International Journal of Pharmaceutics*, 334, 62-70.

EMA (2006) Guideline on the pharmaceutical quality of inhalation and nasal products. *Committee for medicinal products for human use (CHMP).* [Online]. [Accessed 14th August 2017]. Available at http://www.ema.europa.eu/ema/

EMA (2017) Cyclodextrins used as excipients. *Committee for Human Medicinal Product (CHMP).* [Online]. [Accessed 15th July 2018]. Available at http://www.ema.europa.eu/ema/

FATHI, M., ZANGABAD, P. S., AGHANEJAD, A., BARAR, J., ERFAN-NIYA, H. & OMIDI, Y. (2017) Folate-conjugated thermosensitive O-maleoyl modified chitosan micellar nanoparticles for targeted delivery of erlotinib. *Carbohydrate Polymers*, 172, 130-141.

FROHNA, P., LU, J., EPPLER, S., HAMILTON, M., WOLF, J., RAKHIT, A., LING, J., KENKARE-MITRA, S. R. & LUM, B. L. (2006) Evaluation of the absolute oral bioavailability and bioequivalence of erlotinib, an inhibitor of the epidermal growth factor receptor tyrosine kinase, in a randomized, crossover study in healthy subjects. *Journal of Clinical Pharmacology*, 46, 282-90.

GADGEEL, S. M., ALI, S., PHILIP, P. A., WOZNIAK, A. & SARKAR, F. H. (2009) Genistein enhances the effect of epidermal growth factor receptor tyrosine kinase inhibitors and inhibits nuclear factor kappa B in nonsmall cell lung cancer cell lines. *Cancer*, 115, 2165-2176.

GANTA, S. & AMIJI, M. (2009) Coadministration of paclitaxel and curcumin in nanoemulsion formulations to overcome multidrug resistance in tumor cells. *Molecular Pharmaceutics*, 6, 928-939.

GELLER, D. E., WEERS, J. & HEUERDING, S. (2011) Development of an inhaled dry-powder formulation of tobramycin using PulmoSphere™ technology. *Journal of Aerosol Medicine and Pulmonary Drug Delivery*, 24, 175-182.

GILANI, K., NAJAFABADI, A. R., BARGHI, M. & RAFIEE-TEHRANI, M. (2005) The effect of water to ethanol feed ratio on physical properties and aerosolization behavior of spray dried cromolyn sodium particles. *Journal of Pharmaceutical Sciences,* 94, 1048-1059.

GLAXOSMITHKLINE (2017) Prescribing information: Breo Ellipta® inhaler. [Online]. [Accessed 21st February 2018]. Available at https://www.gsksource.com/pharma/content/gsk/source/us/en/brands/breo-asthma/pi/inhaler.html

GLIŃSKI, J., CHAVEPEYER, G. & PLATTEN, J. K. (2000) Surface properties of aqueous solutions of l-leucine. *Biophysical Chemistry,* 84, 99-103.

GONTIJO, S. M. L., GUIMARÃES, P. P. G., VIANA, C. T. R., DENADAI, Â. M. L., GOMES, A. D. M., CAMPOS, P. P., ANDRADE, S. P., SINISTERRA, R. D. & CORTÉS, M. E. (2015) Erlotinib/hydroxypropyl-β-cyclodextrin inclusion complex: characterization and in vitro and in vivo evaluation. *Journal of Inclusion Phenomena and Macrocyclic Chemistry*, 83, 267-279.

GUCHARDI, R., FREI, M., JOHN, E. & KAERGER, J. S. (2008) Influence of fine lactose and magnesium stearate on low dose dry powder inhaler formulations. *International Journal of Pharmaceutics*, 348, 10-17.

GUPTA, B., POUDEL, B. K., REGMI, S., PATHAK, S., RUTTALA, H. B., GAUTAM, M., AN, G. J., JEONG, J. H., CHOI, H. G., YONG, C. S. & KIM, J. O. (2018) Paclitaxel and erlotinib-co-loaded solid lipid core nanocapsules: assessment of physicochemical characteristics and cytotoxicity in non-small cell lung cancer. *Pharmaceutical Research*, 35, 96.

GUZZO, M. R., UEMI, M., DONATE, P. M., NIKOLAOU, S., MACHADO, A. E. H. & OKANO, L. T. (2006) Study of the complexation of fisetin with cyclodextrin. *Journal of Physical Chemistry A*, 110, 10545-10551.

HASSAN, M. S. & LAU, R. W. M. (2009) Effect of particle shape on dry particle inhalation: Study of flowability, aerosolization, and deposition properties. *AAPS PharmSciTech*, 10, 1252-1262.

HE, Y., SU, Z., XUE, L., XU, H. & ZHANG, C. (2016) Co-delivery of erlotinib and doxorubicin by pH-sensitive charge conversion nanocarrier for synergistic therapy. *Journal of Controlled Release*, 229, 80-92.

HIGUCHI, T. & CONNORS, K. A. (1965) Phase-solubility techniques. *Advances in Analytical Chemistry and Instrumentation,* 4, 117-212.

HONG, S. W., PARK, N. S., NOH, M. H., SHIM, J. A., AHN, B. N., KIM, Y. S., KIM, D., LEE, H. K. & HUR, D. Y. (2017) Combination treatment with erlotinib and ampelopsin overcomes erlotinib resistance in NSCLC cells via the Nox2-ROS-Bim pathway. *Lung Cancer*, 106, 115-124.

HONGRAPIPAT, J., KOPEČKOVÁ, P., PRAKONGPAN, S. & KOPEČEK, J. (2008) Enhanced antitumor activity of combinations of free and HPMA copolymer-bound drugs. *International Journal of Pharmaceutics*, 351, 259-270.

HOPPENTOCHT, M., HAGEDOORN, P., FRIJLINK, H. W. & DE BOER, A. H. (2014) Technological and practical challenges of dry powder inhalers and formulations. *Advanced Drug Delivery Reviews,* 75, 18-31.

ICH (1994) Validation of analytical procedures: Text and methodology Q2 (R1). *ICH harmonised tripartite guideline*. [Online]. [Accessed 11th October 2015]. Available at http://www.ich.org.

ICH (2003) Guidance for industry: Q1A(R2) Stability testing of new drug substances and products. *ICH harmonised tripartite guideline*. [Online]. [Accessed 07th March 2018]. Available at http://www.ich.org.

IBRAHIM, M., VERMA, R. & GARCIA-CONTRERAS, L. (2015) Inhalation drug delivery devices: technology update. *Medical Devices: Evidence and Research*, 8, 131-139.

IHLE, N. T., PAINE-MURRIETA, G., BERGGREN, M. I., BAKER, A., TATE, W. R., WIPF, P., ABRAHAM, R. T., KIRKPATRICK, D. L. & POWIS, G. (2005) The phosphatidylinositol-3-kinase inhibitor PX-866 overcomes resistance to the epidermal growth factor receptor inhibitor gefitinib in A-549 human non-small cell lung cancer xenografts. *Molecular Cancer Therapeutics*, 4, 1349-1357.

IRNGARTINGER, M., CAMUGLIA, V., DAMM, M., GOEDE, J. & FRIJLINK, H. W. (2004) Pulmonary delivery of therapeutic peptides via dry powder inhalation: effects of micronisation and manufacturing. *European Journal of Pharmaceutics and Biopharmaceutics,* 58**,** 7-14.

IYER, R. & BHARTHUAR, A. (2010) A review of erlotinib- An oral, selective epidermal growth factor receptor tyrosine kinase inhibitor. *Expert Opinion of Pharmacotherapy*, 11, 311-320.

JAIN, A. C. & ADEYEYE, M. C. (2001) Hygroscopicity, phase solubility and dissolution of various substituted sulfobutylether β-cyclodextrins (SBE) and danazol-SBE inclusion complexes. *International Journal of Pharmaceutics*, 212, 177-186.

JEONG, D., CHOI, J. M., CHOI, Y., JEONG, K., CHO, E. & JUNG, S. (2013) Complexation of fisetin with novel cyclosophoroase dimer to improve solubility and bioavailability. *Carbohydrate Polymers*, 97, 196-202.

JESSON, G., BRISANDER, M., ANDERSSON, P., DEMIRBÜKER, M., DERAND, H., LENNERNÄS, H. & MALMSTEN, M. (2014) Carbon dioxide-mediated generation of hybrid nanoparticles for improved bioavailability of protein kinase inhibitors. *Pharmaceutical Research*, 31, 694-705.

JOHNSON, D. H., SCHILLER, J. H. & BUNN JR, P. A. (2014) Recent clinical advances in lung cancer management. *Journal of Clinical Oncology*, 32, 973-982.

JUNTUNEN-BACKMAN, K., KAJOSAARI, M., LAURIKAINEN, K., MALINEN, A., KAILA, M., MUSTALA, L., KASKI, U., LINNA, O., MARENK, M. & TOIVANEN, P. (2002) Comparison of Easyhaler® metered-dose, dry powder inhaler and a pressurised metered-dose inhaler plus spacer in the treatment of asthma in children. *Clinical Drug Investigation*, 22, 827-835.

KHAN, N., AFAQ, F., KHUSRO, F. H., ADHAMI, V. M., SUH, Y. & MUKHTAR, H. (2012) Dual inhibition of P13K/AKT and mTOR signaling in human non-small cell lung cancer cells by a dietary flavonoid fisetin. *International Journal of Cancer*, 130, 1695-1705.

KHAN, N. & MUKHTAR, H. (2015) Dietary agents for prevention and treatment of lung cancer. Cancer Letters, 359, 155-164.

KHAN, N., SYED, D. N., AHMAD, N. & MUKHTAR, H. (2013) Fisetin: A dietary antioxidant for health promotion. *Antioxidants & Redox Signaling*, 19, 151-162.

KIM, I., BYEON, H. J., KIM, T. H., LEE, E. S., OH, K. T., SHIN, B. S., LEE, K. C. & YOUN, Y. S. (2012) Doxorubicin-loaded highly porous large PLGA microparticles as a sustained-release inhalation system for the treatment of metastatic lung cancer. *Biomaterials*, 33, 5574-5583.

KIM, J., RAMASAMY, T., CHOI, J. Y., KIM, S. T., YOUN, Y. S., CHOI, H. G., YONG, C. S. & KIM, J. O. (2017) PEGylated polypeptide lipid nanocapsules to enhance the anticancer efficacy of erlotinib in non-small cell lung cancer. *Colloids and Surfaces B: Biointerfaces*, 150, 393-401.

KLEEMANN, E., SCHMEHL, T., GESSLER, T., BAKOWSKY, U., KISSEL, T. & SEEGER, W. (2007) Iloprost-containing liposomes for aerosol application in pulmonary arterial hypertension: Formulation aspects and stability. *Pharmaceutical Research*, 24, 277-287.

KURKOV, S. V. & LOFTSSON, T. (2013) Cyclodextrins. *International Journal of Pharmaceutics*, 453, 167-180.

LABIRIS, N. R. & DOLOVICH, M. B. (2003) Pulmonary drug delivery. Part II: The role of inhalant delivery devices and drug formulations in therapeutic effectiveness of aerosolized medications. *British Journal of Clinical Pharmacology*, 56, 600-612.

LAM, A. T. N., YOON, J., GANBOLD, E. O., SINGH, D. K., KIM, D., CHO, K. H., SON, S. J., CHOO, J., LEE, S. Y., KIM, S. & JOO, S. W. (2014) Adsorption and desorption of tyrosine kinase inhibitor erlotinib on gold nanoparticles. *Journal of Colloid and Interface Science*, 425, 96-101.

LANDI, L. & CAPPUZZO, F. (2014) Management of NSCLC: focus on crizotinib. *Expert Opinion on Pharmacotherapy*, 15, 2587-2597.

LÉOTOING, L., WAUQUIER, F., GUICHEUX, J., MIOT-NOIRAULT, E., WITTRANT, Y. & COXAM, V. (2013) The polyphenol fisetin protects bone by repressing NF-κB and MKP-1-dependent signaling pathways in osteoclasts. *PLoS ONE*, 8, e68388.

LEV-ARI, S., STARR, A., KATZBURG, S., BERKOVICH, L., RIMMON, A., BEN-YOSEF, R., VEXLER, A., RON, I. & EARON, G. (2014) Curcumin induces apoptosis and inhibits growth of orthotopic human non-small cell lung cancer xenografts. *The Journal of Nutritional Biochemistry*, 25, 843-850.

LI, F., MEI, H., GAO, Y., XIE, X., NIE, H., LI, T., ZHANG, H. & JIA, L. (2017a) Co-delivery of oxygen and erlotinib by aptamer-modified liposomal complexes to reverse hypoxia-induced drug resistance in lung cancer. *Biomaterials*, 145, 56-71.

LI, F., MEI, H., XIE, X., ZHANG, H., LIU, J., LV, T., NIE, H., GAO, Y. & JIA, L. (2017b) Aptamer-conjugated chitosan-anchored liposomal complexes for targeted delivery of erlotinib to EGFR-mutated lung cancer cells. *The AAPS Journal*, 19, 814-826.

LI, H. Y., NEILL, H., INNOCENT, R., SEVILLE, P., WILLIAMSON, I. & BIRCHALL, J. C. (2003) Enhanced dispersibility and deposition of spray-dried powders for pulmonary gene therapy. *Journal of Drug Targeting,* 11, 425-432.

LI, H. Y., SEVILLE, P. C., WILLIAMSON, I. J. & BIRCHALL, J. C. (2005a) The use of amino acids to enhance the aerosolisation of spray-dried powders for pulmonary gene therapy. *The Journal of Gene Medicine,* 7, 343-353.

LI, R., QUAN, P., LIU, D. F., WEI, F. D., ZHANG, Q. & XU, Q. W. (2009) The influence of cosolvent on the complexation of HP-β-cyclodextrins with oleanolic acid and ursolic acid. *AAPS PharmSciTech,* 10, 1137-1144.

LI, S., DOYLE, P., METZ, S., ROYCE, A. E. & SERAJUDDIN, A. T. M. (2005b) Effect of chloride ion on dissolution of different salt forms of haloperidol, a model basic drug. *Journal of Pharmaceutical Sciences*, 94, 2224-2231.

LI, Y., AHMED, F., ALI, S., PHILIP, P. A., KUCUK, O. & SARKAR, F. H. (2005c) Inactivation of nuclear factor κB by soy isoflavone genistein contributes to increased apoptosis induced by chemotherapeutic agents in human cancer cells. *Cancer Research*, 65, 6934-6942.

LIAO, Y. C., SHIH, Y. W., CHAO, C. H., LEE, X. Y. & CHIANG, T. A. (2009) Involvement of the ERK signaling pathway in fisetin reduces invasion and migration in the human lung cancer cell line A549. *Journal of Agricultural and Food Chemistry*, 57, 8933-8941.

LIPPMANN, M., YEATES, D. B. & ALBERT, R. E. (1980) Deposition, retention, and clearance of inhaled particles. *British Journal of Industrial Medicine*, 37, 337-362.

LIU, L. C., TSAO, T. C. Y., HSU, S. R., WANG, H. C., TSAI, T. C., KAO, J. Y. & WAY, T. D. (2012) EGCG inhibits transforming growth factor-β-mediated epithelial-to-mesenchymal transition via the inhibition of Smad2 and Erk1/2 signaling pathways in nonsmall cell lung cancer cells. *Journal of Agricultural and Food Chemistry*, 60, 9863-9873.

LOFTSSON, T. & BREWSTER, M. E. (2012) Cyclodextrins as functional excipients: Methods to enhance complexation efficiency. *Journal of Pharmaceutical Sciences,* 101, 3019-3032.

LOFTSSON, T., HREINSDÓTTIR, D. & MÁSSON, M. (2005a) Evaluation of cyclodextrin solubilization of drugs. *International Journal of Pharmaceutics*, 302, 18-28.

LOFTSSON, T., JARHO, P., MÁSSON, M. & JÄRVINEN, T. (2005b) Cyclodextrins in drug delivery. *Expert Opinion on Drug Delivery*, 2, 335-351.

LOFTSSON, T., MAGNÚSDÓTTIR, A., MÁSSON, M. & SIGURJÓNSDÓTTIR, J. F. (2002) Self-association and cyclodextrin solubilization of drugs. *Journal of Pharmaceutical Sciences*, 91, 2307-2316.

LU, Z., CHENG, B., HU, Y., ZHANG, Y. & ZOU, G. (2009) Complexation of resveratrol with cyclodextrins: Solubility and antioxidant activity. *Food Chemistry,* 113, 17-20.

MAA, Y. F., NGUYEN, P. A., ANDYA, J. D., DASOVICH, N., SWEENEY, T. D., SHIRE, S. J. & HSU, C. C. (1998) Effect of spray drying and subsequent processing conditions on residual moisture content and physical/biochemical stability of protein inhalation powders. *Pharmaceutical Research,* 15, 768-775.

MANDAL, B., MITTAL, N. K., BALABATHULA, P., THOMA, L. A. & WOOD, G. C. (2016) Development and in vitro evaluation of core-shell type lipid-polymer hybrid nanoparticles for the delivery of erlotinib in non-small cell lung cancer. *European Journal of Pharmaceutical Sciences*, 81, 162-171.

MANUNTA, M. D. I., MCANULTY, R. J., TAGALAKIS, A. D., BOTTOMS, S. E., CAMPBELL, F., HAILES, H. C., TABOR, A. B., LAURENT, G. J., O'CALLAGHAN, C. & HART, S. L. (2011) Nebulisation of receptor-targeted nanocomplexes for gene delivery to the airway epithelium. *PLoS ONE*, 6, e26768.

MARSLIN, G., SHEEBA, C. J., KALAICHELVAN, V. K., MANAVALAN, R., NEELAKANTA REDDY, P. & FRANKLIN, G. (2009) Poly(D,L-lactic-co-glycolic acid) nanoencapsulation reduces erlotinib-induced subacute toxicity in rat. *Journal of Biomedical Nanotechnology*, 5, 464-471.

MATILAINEN, L., TOROPAINEN, T., VIHOLA, H., HIRVONEN, J., JÄRVINEN, T., JARHO, P. & JÄRVINEN, K. (2008) In vitro toxicity and permeation of cyclodextrins in Calu-3 cells. *Journal of Controlled Release*, 126, 10-16.

McINTOSH, M. P., SCHWARTING, N. & RAJEWSKI, R. A. (2004) In vitro and in vivo evaluation of a sulfobutyl ether β-cyclodextrin enabled etomidate formulation. *Journal of Pharmaceutical Sciences*, 93, 2585-2594.

MEENACH, S. A., ANDERSON, K. W., ZACH HILT, J., MCGARRY, R. C. & MANSOUR, H. M. (2013) Characterization and aerosol dispersion performance of advanced spray-dried chemotherapeutic PEGylated phospholipid particles for dry powder inhalation delivery in lung cancer. *European Journal of Pharmaceutical Sciences,* 49**,** 699-711.

MENON, L. G., KUTTAN, R., NAIR, M. G., CHANG, Y. C. & KUTTAN, G. (1998) Effect of isoflavones genistein and daidzein in the inhibition of lung metastasis in mice induced by B16F-10 melanoma cells. *Nutrition and Cancer*, 30, 74-77.

MIGNET, N., SEGUIN, J., ROMANO, M. R., BRULLÈ, L., TOUIL, Y. S., SCHERMAN, D., BESSODES, M. & CHABOT, G. G. (2012) Development of a liposomal formulation of the natural flavonoid fisetin. *International Journal of Pharmaceutics*, 423, 69-76.

MILLIGAN, S. A., BURKE, P., COLEMAN, D. T., BIGELOW, R. L., STEFFAN, J. J., CARROLL, J. L., WILLIAMS, B. J. & CARDELLI, J. A. (2009) The green tea polyphenol EGCG potentiates the antiproliferative activity of c-Met and epidermal growth factor receptor inhibitors in non-small cell lung cancer cells. *Clinical Cancer Research*, 15, 4885-4894.

MOMIN, M. M., ZAHEER, Z., ZAINUDDIN, R. & SANGSHETTI, J. N. (2018) Extended release delivery of erlotinib glutathione nanosponge for targeting lung cancer. *Artificial Cells, Nanomedicine, and Biotechnology*, 46, 1064-1075.

MORTON, S. W., LEE, M. J., DENG, Z. J., DREADEN, E. C., SIOUVE, E., SHOPSOWITZ, K. E., SHAH, N. J., YAFFE, M. B. & HAMMOND, P. T. (2014) A nanoparticle-based combination chemotherapy delivery system for enhanced tumor killing by dynamic rewiring of signaling pathways. *Science Signaling*, 7, 1-27.

NATIONAL INSTITUTE FOR HEALTH AND CARE EXCELLENCE (2011) Lung cancer: diagnosis and management. *NICE Guidance*. [Online]. [Accessed 6th July 2018]. Available at https://www.nice.org.uk/guidance/CG121.

NATIONAL INSTITUTE FOR HEALTH AND CARE EXCELLENCE (2015) Erlotinib and gefitinib for treating non-small-cell lung cancer that has progressed after prior chemotherapy. *NICE Guidance.* [Online]. [Accessed 6th July 2018]. Available at https://www.nice.org.uk/guidance/ta374.

NOLAN, L. M., TAJBER, L., MCDONALD, B. F., BARHAM, A. S., CORRIGAN, O. I. & HEALY, A. M. (2009) Excipient-free nanoporous microparticles of budesonide for pulmonary delivery. *European Journal of Pharmaceutical Sciences*, 37, 593-602.

NOORANI, M., AZARPIRA, N., KARIMIAN, K. & HELI, H. (2017) Erlotinib-loaded albumin nanoparticles: A novel injectable form of erlotinib and its in vivo efficacy against pancreatic adenocarcinoma ASPC-1 and PANC-1 cell lines. *International Journal of Pharmaceutics*, 531, 299-305.

NOVELLO, S., BARLESI, F., CALIFANO, R., CUFER, T., EKMAN, S., LEVRA, M. G., KERR, K., POPAT, S., RECK, M., SENAN, S., SIMO, G. V., VANSTEENKISTE, J. & PETERS, S. (2016) Metastatic non-small-cell lung cancer: ESMO Clinical Practice Guidelines for diagnosis, treatment and follow-up. *Annals of Oncology*, 27, v1-v27.

OBER, C. A., KALOMBO, L., SWAI, H. & GUPTA, R. B. (2013) Preparation of rifampicin/lactose microparticle composites by a supercritical antisolvent-drug excipient mixing technique for inhalation delivery. *Powder Technology*, 236, 132-138.

PAHARI, B., SENGUPTA, B., CHAKRABORTY, S., THOMAS, B., MCGOWAN, D. & SENGUPTA, P. K. (2013) Contrasting binding of fisetin and daidzein in γ-cyclodextrin nanocavity. *Journal of Photochemistry and Photobiology B: Biology*, 118, 33-41.

PAO, W. & GIRARD, N. (2011) New driver mutations in non-small-cell lung cancer. *The Lancet Oncology*, 12, 175-180.

PARI (2018) Pari LC© Sprint reusable nebulizer. *Instructions for use*. [Online]. [Accessed 11th February 2018]. Available at https://www.pari.com/us-en/products/nebulizers/lcr-sprint-reusable-nebulizer/.

PATTON, J. S. & BYRON, P. R. (2007) Inhaling medicines: delivering drugs to the body through the lungs. *Nature Review Drug Discovery*, 6, 67-74.

PELTONEN, L., VALO, H., KOLAKOVIC, R., LAAKSONEN, T. & HIRVONEN, J. (2010) Electrospraying, spray drying and related techniques for production and formulation of drug nanoparticles. Expert Opinion on Drug Delivery, 7, 705-719.

PHENOMENEX (2015) Synergi^{TM}: Full range selectivity for reversed phase separation. [Online]. [Accessed 27th July 2017]. Available at https://www.phenomenex.com/ViewDocument?id=synergi+products.

PILCER, G. & AMIGHI, K. (2010) Formulation strategy and use of excipients in pulmonary drug delivery. *International Journal of Pharmaceutics*, 392, 1-19.

POSTMUS, P. E., KERR, K. M., OUDKERK, M., SENAN, S., WALLER, D. A., VANSTEENKISTE, J., ESCRIU, C. & PETERS, S. (2017) Early and locally advanced non-small-cell lung cancer (NSCLC): ESMO Clinical Practice Guidelines for diagnosis, treatment and follow-up. *Annals of Oncology*, 28, iv1-iv21.

POURSHAHAB, P. S., GILANI, K., MOAZENI, E., ESLAHI, H., FAZELI, M. R. & JAMALIFAR, H. (2011) Preparation and characterization of spray dried inhalable powders containing chitosan nanoparticles for pulmonary delivery of isoniazid. *Journal of Microencapsulation*, 28, 605-613.

PRABHU, R., HEGDE, K., SHABARAYA, A. R. & RAO, M. N. A. (2011) Scavenging potential of the reactive oxygen species by tetra-hydrocurcumin. *Journal of Applied Pharmaceutical Science,* 1, 114-118.

PRALHAD, T. & RAJENDRAKUMAR, K. (2004) Study of freeze-dried quercetin-cyclodextrin binary systems by DSC, FT-IR, X-ray diffraction and SEM analysis. *Journal of Pharmaceutical and Biomedical Analysis,* 34, 333-339.

RABBANI, N. R. & SEVILLE, P. C. (2005) The influence of formulation components on the aerosolisation properties of spray-dried powders. *Journal of Controlled Release,* 110, 130-140.

RAGELLE, H., CRAUSTE-MANCIET, S., SEGUIN, J., BROSSARD, D., SCHERMAN, D., ARNAUD, P. & CHABOT, G. G. (2012) Nanoemulsion formulation of fisetin improves bioavailability and antitumour activity in mice. *International Journal of Pharmaceutics*, 427, 452-459.

RAO, R. D., MLADEK, A. C., LAMONT, J. D., GOBLE, J. M., ERLICHMAN, C., JAMES, C. D. & SARKARIA, J. N. (2005) Disruption of parallel and converging signaling pathways contributes to the synergistic antitumor effects of simultaneous mTOR and EGFR inhibition in GBM cells. *Neoplasia*, 7, 921-929.

RAULA, J., THIELMANN, F., KANSIKAS, J., HIETALA, S., ANNALA, M., SEPPÄLÄ, J., LÄHDE, A. & KAUPPINEN, E. (2008) Investigations on the humidity-induced transformations of salbutamol sulphate particles coated with L-leucine. *Pharmaceutical Research*, 25, 2250-2261.

RAVICHANDRAN, N., SURESH, G., RAMESH, B. & VIJAIYAN SIVA, G. (2011) Fisetin, a novel flavonol attenuates benzo(a)pyrene-induced lung carcinogenesis in Swiss albino mice. *Food and Chemical Toxicology*, 49, 1141-1147.

RECK, M., HEIGENER, D. F., MOK, T., SORIA, J. C. & RABE, K. F. (2013) Management of non-small-cell lung cancer: recent developments. *The Lancet*, 382, 709-719.

REN, L., ZHOU, Y., WEI, P., LI, M. & CHEN, G. (2014) Preparation and pharmacokinetic study of aprepitant-sulfobutyl ether-β-cyclodextrin complex. *AAPS PharmSciTech*, 15, 121-130.

RISS, T. L., MORAVEC, R. A., NILES, A. L., BENINK, H. A., WORZELLA, T. J., MINOR, L. (2015) Cell viability assays. *Assay Guidance Manual*. [Online]. [Accessed 30th January 2018]. Available at https://www.ncbi.nlm.nih.gov/books/NBK144065/

RIZI, K., GREEN, R. J., DONALDSON, M. & WILLIAMS, A. C. (2011) Production of pH-responsive microparticles by spray drying: Investigation of experimental parameter effects on morphological and release properties. *Journal of Pharmaceutical Sciences*, 100, 566-579.

RUDOLPH, C., SCHILLINGER, U., ORTIZ, A., TABATT, K., PLANK, C., MÜLLER, R. H. & ROSENECKER, J. (2004) Application of novel solid lipid nanoparticle (SLN)-gene vector formulations based on a dimeric HIV-1 TAT-peptide in vitro and in vivo. *Pharmaceutical Research*, 21, 1662-1669.

SAHU, B. D., KALVALA, A. K., KONERU, M., MAHESH KUMAR, J., KUNCHA, M., RACHAMALLA, S. S. & SISTLA, R. (2014) Ameliorative effect of fisetin on cisplatin-induced nephrotoxicity in rats via modulation of NF-κB activation and antioxidant defence. *PLoS ONE*, 9, e105070.

SALI, N., CSEPREGI, R., KŐSZEGI, T., KUNSÁGI-MÁTÉ, S., SZENTE, L. & POÓR, M. (2018) Complex formation of flavonoids fisetin and geraldol with β-cyclodextrins. *Journal of Luminescence*, 194, 82-90.

SALUJA, V., AMORIJ, J. P., KAPTEYN, J. C., DE BOER, A. H., FRIJLINK, H. W. & HINRICHS, W. L. J. (2010) A comparison between spray drying and spray freeze drying to produce an influenza subunit vaccine powder for inhalation. *Journal of Controlled Release*, 144, 127-133.

SCALIA, S., HAGHI, M., LOSI, V., TROTTA, V., YOUNG, P. M. & TRAINI, D. (2013) Quercetin solid lipid microparticles: A flavonoid for inhalation lung delivery. *European Journal of Pharmaceutical Sciences*, 49, 278-285.

SCHERING CORPORATION (2010) Medication guide: Foradil® Arolizer®. [Online]. [Accessed on 21st February 2018]. Available at https://www.fda.gov/downloads/Drugs/DrugSafety/ucm088602.pdf

SEGUIN, J., BRULLÈ, L., BOYER, R., LU, Y. M., ROMANO, M. R., TOUIL, Y. S., SCHERMAN, D., BESSODES, M., MIGNET, N. & CHABOT, G. G. (2013) Liposomal encapsulation of the natural flavonoid fisetin improves bioavailability and antitumor efficacy. *International Journal of Pharmaceutics*, 444, 146-154.

SEVILLE, P. C., LEAROYD, T. P., LI, H. Y., WILLIAMSON, I. J. & BIRCHALL, J. C. (2007) Amino acid-modified spray-dried powders with enhanced aerosolisation properties for pulmonary drug delivery. *Powder Technology,* 178, 40-50.

SHANG, Y. J., JIN, X. L., SHANG, X. L., TANG, J. J., LIU, G. Y., DAI, F., QIAN, Y. P., FAN, G. J., LIU, Q. & ZHOU, B. (2010) Antioxidant capacity of curcumin-directed analogues: Structure-activity relationship and influence of microenvironment. *Food Chemistry,* 119, 1435-1442.

SHARMA, S. V., BELL, D. W., SETTLEMAN, J. & HABER, D. A. (2007) Epidermal growth factor receptor mutations in lung cancer. *Nature Reviews Cancer*, 7, 169-181.

SHEKUNOV, B. Y., CHATTOPADHYAY, P., TONG, H. H. Y. & CHOW, A. H. L. (2007) Particle size analysis in pharmaceutics: principles, methods and applications. *Pharmaceutical Research*, 24, 203-227.

SHEN, Q., WANG, Y. & ZHANG, Y. (2011) Improvement of colchicine oral bioavailability by incorporating eugenol in the nanoemulsion as an oil excipient and enhancer. *International Journal of Nanomedicine*, 6, 1237-1243.

SHEPHERD, F. A., RODRIGUES PEREIRA, J., CIULEANU, T., TAN, E. H., HIRSH, V., THONGPRASERT, S., CAMPOS, D., MAOLEEKOONPIROJ, S., SMYLIE, M., MARTINS, R., VAN KOOTEN, M., DEDIU, M., FINDLAY, B., TU, D., JOHNSTON, D., BEZJAK, A., CLARK, G., SANTABÁRBARA, P. &

SEYMOUR, L. (2005) Erlotinib in previously treated non-small-cell lung cancer. *New England Journal of Medicine*, 353, 123-132.

SINGH, C., KODURI, L. V. S. K., SINGH, A. & SURESH, S. (2015) Novel potential for optimization of antitubercular therapy: Pulmonary delivery of rifampicin lipospheres. *Asian Journal of Pharmaceutical Sciences*, 10, 549-562.

SISTLA, R., TATA, V. S. S. K., KASHYAP, Y. V., CHANDRASEKAR, D. & DIWAN, P. V. (2005) Development and validation of a reversed-phase HPLC method for the determination of ezetimibe in pharmaceutical dosage forms. *Journal of Pharmaceutical and Biomedical Analysis,* 39, 517-522.

SMITH, N. F., BAKER, S. D., GONZALEZ, F. J., HARRIS, J. W., FIGG, W. D. & SPARREBOOM, A. (2008) Modulation of erlotinib pharmacokinetics in mice by a novel cytochrome P450 3A4 inhibitor, BAS 100. *British Journal of Cancer*, 98, 1630-1632.

SON, Y. J. & MCCONVILLE, J. T. (2012) Preparation of sustained release rifampicin microparticles for inhalation. *Journal of Pharmacy and Pharmacology*, 64, 1291-1302.

STECKEL, H. & ESKANDAR, F. (2003) Factors affecting aerosol performance during nebulization with jet and ultrasonic nebulizers. European Journal of Pharmaceutical Sciences, 19, 443-455.

STIGLIANI, M., AQUINO, R. P., DEL GAUDIO, P., MENCHERINI, T., SANSONE, F. & RUSSO, P. (2013) Non-steroidal anti-inflammatory drug for pulmonary administration: Design and investigation of ketoprofen lysinate fine dry powders. *International Journal of Pharmaceutics*, 448, 198-204.

TAJBER, L., CORRIGAN, O. I. & HEALY, A. M. (2009) Spray drying of budesonide, formoterol fumarate and their composites-II. Statistical factorial design and in vitro deposition properties. *International Journal of Pharmaceutics,* 367**,** 86-96.

TAYLOR, K. M. G. (2018) Pulmonary drug delivery. IN AULTON, M. E. & TAYLOR, K. M. G. (Eds.) *Aulton's pharmaceutics: the design and manufacture of medicines*. 5 ed. London, Elsevier Ltd., pp. 653-670.

TAYLOR, K. M. G., VENTHOYE, G. & CHAWLA, A. (1992) Pentamidine isethionate delivery from jet nebulisers. International Journal of Pharmaceutics, 85, 203-208.

TELKO, M. J. & HICKEY, A. J. (2005) Dry Powder Inhaler Formulation. *Respiratory Care*, 50, 1209-1227.

TOLMAN, J. A., WIEDERHOLD, N. P., MCCONVILLE, J. T., NAJVAR, L. K., BOCANEGRA, R., PETERS, J. I., COALSON, J. J., GRAYBILL, J. R., PATTERSON, T. F. & WILLIAMS, R. O. (2009) Inhaled voriconazole for prevention of invasive pulmonary aspergillosis. *Antimicrobial Agents and Chemotherapy*, 53, 2613-2615.

TOMODA, K., OHKOSHI, T., HIROTA, K., SONAVANE, G. S., NAKAJIMA, T., TERADA, H., KOMURO, M., KITAZATO, K. & MAKINO, K. (2009) Preparation and properties of inhalable nanocomposite particles for treatment of lung cancer. *Colloids and Surfaces B: Biointerfaces*, 71, 177-182.

TÓTH, G., JÁNOSKA, Á., SZABÓ, Z. I., VÖLGYI, G., ORGOVÁN, G., SZENTE, L. & NOSZÁL, B. (2016) Physicochemical characterisation and cyclodextrin complexation of erlotinib. *Supramolecular Chemistry*, 28, 656-664.

TOUIL, Y. S., SEGUIN, J., SCHERMAN, D. & CHABOT, G. G. (2011) Improved antiangiogenic and antitumour activity of the combination of the natural flavonoid fisetin and cyclophosphamide in Lewis lung carcinoma-bearing mice. *Cancer Chemotherapy and Pharmacology*, 68, 445-455.

TRAINI, D. & YOUNG, P. M. (2009) Delivery of antibiotics to the respiratory tract: an update. *Expert Opinion on Drug Delivery*, 6, 897-905.

TRAVIS, W. D. (2011) Pathology of lung cancer. *Clinics in Chest Medicine*, 32, 669-692.

TRAVIS, W. D., BRAMBILLA, E., NICHOLSON, A. G., YATABE, Y., AUSTIN, J. H. M., BEASLEY, M. B., CHIRIEAC, L. R., DACIC, S., ISHIKAWA, Y., KERR, K. M., NOGUCHI, M., PELOSI, G., POWELL, C. A., TSAO, M. S. & WISTUBA, I. (2015) The 2015 World Health Organization classification of lung tumors- Impact of genetic, clinical and radiologic advances since the 2004 classification. *Journal of Thoracic Oncology*, 10, 1243-1260.

TRIPATHI, R., SAMADDER, T., GUPTA, S., SUROLIA, A. & SHAHA, C. (2011) Anticancer activity of a combination of cisplatin and fisetin in embryonal carcinoma cells and xenograft tumors. *Molecular Cancer Therapeutics*, 10, 255-268.

TRUONG, D. H., TRAN, T. H., RAMASAMY, T., CHOI, J. Y., LEE, H. H., MOON, C., CHOI, H. G., YONG, C. S. & KIM, J. O. (2016) Development of solid self-emulsifying formulation for improving the oral bioavailability of erlotinib. *AAPS PharmSciTech*, 17, 466-473.

VANBEVER, R., BEN-JEBRIA, A., MINTZES, J., LANGER, R. & EDWARDS, D. A. (1999) Sustained release of insulin from insoluble inhaled particles. *Drug Development and Research*, 48, 178-185.

VECELLIO, L. (2006) The mesh nebuliser: a recent technical innovation for aerosol delivery. *Breathe*, 2, 253-260.

VEHRING, R. (2008) Pharmaceutical particle engineering via spray drying. *Pharmaceutical Research*, 25, 999-1022.

VRIGNAUD, S., HUREAUX, J., WACK, S., BENOIT, J. P. & SAULNIER, P. (2012) Design, optimization and in vitro evaluation of reverse micelle-loaded lipid nanocarriers containing erlotinib hydrochloride. *International Journal of Pharmaceutics*, 436, 194-200.

WALLENTINE, C. B., SHIMODE, N., EGAN, T. D. & PACE, N. L. (2011) Propofol in a modified cyclodextrin formulation: first human study of dose-response with emphasis on injection pain. *Anesthesia & Analgesia*, 113, 738-741.

WANG, D., CHEN, G. & REN, L. (2017) Preparation and characterization of the sulfobutylether-beta-cyclodextrin inclusion complex of amiodarone hydrochloride with enhanced oral bioavailability in fasted state. *AAPS PharmSciTech*, 18, 1526-1535.

WHO (2017) Cancer: Fact sheet. *Media Centre.* [Online]. [Accessed 15th November 2017]. Available at http://www.who.int/mediacentre/factsheets/fs297/en/

XU, H., HE, C., LIU, Y., JIANG, J. & MA, T. (2017) Novel therapeutic modalities and drug delivery- erlotinib liposomes modified with galactosylated lipid: in vitro and in vivo investigations. Artificial Cells, *Nanomedicine, and Biotechnology*, 1-6.

YANG, K. M., SHIN, I. C., PARK, J. W., KIM, K. S., KIM, D. K., PARK, K. & KIM, K. (2017) Nanoparticulation improves bioavailability of erlotinib. *Drug Development and Industrial Pharmacy*, 43, 1557-1565.

YATSU, F. K. J., KOESTER, L. S., LULA, I., PASSOS, J. J., SINISTERRA, R. & BASSANI, V. L. (2013) Multiple complexation of cyclodextrin with soy isoflavones present in an enriched fraction. *Carbohydrate Polymers*, 98, 726-735.

ZENG, X. M., MARTIN, G. P., TEE, S.-K., GHOUSH, A. A. & MARRIOTT, C. (1999) Effects of particle size and adding sequence of fine lactose on the deposition of salbutamol sulphate from a dry powder formulation. *International Journal of Pharmaceutics*, 182, 133-144.

ZHANG, J. Q., JIANG, K. M., AN, K., REN, S. H., XIE, X. G., JIN, Y. & LIN, J. (2015) Novel water-soluble fisetin/cyclodextrins inclusion complexes: Preparation, characterization, molecular docking and bioavailability. *Carbohydrate Research*, 418, 20-28.

ZHANG, K. S., CHEN, H. Q., CHEN, Y. S., QIU, K. F., ZHENG, X. B., LI, G. C., YANG, H. D. & WEN, C. J. (2014) Bisphenol A stimulates human lung cancer cell migration via upregulation of matrix metalloproteinases by GPER/EGFR/ERK1/2 signal pathway. *Biomedicine & Pharmacotherapy*, 68, 1037-1043.

ZHANG, L., HUANG, Y., ZHUO, W., ZHU, Y., ZHU, B. & CHEN, Z. (2016) Fisetin, a dietary phytochemical, overcomes erlotinib-resistance of lung adenocarcinoma cells through inhibition of MAPK and AKT pathways. *American Journal of Translational Research*, 8, 4857-4868.

ZHENG, Y. & CHOW, A. H. L. (2009) Production and characterisation of a spray-dried hydroxypropyl-β-cyclodextrin/quercetin complex. *Drug Development and Industrial Pharmacy,* 35, 727-734.

ZHOU, J., ZHAO, W. Y., MA, X., JU, R. J., LI, X. Y., LI, N., SUN, M. G., SHI, J. F., ZHANG, C. X. & LU, W. L. (2013) The anticancer efficacy of paclitaxel liposomes modified with mitochondrial targeting conjugate in resistant lung cancer. *Biomaterials*, 34, 3626-3638.

ZHUO, W., ZHANG, L., ZHU, Y., ZHU, B. & CHEN, Z. (2015) Fisetin, a dietary bioflavonoid, reverses acquired cisplatin-resistance of lung adenocarcinoma cells through MAPK/Survivin/Caspase pathway. *American Journal of Translational Research*, 7, 2045-2052.

ZHOU, X., TAO, H. & SHI, K. H. (2018) Development of a nanoliposomal formulation of erlotinib for lung cancer and in vitro/in vivo antitumoral evaluation. *Drug Design, Development and Therapy*, 12, 1-8.

ZHOU, Z., KENNELL, C., JAFARI, M., LEE, J. Y., RUIZ-TORRES, S. J., WALTZ, S. E. & LEE, J. H. (2017) Sequential delivery of erlotinib and doxorubicin for enhanced triple negative breast cancer treatment using polymeric nanoparticle. *International Journal of Pharmaceutics*, 530, 300-307.
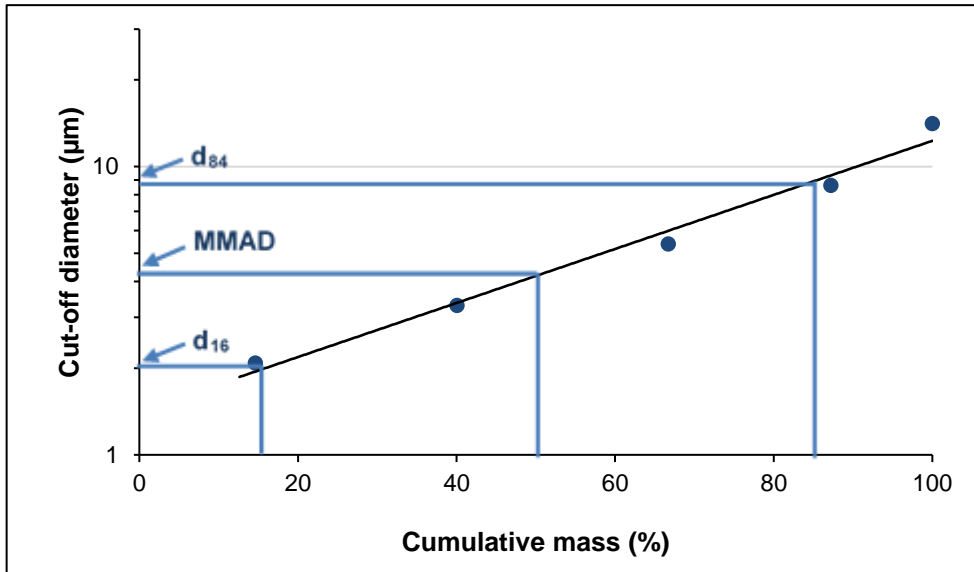
Appendices
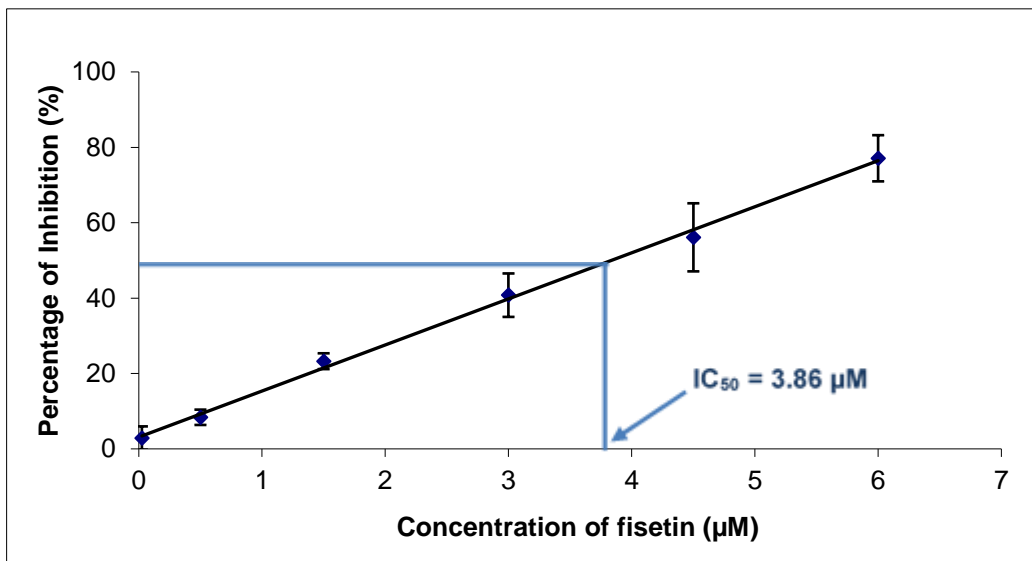
Appendix A Inhibition curve of spray-dried fisetin-SBE-β-CD complex solution in DPPH assay; Interpolation of the graph to find the IC_{50}.
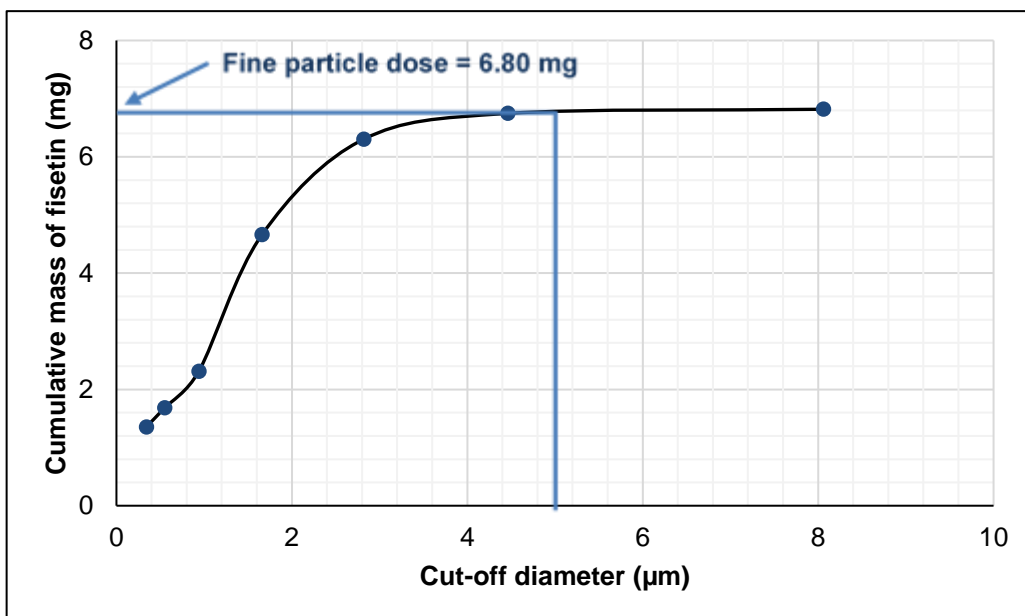

Appendix B Cumulative mass plot of fisetin in formulation SD_20%Eth20%Leu in the NGI; Interpolation of the graph to find the fine particle dose (FPD).
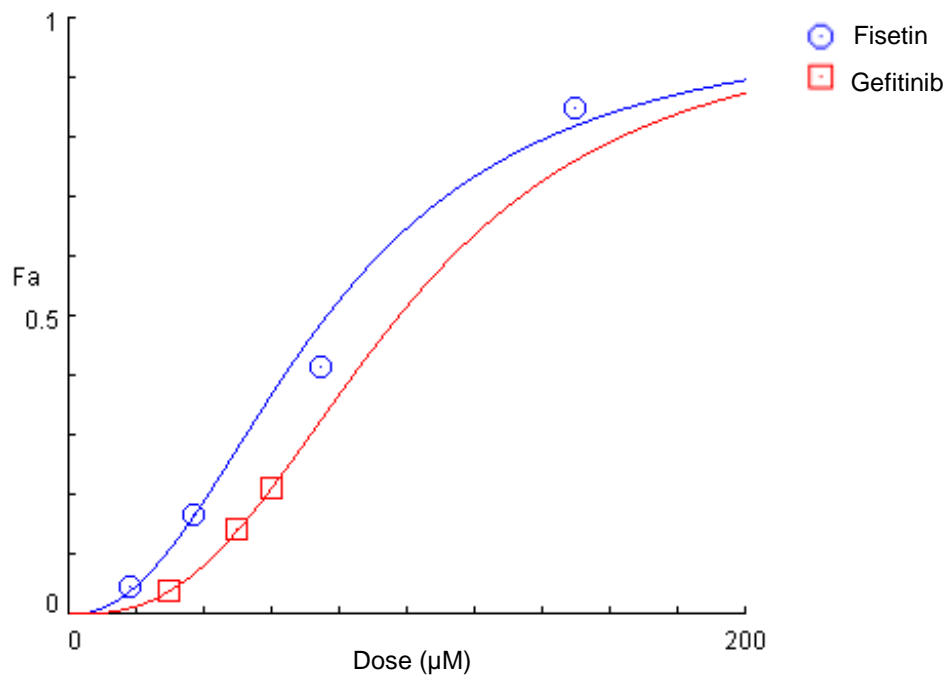
Appendix C Example of cumulative fraction of active substance versus cut-off diameter on log probability scale, in the determination of MMAD and GSD.
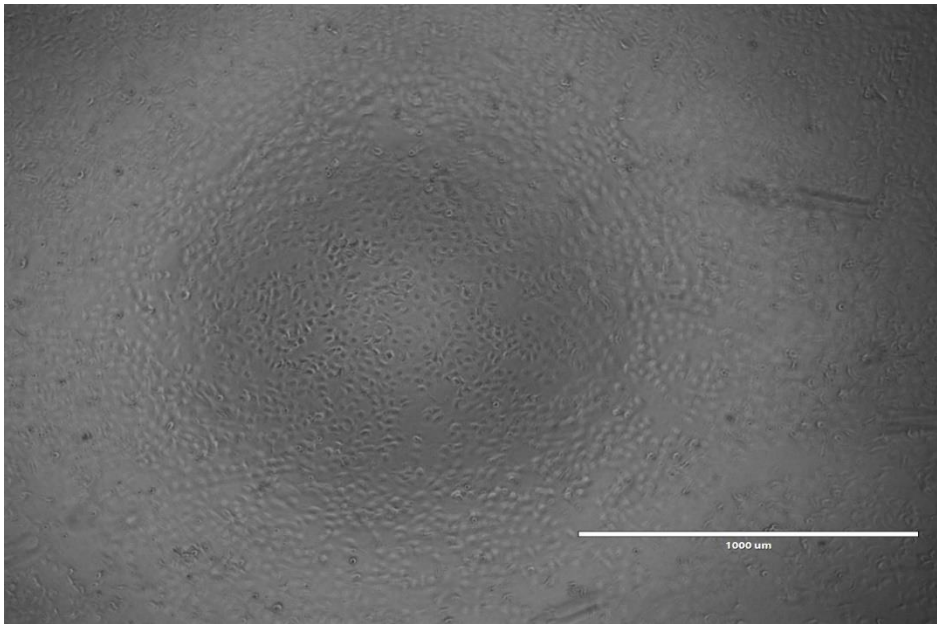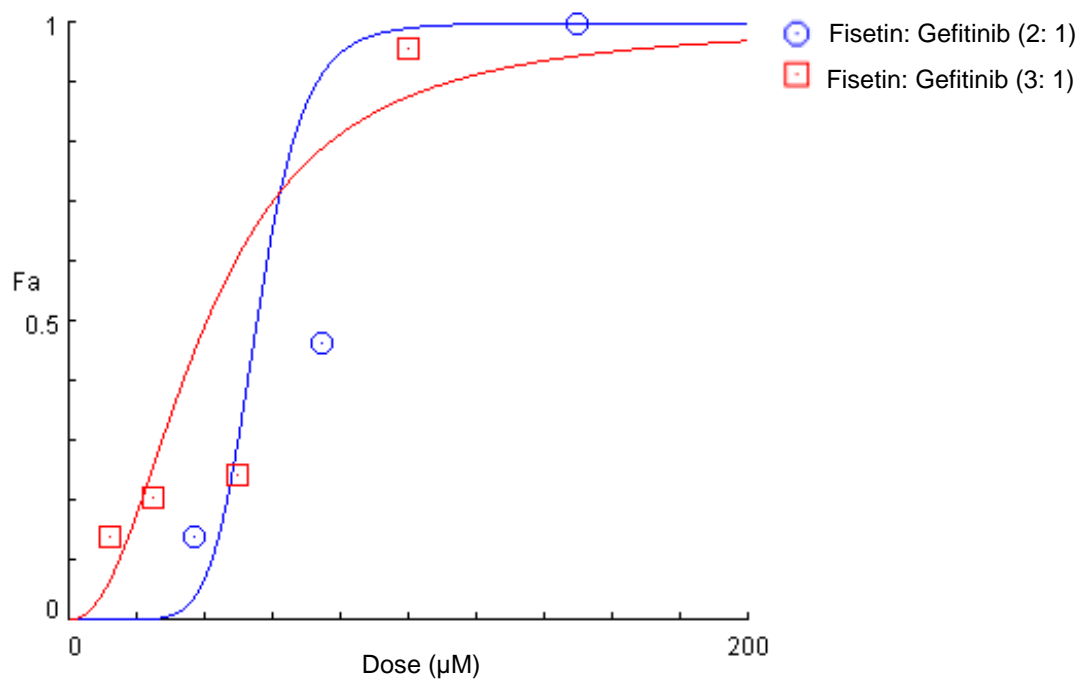

Appendix D Inverted microscope image of the A549 cell line after 24 hr incubation in 96-well plate, prior to the treatment.
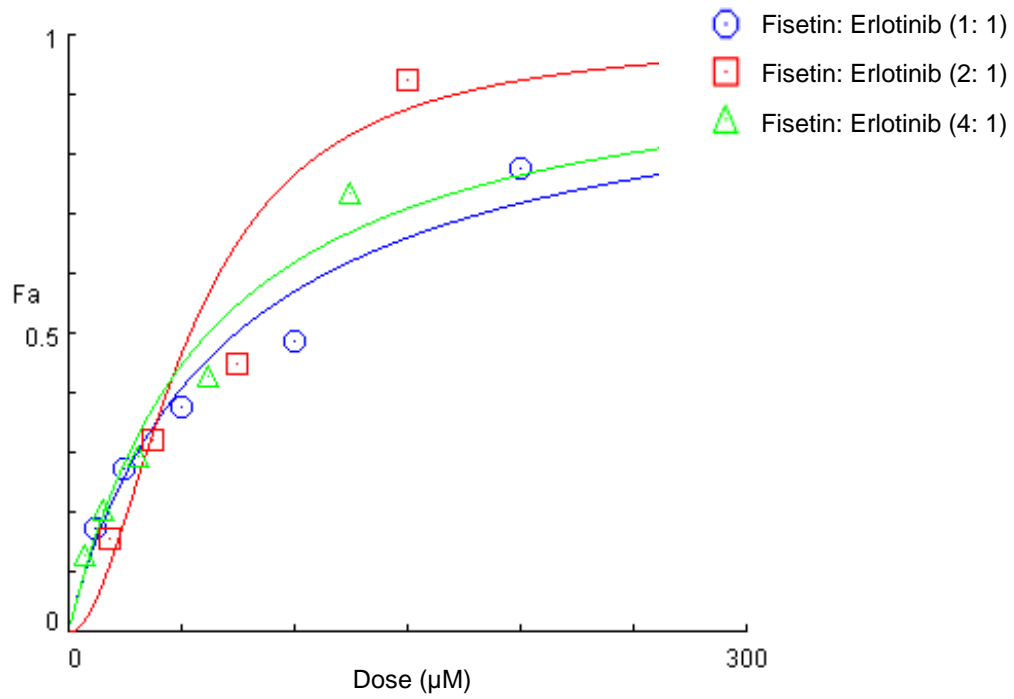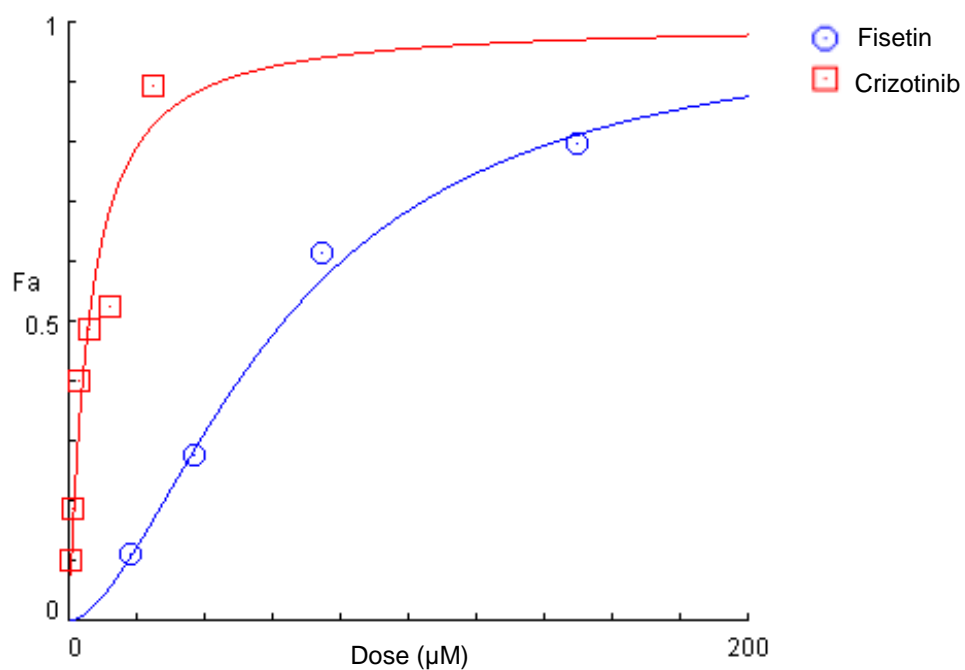
Appendix E Fraction affected (Fa) plot of fisetin and erlotinib combinations.
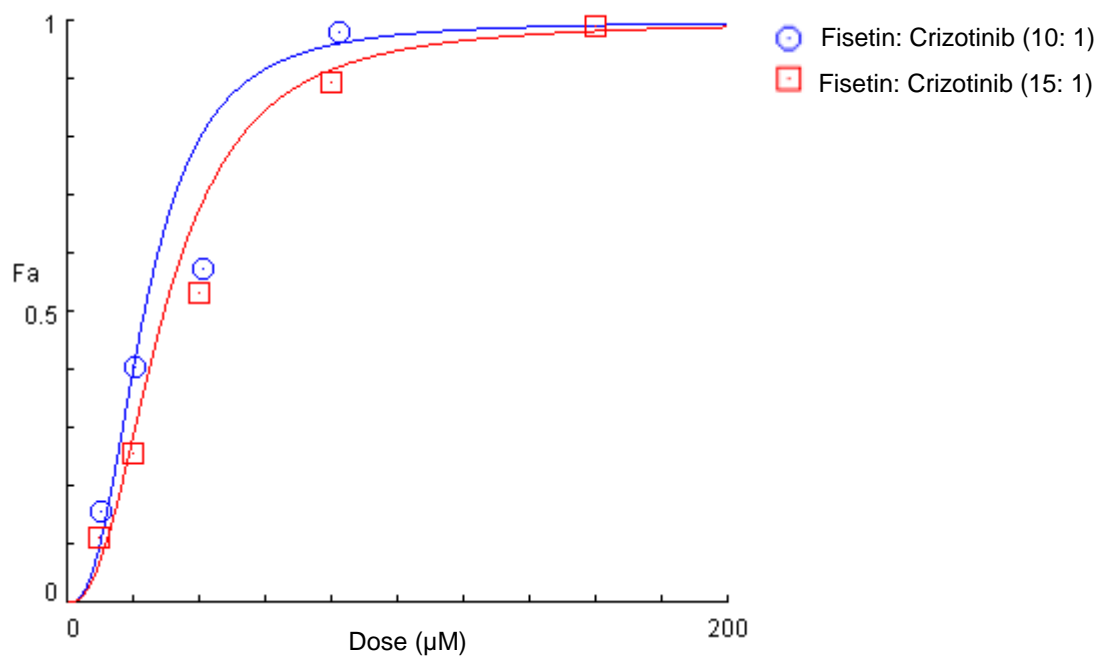

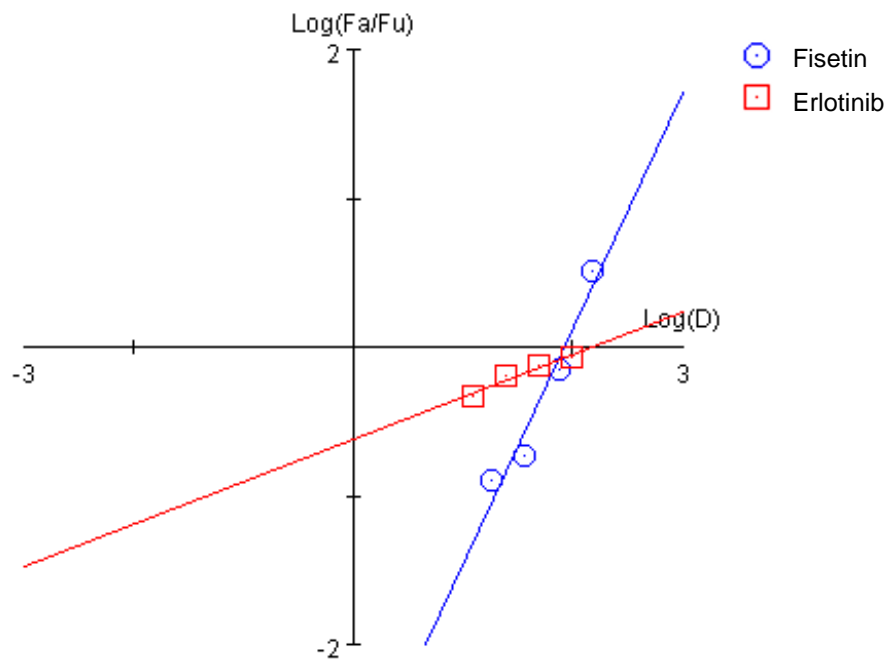Appendix F Fraction affected (Fa) plot of fisetin and gefitinib.

Appendix G Fraction affected (Fa) plot of fisetin and gefitinib combinations.
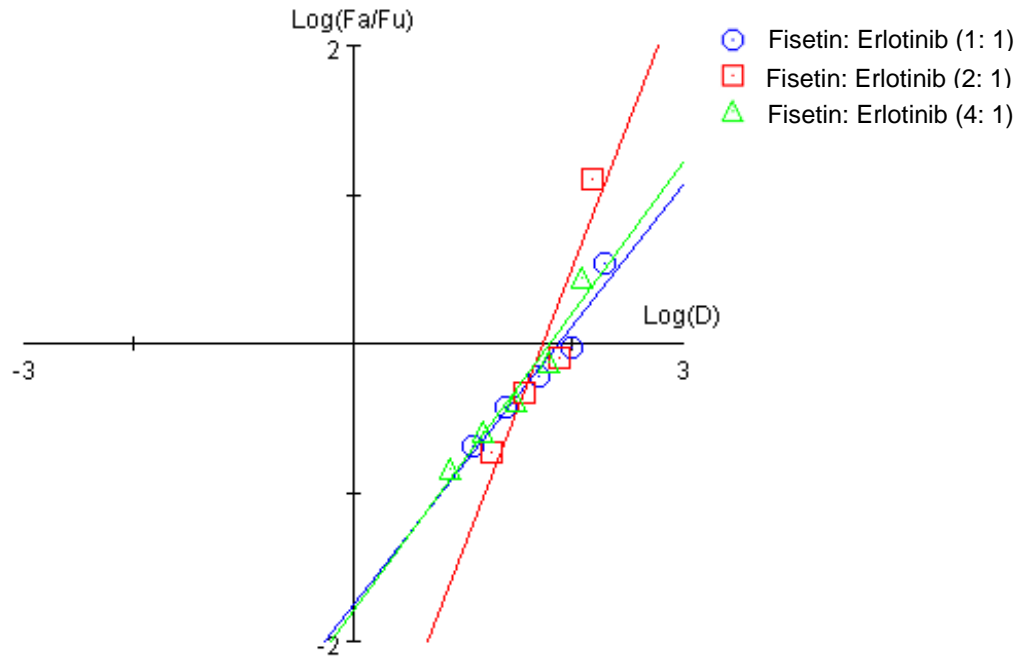

Appendix H Fraction affected (Fa) plot of fisetin and crizotinib.

Appendix I Fraction affected (Fa) plot of fisetin and crizotinib combinations.

Appendix J Median effect plot of fisetin and erlotinib.

Appendix K Median effect plot of fisetin and erlotinib combinations.

Publication and presentations

Publication

MOHTAR, N., TAYLOR, K. M. G., SHEIKH, K., SOMAVARAPU, S. (2017) Design and development of dry powder sulfobutylether-β-cyclodextrin complex for pulmonary delivery of fisetin, *European Journal of Pharmaceutics and Biopharmaceutics*, 113, 1-10.

Poster presentations

MOHTAR, N., SHEIKH, K., TAYLOR, K. M. G., SOMAVARAPU, S. (2015) Sulfobutylether-β-cyclodextrin (SBE-β-CD) fisetin complex dry powder formulation for lung delivery. AAPS Annual Meeting and Exposition, Florida (USA), 25-29 October 2015.

MOHTAR, N., TAYLOR, K. M. G., SHEIKH, K., SOMAVARAPU, S. (2016) Production of a dry powder sulfobutylether-β-cyclodextrin (SBE-β-CD) complex for pulmonary delivery of fisetin. APS 7th International PharmSci Conference, Glasgow (UK), 5-7 September 2016.

MOHTAR, N., TAYLOR, K. M. G., SOMAVARAPU, S. (2017) Erlotinib-fisetin-SBE-β-CD complex for pulmonary delivery as an improved treatment for non-small cell lung cancer (NSCLC). Drug Delivery to Lungs 2017, Edinburgh (UK), 6-8 December 2017.

Internal UCL Presentations

MOHTAR, N., TAYLOR, K. M. G., SHEIKH, K., SOMAVARAPU, S. (2016) Development of a dry powder sulfobutylether-β-cyclodextrin (SBE-β-CD) complex for pulmonary delivery of fisetin. UCL School of Pharmacy PhD Research Day, London (UK), April 2016. Poster presentation.

MOHTAR, N., TAYLOR, K. M. G., SOMAVARAPU, S. (2017) Inhalable erlotinib-fisetin-sulfobutylether-β-cyclodextrin complex in the treatment of non-small cell lung cancer (NSCLC). UCL School of Pharmacy PhD Research Day, London (UK), September 2017. Oral presentation.